

# Chapter -3

*Results and Discussions*

---

## **RESULTS AND DISCUSSION**

Fresh leaves and root bark of *A. excelsa* Roxb. along with flowers and stem of *Butea monosperma* Lam. were collected from local area of Amravati, Maharashtra, India and were identified by comparing with the herbarium specimen. Voucher specimen (No. Pharmacy/05-06/AE/ML), (No. Pharmacy/05-06/BUT/ML) respectively were submitted in the Pharmacy Department, The M S University of Baroda, Vadodara.

### **3.1 Studies on *Ailanthus excelsa* Roxb**

#### **3.1.1 Extraction of plant material**

Successive extracts of *Ailanthus* leaves in (petroleum ether, diethyl ether, chloroform, ethyl acetate, methanol, water) and root bark in (petroleum ether, benzene, chloroform, ethyl acetate, methanol, and water) were prepared by soxhlet extraction method. The extracts were concentrated, dried under vacuum and subjected to preliminary phytochemical analysis.

For leaves and root bark maximum extractive values were obtained with polar solvents like methanol and water, whereas it's less in non polar solvents. Percentage extractive values are reported in (Table-1.1).

**Table-1.1 Percentage extractive values of leaves and root bark of *A. excelsa***

A. excelsa			
Sr.No.	Solvent used		
<b>Leaves</b>			
	Color	&	Average Extractive value % (w/w)
	Consistency		
1	Petroleum ether	Greenish-yellow, semisolid, oily.	4.79
2	Diethyl ether	Dark green, soft mass	0.81
3	Chloroform	Dark green, soft mass	0.31
4	Ethyl acetate	Dark green semisolid mass.	2.95
5	Methanol	Dark brown semisolid mass	20.61
6	Water	Coffee brown, solid mass	8.45
<b>Root bark</b>			
	Color	&	Average Extractive value % (w/w)
	Consistency		
		Yellowish brown, waxy mass	0.51
		Reddish brown, semisolid mass	0.55
		Reddish brown, semisolid mass	0.21
		Reddish brown, semisolid mass	0.18
		Dark brown semisolid mass	20.0
		Coffee brown, solid mass	17.2

### 3.1.2 Qualitative chemical tests

Qualitative chemical tests showed the presence of flavonoids, steroids, saponins, sugars and amino acids in various extracts of leaves, while root bark showed presence of steroids, triterpenoids, tannins and alkaloids. Alkaloids were present in most of the extracts of root bark (Table-1.2).

**Table-1.2 Qualitative chemical tests for different extracts of leaves and root bark of *A. excelsa***

Class of compounds	Plant drugs													
	<i>Ailanthus leaves</i>							<i>Ailanthus root bark</i>						
	P	D	C	E	SM	SA	P	B	C	E	SM	SA		
Alkaloids	-	-	-	-	-	-	-	+	+	+	+	-		
Carbohydrates	-	+	-	+	+	+	-	+	-	+	+	+		
Steroids/Terpenoids	+	+	+	+	+	-	+	+	+	+	+	-		
Proteins & Amino acids	-	-	-	-	+	+	+	-	-	+	+	+		
Saponins	-	-	-	-	-	-	-	-	-	-	-	-		
Fixed oils/Fats	+	+	-	-	-	-	-	-	-	-	-	-		
Flavonoids	-	-	-	+	+	-	-	-	-	-	-	-		
Phenolics	-	-	+	+	+	+	-	+	+	+	+	-		
Tannins	-	-	-	-	+	-	-	+	+	+	+	-		

+ Present, - Absent

P-Petroleum ether extract  
 B-Benzene  
 C-Chloroform extract  
 D-Diethyl ether extract  
 E-Ethyl acetate extract  
 SM-Successive methanol extract  
 SA-Successive aqueous extract

### 3.1.3 Elemental analysis

Elemental analysis of Ailanthus leaves and root bark was done by Atomic absorption spectrophotometer, where both leaves and root bark showed high concentration of potassium. Root bark showed higher concentration of iron and lead as compared to leaves. (Table-1.3)

**Table-1.3- Elemental analysis of Ailanthus leaves and root bark.**

	Elemental analysis							
	Manganese	Zinc	Copper	Sodium	Potassium	Iron	Lead	Cadm
Ailanthus leaf	27.19	21.58	7.6	240.44	9380.05	140.77	6.65	NIL
Ailanthus root bark	33.88	10.04	10.03	207.97	10881.65	766.44	36.42	NIL

All parameters are expressed in PPM

### 3.1.4 Evaluation of Antioxidant activity of Ailanthus leaves extracts

#### 3.1.4.1 In-vitro antioxidant activity

All the successive extracts of Ailanthus leaves along with total methanol and total aqueous extract were screened for in-vitro antioxidant activity.

##### 3.1.4.1.1 Reducing power assay

Diethyl ether, ethyl acetate, total aqueous, chloroform, and successive aqueous extracts were found to possess significant reducing power. Diethyl ether and ethyl acetate extracts were more active compared to others. The extracts exhibited a concentration dependent increase in reducing power. Compared with ascorbic acid the reducing powers of these extracts were lesser (Fig-3.1A).

##### 3.1.4.1.2 Scavenging of DPPH radical

Diethyl ether, successive methanol, ethyl acetate, and chloroform extracts showed a concentration dependent antiradical activity by scavenging DPPH radical with an EC<sub>50</sub> value of 17.55, 26.75, 38.55 and 52.37 µg/ml, respectively. Diethyl ether and chloroform extracts were found to be more potent compared to other two. The scavenging effects were lesser compared to reference standard rutin (EC<sub>50</sub>: 2.85 µg/ml) (Fig-3.1B).

#### **3.1.4.1.3 Inhibition of superoxide radical**

Diethyl ether and ethyl acetate extracts exhibit better inhibition of superoxide radical with an EC<sub>50</sub> value of 176.89 and 180.83µg/ml, respectively, while chloroform and successive methanol extracts showed 50% inhibition at a higher concentration of 241.48 and 291.05µg/ml. The scavenging effects were lesser compared to reference standard quercetin (EC<sub>50</sub>:10.84 µg/ml) (Fig-3.1C).

#### **3.1.4.1.4 Inhibition of nitric oxide radical**

Concentration of diethyl ether, ethyl acetate, chloroform and successive methanol extracts required for 50% inhibition were found to be 86.54, 124.23, 149.76 and 177.31µg/ml respectively. Diethyl ether extract was found to be more potent compared to others. Curcumin used as a reference compound, showed 50% inhibition at 34.23µg/ml (Fig-3.1D).

#### **3.1.4.1.5 Inhibition of hydroxyl radical**

Effect of successive extracts and total extracts of Ailanthus leaves were studied on deoxyribose damage induced by Fe<sup>3+</sup>/H<sub>2</sub>O<sub>2</sub> is shown in (Fig-3.1E). Diethyl ether and ethyl acetate extracts were found to show better inhibition compared to chloroform and successive methanol extracts with EC<sub>50</sub> 68.88, 77.86, 89.45 and 96.73µg/ml, respectively. The results were compared with reference standard curcumin (EC<sub>50</sub>: 0.96µg/ml), which was more effective than the fractions tested.

#### **3.1.4.1.6 Inhibition of erythrocyte hemolysis**

Diethyl ether, successive methanol, ethyl acetate and chloroform extracts were found to inhibit the hemolysis of erythrocytes with EC<sub>50</sub> values of 0.77, 20.89, 25.87, and 36.97µg/ml respectively. Diethyl ether extract was found to be more potent than ascorbic acid (EC<sub>50</sub>: 3.07µg/ml). (Fig-3.1F)

#### **3.1.4.1.7 Rapid screening for antioxidant compounds**

Ethyl acetate, successive methanol, total methanol and diethyl ether extracts were found to contain antiradical components, compared to other extracts (Fig-3.15).

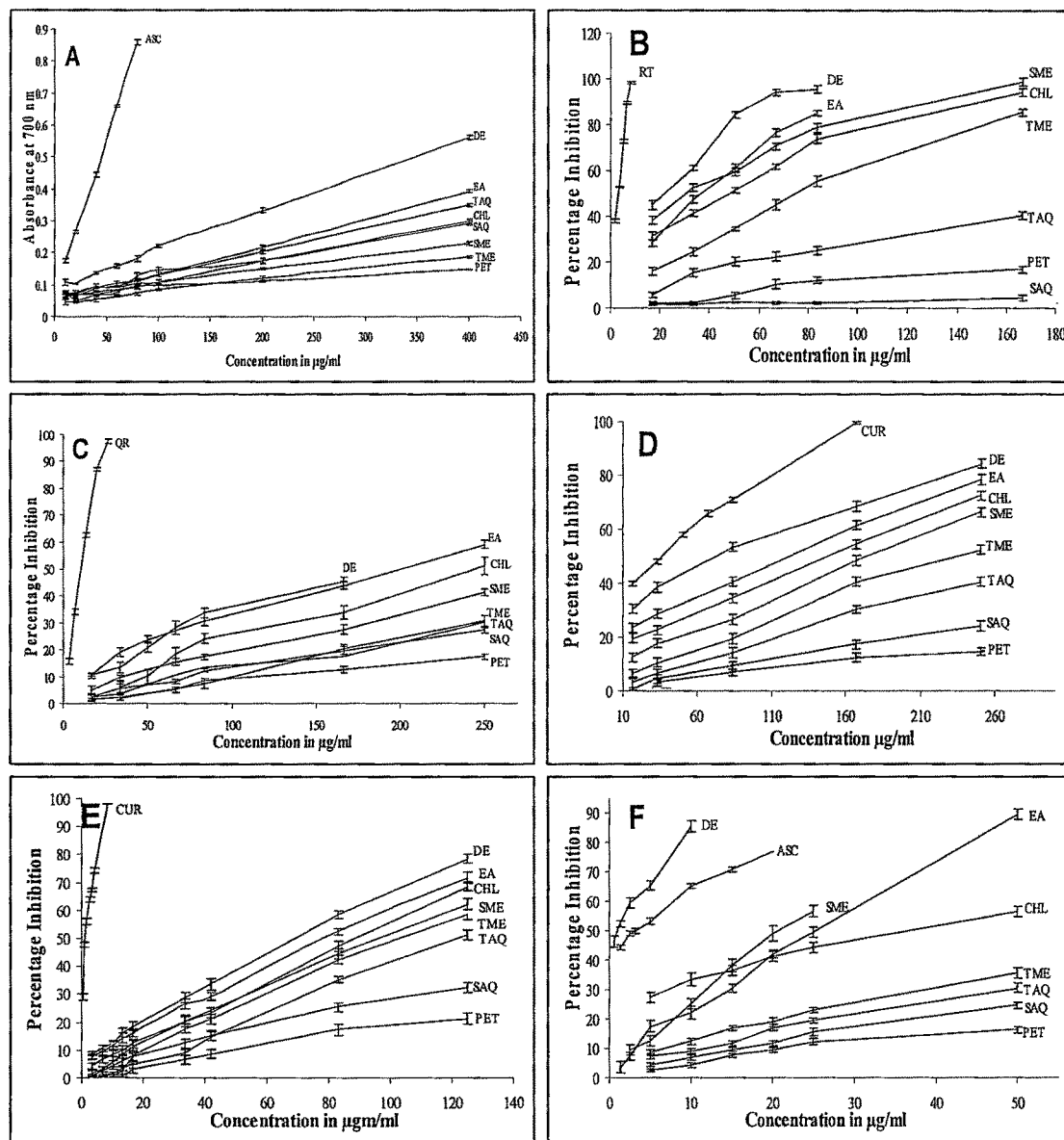


**Fig-3.1 XY- Scatters for *in vitro* studies on different extracts of Ailanthus leaves.**

Results are average of three determinations and shown as Mean  $\pm$  SD. A) Reducing power assay, B) DPPH assay, C) Superoxide radical scavenging assay, D) Nitric oxide radical scavenging assay, E) Hydroxyl radical scavenging assay, F) Inhibition of erythrocytes lysis by extracts.

Abbreviations used in figure: EA-Ethyl acetate extract, TAQ-Total aqueous extract, TME-Total methanol extract, SME- Successive methanol extract, SAQ-Successive aqueous extract, CHL-Chloroform extract, DE-Diethyl ether, PET-Petroleum ether extract, ASC-Ascorbic acid, CUR-Curcumin, RT-Rutin, QUR-Quercetin.

### 3.1.4.1.8 Total phenolic content

Diethyl ether and ethyl acetate extracts showed higher concentration of phenolics with 6.89 and 5.6% w/w, respectively (Fig-3.2). Gallic acid was used as a standard for the calibration.

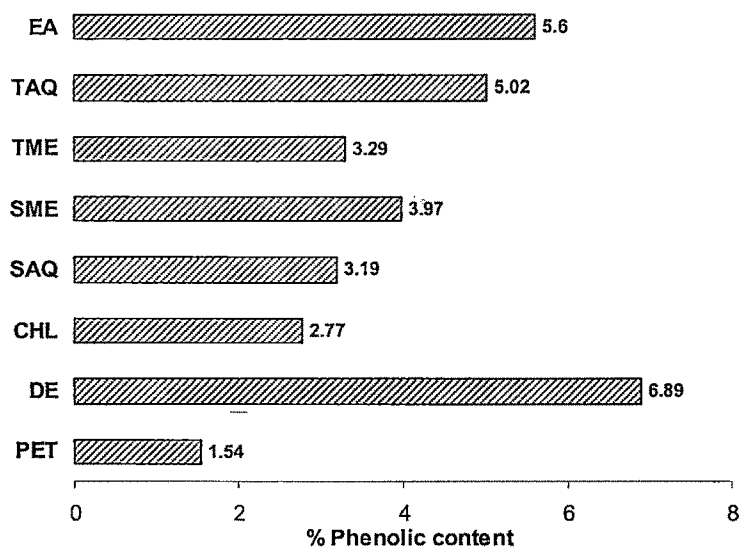


**Fig-3.2 Total phenolic content in successive and total extracts of Ailanthus leaves.**

Abbreviations used in figure: EA-Ethyl acetate extract, TAQ-Total aqueous extract, TME-Total methanol extract, SME- Successive methanol extract, SAQ-Successive aqueous extract, CHL-Chloroform extract, DE-Diethyl ether, PET-Petroleum ether extract.

### 3.1.4.2 Toxicity studies

Chloroform (AECL), ethyl acetate (AEEA), diethyl ether (AEDT) and successive methanol extract (AEME), did not show any mortality at a single oral dose of 2000mg/kg body weight. Histopathological examination of the visceral organs did not show any signs of necrosis or damage. Extracts did not affect the normal architect of liver, heart and kidney. AEDT and AECL treated mice showed increased body weight. No signs of reactions like tremors, convulsions, salivation, and diarrhoea were observed. Safe dose 200mg/kg body weight was used for further in vivo studies (Table-1.4).

**Table-1.4 Effect of leaf extracts on body weight of mice under toxicity studies**

<b>Extracts</b>	<b>1<sup>st</sup> Day</b>	<b>8<sup>th</sup> Day</b>	<b>14<sup>th</sup> day</b>
AEDT	33.33±2.35	40±7.07	41.66±4.71
AECHL	33.33±2.35	36.6±2.35	38.33±2.35
AEEA	33.33±2.35	35.0±7.07	36.66±4.71
AEME	35.0±4.08	36.66±8.49	36.66±8.49

Values shown as Mean ± SD, (n=3)

### 3.1.4.3 In-vivo antioxidant activity

AEDT, AEEA, AECL and AEME from Ailanthus leaves were screened for in-vivo antioxidant activity using isoproterenol (ISO) induced myocardial infarction (MI) and liver damage in rats. Results are shown in (Table-1.5 & 1.6, Fig-3.3 & 3.4)

**Table-1.5 Effect of different extracts of Ailanthus leaves on endogenous antioxidant enzymes.**

Groups	SOD	CAT	GSH	LPO
CONTROL	18.29±1.71	798.76±33.63	14.95±0.67	1.38±0.13
ISO	10.24±0.78*	368.11±33.33***	11.87±0.38**	4.59±0.22***
AEEA	23.8±6.3 <sup>ns</sup>	818.52±62.66 <sup>ns</sup>	25.21±0.47***	1.99±0.07 <sup>ns</sup>
AEEA+ISO	20.77±1.52###	788.04±51.14###	23.61±0.45###	2.25±0.24###
AEDT	24.43±1.87 <sup>ns</sup>	776.53±37.21 <sup>ns</sup>	20.53±0.8***	1.98±0.21 <sup>ns</sup>
AEDT+ISO	22.45±1.33###	766.71±69.53###	17.47±0.34###	2.49±0.23###
AECL	17.1±1.16 <sup>ns</sup>	738.82±72.16 <sup>ns</sup>	20.63±0.59***	3.72±0.18***
AECL+ISO	15.29±1.43 <sup>ns</sup>	671.9±45.46#	17.14±0.49###	13.43±0.44###
AEME	13.62±2.31 <sup>ns</sup>	780.86±77.81 <sup>ns</sup>	18.77±0.77***	1.52±0.09 <sup>ns</sup>
AEME+ISO	7.78±1.16 <sup>ns</sup>	421.04±48.35 <sup>ns</sup>	13.64±0.37 <sup>ns</sup>	5.38±0.41 <sup>ns</sup>

Statistical analysis was done by using ANOVA

Post test applied: Tukey-Kramer multiple comparison Test

Values are expressed as mean ± SEM.

\*p<0.05; \*\*p<0.01; \*\*\*p<0.001; <sup>ns</sup>p>0.05 = non significant, (n=6)

ISO treated group and extract alone pretreated groups were compared with control group (\*Compared with control group).

Extract pretreated group injected with ISO were compared with ISO group (#compared with ISO treated group).

**Table-1.6 Effect of different extracts of Ailanthus leaves on cardiac and liver serum marker enzymes**

Groups	CKMB	LDH	SGPT	SGOT	ALKP	Uric acid
CON	585.87±41.58	1417.3±63.91	60.66±1.45	131±11.51	312.5±21.11	0.99±0.05
ISO	850.86±31.89***	1877.8±42.94***	60.66±0.88 <sup>ns</sup>	183±7.08***	475±22.58***	1.55±0.06***
AEEA	607.12±31.84 <sup>ns</sup>	1426.3±55.53 <sup>ns</sup>	61.2±1.45 <sup>ns</sup>	126.98±3.35 <sup>ns</sup>	322.08±30.25 <sup>ns</sup>	0.6±0.02*
AEEA+ISO	643.03±49.04#	1453.8±58.74##	64.33±0.44 <sup>ns</sup>	138±5.29##	328.58±21.88#	1.03±0.1##
AEDT	1314.4±42.57***	1859±57.37***	63.7±2.04 <sup>ns</sup>	133.44±2.62 <sup>ns</sup>	398.27±22.6 <sup>ns</sup>	0.55±.04**
AEDT+ISO	1562.7±43.34##	3472.3±89.52##	61.08±1.21 <sup>ns</sup>	156±6.38 <sup>ns</sup>	523±23.5 <sup>ns</sup>	0.86±0.04###
AECL	537.66±3.15 <sup>ns</sup>	829.75±26.38***	74.2±1.45***	145.42±2.91 <sup>ns</sup>	328.83±24.65 <sup>ns</sup>	1.51±0.01 <sup>ns</sup>
AECL+ISO	575.27±39.26##	1457±78.63##	75.33±1.01###	157.33±2.77 <sup>ns</sup>	350.67±23.38#	1.94±0.04#
AEME	669.25±50.75 <sup>ns</sup>	1478.7±42.58 <sup>ns</sup>	82.95±0.29***	136.52±3.69 <sup>ns</sup>	324.67±16.65 <sup>ns</sup>	1.8±0.02***
AEME+ISO	539.33±42.96##	1872±40.66 <sup>ns</sup>	78.66±1.74###	174.33±10.66 <sup>ns</sup>	349.25±16.89#	2.39±0.16##

Statistical analysis was done by using ANOVA

Post test applied: Tukey-Kramer multiple comparison Test

Values are expressed as mean ± SEM.

\*p<0.05; \*\*p<0.01; \*\*\*p<0.001; <sup>ns</sup>p>0.05 = non significant, (n=6)

ISO treated group and extract alone pretreated groups were compared with control group (\*Compared with control group).

Extract pretreated group injected with ISO were compared with ISO group (#compared with ISO treated group).

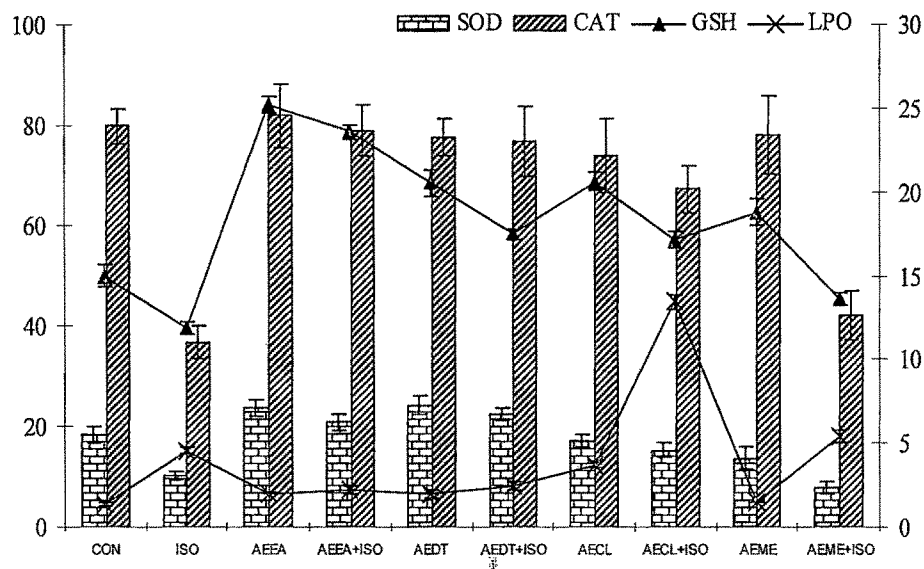


**Fig-3.3** Effect of Ailanthus extracts on endogenous antioxidant enzymes in ISO induced myocardial infarction.

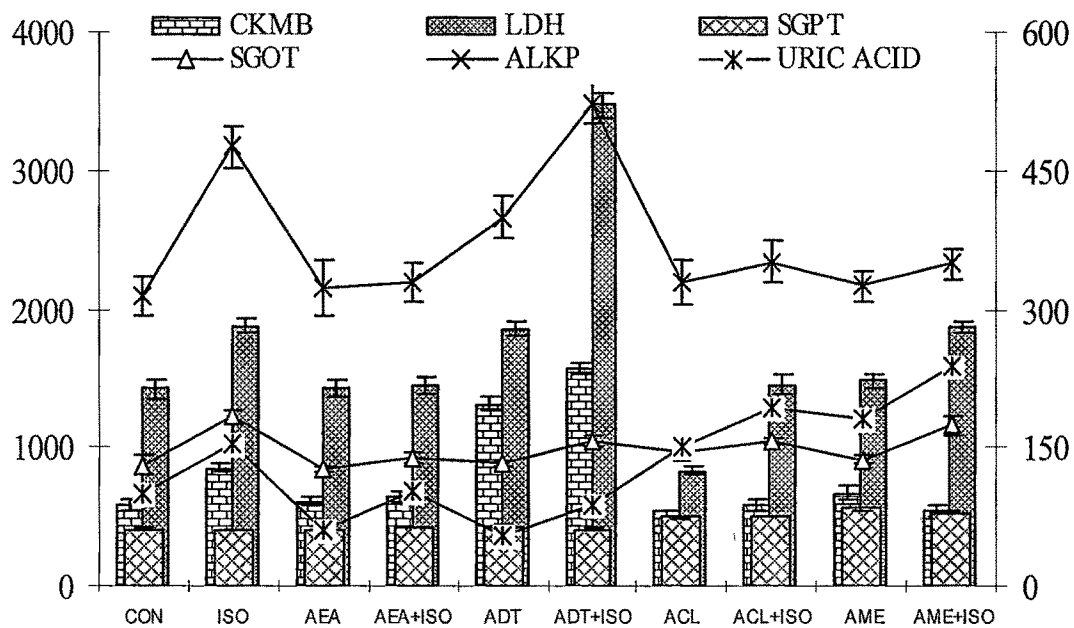


**Fig-3.4** Effect of Ailanthus extracts on serum cardiac and liver marker enzymes.

#### **3.1.4.3.1 Effect on Body weight**

No significant variation in body weight was observed, except AEME alone pretreated rats showed significant increase in body weight on 17<sup>th</sup> day when compared with the 1<sup>st</sup> day weight. (Table-1.7, Fig-3.5)

#### **3.1.4.3.2 Effect on Heart weight/ Body weight ratio**

ISO group showed increase in Heart/body weight ratio ( $p < 0.01$ ) compared to control group. AEDT pretreated group injected with ISO showed significant reduction in the ratio compared to ISO group ( $p < 0.05$ ), while AECHL, AEME, AEEA pretreated group showed no significant reduction in ISO affected ratio compared to ISO group.

AEDT and AECHL alone pretreated group show increase in ratio ( $p > 0.05$ ) while AEME and AEEA alone pretreated groups did not show any change when compared with control group (Fig-3.6)

#### **3.1.4.3.3 Histopathological studies**

Microscopic examination of ISO treated rats showed myocardial necrosis foci intercalated among normal muscle fibers. In the necrosis foci there were lymphocytic exudates, atrophy of the remaining normal muscle and also elongation, undulation of the fibers and formation of contractile band lesions characteristic of the pre-infarction stage.

The rats pretreated with ethyl acetate extracts found to reverse these changes. In the present study, chloroform and ethyl acetate extract of Ailanthus leaves were found to possess significant antioxidant activity and provides significant protection against ISO induced myocardial infarction, compared to other extracts. (Fig-3.7)

Table-1.7 Effect of Ailanthus extracts on weight of rats during treatment.

Day	Animal Weights (Gms)										
	CON	ISO	AEAA	AEAA+ISO	AEDT	AEDT+ISO	AEME	AEME+ISO	AECL	AECL+ISO	
1st	343.33±8.72	313.33±3.6	298.33±7.9	303.33±5.46	300±7.5	308.33±8.33	303.33±3	313.33±13.86	303.33±7.9	323.33±6.5	
8th	333.33±11.1	323.33±3.6	291.67±8.3	295±6.29	298.33±6.6	313.33±5.83	305±3.81	313.33±11.57	301.67±6	326.67±5.06	
15 <sup>th</sup>	343.33±7.37	330±5.2	295±7.63	301.67±5.83	305±5.77	315±6.29	315±5.2	321.67±13.71	298.33±5.4	326.67±5.06	
17 <sup>th</sup>	353.33±4.94	328.33±6.5	300±8.78	301.67±7.12	311.67±6	320±6.61	325±.2**	308.33±10.24	305±6.61	323.33±4.41	

Statistical analysis was done by using ANOVA

Post test applied: Dunnett multiple comparisons test.

Values are expressed as mean ± SEM.

\*p<0.05; \*\*p<0.01; \*\*\*p<0.001; <sup>ns</sup>p>0.05 = non significant, (n=6)

\* Compared with first day weight.

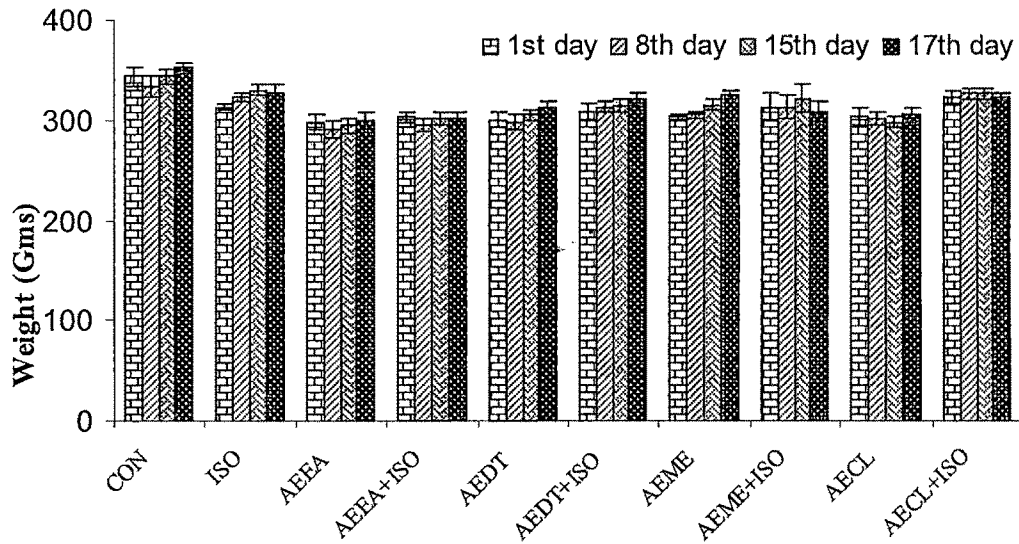


**Fig-3.5 Effect of Ailanthus extracts on body weight of rats.**

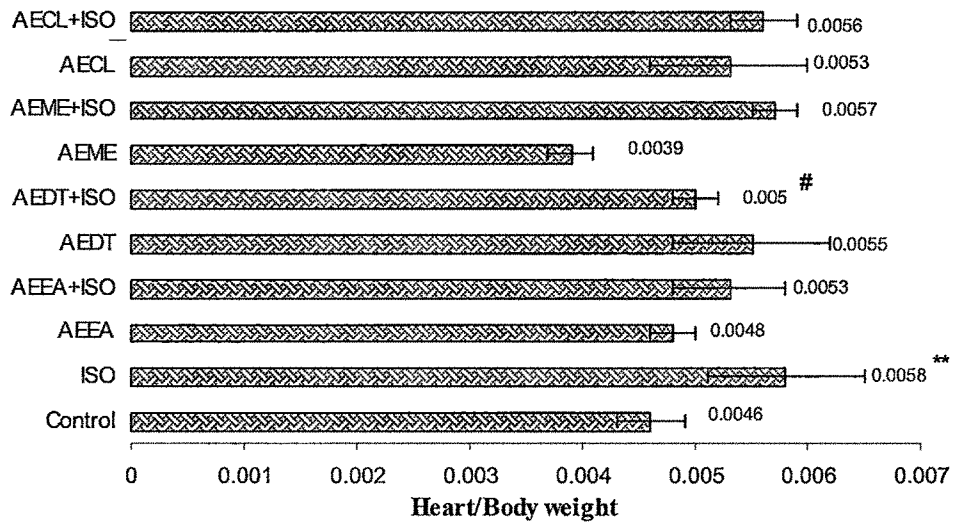


**Fig-3.6 Effect of Ailanthus extracts on Heart weight/body weight ratio.**

Statistical analysis was done by using ANOVA  
 Post test: Tukey-Kramer multiple comparison Test  
 Values are expressed as mean ± SEM.  
 \*p<0.05; \*\*p<0.01; \*\*\*p<0.001; nsp>0.05 = non significant, (n=6)  
 #compared with ISO treated group  
 \*Compared with normal group

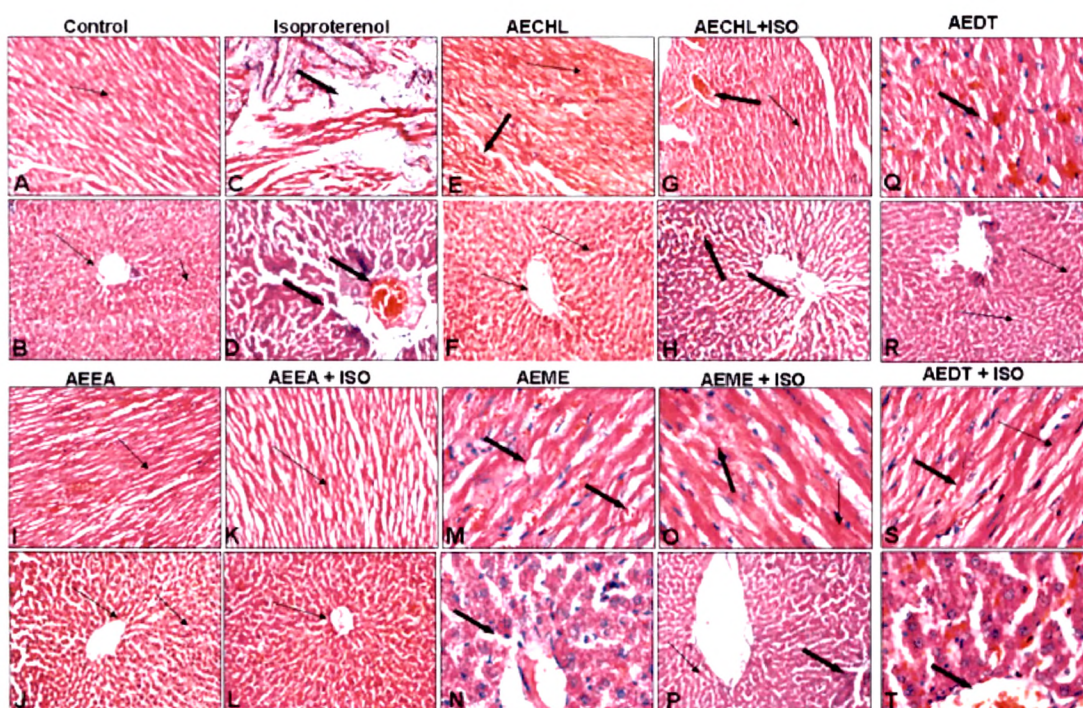


**Fig-3.7 Histopathology of heart and liver showing effect of Ailanthus leaves extracts in ISO induced myocardial and liver damage.**

In the present study ISO treated groups showed significant reduction in the endogenous antioxidant enzyme levels of SOD, CAT, and GSH with increased LPO. ISO also increased levels of serum cardiac and liver marker enzymes like CKMB, LDH, GOT, ALKP and uric acid without any change in GPT level, when compared with the control group.

Treatment with AEEA and AEDT was found to reverse these ISO induced changes, confirmed by significant increase in the levels of endogenous antioxidant enzymes. Further AEEA showed pronounced effect by significantly decreasing the ISO elevated levels of cardiac and liver marker enzymes along with uric acid and at the same time AEEA alone pretreated group did not showed any significant change in endogenous antioxidant and LPO levels and show significant increase in the GSH level when compared with control group. While AEDT significantly increases the CKMB, LDH level with non significant

change in liver marker enzymes and just manage to reduce the serum uric acid level, when compared with ISO group. Even AEDT alone pretreated group showed significant increased in CKMB, LDH level with non significant increase in serum GOT, GPT and ALKP level, and just manage to reduce the uric acid level significantly. Thus AEDT failed to reverse the ISO induced cardiac and liver damage even after having significant antioxidant property.

When compared with ISO group, AECL treated group was found to reverse the ISO affected levels of endogenous antioxidant enzymes except SOD with significant increase in LPO level, while AEME pretreated group did not showed any significant change in ISO affected enzymes and LPO level when compared with ISO group. Both AECL and AEME alone pretreated groups did not show any significant change in these levels compared to control group.

AEEA was found to protect the cardiovascular and hepatic system by increasing the level of endogenous antioxidant enzymes. The result provides a strong support for the use of this plant as cardiac and liver tonic. This may also further supported by the presence of flavonoids like apigenin, kaempferol, luteoline and quercetin in leaves. All these flavonoids are present in glucoside form and are already reported as antioxidant. HPTLC and spectrofluorometric analysis showed high concentration of apigenin and quercetin in the ethyl acetate fraction. Thus, the data support potential of ethyl acetate extract of *Ailanthus* leaves for antioxidant action.

### 3.1.5 Evaluation of antioxidant activity of ethyl acetate extract of Ailanthus leaves (AEEA) using Cardiac cell line-H9c2

#### 3.1.5.1 Percentage cell viability (H9c2)

The effect of AEEA on viability of rat myocardial cell line H9c2 was done by incubation of cells with various concentrations of AEEA for a different time interval and the viability of cells was then determined. (Table-1.8, Fig-3.8)

AEEA (2-50 µg/ml) after 3hrs of incubation did not show any significant change in %- cell viability, but at 100µg/ml, 11.68% decrease was observed in cell viability as compared to that of control.

AEEA at the concentration range of 2-100µg/ml, after 6hrs of incubation showed 86.57 to 56.85% of cell viability, while after 20hrs 95.53 to 8.13%.

The results indicate that AEEA showed its effect in concentration and time dependent manner. As both the concentration and time increased cell viability was found to be decreased. The results obtained for AEEA provides a lead for dose fixation for further studies carried out stated below.

**Table-1.8 Effect of AEEA from Ailanthus leaves on % - viability of H9c2 cells**

<b>AEEA (µg/ml)</b>	<b>3 Hr</b>	<b>9 Hr</b>	<b>20 Hr</b>
Control	100±2.99	100±1.14	100±4.72
2	98.2±2.09	86.57±2.28	95.53±2.62
5	100.59±0.59	86.28±4.28	97.9±1.83
10	104.19±3.59	87.71±1.14	100.52±0.26
15	106.99±4.35	89.69±4.34	90.81±1.57
20	109.58±4.19	95.14±3.42	38.05±2.09
50	100±2.09	83.14±8.22	15.74±3.14
100	88.32±2.09	56.85±3.71	8.13±0.52

Values are expressed as mean ± SD of % cell viability (average of three determinations)

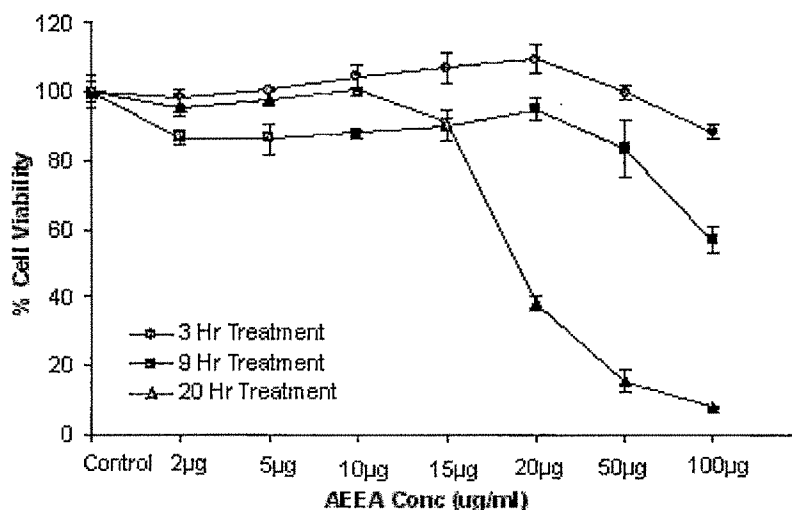


**Fig-3.8 Effect of various concentration of AEEA on %- viability of H9c2 cells at different time interval**

### **3.1.5.2 Effect of AEEA from *Ailanthus* leaves on H<sub>2</sub>O<sub>2</sub> induced stress in H9c2 cells**

H9c2 cells after incubation for 3hrs with AEEA in the concentration range of 1 to 50µg/ml, when challenged with H<sub>2</sub>O<sub>2</sub> showed 32.36, 34.42, 40.74, 51.63, 59.69, 45.96, and 21.35% of cell viability, when compared with only H<sub>2</sub>O<sub>2</sub> treated cells with 21.13% of cell viability. AEEA after 6hrs of incubation showed 33.95, 34.65, 50.93, 50.93, 59.3, 52.55, and 26.04% of cell viability in the concentration rang of 1 to 50µg/ml, when compared with H<sub>2</sub>O<sub>2</sub> control (27.2%) while after 12 hrs incubation AEEA (1-50µg /ml) showed 32.26, 34.64, 26.32, 29.56, 30.48, 28.17 and 12.7% of cell viability when compared to only H<sub>2</sub>O<sub>2</sub> treated cells with 29.33% of cell viability. AEEA was found to reverse the H<sub>2</sub>O<sub>2</sub> (35µM) induce stress in H9c2 cells. (Table-1.9, Fig-3.9)

The result suggested that AEEA reverse the H<sub>2</sub>O<sub>2</sub> induced stress in H9c2 cells in a concentration and time dependent manner. AEEA showed significant protection upto 6hrs which is same as that exhibited by the known antioxidants. The results also optimized the dose range of AEEA to be used for further studies carried out.

**Table-1.9 Effect of pretreatment of AEEA on H<sub>2</sub>O<sub>2</sub> affected viability of H9c2 cells**

<b>AEEA (<math>\mu\text{g/ml}</math>)</b>	<b>3 Hr</b>	<b>6 Hr</b>	<b>12 Hr</b>
Control	100 $\pm$ 5.01	100 $\pm$ 2.55	100 $\pm$ 4.61
H <sub>2</sub> O <sub>2</sub>	21.13 $\pm$ 2.61	27.2 $\pm$ 4.65	29.33 $\pm$ 1.84
1	32.36 $\pm$ 11.54	33.95 $\pm$ 2.32	32.26 $\pm$ 2.30
2	34.42 $\pm$ 6.10	34.65 $\pm$ 6.97	34.64 $\pm$ 6.92
5	40.74 $\pm$ 3.70	50.93 $\pm$ 9.30	26.32 $\pm$ 2.30
10	51.63 $\pm$ 3.48	50.93 $\pm$ 6.97	29.56 $\pm$ 2.30
15	59.69 $\pm$ 8.93	59.3 $\pm$ 9.30	30.48 $\pm$ 2.30
20	45.96 $\pm$ 3.26	52.55 $\pm$ 6.97	28.17 $\pm$ 1.61
50	21.35 $\pm$ 2.83	26.04 $\pm$ 4.65	12.7 $\pm$ 2.07

Values are expressed as mean  $\pm$  SD of % cell viability (average of three determinations)

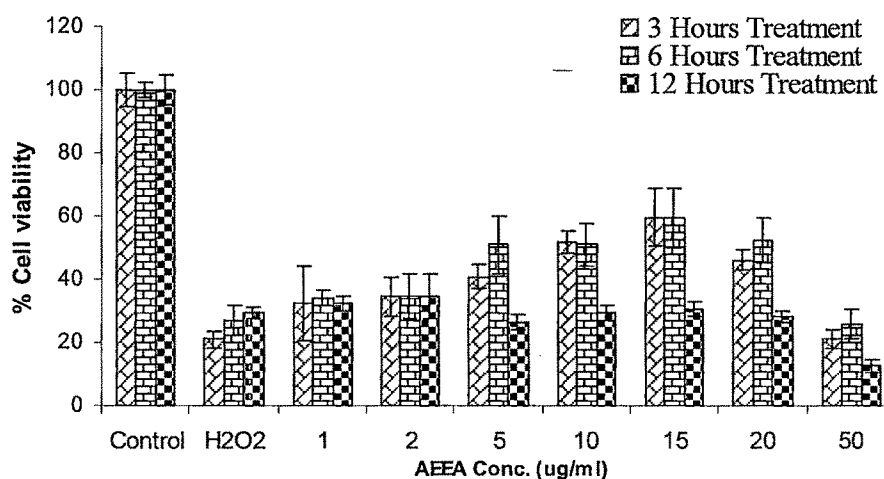


**Fig-3.9 Effect of pretreatment of AEEA on H<sub>2</sub>O<sub>2</sub> affected viability of H9c2 cells**

### **3.1.5.3 Effect of AEEA pretreatment on H<sub>2</sub>O<sub>2</sub> induced increase in intracellular ROS level**

It is already established that H<sub>2</sub>O<sub>2</sub> causes generation of ROS. H9c2 cells, pretreated with AEEA for 6hrs were exposed to 35μM of H<sub>2</sub>O<sub>2</sub>, and ROS was assessed by flow cytometric analysis after loading the cells with the ROS-sensitive dye 2', 7'-Dichlorofluorescein Diacetate (DCFH-DA). An increase in fluorescence intensity was observed in the H<sub>2</sub>O<sub>2</sub>-treated cells from 4.69% to 37.56% (Fig- 3.10A & B) The effect of this phenomenon was attenuated by AEEA pretreatment. H9c2 cells when treated with 5-15μg/ml of AEEA caused a decrease in the mean fluorescence intensity from 37.56% to 9.07% (Fig-3.10B, C, D & E) whereas at higher concentration (20μg/ml) an increase in fluorescence intensity was observed upto 21.86% this may be due to the prooxidant effect of AEEA (Fig-3.10F).

The H<sub>2</sub>O<sub>2</sub> treated cells were treated under the same conditions and subjected to confocal microscopy, a dramatic increase in fluorescence intensity was observed due to generation of ROS, which was reversed by pretreatment with different concentration of AEEA (5-20μg/ml) (Fig-3.11B, C, D, E & F).

Thus AEEA pretreatment showed concentration dependent protection against H<sub>2</sub>O<sub>2</sub> induced ROS formation in H9c2 cells

### **3.1.5.4 Effect of AEEA on xanthine-xanthine oxidase induced increase in intracellular ROS level**

The H9c2 cells loaded with ROS sensitive dye DHE and treated with xanthine-xanthine oxidase (X+XO) were assessed on FACs showed an increased fluorescence intensity of the dye from 4.36 to 60.40% indicating the generation of ROS (Fig- 3.10G to 3.10H). This effect was reversed when the cells were pretreated with different concentration of AEEA (5-15μg/ml), which showed decrease in fluorescence intensity from 60.40 to 4.50% (Fig- 3.10H to 3.10K).

When the H9c2 cells treated with xanthine-xanthine oxidase were examined using confocal microscopy showed enhancement of generation of O<sub>2</sub><sup>•-</sup> (Fig- 3.11G & 3.11H). The treatment of AEEA (5-15μg/ml) was found to reverse the above change and also showed a concentration dependent effect in neutralizing the X+XO induced ROS formation in H9c2 cells (Fig- 3.11H to 3.11L).

### **3.1.5.5 Effects of AEEA on H<sub>2</sub>O<sub>2</sub> affected mitochondrial membrane potential ( $\Delta\Psi_m$ ) in H9c2 cells.**

Mitochondria is the limiting factor in the apoptosis pathway in many experimental systems. Disruption of mitochondrial membrane potential ( $\Delta\Psi_m$ ) is established as indicator of mitochondrial damage in the progression of apoptosis. Thus loss of membrane potential is a limiting factor in the apoptotic pathway. A mitochondrial voltage dependent dye 3, 3'-dihexyloxacarbocyanine iodide (DiOC<sub>6</sub>), is employed to observe the changes in membrane potential. The intensity of DiOC<sub>6</sub> fluorescence was significantly reduced after exposing the cells to H<sub>2</sub>O<sub>2</sub> (35 $\mu$ M) for 2hrs when observed in confocal microscopy. (Fig-3.11M & 3.11N). Pretreatment with AEEA (5-15 $\mu$ g/ml) for 6hrs increased the fluorescence intensity of H<sub>2</sub>O<sub>2</sub> treated cells (Fig-3.11O-3.11Q). Further increase in AEEA concentration (20 $\mu$ g/ml) showed decrease fluorescence intensity which may be due to prooxidant activity of AEEA (Fig- 3.11R)

Mitochondrial membrane potential is also measured by tetramethyl rhodamine (TMRE). TMRE is a cell permeable cationic dye that has a strong fluorescent signal and exhibits low membrane potential independent binding. H<sub>2</sub>O<sub>2</sub> reduced the membrane potential in H9c2 cells marked with increased fluorescence intensity from 10.25 to 41.80% when assessed by flow cytometric analysis after loading the cells with the membrane potential sensitive dye TMRE (Fig-3.10M & 3.10N). Pretreatment with various concentration of AEEA (5- 15 $\mu$ g/ml) increased the membrane potential confirmed by decreased fluorescence intensity from 41.80 to 11.05% (Fig-3.10M-3.10O), but at higher concentration 20  $\mu$ g/ml, membrane potential gets reduced, which may be due to the prooxidant effect of AEEA (Fig- 3.10R).

Pretreatment of AEEA thus found to increase the H<sub>2</sub>O<sub>2</sub> affected mitochondrial membrane potential ( $\Delta\Psi_m$ ) but at higher concentration this effect gets abolished which may be due its prooxidant AEEA.

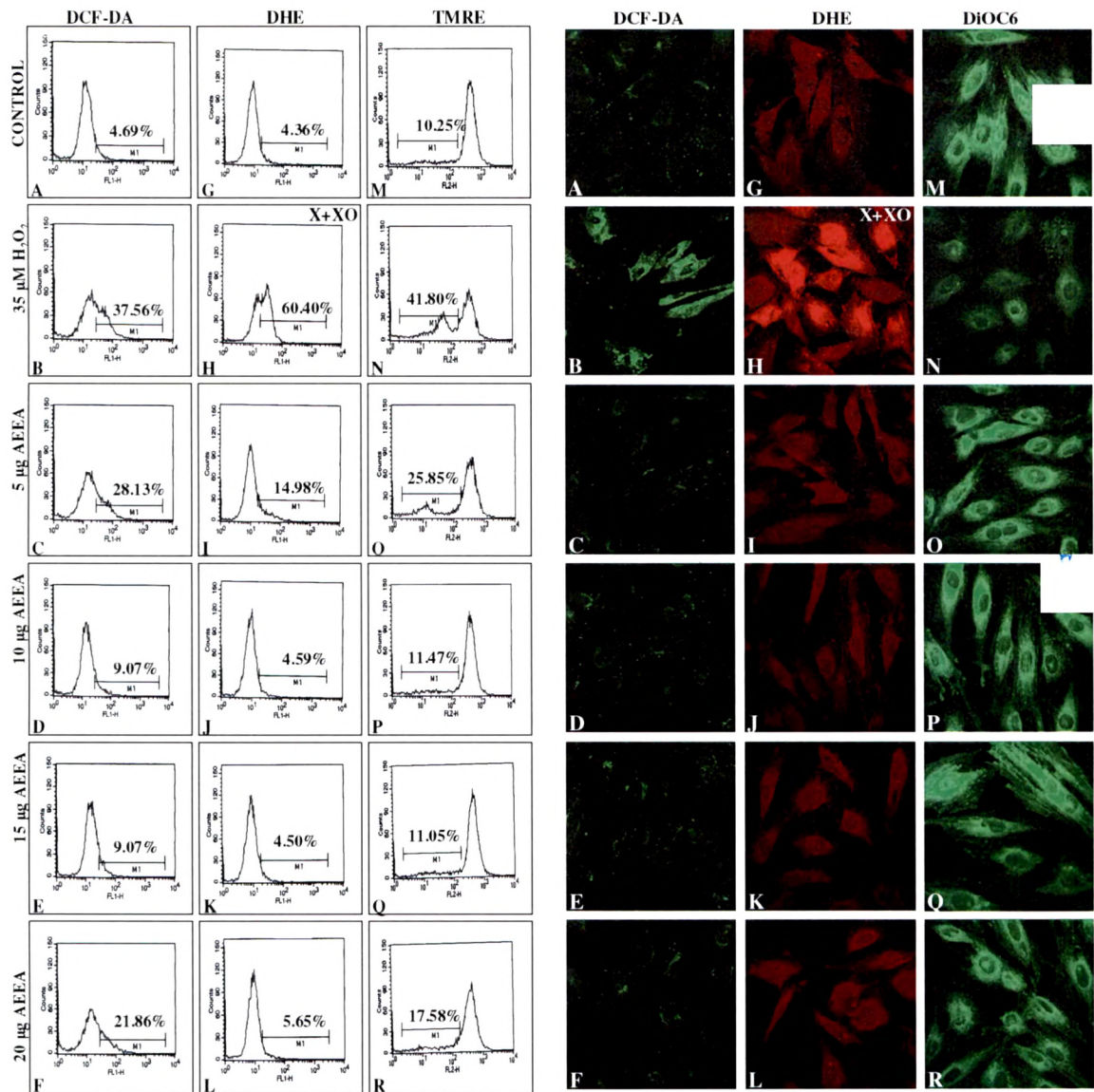


**Fig-3.10 (A-R) Flow activated cytometric analysis of H9c2 cells pretreated with different concentration of AEEA and challenged with H<sub>2</sub>O<sub>2</sub> and Xanthine-xanthine oxidase after loading with different molecular probes.**

**Fig-3.11 (A-R) Confocal images of H9c2 cells loaded with different molecular probes showing the effect of AEEA on H<sub>2</sub>O<sub>2</sub> and Xanthine-xanthine oxidase induced stress.**

### **3.1.6 Chromatographic studies**

TLC fingerprint of ethyl acetate, diethyl ether, chloroform, successive methanol and total methanol were derived in order to develop the standards and to know the compounds present. Quantification of compounds in different bioactive extracts was also done using HPTLC (Fig-3.12)

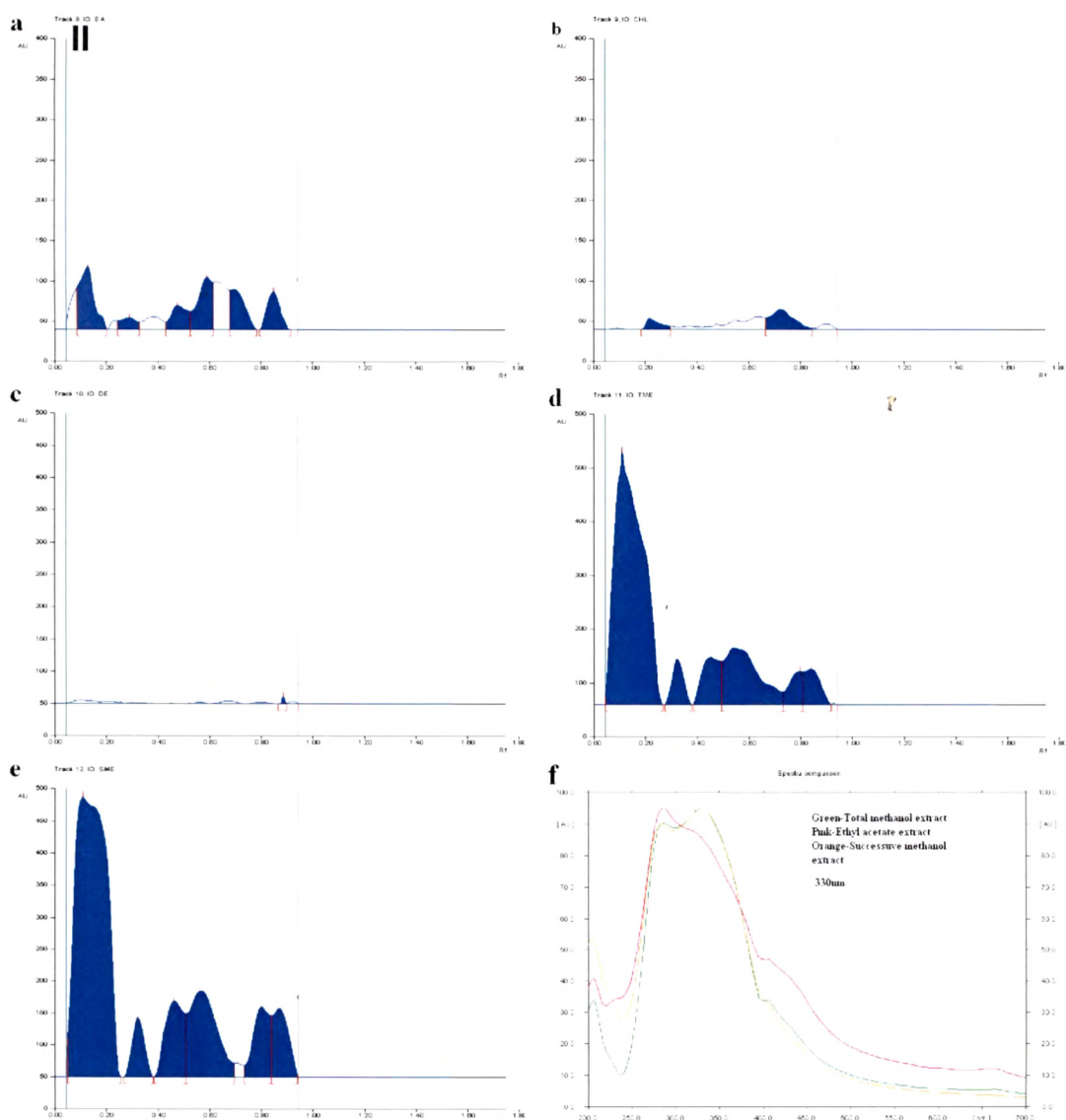
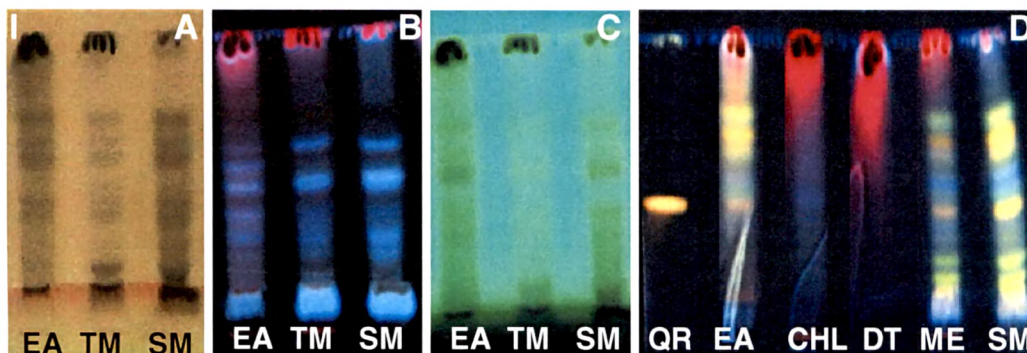


**Fig-3.12-I-TLC showing nature of compounds in different extracts of leaves of *A. excelsa***

**EA**-Ethyl acetate extract, **TM**-Total methanol extract, **SM**-Successive methanolic extract, **QR**-Quercetin-reference standard, **CHL**-Chloroform extract, **DT**-Diethyl ether extract.

Solvent system-Ethyl acetate: Formic acid: Glacial acetic acid: Water, (14.28:1.42:1.42:2.85 v/v).

**Fig-3.12-Plate (IA-ID)**

IA) Treated with ferric chloride, black coloration showed the presence of phenolic compounds.

IB) Compounds visible at 366nm

IC) Compounds visible at 254nm

ID) Extracts showing the presence of quercetin and other phenolics after treatment with natural product reagent, visible at 366nm. Same plate was scanned at 366nm, data shown in (Table-1.10).

**Fig-3.12-II-Chromatogram of different extracts of Ailanthus leaves scanned at 366nm after spraying with NP reagent.**

- a) Ethyl acetate extract,
- b) Chloroform extract
- c) Diethyl ether extract
- d) Total methanol extract
- e) Successive methanol extract
- f) Spectra of quercetin identified in different extracts

**Table-1.10 TLC fingerprinting for different extracts of *A. excelsa* leaves after treatment with NP reagent and scanning at 366nm.**

<i>Ethyl acetate extract</i>			<i>Chloroform extract</i>			<i>Diethyl ether extract</i>			<i>Total methanol</i>			<i>Successive methanol</i>		
Rf	$\lambda_{max}$	Relative % area	Rf	$\lambda_{max}$	Relative % area	Rf	$\lambda_{max}$	Relative % area	Rf	$\lambda_{max}$	Relative % area	Rf	$\lambda_{max}$	Relative % area
0.13	284	27.54	0.22	288	24.54	0.89	316	100	0.11	283	62.10	0.11	279	57.09
0.29	320	5.82	0.72	290	75.46				0.33	337	4.69	0.32	339	4.59
0.48	308	11.67							0.45	331	7.48	0.46	333	8.94
0.58	330	22.82							0.58	330	16.88	0.57	330	15.07
0.70	279	17.52							0.80	321	3.87	0.80	331	7.38
0.85	288	14.62							0.84	323	5.06	0.87	324	6.94

\*Solvent system 1-ethyl acetate: formic acid: glacial acetic acid: water (14.28:1.42:2.85 v/v), treated with Natural product reagent and scanned at 366nm

TLC studies showed the presence of phenolic compounds in different extracts of *A. excelsa* leaves (Fig-3.12-I). TLC plate after treatment with alcoholic ferric chloride solution showed black coloration due to the presence of phenolic compounds (Fig-3.12-IA). Fig-3.12-ID showed the presence of phenolic compounds in successive methanol, ethyl acetate and total methanol extracts after spraying with natural product reagent and also detected the presence of quercetin in ethyl acetate, successive methanol and total methanol extracts of leaves, which was quantified by HPTLC. Chloroform and diethyl ether extracts did not show presence of these compounds (Table-1.10).

**3.1.7 Estimation of quercetin in different extracts of Ailanthus leaves by HPTLC (Table-1.12 Fig-3.14).**

**Table-1.12 Percentage of quercetin in different extracts of Ailanthus leaves.**

Extracts	% - of Quercetin	
	Height	Area
Ethyl acetate extract	0.263	0.219
T. methanol extract	0.259	0.234
Successive methanol extract	0.239	0.24

Highest concentration of quercetin was found in ethyl acetate extract as per height, while as per area it was higher in successive methanol extract. Quercetin was not detected in diethyl ether and chloroform extract.

Track	Vial	Rf	Amount Fraction	Height	X(calc)	Area	X(calc)	Sample ID/ Remark
1	1							not evaluated
2	1	0.58	25.00 ng	11.02		249.27		
3	1	0.58	50.00 ng	32.02		647.24		
4	1	0.58	75.00 ng	50.04		1059.54		
5	1							not evaluated
6	1	0.60	100.00 ng	65.05		1580.65		
7	1							not evaluated
8	2	0.56		33.06	54.30 ng	790.82	66.75 ng	EA
9	2	0.55		30.01	49.66 ng	698.03	56.80 ng	EA
10	3	0.55		23.38	48.87 ng	646.75	51.84 ng	TME
11	4	0.54		26.09	60.10 ng	729.80	59.88 ng	SME
12	3							TME not detected or d

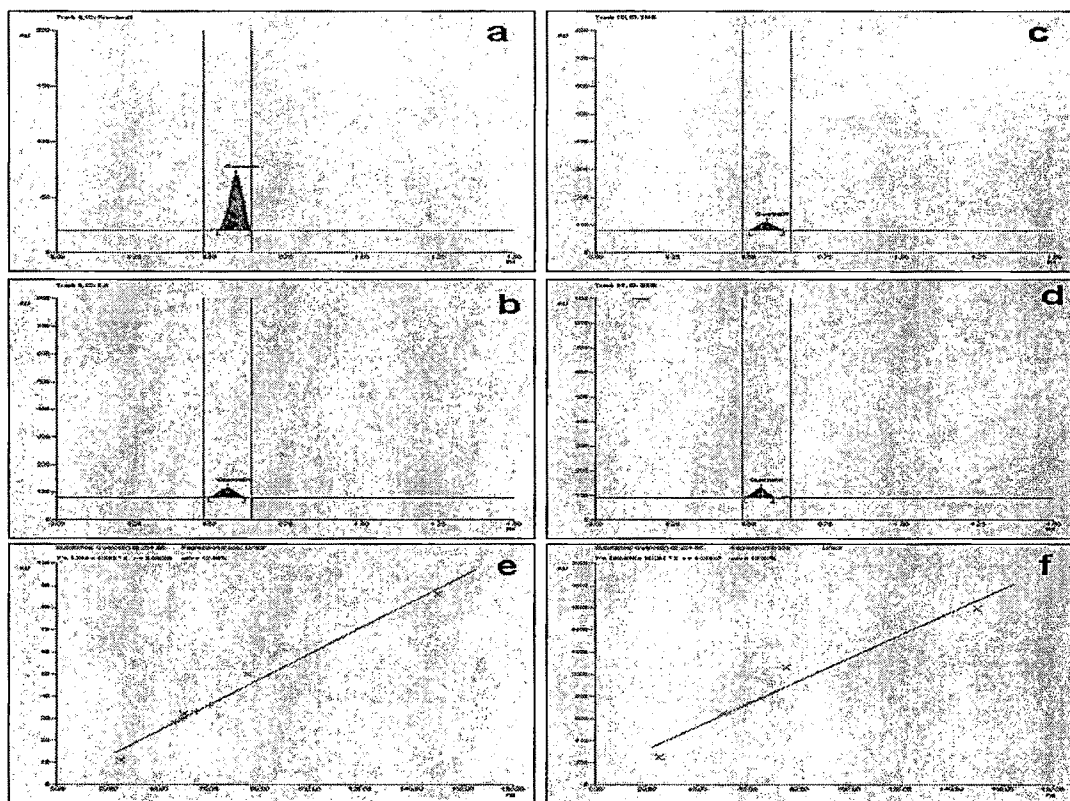


**Fig-3.14 Quantification of quercetin in different extracts of Ailanthus leaves by HPTLC.**

**Table-**Detection & quantification of quercetin in extracts, (a-d)-Chromatogram for standard quercetin and that in extracts, (e-f)-Linearity of standard quercetin as per height and area of peak, Standard level used-(25-250ng)

Solvent system- Ethyl acetate: formic acid: glacial acetic acid: water (14.28:1.42:1.42:2.85 v/v), Scanning wavelength-254nm

**3.1.8 Fluorimetric estimation of apigenin in different extracts of Ailanthus leaves** (Table-1.11, Fig-3.13)

Calibration range for standard apigenin (2.5-25ng/ml)

Excitation wavelength: 333

Emission wavelength: 624

Scale:  $\delta$ - Scale-1

Concentration of extract used (50ng/ml).

**Table-1.11 Fluorimetric estimation of apigenin in different extracts of Ailanthus leaves**

Sr No.	Conc. ng/ml	% Relative Intensity	Conc. ng/ml	% apigenin present
1	T. methanol extract	30.2	9.43	18.86
2	Diethyl ether extract	25.1	6.35	12.7
3	Ethyl acetate extract	38.4	14.38	28.76
4	Chloroform extract	30.2	9.43	18.86
5	S. methanol extract	32.2	10.63	21.6

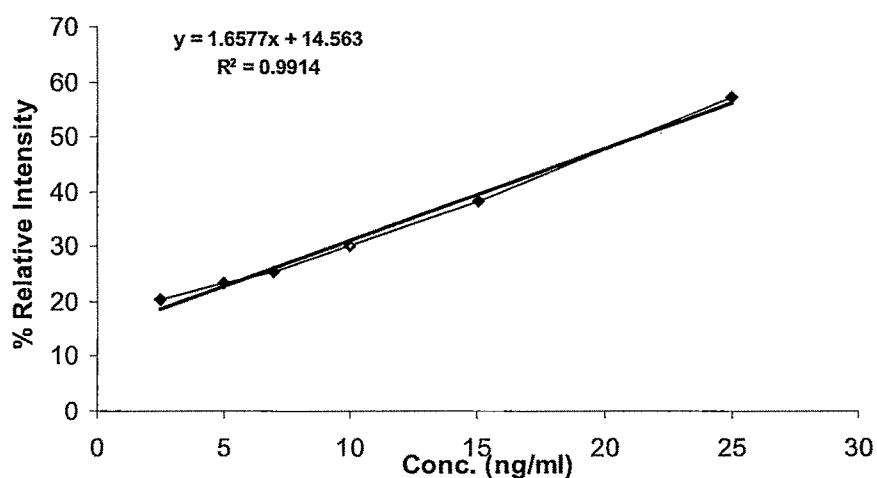


**Fig-3.13 Calibration plot for standard apigenin using spectrofluorimetry**

### **3.1.9 TLC Fingerprinting profile for Ailanthus leaves**

TLC fingerprint profile was developed for ethyl acetate, chloroform and diethyl ether extract of *A. excelsa* leaves the data was recorded (Table-1.13, Fig-3.15). It includes total number of compounds resolved with their respective R<sub>f</sub>, λ<sub>max</sub> and % relative area.

Solvent system- Toluene: Dioxan: Glacial acetic acid (90:25:4v/v)

Spray reagent- DPPH reagent

Scanning wavelength-254, 366 and 520nm

## HPTLC fingerprinting for various extracts of *Ailanthus* leaves

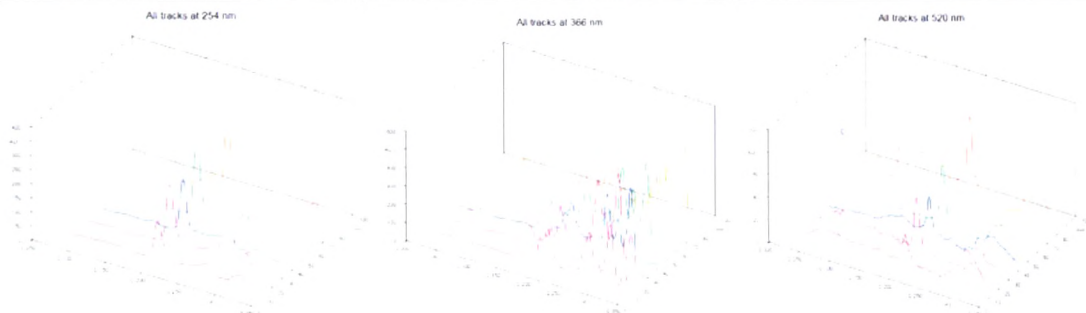
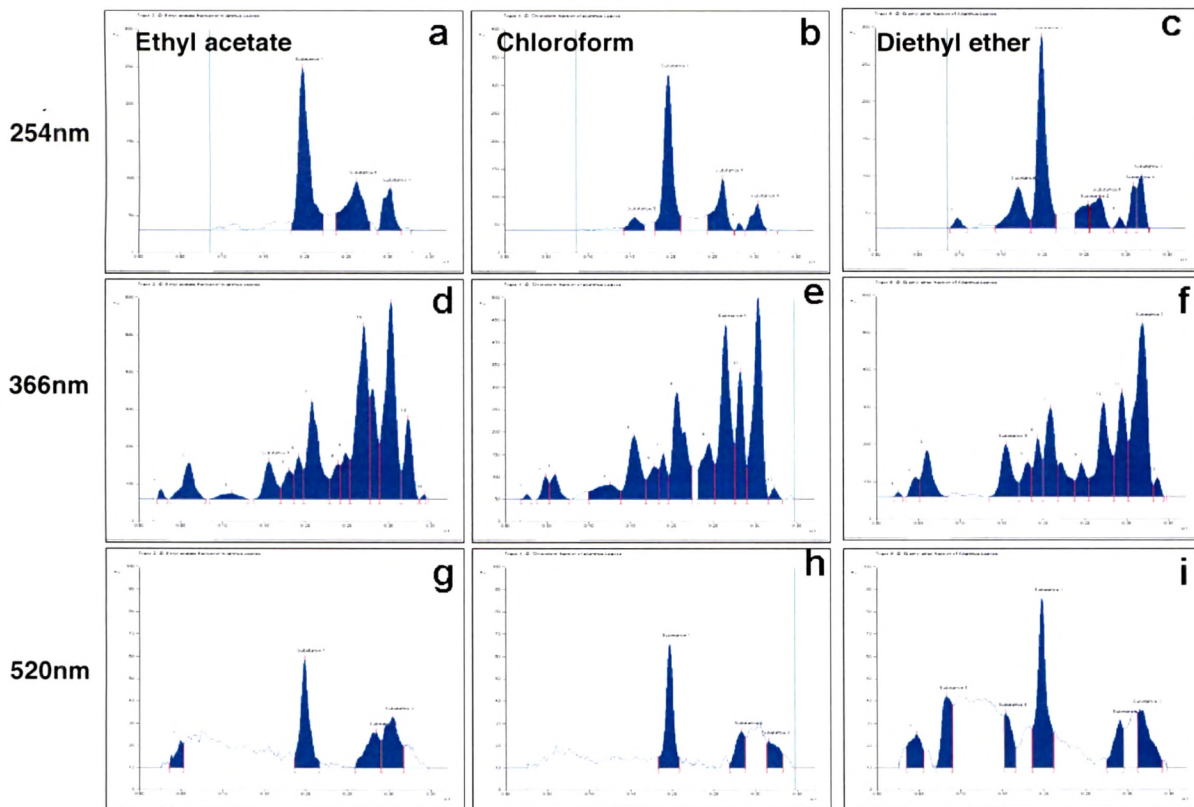
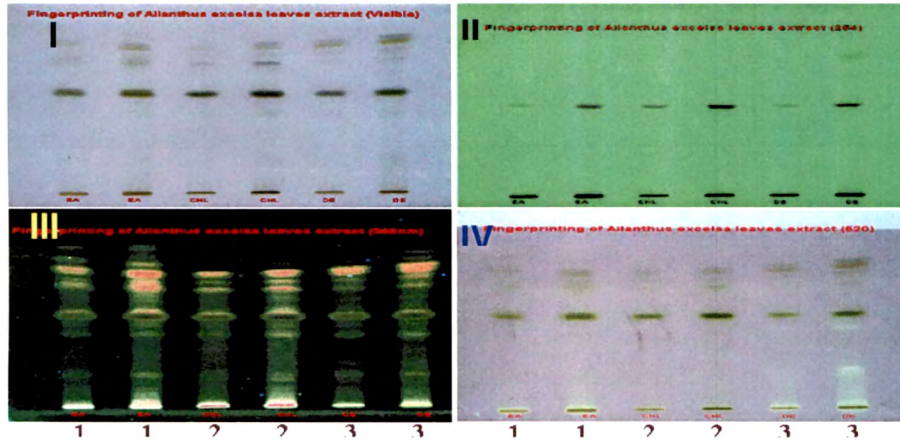


**Fig-3.15 HPTLC fingerprinting for various extracts of Ailanthus leaves**

i) TLC plates I) Visible region II) 254nm, III) 366nm and IV) Sprayed with DPPH reagent (Showing presence of radical scavengers in ethyl acetate and diethyl ether extracts), (Track-1-Ethyl acetate, Track-2-Chloroform extract, Track-3-Diethyl ether extract)

ii) Chromatograms- for ethyl acetate (a, d, g), chloroform (b, e, h) and diethyl ether (c, f, i) extract scanned at 254, 366 and 520nm (after treatment with DPPH reagent in methanol)

iii) 3-D- presentation of the chromatogram at 254, 366 and 520nm

**Table-1.13 TLC fingerprint for ethyl acetate, chloroform and diethyl ether extract of Ailanthus leaves**

<i>Ethyl acetate extract</i>			<i>Chloroform extract</i>			<i>Diethyl ether extract</i>		
Rf	$\lambda_{\max}$	Relative % area	Rf	$\lambda_{\max}$	Relative % area	Rf	$\lambda_{\max}$	Relative % area
<b>Scanning at 254nm</b>								
0.20	405	58.81	0.16	410	6.30	0.10	315	2.05
0.27	414	24.82	0.20	395	59.54	0.17	311	15.66
0.31	407	16.36	0.26	402	22.65	0.20	403	45.98
			0.28	400	1.37	0.25	200	7.17
			0.30	406	10.13	0.27	407	10.03
						0.29	401	1.76
						0.31	443	7.04
						0.32	406	10.32
<b>Scanning at 366nm</b>								
0.03	400	0.51	0.03	402	0.27	0.03	400	0.25
0.06	405	4.70	0.05	407	1.70	0.05	405	1.91
0.11	315	1.14	0.06	405	2.36	0.06	406	5.92
0.16	408	4.67	0.13	401	3.75	0.16	408	7.66
0.18	309	2.93	0.16	410	9.15	0.18	311	3.98
0.19	310	3.54	0.18	311	3.53	0.19	311	5.38
0.21	405	13.2	0.19	310	3.72	0.21	405	10.60
0.24	425	3.14	0.21	406	15.27	0.22	410	4.66
0.25	200	4.03	0.25	200	7.70	0.25	201	3.84
0.27	414	22.2	0.27	414	19.99	0.27	416	14.01
0.28	400	8.09	0.28	400	10.65	0.30	415	12.40
0.30	415	24.2	0.30	415	21.11	0.32	414	27.90
0.32	414	7.31	0.32	413	0.81	0.34	615	1.49
0.34	616	0.17						
<b>Scanning at 520nm</b>								
0.05	405	9.34	0.20	397	58.97	0.05	425	9.66
0.20	414	39.79	0.28	523	21.08	0.08	700	16.34
0.29	670	20.78	0.32	528	19.95	0.15	424	10.26
0.30	415	30.09				0.20	410	36.29
						0.29	670	10.23
						0.32	414	17.22

\*Solvent system- Toluene: Dioxan: Glacial acetic acid (90:25:4v/v), and treated with DPPH reagent and scanned at 520nm.

**TLC fingerprinting of total methanol and successive methanol extracts of Ailanthus leaves**

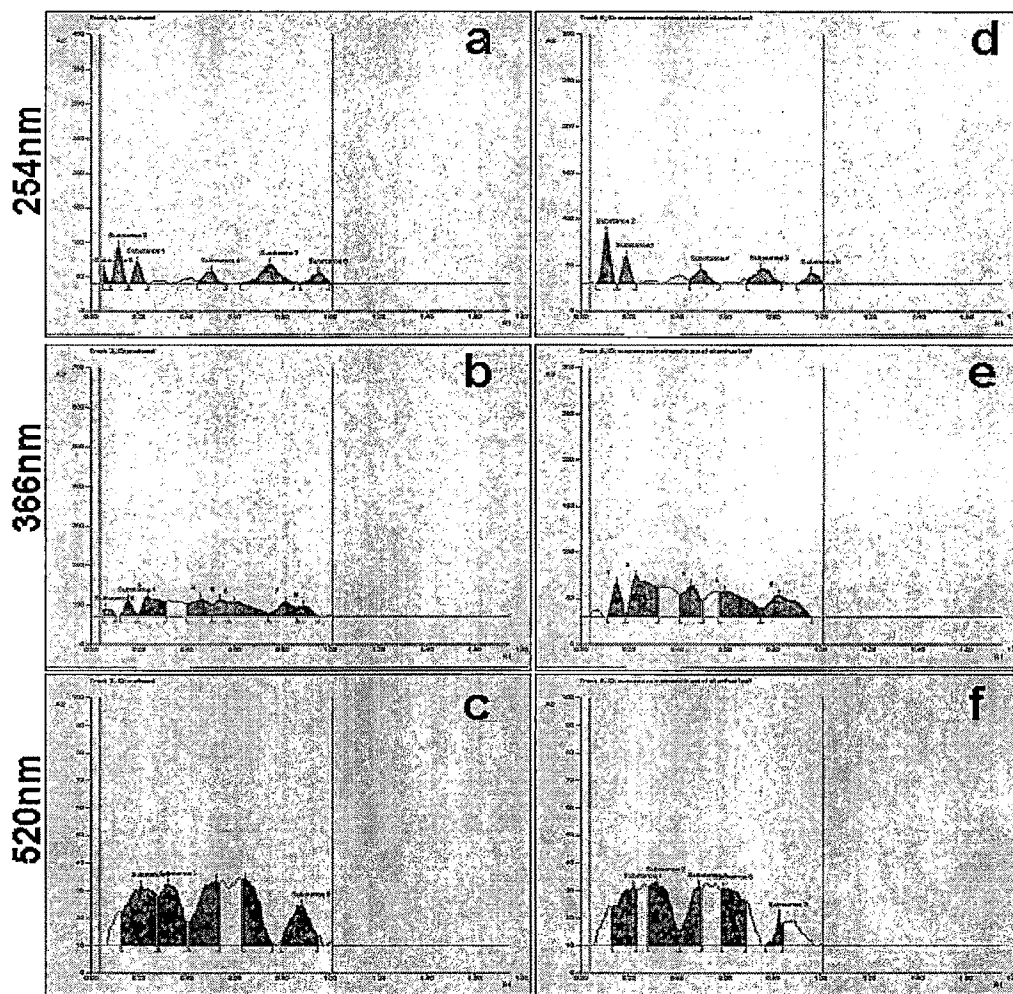
TLC fingerprint profile for total methanol and successive methanol extract of *A. excelsa* leaves was developed and recorded (Table-1.14, Fig-3.16).

Table shows total number of compounds resolved with their respective R<sub>f</sub>, λ<sub>max</sub> and % relative area.

**Table-1.14 TLC fingerprint for Total methanol and successive methanol extracts of Ailanthus leaves**

Total methanol extract			S. methanol extract		
R <sub>f</sub>	λ <sub>max</sub>	Relative % area	R <sub>f</sub>	λ <sub>max</sub>	Relative % area
<b>Scanning at 254nm</b>					
0.06	336	4.13	0.11	343	31.63
0.12	342	23.20	0.19	343	18.11
0.20	343	14.25	0.50	341	16.68
0.51	339	13.45	0.75	325	22.37
0.75	314	31.79	0.96	341	11.22
0.95	343	13.17			
<b>Scanning at 366nm</b>					
0.06	336	3.63	0.15	340	10.05
0.16	342	7.29	0.23	346	29.03
0.23	346	20.83	0.46	350	17.18
0.46	350	17.59	0.60	315	23.38
0.54	340	11.88	0.83	316	20.35
0.60	315	18.83			
0.81	317	12.77			
0.89	316	7.19			
<b>Scanning at 520nm</b>					
0.21	345	25.90	0.22	346	23.96
0.33	318	20.77	0.32	321	29.12
0.53	326	21.95	0.49	345	17.20
0.65	313	17.90	0.60	315	25.36
0.89	316	13.48	0.83	313	4.37

Solvent system- Chloroform: Acetone: Formic acid (75:17: 9v/v), treated with DPPH reagent and scanned at 520nm.



**Fig-3.16 Chromatograms- for total methanol (a, b, c) and successive methanol (d, e, f) extracts, scanned at 254, 366 and 520nm (after treatment with DPPH reagent in methanol)**

These fingerprint data helps in ascertaining the total number of chemical moieties which are common in these extracts and also provides an idea regarding the isolation of bioactive compounds.

Thus above study revealed the antioxidant potential of ethyl acetate extract of *A. excelsa* leaves, where it showed significant radical scavenging effect by various in vitro and ex-vivo methods. AEEA showed high concentration of phenolic content and a significant protection against ISO induced MI without showing any toxic effect. AEEA also showed concentration dependent effect on H9c2 cells where at higher concentration it showed prooxidant effect like most of the well known antioxidants. AEEA prevents the generation of H<sub>2</sub>O<sub>2</sub> and xanthine-xanthine oxidase induced ROS in H9c2 cells and thus showed protective effect. Chromatographic studies showed the presence of phenolics and specifically flavonoids in AEEA, which are known to possess antioxidant activity. Further study is needed to isolate these flavonoids and to study their effect on ROS. Flavonoids like apigenin, kaempferol, luteolin are already reported, further study can identify other flavonoid in leaves. Better results can further be achieved by preparing flavonoids rich fraction from leaves and evaluating its activity, as study the flavonoids were distributed in ethyl acetate, and successive methanol extracts.

Present study showed that, flavonoids in leaves are responsible for the antioxidant effect of *A. excelsa*, by increasing the endogenous antioxidant levels these compounds protects liver and cardiovascular system thus fulfilling the claims made in traditional literature.

## **3.2 Studies on *Ailanthus excelsa* root bark:**

### **3.2.1 Evaluation of Antioxidant activity**

#### **3.2.1.1 *In-vitro* antioxidant activity**

The successive extracts of root bark along with its total methanol and total aqueous extracts were screened for in-vitro antioxidant activity. The results revealed that chloroform, ethyl acetate, benzene and successive methanol extract were more active compared to other extracts. These extracts were screened for ex-vivo studies using human blood erythrocytes lysis mediated by AAPH. The ethyl acetate and successive methanol extract showed significant reduction in erythrocytes lysis compared to chloroform and ethyl acetate extracts.

##### **3.2.1.1.1 Reducing power assay**

Ethyl acetate, chloroform, successive methanol and benzene extracts were found to possess significant reducing power. The extracts exhibited a concentration dependent increase in reducing power. Ethyl acetate and chloroform extract were equally active. Compared with ascorbic acid the reducing powers of these extracts were lesser (Fig-3.17A).

##### **3.2.1.1.2 Scavenging of DPPH radical**

Ethyl acetate, successive methanol, chloroform and benzene extracts showed a concentration dependent antiradical activity by scavenging DPPH radical with an EC<sub>50</sub> value of 66.61, 170.024, 188.69, 225.46µg/ml respectively. Ethyl acetate extract was found to be more potent compared to others. The scavenging effects were lesser compared to reference standard rutin (EC<sub>50</sub>: 2.85 µg/ml) (Fig-3.17B).

##### **3.2.1.1.3 Inhibition of erythrocyte hemolysis**

Ethyl acetate, successive methanol, chloroform and benzene extracts were found to inhibit the hemolysis of erythrocytes with EC<sub>50</sub> values of 0.147, 19.34, 31.97 and 37.27µg/ml respectively. Ethyl acetate extract was found to be more potent than ascorbic acid (EC<sub>50</sub>: 3.07µg/ml). (Fig-3.17C)

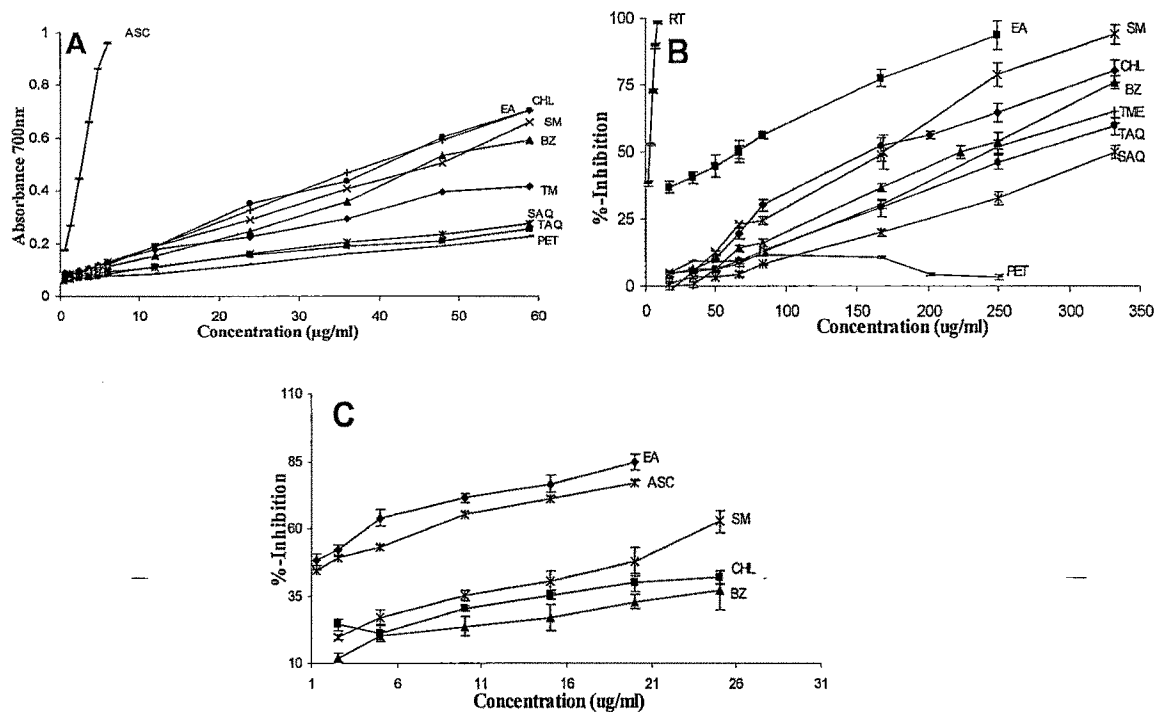


**Fig-3.17 XY- Scatters for *in vitro* studies on different extracts of Ailanthus root bark. Results are average of three determinations and shown as Mean  $\pm$  SD. A) Reducing power assay, B) DPPH radical scavenging assay, C) Inhibition of erythrocytes lysis by extracts**

**Abbreviations used in figure:** EA-Ethyl acetate extract, TAQ-Total aqueous extract, TM-Total methanol extract, SM- Successive methanol extract, SAQ-Successive aqueous extract, CHL-Chloroform extract, - Benzene, PET-Petroleum ether extract, ASC-Ascorbic acid, RT-Rutin.

Alkaloids were common constituents of most of the extracts therefore total alkaloidal extract of root bark was prepared and used it for radical scavenging activity. The extract was designated here as (AFRB) (Fig-3.19).

### **3.2.1.2 In vitro antioxidant activity for Alkaloidal extract of Ailanthus root bark (AFRB)**

AFRB showed concentration dependent increase in reducing power, when compared with ascorbic acid the reducing powers of AFRB was lesser (Fig-3.20A).

AFRB showed a significant antiradical activity by scavenging DPPH radical with an  $EC_{50}$  value of 150.09 $\mu$ g/ml which was lesser compared to reference standard rutin ( $EC_{50}$ : 2.85  $\mu$ g/ml) (Fig-3.20B).

AFRB exhibit better inhibition of superoxide radical with an  $EC_{50}$  value of 169.35 $\mu$ g/ml. The scavenging effects was lesser compared to reference standard quercetin ( $EC_{50}$ :10.84  $\mu$ g/ml) (Fig-3.20C). Further AFRB was found to inhibit the hemolysis of erythrocytes with  $EC_{50}$  values of 121 $\mu$ g/ml. This inhibitory effect was lesser than ascorbic acid ( $EC_{50}$ : 3.07 $\mu$ g/ml). (Fig-3.20D)

These results shows that AFRB posses radical scavenging activity, though this effect was not so pronounced compared to other extracts of Ailanthus root bark.

#### **3.2.1.2.1 Rapid screening for antioxidant compounds**

Chloroform and benzene extracts were found to contain high concentration of antiradical components, compared to AFRB, ethyl acetate and successive methanol extracts (Fig-3.28-TLC/ DPPH).

#### **3.2.1.2.2 Total phenolic content**

Chloroform, ethyl acetate, benzene and AFRB showed higher concentration of phenolics with 5.04, 4.87, 4.42, 4.12% w/w, respectively (Fig-3.18). Gallic acid was used as a standard for the calibration.

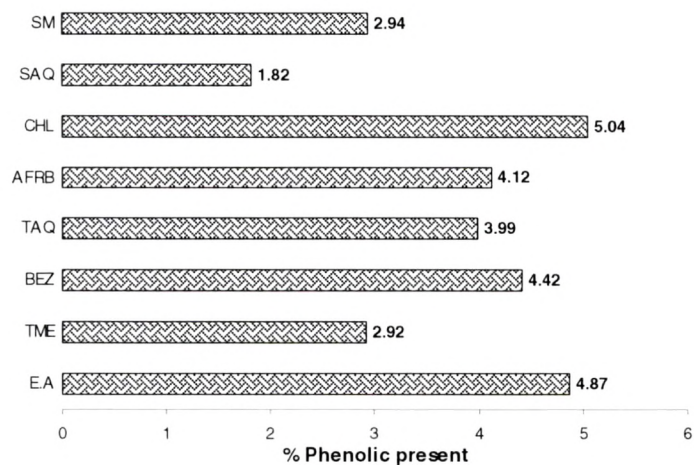


**Fig-3.18 % Phenolics present in different extracts of Root bark of *A. excelsa*.**

**Abbreviations used in figure:** EA-Ethyl acetate extract, TAQ-Total aqueous extract, TME-Total methanol extract, SM- Successive methanol extract, SAQ-Successive aqueous extract, CHL-Chloroform extract, BZ- Benzene extract AFRB-Alkaloidal fraction of root bark.

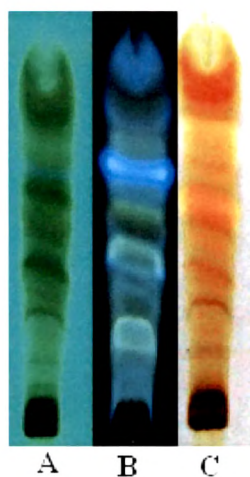


**Fig-3.19 TLC plate showing Alkaloidal fraction of root bark**

Solvent system: Chloroform: Methanol (9:1), A) 254nm, B) 366nm and C) Treated with Dragendorff's reagent

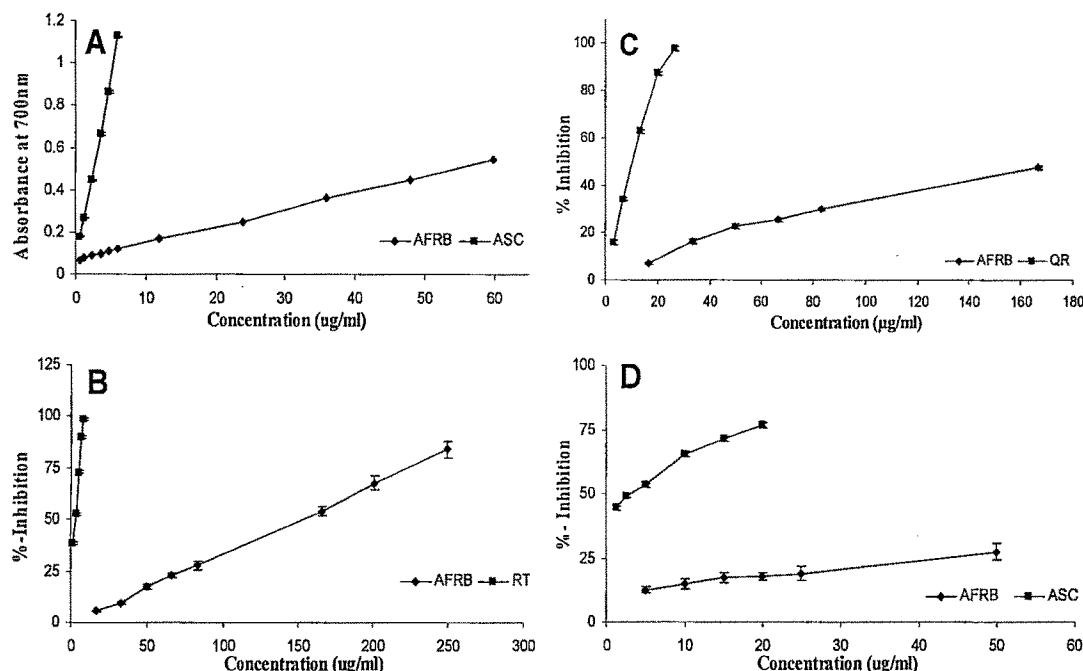


**Fig-3.20 XY- Scatters for *in vitro* studies on alkaloidal extract of *A. excelsa* root bark (AFRB).** Results are average of three determinations and shown as Mean  $\pm$  SD. A) Reducing power assay, B) DPPH radical scavenging assay, C) Superoxide radical scavenging assay D) Inhibition of erythrocytes lysis by extracts  
Abbreviations used in figure: AFRB-alkaloidal fraction of root bark, QR- Quercetin, ASC-Ascorbic acid, RT-Rutin.

### 3.2.2 Toxicity study in mice

Toxicity study of total methanol, total aqueous, chloroform (AECHL), benzene, ethyl acetate, extracts and alkaloidal fraction was determined as per OECD guidelines in female albino mice. Details regarding the toxicity of different extracts of root bark are shown in (Table-1.15)

Histopathological examination of the visceral organs in mice (2000mg/kg b.w.) showed damaged myocytes with total loss of myocardial muscle integrity, comparatively this effect was less in ethyl acetate, AFRB and total methanol treated mice. Chloroform, benzene and AFRB showed hepatic damage with necrotic area and bifurcated central artery, while methanol and ethyl acetate treated mice did not affect liver anatomy. In the same way all the extract were found to affect the kidney, where they showed tubular elongation and

vacuolization, loss of glomeruli with lots of empty spaces. Hemorrhagic areas were observed with diffused tubular walls.

Thus single toxic dose of all the extracts and AFRB showed severe cardiac and kidney damage with mortality in mice. The reason for death might be due to cardiac effects. (Fig-3.21)

**Table-1.15 Effect of various extracts of root bark on mice under toxicity study.**

Extracts	Dose level mg/kg body weight			
	2000mg/kg	550mg/kg	175mg/kg	55mg/kg
Methanol	Died within 6hrs	Died after 24hrs	Non-toxic	-----
Aqueous	Non-Toxic	-----	-----	-----
Ethyl acetate	Died within 6hrs	Non-Toxic	-----	-----
Chloroform	Died within 6hrs	Died within 12hrs	Died after 3days	Non toxic
Benzene	Died within 6hrs	Non-Toxic	-----	-----
AFRB	Died within 6hrs	Died within 12hrs	Died after 3days	Non toxic

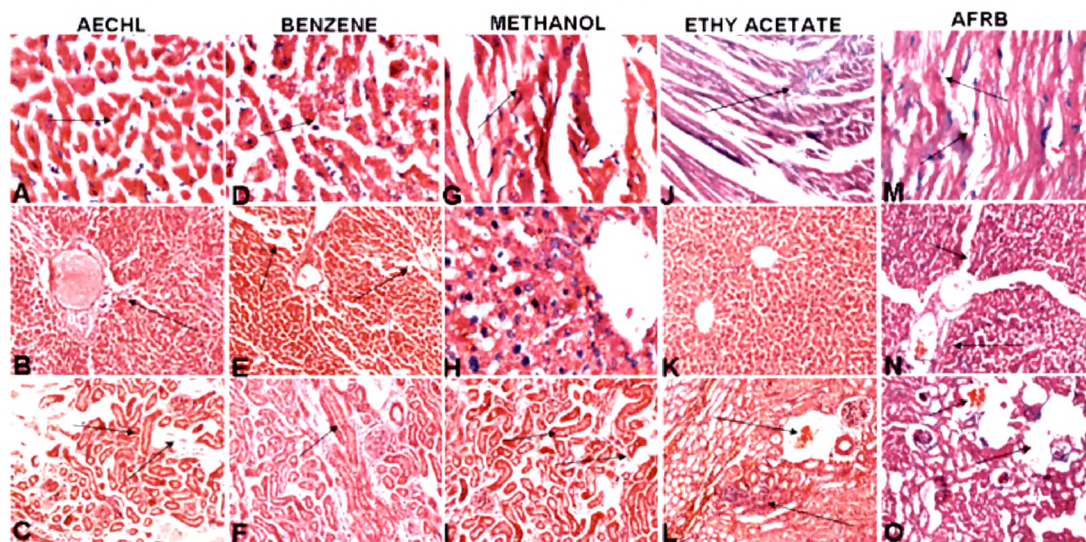


**Fig-3.21 Microscopic photographs of visceral organs of mice administered with a single oral dose of extract (2000mg/kg body weight). The sections are stained with (H & E). Effect on heart (A, D, G, J & M), effect on liver (B, E, H, K & N), effect on kidney (C, F, I, L & O), Arrows in the slides indicates the damaged and necrotic areas in.**

As per the reported literature of Ailanthus root bark on cardiovascular system the effect of long term treatment of AECHL was also analyzed in male albino rats of SD strain.

The treatment of AECHL (5.5mg/kg) for 10 days showed non significant change in WBC, RBC and haemoglobin content, but the PLT count was found to be increased ( $p < 0.05$ ). While on day 21<sup>st</sup> increase occurs in WBC ( $p < 0.05$ ) and PLT ( $p < 0.01$ ) count with non significant decrease in RBC ( $p > 0.05$ ). Even the haemoglobin content was found to be decreased ( $p < 0.01$ ) when compared with day 1<sup>st</sup>. (Table-1.16, Fig-3.22)

**Table-1.16 Effect of AECHL on complete blood count in rats**

Days	WBC/ $\mu$ l	RBC/ $\mu$ l	PLT/ $\mu$ l	Hbg (g/dl)
1 <sup>st</sup> day	$7.067 \times 10^3 \pm 0.45$	$8.105 \times 10^6 \pm 0.55$	$5.677 \times 10^5 \pm 4.79$	$17.42 \pm 0.25$
10 <sup>th</sup> day	$8.5 \times 10^3 \pm 1.37^{ns}$	$8.49 \times 10^6 \pm 0.25^{ns}$	$6.571 \times 10^5 \pm 4.20^*$	$16.8 \pm 0.67^{ns}$
21 <sup>st</sup> day	$9.02 \times 10^3 \pm 1.46^*$	$7.88 \times 10^6 \pm 0.39^{ns}$	$7.336 \times 10^5 \pm 5.59^{**}$	$15.57 \pm 0.67^{**}$

Statistical analysis was done by using ANOVA  
Post test applied: Dunnett Multiple Comparison Test  
Values are expressed as mean  $\pm$  SEM.

\* $p < 0.05$ ; \*\* $p < 0.01$ ; \*\*\* $p < 0.001$ ;  $^{ns}p > 0.05$  = non significant, (n=6)

Comparison is made between 1<sup>st</sup> day data with 10<sup>th</sup> and 21 day data.

**Abbreviations:** WBC-White blood cells, RBC-Red blood cells, PLT-Platelets, Hbg-hemoglobin

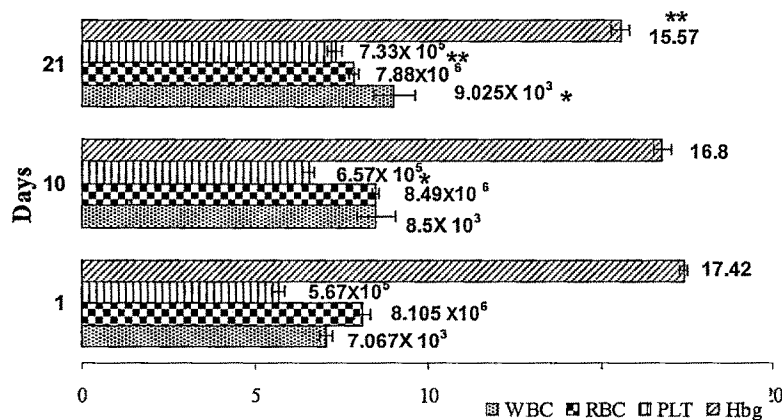


**Fig-3.22 Effect of AECHL on complete blood count in rats**

The long term treatment of chloroform extract of root bark (AECHL) in rats showed increase in WBC and platelet counts with decreased RBC and hemoglobin content.

AECHL (5mg/kg) treatment for 21 days showed no change in total bilirubin level but it showed significant increase in direct bilirubin ( $P<0.01$ ) and reduction in indirect bilirubin ( $P<0.001$ ). Further AECHL did not show any significant change in uric acid and creatinine level, but the serum cortisol level was found to be increased ( $P<0.01$ ) when compared with control group. AECHL treatment showed reduction in serum levels of GPT ( $P<0.001$ ), GOT ( $P<0.001$ ), ALKP ( $P<0.05$ ) and LDH ( $P<0.001$ ) with significant increase in the levels of brain dopamine ( $P<0.001$ ) and CKMB ( $P<0.01$ ) when compared with control group. (Table-1.17 & 1.18, Fig-3.23 & 3.24)

An increased level of serum cortisol indicates that administration of AECHL may affect the normal carbohydrate metabolism and increased stress in rats, in response to this serum cortisol level get increased. This increased cortisol may be the reason for intestinal ulcer, muscle damage and initial increased blood pressure in rats. The condition is like Cushing's syndrome, in which there is increased blood pressure and sometimes mental disturbances due to excess of cortisol.

AECHL may also act by increasing the secretion of adrenocorticotrophic hormone through stimulation of pituitary gland which may lead to increased cortisol level with excessive stimulation of adrenal glands.

Excess of creatinine in serum after AECHL administration may be due to muscular break down, which leads to loss of high amount of energy stored in the form of ATP which is required for the normal muscle contraction.

Dopamine is an intermediate in the synthesis of norepinephrine and occurs in caudate nucleus. Increased dopamine level might be due to the stimulation of sympathetic stimulation caused by AECHL.

Uric acid is an end product of nucleic acid metabolism, increased serum levels of uric acid with AECHL indicates increased nucleic acid metabolism.

Increased bilirubin with AECHL may be due to break down of blood pigment hemoglobin, which inturn showed increased levels of serum bilirubin and decrease hemoglobin content in AECHL treated rats.

Increased level of CKMB with AECHL treatment might be due to loss of normal myocardial architecture.

Histopathological examination of section of organs after long term treatment with AECHL (5mg/kg. b.w) showed damaged liver with lots of necrotic areas. No such effect was seen in kidney sections. Severe myocardial damage was observed with loss of muscle integrity and displacement of nuclei.

Development of lesions from the inner side of intestine occurs which grows slowly to form tumor like mass, this lesions formation might be due to increased serum cortisol level. Normal anatomy of stomach showed secretory epithelial sheath containing secretory cells on the inner wall of the stomach, along with surface mucosal cells, AECHL treatment showed loss of this secretory epithelial sheath at several places from the inner side of stomach. (Fig-3.27).

**Table-1.17 Effect of AECHL on serum marker enzymes of rat**

Groups	T. bilirubin	D. bilirubin	I. bilirubin	Uric acid	Cortisol	Creatinine
CONTROL	0.426±0.016	0.073±0.008	0.353±0.008	1.367±0.108	0.547±0.049	0.853±0.060
AECL	0.423±0.024	0.163±0.039**	0.26±0.017***	1.433±0.156	1.413±0.095**	1.003±0.127

Values are expressed as mean ± SEM.

Data presented as Mean ± SD.

Statistical analysis was done by using "Paired t test"

(n=6), ns=P>0.05, \*P<0.05, \*\*P<0.01, \*\*\*P<0.001

Comparison made with control group

**Fig 1.18 Effect of AECHL on cardiac and liver marker enzymes**

	SGPT	SGOT	ALKP	DOPAMINE	CKMB	LDH
CONTROL	53.66±3.89	142.33±2.27	387±6.48	39±2.6	679.03±46.43	931.67±23.97
AECHL	40±3.39***	111.33±4.71***	357.33±14.83*	74.66±4.6***	930.9±67.56**	686.57±49.22***

Values are expressed as mean ± SEM.

Data presented as Mean ± SD.

Statistical analysis was done by using "Paired t test"

(n=6), ns=P>0.05, \*P<0.05, \*\*P<0.01, \*\*\*P<0.001

Comparison made with control group

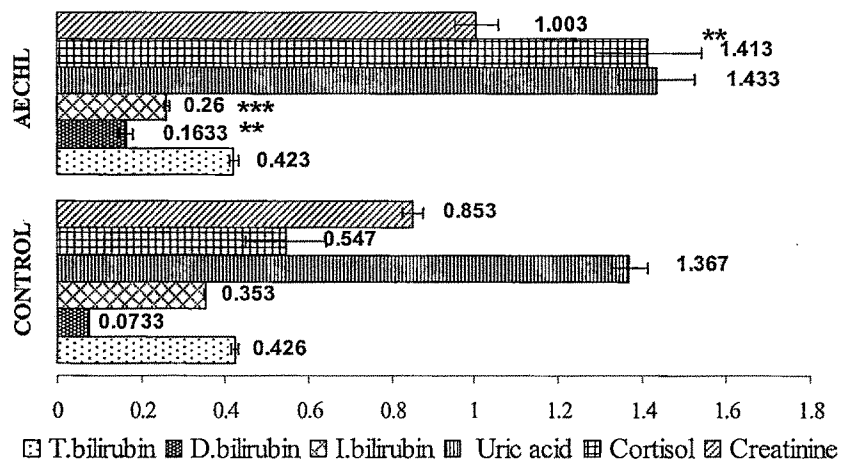


**Fig- 3.23 Effect of AECHL (5.5mg/kg b.w, p.o.) on serum levels of bilirubin, uric acid cortisol and creatinine in rats.**

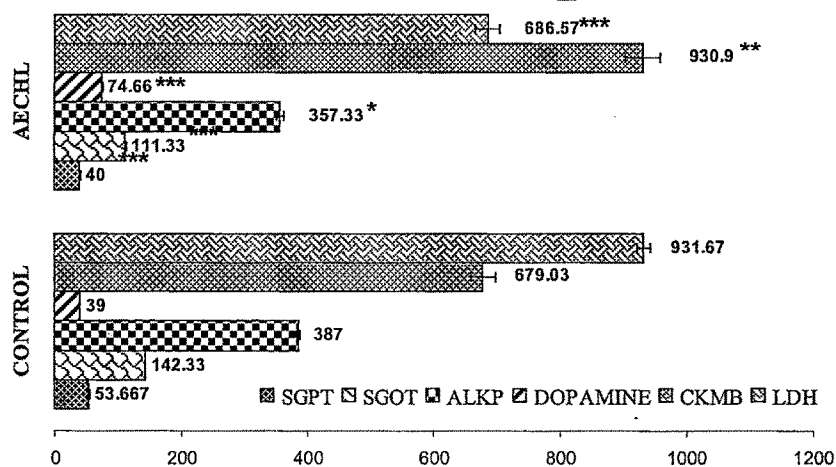


**Fig- 3.24 Effect of AECHL (5.5mg/kg b.w, p.o.) on serum levels of GOT, GPT, ALKP, CKMB, LDH and brain dopamine (brain homogenate) in rats.**

### **3.2.2.3 Effect of AECHL on haemodynamic properties of rat heart**

The effect of AECHL on cardiovascular system after a single dose (2000mg/kg b.w.) administration in rats was determined from changes in blood pressure (BP), electrocardiograph (ECG), max pressure (mmHg), min pressure (mmHg), systolic duration (s), diastolic duration (s), cycle duration (s), max dP/dt (mmHg/s), min dP/dt (mmHg/s), contractility index (1/s) and pressure time index (mmHg.s) recorded with Power Lab instrument using Millar catheter. Data shown in (Table-1.19 & 1.20, Fig-3.25 & 3.26)

After 2 hours of AECHL treatment the baseline changes in the ECG pattern with waveform ECG was seen. An elevation of QRS complex wave and the time for QRS complex also decreased from 15 ms to 12 ms. There was a dip in the QRS complex peak height accompanied by increase in the refractory period (relaxation time) of the heart which continues to persist till 3 to 3.50 hours

After that there is a sharp decline in the QRS wave observed which dips down drastically and occurrence was of Bigemini which is a sign of ectopic focus or ventricular arrhythmia. The frequency of QRS wave decreased with a decrease in the amplitude as well. The animal died after 270min of treatment.

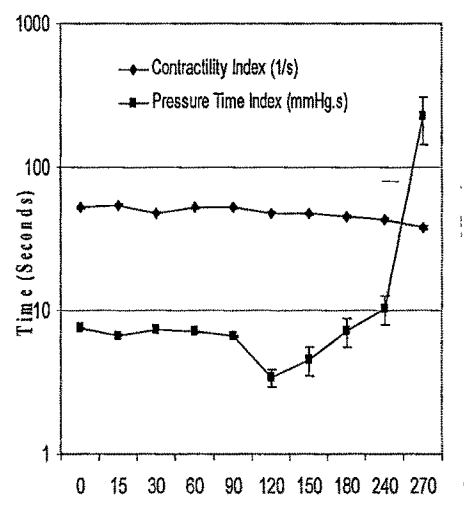
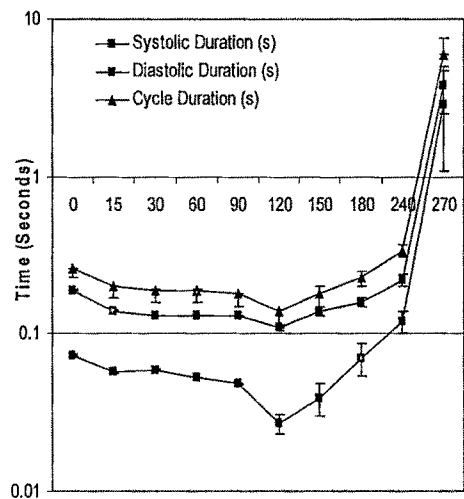
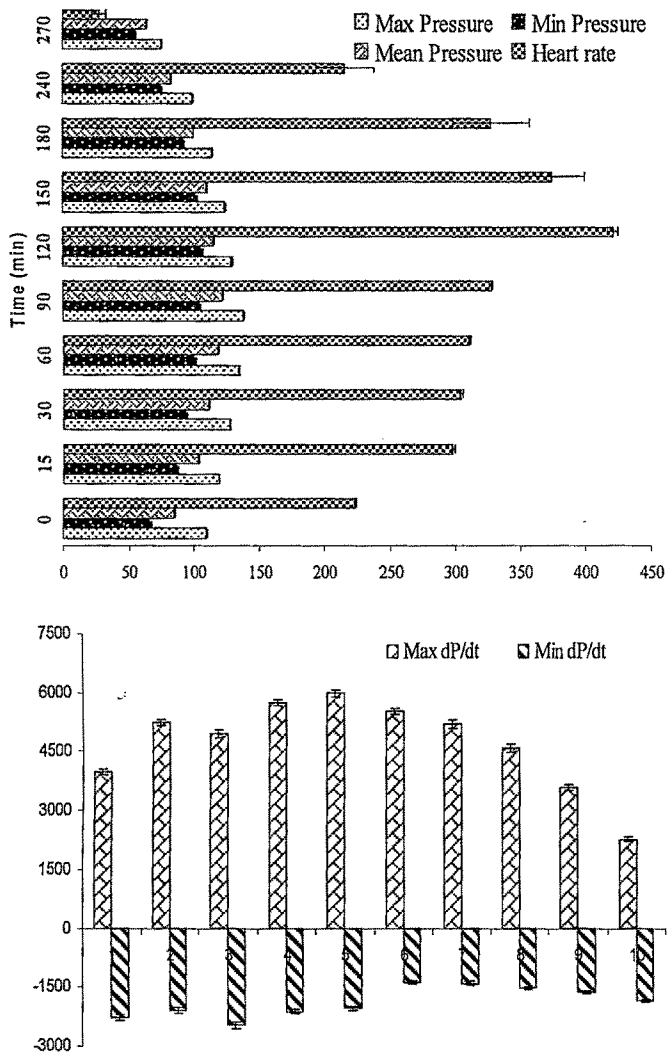


**Fig- 3.25 Effect of AECHL on mechanical properties of rat heart**

**Table-1.19 Effect of AECHL on various mechanical properties rat heart.**

Time (Min)	Mean							
	Max Pressure (mmHg)	Min Pressure (mmHg)	Pressure (mmHg)	Systolic Duration (s)	Diastolic Duration (s)	Heart Rate (BPM)	Rate	
Control	110.03±0.27	65.23±0.22	85.04±0.28	0.073±0.0008	0.19±0.001	223.6±1.04		
15	119.53±0.24**	86.17±0.17**	103.91±0.23**	0.057±0.0004	0.14±0.001	298.21±1.5**		
30	127.93±0.34**	93.03±0.29**	111.81±0.27**	0.059±0.0004	0.13±0.0008	304.18±1.35**		
60	134.97±0.37**	99.64±0.2**	118.65±0.29**	0.053±0.0002	0.13±0.0005	310.9±0.8**		
90	138.15±0.41**	103.82±0.33**	122.07±0.41**	0.048±0.0004	0.13±0.0007	327.64±1.3**		
120	129.04±0.71**	105±0.43**	115.28±0.5**	0.027±0.004	0.11±0.001	420.59±3.8**		
150	124.07±0.37**	100.69±0.4**1	110.29±0.39**	0.039±0.009	0.14±0.02	374.05±24.3**		
180	114.35±0.3**	91.25±0.4**	99.9±0.37**	0.07±0.016	0.16±0.02	327.54±29.7**		
240	99.4±0.26##	74.7±0.53**	82.76±0.28##	0.12±0.02	0.22±0.03	215.59±21.9		
270	75.47±0.18##	53.96±0.45##	63.96±0.39##	2.87±1.78**	3.79±1.59**	27.61±5.4##		

Values are expressed as mean ± SEM.

Data presented as Mean ± SD.

Statistical analysis was done by using ANOVA

Post test- Dunnett Multiple Comparison Test

(n=6), ns=P>0.05, \*P<0.05, \*\*P<0.01, \*\*\*P<0.001

Comparison made with control group

Heart rate: Beats per minutes

# compared with the control group animals, #Increased, #Decreased

**Table-1.20 Effect of AECHL on various mechanical properties rat heart.**

Time (Min)	Cycle Duration (s)	Max-dP/dt (mmHg/s)	Min-dP/dt (mmHg/s)	Contractility Index (1/s)	Pressure-Time Index (mmHg.s)
Control	0.26±0.001	3973.4±64.09	2273.4±61.6	52.19±0.91	7.5±0.06
15	0.2±0.001	5234.4±65.49*	2100±64.5	52.77±0.75	6.7±0.05
30	0.19±0.0008	4943.8±101**	2475±86.4	48.14±1.03*	7.32±0.05
60	0.19±0.0005	5734.4±69.52**	2126.6±60.6	52.25±0.72	7.09±0.03
90	0.18±0.0007	5971.9±75.01**	2034.4±53.6#	52.11±0.65	6.6±0.07
120	0.14±0.001	5515.6±77.3**	1379.7±40.2##	47.68±0.59##	3.42±0.5
150	0.18±0.02	5203.1±97.8**	1400±38.7##	47.21±0.96##	4.53±1.02
180	0.23±0.02	4603.1±108**	1531.3±32.1##	45.38±1.1##	7.2±1.65
240	0.34±0.03	3590.6±65.4**	1639.1±39.9##	42.91±0.88##	10.26±2.29
270	5.98±1.59**	2264.1±50**	1856.3±41.5##	37.62±1.1##	225.37±81.2**

Values are expressed as mean ± SEM.

Data presented as Mean ± SD.

Statistical analysis was done by using ANOVA

Post test- Dunnett Multiple Comparison Test

(n=6), ns>P>0.05, \*P<0.05, \*\*P<0.01, \*\*\*P<0.001

Comparison made with control group

Heart rate: Beats per minutes

# compared with the control group animals, †Increased, #Decreased

A gradual increase in systolic, diastolic and mean blood pressure, with decreased systolic, diastolic and cycle duration was observed with single dose administration of AECHL (2000mg/kg b.w. p.o). AECHL also increased the heart rate with reduction in the contractility and pressure time index. An increase in Max dP/dt and Min dP/dt was observed. These data supports that the AECHL shows sympathomimetic effect on cardiovascular system. However this effect was abolished 120mins after AECHL treatment as shown by reduced systolic, diastolic and mean blood pressure, increased systolic, diastolic and cycle duration time. The heart rate was decreased with a reduction in contractility index and increase in pressure time index. All these parameters were changed significantly when compared with those of control group. Thus AECHL showed reversal of its sympathomimetic effect with time.

The initial sympathomimetic effect of AECHL may be due to the stimulation of sympathetic nervous system, releasing the sympathetic neurotransmitter responsible for increasing the cardiac functions. The effect may also be due to increase in intracellular calcium level which further leads to release of calcium from the storage, sarcoplasmic reticulum, leading to increased brushing action of myocardial contractile proteins actin and myosin resulting in increased contraction.

The reversal of sympathomimetic action with time may be due to aggravation of intracellular calcium level causing fatigueness of myocardium, leading to heart failure. This effect of AECHL was clearly indicated in the ECG recording, which showed elevation of QRS complex wave with a decrease in time taken for wave formation as correlated with decrease in systolic, diastolic duration, contractility and pressure time index.

A gradual dip in the QRS complex peak height accompanied by increase in the refractory period, followed by a sharp decline in the QRS wave, dips down drastically with an occurrence of Bigemini which is a sign of ectopic focus or ventricular arrhythmia. These changes can be correlated with increased systolic, diastolic and cycle duration along with increased contractility and pressure index. All these changes lead to drastic fall in blood pressure and heart rate causing death of animals.

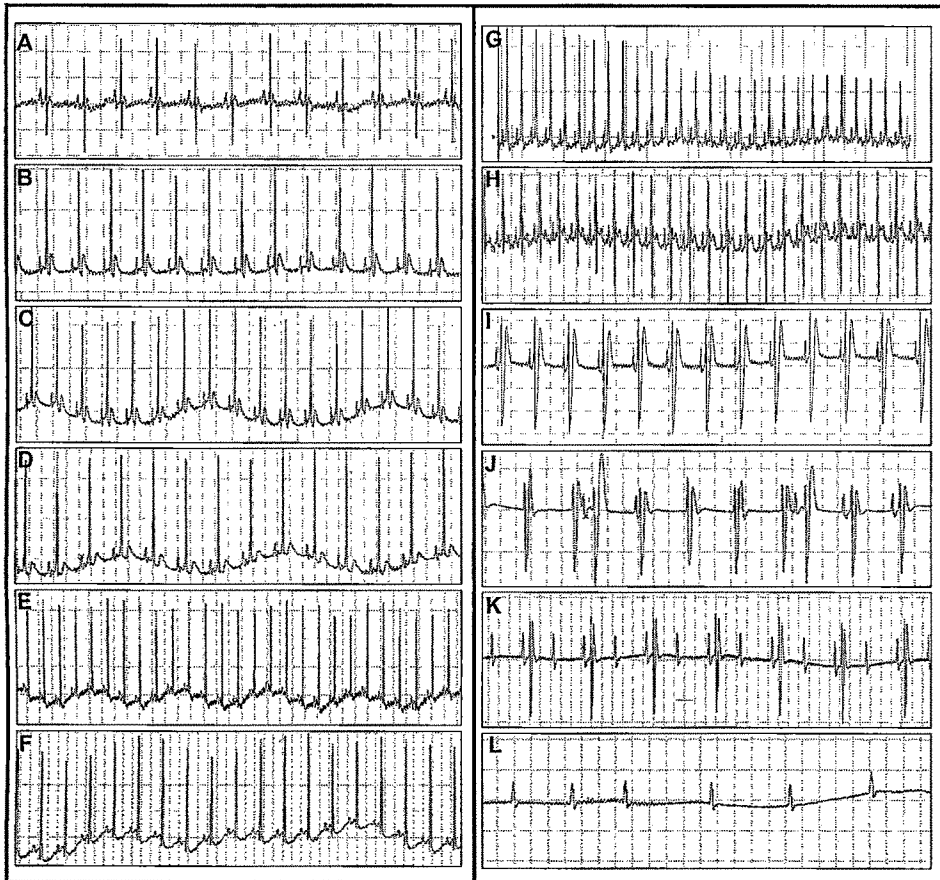


**Fig-3.26 Electrocardiogram of rat treated with Chloroform extract of *A. excelsa* root bark (AECHL)**

The P, QRS, and T waves in normal sinus rhythm are shown in **(Panel A)** and treated **(Panel B)**. We see baseline changes with wave form ECG **(Panel C)**. There is elevation of QRS complex and the time for QRS complex also decreases from 15 ms to 12 ms. T wave elevation (T wave found to be lengthened with wavy base) **(Panel D)**. T wave cant seen with improper P wave **(Panel E)**. There is a dip in the QRS complex peak height accompanied by increase in the refractory period (relaxation time) **(Panel F)**. QRS wave amplitude decreased, **(Panel G)**. Here there is sharp decline in the QRS wave which dips down drastically and occurrence of Bigemini which is a sign of ectopic focus or ventricular arrhythmia. The frequency of QRS wave decreases with a decrease in the amplitude as well. T wave elevation occurs here **(Panel H)**. Here again frequency of QRS complex reduced further with deep depression in QRS complex. P and T wave further elevated **(Panel I)**. Extra P wave formation was observed with T wave elevation. QRS complex was found to be further reduced, with increased QRS depression. **(Panel J)** Here QRS and T wave completely vanished. **(Panel K)** Amplitude and frequency of P wave formation further reduced. The animal dies after 4 hour 30 min. **(Panel L)**

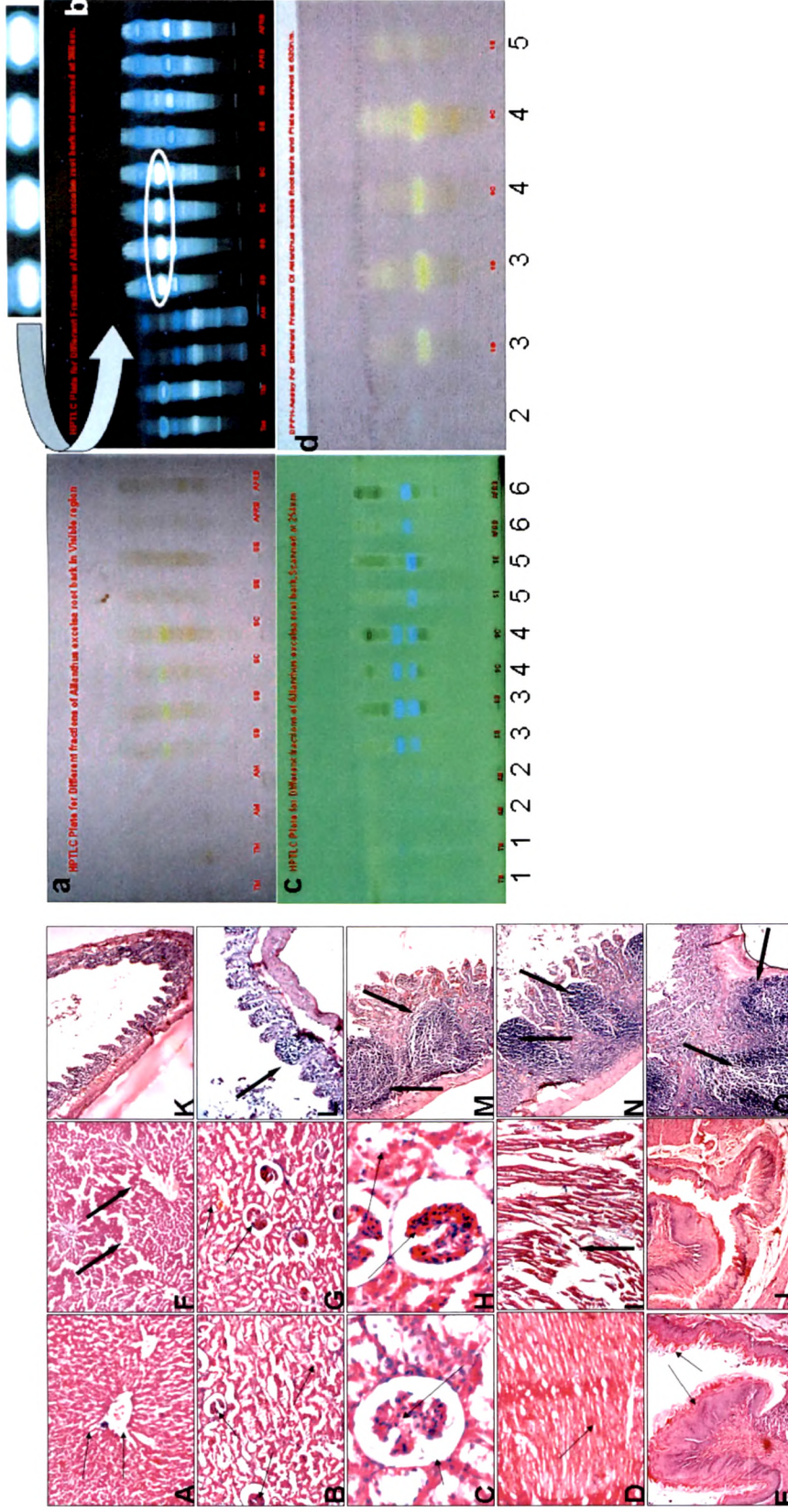


**Fig-3.27 Photomicrographs showing the effect of AECHL on rat organs (Stained with H & E)**

Normal- A) Liver, B) Kidney, C) Kidney-glomeruli, D) Myocardium, E) Intestine (Arrows showing normal architect of organs)  
 AECHL treated - F) Liver, G) Kidney, H) Kidney, I) Myocardium, J) Stomach, K) Intestine. (Solid arrows showing effect of AECHL 5mg/kg, b.w)

**Fig-3.28 TLC plates showing different extracts of Ailanthus root bark in a) Visible, b) 366nm, c) 254nm, d) After spraying with DPPH**

Track-1- Total methanol extract, Track-2-Successive methanol extract, Track-3- Successive benzene extract, Track-4-Successive chloroform extract, Track-5- Successive ethyl acetate extract, Track-6-Alkaloidal extract (AFRB), Solvent system: Chloroform: Methanol (9:1), Spray reagent: DPPH in Methanol. Circle showing the presence of common major compound in benzene and chloroform extract.

### 3.2.4 TLC study for different extracts of Ailanthus root bark

In chromatographic study (Fig-3.28) Plate (a) showed different extracts of Ailanthus root bark developed in chloroform: methanol (9:1), and compound resolved can be seen in visible region. Plate (b) showed plate observed under UV at 366nm, where most of the compounds are visible, circle showed common compounds which are present in chloroform and benzene extract at high concentration, and these extract shows toxic effect in mice and out of these two chloroform extract showed severe effect on cardiovascular system. So compound shown with arrow was isolated by column chromatography and was used for further studies. Plate (c) Showed compounds visible at 254nm. Plate (d) Shows close view of the compound from chloroform and benzene extract (same compound shown in circle at plate b) showing yellow color with DPPH reagent thus proving it as radical scavenger (Fig-3.28).

### TLC fingerprinting of alkaloidal extract of root bark (AFRB)

HPTLC finger print profile was established for AFRB. A stock solution (1mg/ml) was prepared in chloroform. Developed on pre-coated Silica gel G60 F254 TLC plates using CAMAG Linomat V Automatic Sample Spotter and the plates were developed in solvent systems of different polarities to resolve polar and non-polar components of the AFRB. The plates were scanned using TLC Scanner 3 (CAMAG) at 254 nm and 366 nm and Rf values, spectra,  $\lambda$  max and peak areas of resolved bands were recorded. Relative percentage area of each band was calculated from peak areas (Table-1.21, Fig-3.29).

**Table-1.21 TLC fingerprinting for Alkaloidal extract of root bark of *A. excelsa***

Scanning wavelength	Solvent system 1*				Solvent system 2**			
	Rf	$\lambda_{\text{Dmax}}$	Relative area	%	Rf	$\lambda_{\text{Dmax}}$	Relative area	%
254nm (Under UV)	0.31	112	4.34		0.18	598	4.42	
	0.59	197	27.62		0.28	625	11.89	
	0.78	194	24.53		0.36	625	5.38	
	0.87	225	43.51		0.41	332	15.25	
					0.60	399	17.81	
					0.90	361	36.36	
					0.98	227	5.81	
366nm (Under UV)	0.31	112	1.56		0.10	641	1.89	
	0.51	198	5.83		0.18	621	2.89	
	0.61	192	28.35		0.29	606	10.68	
	0.78	194	7.89		0.35	618	2.44	
	0.89	228	56.37		0.39	332	16.15	
					0.44	610	2.67	
					0.48	622	9.58	
					0.52	622	1.10	
					0.60	400	4.42	
					0.69	622	3.32	
					0.78	345	26.67	
520nm (After Derivatization)					0.90	361	15.52	
					0.98	227	2.70	
					0.15	293	3.45	
					0.19	292	12.34	
					0.25	295	7.92	
					0.53	255	12.52	
					0.66	296	11.55	
				0.82	259	11.69		
				0.84	259	7.81		
				0.90	468	32.73		

\*Solvent system 1-Butanol: Acetic acid: Water (4:1:5 v/v), \*\*Solvent system 2- Chloroform: Methanol (9:1 v/v), treated with Dragendorffs reagent.

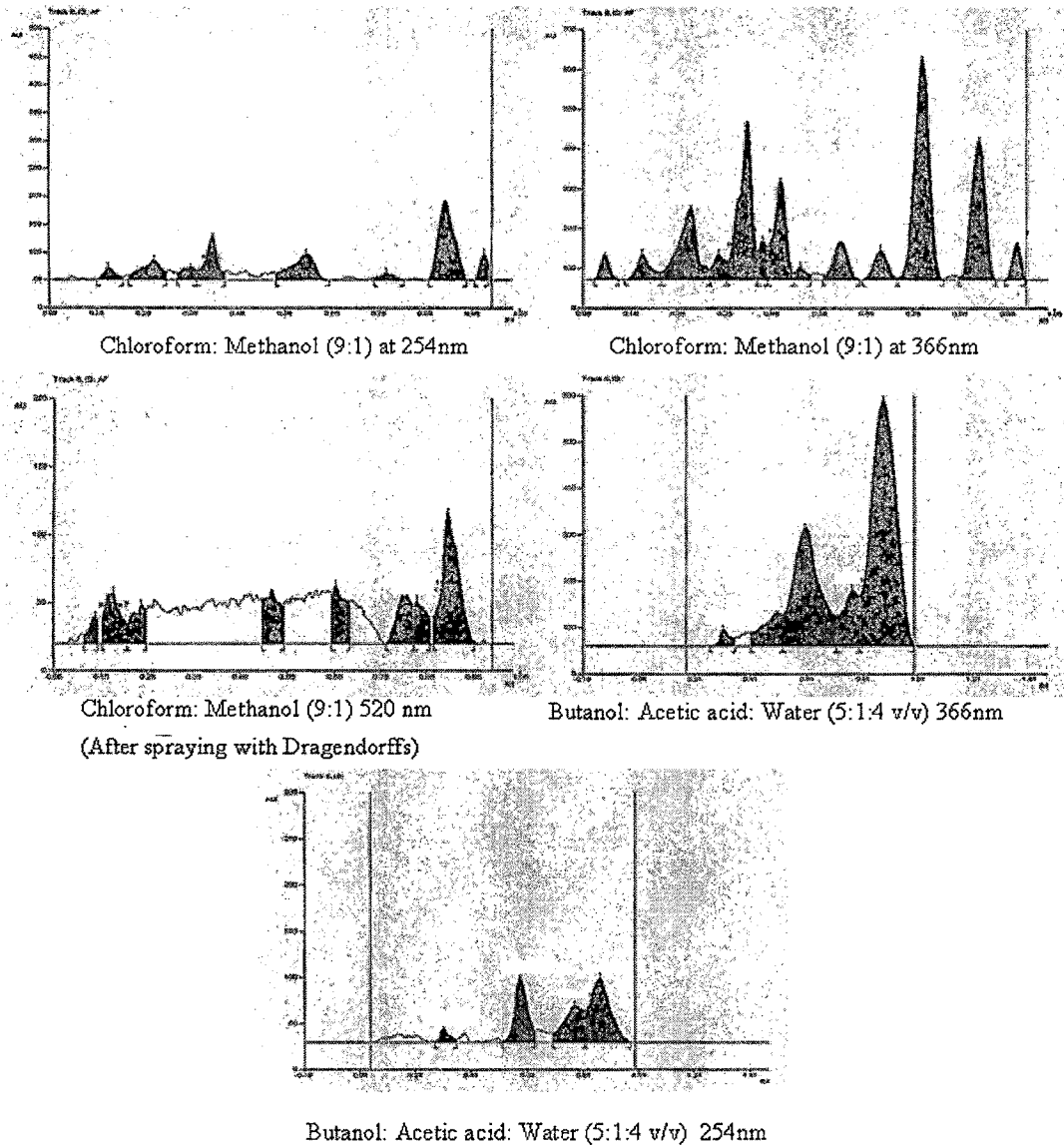


**Fig-3.29 TLC Chromatogram of AFRB developed in different solvent system and scanned at 254, 366 nm and 520nm.**

The results of the studies on Ailanthus root bark as described in present chapter indicated that the radical scavenging activity was shown by different extracts. Since alkaloids are chief constituents present in the extracts, a separate total alkaloidal extract of the root bark was prepared and when subjected for evaluating radical scavenging property a significant effect was obtained. The other extracts as well as the alkaloidal extract when subjected to toxicological studies, all the extracts were toxic except aqueous extract which did not shows any radical scavenging activity.

Since the root form one of the major components of a very important preparation of ayurvedic system Dashmularista prescribed as rejuvenator. Another reason was the controversy in mentioning the usage of roots, some texts of Ayurveda described these as cardio toxic, while other states that it causes cardiac trouble. Hence the most active chloroform extract though toxic was further studied for the antioxidants found active in *in vitro* and rapid screening. The compound present in chloroform and benzene extracts (Fig-3.28d) was further taken up for detailed study on cardiovascular system as described in this chapter.

The non alkaloidal compounds isolated from chloroform extract of root bark and were subjected for detailed studies.

### **3.2.5 Isolation of compounds from chloroform extract of *Ailanthus* root bark**

The successive chloroform extract (1.5gm) of powdered root bark of *Ailanthus excelsa*, was subjected to column chromatography over silica gel and eluted with chloroform: methanol mixtures. Elutes of 50ml each were collected and analyzed by TLC. The first few elute of chloroform consisted of sticky dark brown mass were rejected, while the fraction eluted at, (98:2v/v) consisted of deep green color fluorescence was collected. These fractions when observed at 366nm show deep green fluorescence. The column was further eluted with increasing amount of methanol to remove the fluorescent fraction completely. These elutes were analyzed by TLC (chloroform: methanol, 9:1v/v) and mixed accordingly. The fraction was concentrated and developed on PTLC using chloroform: methanol (9:1v/v). The fluorescent green colored band at 366nm was collected. The silica with compound was dispersed in methanol and the compound separated by centrifugation at 2500rpm, further purification was done in a same manner. Compound obtained (79.35mg) was designated as (AECHL-2). Elution of column with further increasing polarity (chloroform: methanol 90:10v/v) yields light hairy white colored solid mass after concentrating elutes. This mass when subjected to TLC showed three spots which was purified by repeated recrystallization in methanol. After purification it showed single blue colored band at 254nm, and gets pink after treatment with anisaldehyde sulphuric acid reagent when developed on TLC chloroform: methanol (9:1v/v). The compound was designated as AECHL-1 (Yield-180mg). Both AECHL-1 and AECHL-2 were characterized by UV, IR, NMR and mass spectroscopy.

#### **3.2.5.1 Characterization of AECHL-1**

Compound AECHL-1 when subjected to characterization showed following characteristic IR, NMR and mass spectra.

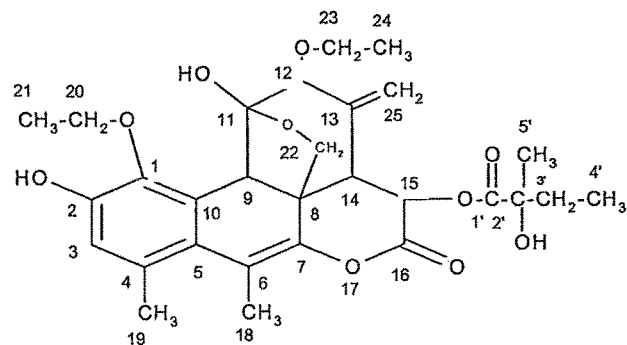
IR (KBr): 3425, 3419 (hydroxyl group), 2972, 2966, 2923, 2873 (alkyl C-H stretch), 1733 ( $\delta$  lactone), 1718 (Bi acetyl), 1680 (C=O conjugation with alkene), 1652 (-C=C stretching), 1600 (aromatic), 1492, 1454, 1394 (methyl stretching), 1222 ( $\delta$  lactone), 1184, 1110, 1051, 1031 (acetals), 1018 nm (alkanes).

<sup>1</sup>H-NMR (DMSO, 400 Hz) δ: 0.95 (3H, t, 4'-CH<sub>3</sub>), δ:1.15 (3H, d, H-24), δ:1.235 (3H, d, 5'-CH<sub>3</sub>), δ: 1.5 (2H, ddd, 5'-CH<sub>2</sub>), δ: 1.73 (3H, ddd, H-21), δ: 1.83 (1H, s, H-9), δ: 1.87 (1 H, s, H-14), δ: 1.9 (2H, s, H-18), δ: 2.16 (3H, s, H-18), δ: 2.3 (3H, d, H-19) δ: 2.71 (2H, s, H-20), δ: 3.45 (2H, dd, H-23) , δ:3.65 (2H, d, H-22), δ: 3.95 (1 H, t, H-12) , δ: 4.05 (2H, s, H-22) , δ: 5.30 (1H, s, H-15), δ: 5.46 (1H, s, OH- 2), δ: 5.73 (1H, d,OH-2') , δ: 6.89 (1 H, s, H-3) , δ: 8.82 (1H, s, OH-11).

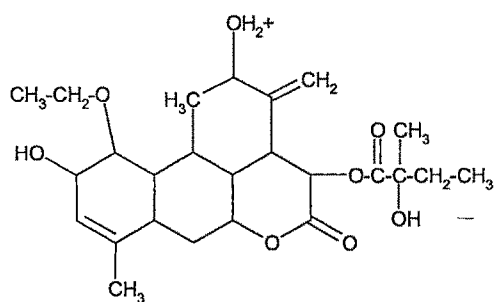
Chemical shifts are given in ppm on the δ-scale, s = singlet, d = doublet, t = triplet.

The m.s. showed the following principal peaks: *m/z*: 1068 due to dimer formation. The actual [M<sup>+</sup>] was considered to be 543.8, 463.3 [M-C<sub>4</sub>H<sub>1</sub>O<sub>2</sub>], 461.4 [M- C<sub>4</sub>H<sub>2</sub>O<sub>2</sub>], 459.4 [M- C<sub>4</sub>H<sub>4</sub>O<sub>2</sub>], 361.2 [M- C<sub>9</sub>H<sub>11</sub>O<sub>4</sub>].

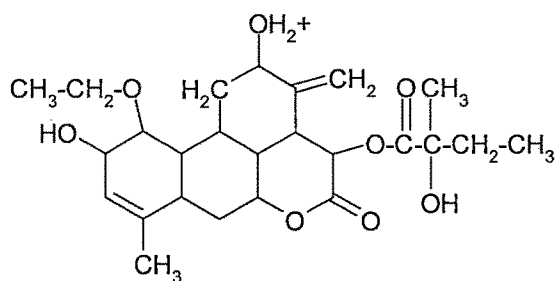
Compound AECHL-1 is a solid, mp. 248-250°C possessed a molecular formula of C<sub>29</sub> H<sub>36</sub>O<sub>10</sub> as indicated by EI and ES mass spectra. The IR spectrum showed the presence of hydroxyl (s) (3425nm, 3419nm), δ lactone (1733nm), and aromatic moiety (1600nm). The UV spectrum gave a characteristic absorption maximum at 235nm, indicating the presence of auxochromic groups like hydroxyl and ketone. The <sup>1</sup>H- NMR spectrum of AECHL-1 revealed the presence of an aromatic proton δ 6.89 and a singlet at δ 5.30 which is characteristic of the ester function at C-15. H-22 appeared as an AB system as a singlet at δ 4.05 and doublet at δ 3.65 and H-12 appeared as a triplet at δ 3.95. The methyl group H-19 on the aromatic ring appeared as singlet at δ 2.3. A doublet at δ 1.235 for six protons is assigned at H-5'. H- 4' appeared as a triplet at δ 0.95. The methyl group, H-18 appeared as a singlet at δ 2.16 (Fig-3.30)



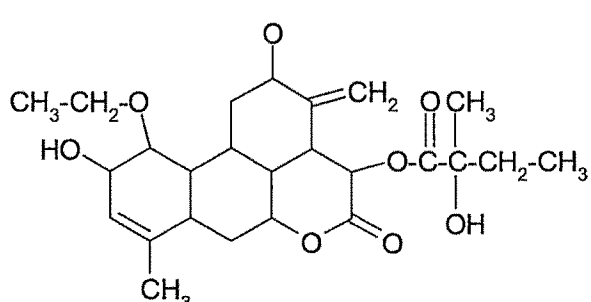
AECHL [m/z : 543 C<sub>29</sub>H<sub>36</sub>O<sub>10</sub>]



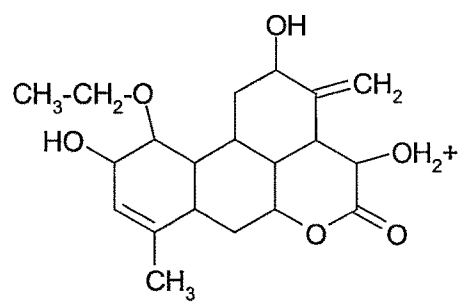
[m/z : 463 C<sub>25</sub>H<sub>35</sub>O<sub>8</sub>]



[m/z : 461 C<sub>25</sub>H<sub>33</sub>O<sub>8</sub>]



m/z : 459 C<sub>25</sub>H<sub>31</sub>O<sub>8</sub>



m/z : 361.2 C<sub>20</sub>H<sub>25</sub>O<sub>6</sub>

Fig-3.30 Structure of AECHL-1 with its mass fragments

### 3.2.5.2 Characterization of AECHL-2

Compound AECHL-2 when subjected to characterization showed following characteristic IR, NMR and mass spectra.

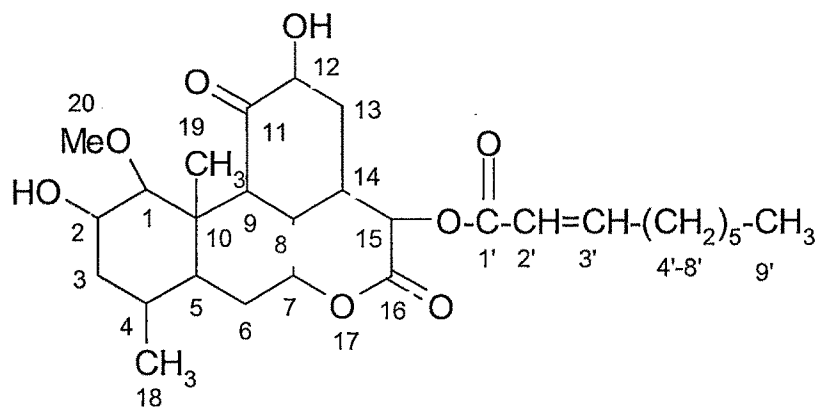
IR (KBr): 3683, 3072 (hydroxyl group), 2981, 2960, 2925, 2867, 2842 (alkyl C-H stretch), 1787 (C=O stretching of lactone), 1728 ( $\alpha$ ,  $\beta$ -unsaturated ester), 1712 (C=O stretching), 1693, 1643 (-C=C stretching), 1593 (ketone), 1531 (alkanes), 1485 (alkanes), 1384 (methyl stretching), 1371 (O-H in plane bending), 1186 (C-(C=O)-C stretching), 1147 (C-O stretching), 1110 (C-O-C stretching), 1056, 1095 (=C-H wagging), 1031 (In plane C-H bend), 792 (Out-of plane C-H bend), 667nm (O-H out of plane bending).

$^1\text{H-NMR}$  (DMSO, 400 Hz)  $\delta$ : 0.85 (3H, d, H-9'),  $\delta$ : 0.89 (3H, d, H-19),  $\delta$ : 1.07 (3H, s, H-18),  $\delta$ : 1.11 (1H, d, H-20),  $\delta$ : 1.25 (H, s, H-14),  $\delta$ : 1.28 (6H, d, H-5'-8'),  $\delta$ : 1.33 (2H, s, H-4'),  $\delta$ : 1.40 (2H, s, H-8, H-9),  $\delta$ : 1.59 (3H, s, H-5, H-6),  $\delta$ : 1.99 (2H, s, H-13)  $\delta$ : 2.17 (1H, s, H-15),  $\delta$ : 2.31 (2H, s, H-3, H-3'),  $\delta$ : 2.97 (1H, s, H-2'),  $\delta$ : 3.51 (3H, s, H-1, H-2, H-12),  $\delta$ : 7.45 (2H, t, 2-OH, 12-OH).

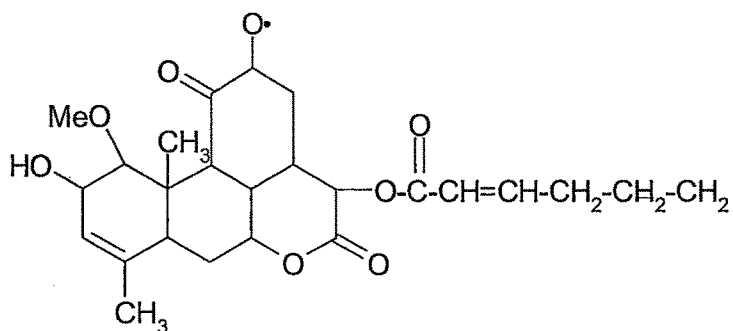
Chemical shifts are given in ppm on the  $\delta$ -scale, s = singlet, d = doublet, t = triplet.

The m.s. showed the following principal peaks:  $m/z$ : The  $[\text{M}^+]$  was found to be 504  $[\text{C}_{28}\text{H}_{40}\text{O}_8]$ , 459.5  $[\text{M}-\text{C}_3\text{H}_8]$ , 355.2  $[\text{M}-\text{C}_9\text{H}_{17}\text{O}_2]$ , 345.2  $[\text{M}-\text{C}_{10}\text{H}_{18}\text{O}_2]$ , 251.1  $[\text{M}-\text{C}_{14}\text{H}_{21}\text{O}_4]$ , 238.8  $[\text{C}_{15}\text{H}_{22}\text{O}_4]$ .

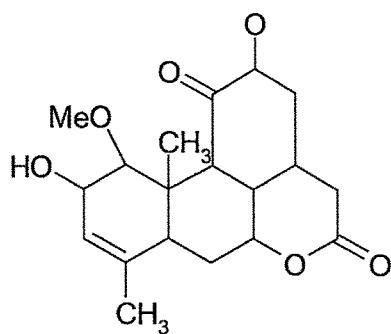
Compound AECHL-2 is an orange color solid gives very bright green fluorescence at 366nm, mp. 180-184°C, has a molecular formula of  $\text{C}_{28}\text{H}_{40}\text{O}_8$  as indicated by EI and ES mass spectra. The IR spectrum showed the presence of hydroxyl (s) (3683nm, 3072nm), unsaturated ester (1728 nm) and methoxy group (1110 nm). The UV spectrum gave a characteristic absorption maximum at 243 nm, indicating the presence of auxochromic groups like hydroxyl and ketone. The  $^1\text{H-NMR}$  spectrum of AECHL-2 revealed the presence of terminal methyl groups as doublets at  $\delta$ -0.85 and  $\delta$ -0.89. A doublet at  $\delta$  1.28 for six protons was assigned to H-5' to H-8' and H-4' appeared as a singlet at  $\delta$  1.33 (Fig-3.31).



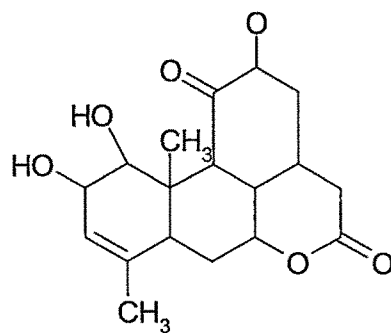
$m/z : 504 [C_{28}H_{40}O_8]$



$m/z : 459.5 [C_{25}H_{32}O_8]$



$m/z : 355.2 [C_{19}H_{23}O_6]$



$m/z : 345.2 [C_{18}H_{22}O_6]$

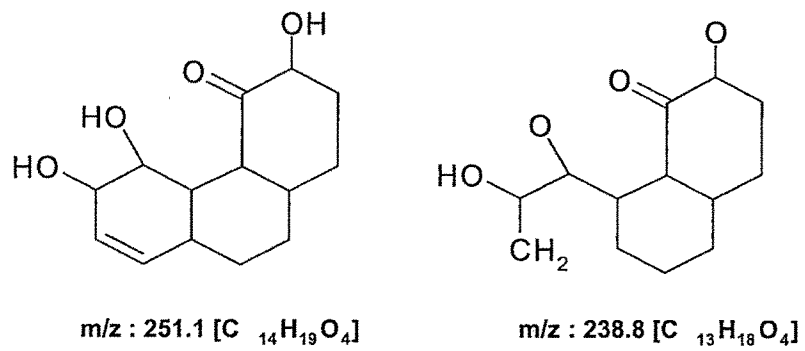


**Fig-3.31 Structure for AECHL-2 and its mass fragments**

### 3.2.6 Studies on AECHL-1 isolated from root bark of *Ailanthus excelsa*

#### 3.2.6.1 Effect of AECHL-1 on % cell viability of H9c2 cells

AECHL-1 was studied for its effect on % viability of H9c2 cells by MTT assay. After treatment with AECHL-1 (5, 10, 20, 50 and 100 µg/ml), for 12, 24, 48 and 72 hrs, cell viability was found to be decreased in concentration and time dependent manner. AECHL-1 (100 µg/ml) showed 59.7, 67.96, 32.42, and 30.89% cell viability after 12, 24, 48 and 72 Hrs of incubation when compared with that of vehicle control (Table-1.22, Fig-3.32, and 3.37A-F)

Thus AECHL-1 showed decreased cell viability in concentration and time dependent manner, showing it to be cytotoxic.

**Table-1.22 Effect of AECHL-1 % - viability of H9c2 cells**

<b>Conc. (µg/ml)</b>	<b>12Hrs</b>	<b>24Hrs</b>	<b>48Hrs</b>	<b>72Hrs</b>
Control	100±1.55	100±3.23	100±2.79	100±1.57
V. Control	105.28±2.59	105.28±3.57	102.15±1.72	105.23±5.50
5	85.99±2.45	88.99±1.45	71.57±4.21	69.37±1.30
10	87.96±1.47	85.55±4.51	65.26±3.15	64.37±2.61
20	83.78±1.22	81.87±0.48	63.78±1.68	59.16±1.83
50	72.97±0.49	77.83±1.29	48.21±1.68	39.79±0.26
100	59.7±1.96	67.96±2.91	32.42±2.94	30.89±.30

Values are expressed as mean ± SD of % cell viability (average of three determinations)

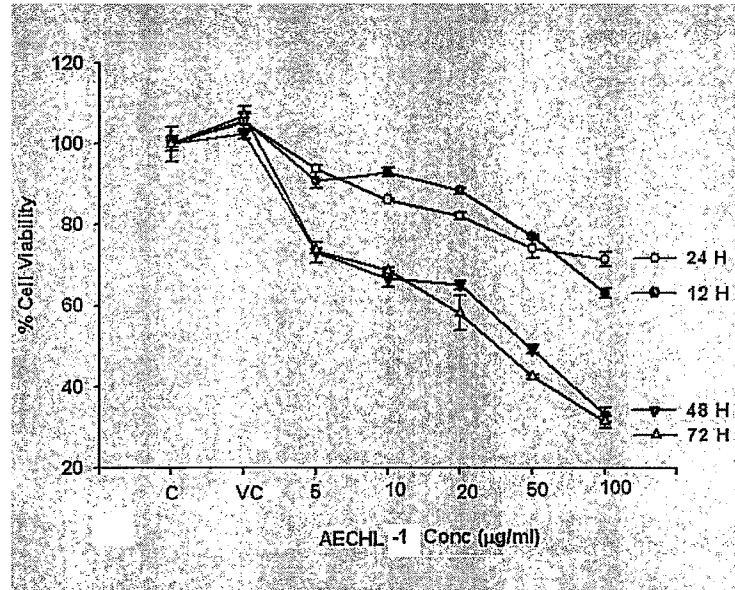


**Fig-3.32 Effect of various concentration of AECHL-1 on %-viability of H9c2 cells at different time interval**

### 3.2.6.2 Annexin-PI Staining for AECHL-1

Annexin V- PI staining was done in order to study the nature of cell death caused by AECHL-1 (Fig-3.33)

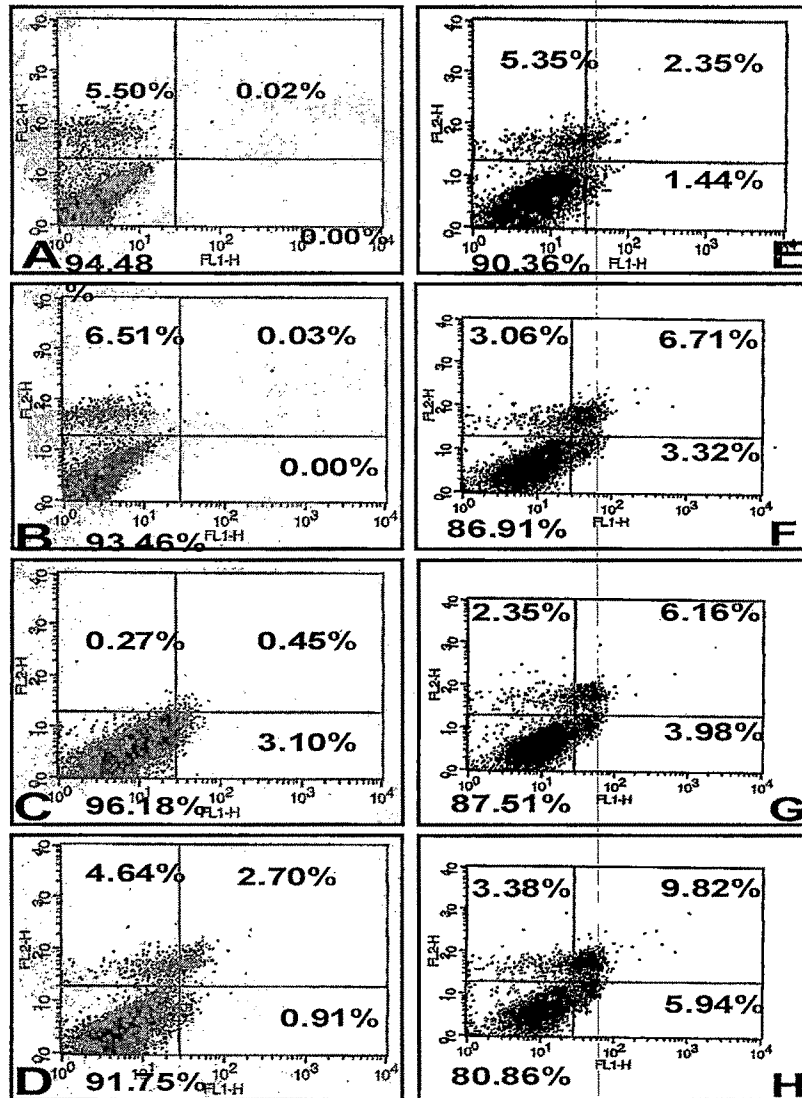


**Fig-3.33 Annexin-V and PI staining of the H9c2 cells treated with AECHL-1 for 48hrs.**

A) Unstained cells, B) PI stained cells, C) Annexin stained cells, D) Both Annexin and PI stained cells considered as control E) Annexin + PI treated with 0.2% DMSO considered as Vehicle control, F) Treated with AECHL-1 (10µg/ml) G) AECHL-1 (20µg/ml), H) AECHL-1 (50µg/ml). The percentage of cells in each quadrant is indicated.

In the above cytogram unstained and PI stained cells did not showed any apoptotic/necrotic cells (**fig. A & B**). vehicle control (0.2% DMSO) group (**fig E**) showed 1.44% of apoptotic cells and 2.35% necrotic cells with no significant change compared to that of control group (stained with Annexin V along with PI) (**fig. D**) with 0.91%, 2.70 respectively. In the above cytogram vehicle control (0.2% DMSO) group (**fig E**) showed 1.44% of apoptotic cells with no significant change compared to that of control group (stained with Annexin V and PI) (**fig. D**) with 0.91%. 48hr treatment with AECHL-1 (10 $\mu$ g/ml) showed increased in that of apoptotic cell 3.32% and late apoptotic/necrotic cells 6.71% (**fig. F**). Again AECHL-1 at 20 and 50 $\mu$ g/ml showed increased level of apoptotic cells ie 3.98%, 5.94% and late apoptotic/necrotic ie 6.16%, 9.82% respectively when compared with the vehicle control group (**fig G & H**).

Annexin-V and PI staining of the H9c2 cells treated with AECHL-1 was done and analyzed by FACs at the excitation wavelength 488nm. No significant difference between the control and vehicle treated group. Treatment with AECHL-1 showed increased both apoptotic and necrotic/late apoptotic cell death. As the concentration of AECHL-1 increased from 10 to 50 $\mu$ g/ml both necrotic and apoptotic cell percentage increased. Necrosis was found to be more prominent compared to apoptotic cells.

### **3.2.6.3 Effect of AECHL-1 on rat neonatal myocytes**

To study the effect of AECHL-1 on cardiovascular system, rat neonatal ventricular myocytes were isolated and after treatment with AECHL-1, mechanical properties of myocytes were assessed using an IonOptix MyoCam system. Cell mechanics were assessed using the peak shortening (PS), time-to-90% peak shortening (TPS), time-to-90% relengthening (TR<sub>90</sub>) along with maximal velocities of shortening (+dL/dt) and relengthening (-dL/dt). (Table-1.23, Fig-3.34)

**Table-1.23 Effect of AECHL-1 on mechanical properties of rat neonatal myocytes**

Treatment	Cell length	PS	TPS	TR <sub>90</sub>	+dL/dt	-dL/dt
CONTROL	17.88±0.68	31.89±4.05	6.41±0.65	6.91±0.49	103.65±6.72	56.15±4.86
AECHL-1 (2.5µg)	46.52±0.06***	2.22±0.2***	7.63±0.66 <sup>ns</sup>	7.96±0.53 <sup>ns</sup>	63.45±2.93**	70.71±5.71
AECHL-1 (5.0µg)	43.41±1.08***	24.5±2.23 <sup>ns</sup>	7.49±0.62 <sup>ns</sup>	8±0.34 <sup>ns</sup>	144.96±6.17*	156.23±6.23***
AECHL-1 5µg+Cal	50.31±0.73***##	22.25±1.79 <sup>ns</sup>	7.48±0.94 <sup>ns</sup>	8.21±0.47 <sup>ns</sup>	211.45±10.17***##	216.27±4.44***##
AECHL-1 7.5µg+Cal	49.02±0.93***##	15.2±1.35***#	8.74±0.41 <sup>ns</sup>	8.51±0.4 <sup>ns</sup>	141.44±9.76** <sup>ns</sup>	99.19±7.07***##
AECHL-1 10µg+Cal	43.56±0.05***##	1.87±0.19***##	4.98±0.73 <sup>ns</sup>	4.02±0.56***##	10.37±0.94***##	7.82±1.02***##

Statistical analysis was done by using ANOVA

Post test applied: Tukey-Kramer multiple comparison Test

Values are expressed as mean ± SEM.

\*p<0.05; \*\*p<0.01; \*\*\*p<0.001; <sup>ns</sup>p>0.05 = non significant, (n=20-25 myocytes)

For TPS: P value is 0.0087 is considered very significant.

For Other parameters: P value is < 0.0001, considered extremely significant

\*Compared with the control group

#Compared with AECHL-1 (5ug)

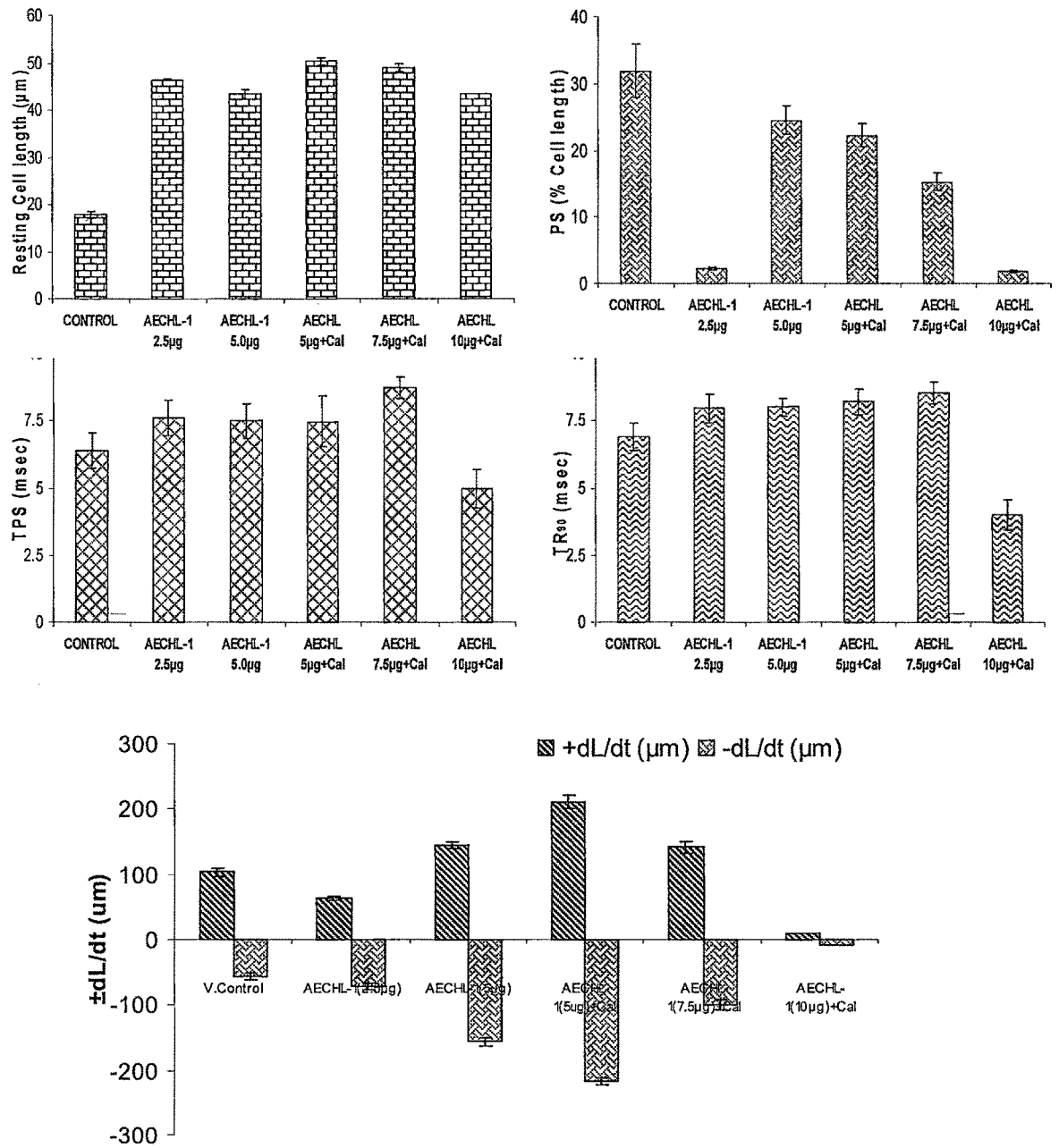


**Fig-3.34 Mechanical properties of ventricular myocytes of 2-3 days old infants**  
**A:** resting cell length. **B:** peak shortening (PS; as percentage cell length). **C:** time to peak shortening (TPS). **D:** time to 90% relengthening (TR<sub>90</sub>). **E:** maximal velocity of shortening (+dL/dt). **F:** maximal velocity of relengthening (-dL/dt).

AECHL-1 (conc. 2.5, 5 $\mu$ g) increased the resting cell length to 46.52 and 43.51 $\mu$ m respectively ( $P < 0.001$ ), compared to control 17.88 $\mu$ m. When AECHL-1 was supplemented with 1mM of calcium it further increases the resting cell length to 50.31, 49.02, 43.56 $\mu$ m ( $P < 0.001$ ) at concentration (5, 7.5, 10 $\mu$ g) respectively when compared with control. But this effect of AECHL-1 along with calcium was found to be decreased with increasing concentration of AECHL-1, when compared with AECHL1-(5 $\mu$ g) + calcium.

AECHL-1 also reduced the peak shortening (PS) to 2.22 ( $P < 0.001$ ) and 24.5% ( $p > 0.05$ ) compared to that of control with 31.89% at (conc. 2.5, 5 $\mu$ g). When supplemented with 1mM of calcium (PS) was further reduced to 22.25, 15.2, 1.87% with increasing concentration of AECHL-1, ie (5, 7.5, 10 $\mu$ g) respectively, compared to control ( $P < 0.001$ ) and (AECHL-5 $\mu$ g+ calcium) ( $P < 0.001$ ). The depression was higher at 10 $\mu$ g of AECHL-1 along with calcium.

AECHL-1 increases the time for peak shortening (TPS) with increased concentration ie. 7.63, 7.49 msec ( $P > 0.05$ ) at of 2.5 and 5 $\mu$ g respectively compared to control with 6.41 msec. This effect of AECHL-1 was further increased with calcium, ie. 8.74 msec at 7.5 $\mu$ g of AECHL-1, but gets abolished at 10 $\mu$ g of AECHL-1 with calcium. ie. 4.98msec ( $P > 0.05$ ) when compared with control and AECHL-1 (5 $\mu$ g) + calcium.

In the same way AECHL-1 increases the ( $TR_{90}$ ) with increasing concentration ie. 7.96, 8 msec with 2.5 and 5.0 $\mu$ g ( $P > 0.05$ ) of AECHL-1 when compared with the control 6.91msec. This effect of AECHL-1 was further increased with calcium supplementation, ie. 8.21, 8.51msec ( $P > 0.05$ ), at 5 and 7.5 $\mu$ g compared to control 6.91msec. Further increase in AECHL-1 concentration ie 10 $\mu$ g results in sudden decrease in  $TR_{90}$  to 4.02 msec ( $P < 0.001$ ) when compared with control and AECHL-1 (5 $\mu$ g+ calcium).

AECHL-1 showed initial stimulation of neonatal cardiomyocytes which gets abolished with increasing concentration (Fig-3.34).

#### **3.2.6.4 Effect of AECHL-1 on cytosolic and nuclear calcium in H9c2 cells**

Fluo-3 acetoxymethyl (AM) ester was used as the fluorescent indicator, which gets excited at 488nm and it emits a yellowish green fluorescence at 525nm when bound with calcium ions. The intensity of calcium depends on the free calcium concentration. When loaded on cells, intra cellular esterases break down the fluo 3AM ester into acetoxymethyl and fluo 3 which can readily combines with free intracellular calcium ions.

Flow activated cytometry and confocal analysis of H9c2 cells treated with AECHL-1 and stained with the molecular probe fluo 3 AM was done in order to analyze the effect of AECHL-1 on intracellular calcium uptake. With fluo 3-AM, the baseline fluorescence was located in the cytoplasm and with increasing concentration of AECHL-1 calcium concentration in the perinuclear was found to be significantly increased when compared with the control cells.

After 20 and 60 mins incubation of H9c2 cells with AECHL-1 (10µg/ml) increased the fluorescence intensity to 4.90 and 10.48% respectively (Fig-3.36a-c), while treatment with 20µg/ml for the same period increased the fluorescence intensity to 9.93 and 27.44% respectively (Fig-3.36b-d) compared to that of untreated (1.80%). Thus AECHL-1 showed time and concentration dependent increase in intracellular calcium uptake.

The results were confirmed by using data analyzed for unstained (0.00%), stained (1.80%), EGTA (0.10%), calcium (16.44%), ionomycin (17.59%), Calcium + Ionomycin (65.36%) respectively (Fig- 3.35a-i).

Where, cells after loading with fluo-3 shows increased fluorescence intensity in the perinuclear region of cells, unstained cells did not showed any region of fluorescence. Addition of EGTA showed decrease in fluorescence intensity in the perinuclear region and increased intensity in nucleus with death of cells. Calcium supplement showed increased fluorescence intensity which further increased after incubation with ionomycin (Fig-3.35A-E).

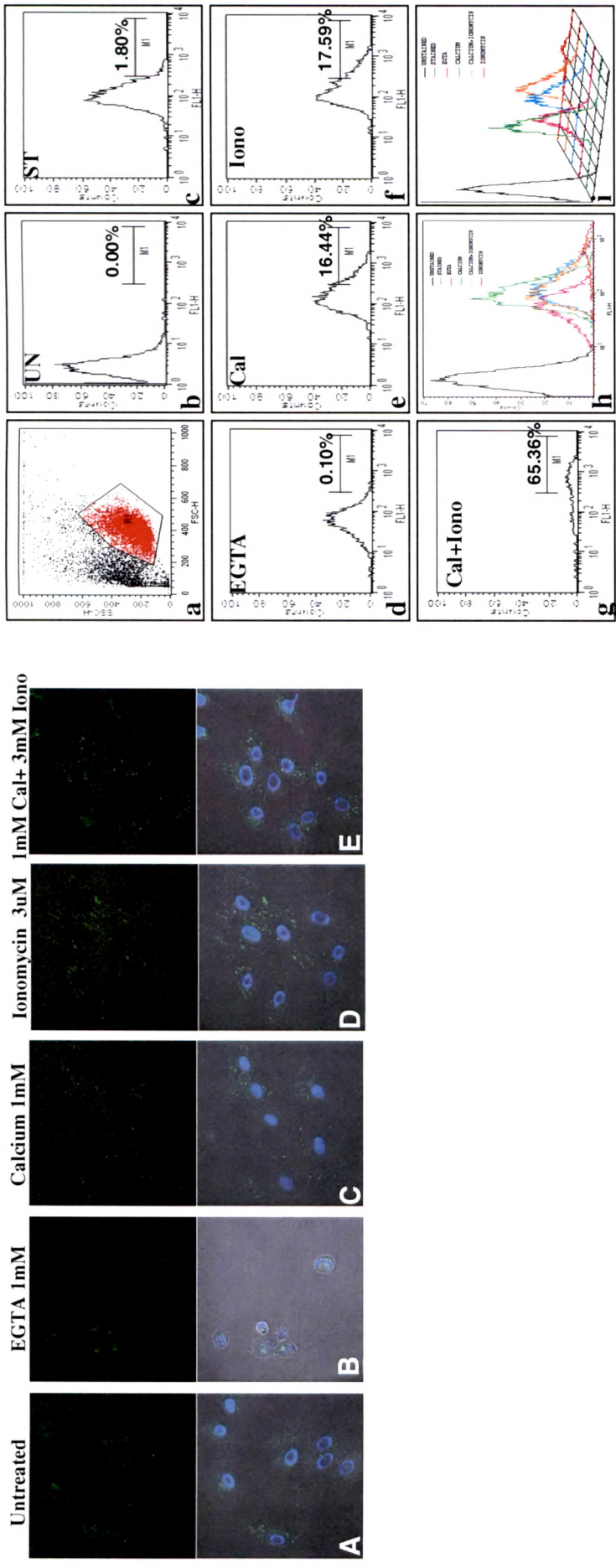


**Fig-3.35 Effect of Ionomycin and EGTA intracellular calcium levels in H9c2 cell lines after loading with fluo 3 AM A-E) Confocal images, a-i) FACS images of H9c2 cells after pretreatment with AECHE-1 and loaded with fluo 3 AM**

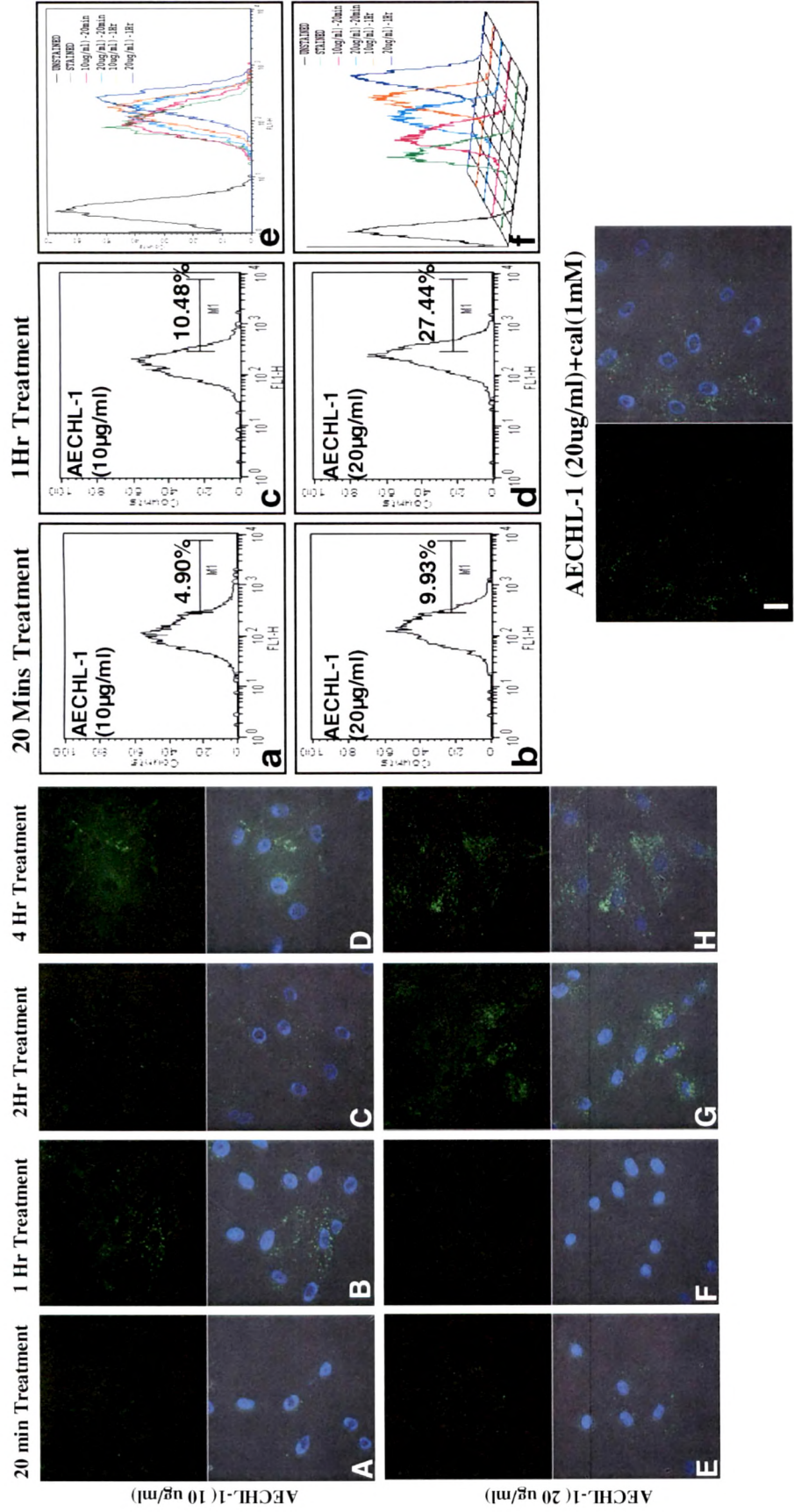


**Fig-3.36 Effect of AECHL-1 on intracellular calcium levels in H9c2 cell lines after loading with fluo 3 AM. A-f) Confocal images, a-f) FACS images of H9c2 cells after pretreatment with AECHL-1 and loaded with fluo 3 AM**

The above data was further confirmed by confocal analysis, where after 4 hrs of treatment EGTA treated cells found to be died (fig-3.35 B), and fluorescence intensity of calcium marker probe fluo-3 AM was increased as Untreated < Calcium 1mM < Ionomycin 3 $\mu$ M < Calcium + Ionomycin.

In the same way H9c2 cells were incubated with AECHL-1 (10 and 20 $\mu$ g/ml) for different time interval ie 20min, 1, 2, 3 and 4 hrs respectively. After incubation time cells were treated with fluo 3 AM for the detection of intracellular calcium.

Incubation with 10 $\mu$ g/ml of AECHL-1 showed increased intracellular calcium level after 1hr and 4 hr based on the intensity of fluorescence seen in (fig-3.36 A-D). The intensity was more in 4hr treatment. While incubation with 20 $\mu$ g/ml of AECHL-1 showed increased calcium level after 2 nad 4 hrs incubation (Fig-3.36E-H).

Incubation with 20 $\mu$ g/ml of AECHL-1 and 1mM of calcium did not show any significant change after 4hrs of treatment (Fig-3.36 I).

Thus AECHL-1 was found to increase an intracellular calcium level in perinuclear area.

Calcium ions have a wide variety of important functions in the activity of the cardiovascular system. They control transmitter release, synaptic plasticity; firing rate, gene expression, and cell death (Meir A, 1999; Clapham DE, 1995). There is no doubt that calcium ions entering through the surface membrane have a major function in many of these processes. In recent years, however, a growing body of evidence suggests that calcium released from intracellular stores may play an important role in calcium control of neuronal function (David G, 1998; Eilers J, 1996). Hence, the study of intracellular calcium dynamics is significant in this context. Thus it is an exciting way to study such dynamics through the examination of calcium sparks.

### **3.2.6.5 Effect of AECHL-1 on intracellular ROS level**

In order to detect the effect of AECHL-1 on intracellular ROS, H9c2 cells were treated with AECHL-1 (10 & 50 µg/ml) and incubated for 24hrs. ROS was assessed by flow cytometric analysis after loading the cells with the ROS-sensitive dye DCFH-DA. As shown in (Fig- 3.39A-D), an increase in DCF was observed in the AECHL-1 treated cells, with the mean fluorescence intensity increased from 4.45% to 46.38%. For further confirmation, the cells treated with AECHL-1 (10-100 µg/ml) under the same conditions were subjected to confocal microscopy. As shown in (Fig-3.38a-f), no change in fluorescence intensity was observed when compared with the vehicle treated cells.

### **3.2.6.6 Effects of AECHL-1 on mitochondrial membrane potential ( $\Delta\Psi_m$ )**

Loss of ( $\Delta\Psi_m$ ) is a limiting factor in the apoptotic pathway. DiOC<sub>6</sub>, a mitochondrial voltage dependent dye was employed to observe the changes in membrane potential. After exposing the cells to AECHL-1 (10-50 µg/ml) for 24hrs, DiOC<sub>6</sub> intensity was significantly increased, while at 100 µg/ml concentration fluorescence intensity was decreased, when analyzed in confocal microscopy compared to the vehicle treated (Fig-3.38M - R).

AECHL-1 increased the mitochondrial membrane potential at lower concentration while it was decreased at higher concentration. (Fig- 3.38N-Q).

During this study we observed the formation of crystalline sheath around the microtubules after treatment of H9c2 cells with AECHL-1 and loading with DiOC<sub>6</sub> (Fig-3.38B)

Membrane potential was further measured by using cell permeable cationic dye tetramethyl rhodamine (TMRE). AECHL-1 (10 & 50 µg/ml) reduced the membrane potential in H9c2 cells marked with increase fluorescence intensity from 15.20 to 30.08% when assessed by flow cytometric analysis after loading the cells with the  $\Delta\Psi_m$ -sensitive dye TMRE (Fig-3.39M-P).

Thus AECHL-1 showed concentration dependent loss of mitochondrial membrane potential.

#### **3.2.6.7 Effect of AECHL-1 on endogenous nitric oxide (NO) in H9c2 cells**

H9c2 cells pretreated with AECHL-1 for 24hrs after loading with DAF-2DA showed no change in fluorescence intensity when analyzed by confocal microscopy, but significant changes in cell morphology were observed (Fig-3.38B). Thus AECHL-1 did not showed generation of nitric oxide radicals in H9c2 cells.

#### **3.2.6.8 Effect of AECHL-1 on generation of superoxide radicals in H9c2 cells**

AECHL-1 treatment causes generation of  $O_2^{\cdot -}$ . Dihydroethidium (DHE) is a specific fluorescent dye for  $O_2^{\cdot -}$  was added to cells for tracking generation of ROS. Treatment of H9c2 cells with AECHL-1 (10-50 $\mu$ g/ml) increases the fluorescence intensity from 4.45 to 63.63% when assessed by flow cytometric analysis after loading the cells with the ROS-sensitive dye DHE (Fig-3.39E-H). This effect was further confirmed by confocal examination which showed  $O_2^{\cdot -}$  was dramatically enhanced in AECHL-1 (10-100 $\mu$ g/ml) exposed cells when compared with the vehicle treated cells (Fig-3.38G-I). H9c2 cells pretreated with SOD (50U) were found to reverse these AECHL-1 induced changes, confirmed by decreased fluorescence intensity in AECHL-1 pretreated cells (Fig-3.38B). Thus AECHL-1 was found to increase the intracellular superoxide radical formation which can be reversed with SOD.

#### **3.2.6.9 Effect of AECHL-1 on peroxynitrite formation in H9c2 cells.**

Pretreatment of H9c2 cells with AECHL-1 (10-50 $\mu$ g/ml), showed increased fluorescence intensity from 5.09 to 23.89% after loading with DHR 123 and assessing with FACs (Fig-3.39I-L).

This effect of AECHL-1 was not observed when H9c2 cells analyzed by confocal microscopy (Fig-3.38m-r). Thus AECHL-1 showed generation of peroxynitrite radicals in myocytes.

Peroxynitrite (ONOO $\cdot$ ) (PN) is a potent oxidant and nitrating species proposed as direct effectors of myocardial damage in numerous cardiac pathologies. This reactive species can be formed by the combination of superoxide ( $\cdot O_2^-$ ) and nitric oxide ( $\cdot NO$ ) radicals, generated *in vivo* (Balavoine, 1999) by, for example, endothelial cells, Kupffer cells, neutrophils and macrophages. ONOO $\cdot$  is a

relatively stable species compared with free radicals but once protonated gives highly reactive peroxyxynitrous acid (ONOOH) (Balavoine, 1999), decomposing with a very short half-life (1.9 s) at 37°C to form various cytotoxicants (Patel, 1999). ONOO<sup>-</sup> can induce the oxidation of thiol (-SH) groups on proteins, nitration of tyrosine, lipid peroxidation and also nitrosation reactions, affecting cell metabolism and signal transduction. It can ultimately contribute to cellular and tissue injury with DNA strand breakage and apoptotic cell death.

PN generation is favored when the production of both NO and O<sub>2</sub><sup>-</sup> is enhanced, as may occur during inflammation, circulatory shock and reperfusion injury (Liaudet L, 2000). In heart, PN generation occurs during myocardial infarction (Liaudet L, 2001), heart failure (Pacher P, 200) and cardiomyopathy due to anthracyclines (Pacher P, 2003). PN is generated in large amounts in the myocardium during myocardial reperfusion injury (Liaudet L, 2001), chronic heart failure (Pacher P, 200), circulatory shock (Lancel S, 2004) and anthracycline cardiomyopathy (Pacher P, 2003). Thus PN has generally been considered as directly biotoxic towards cardiomyocytes.

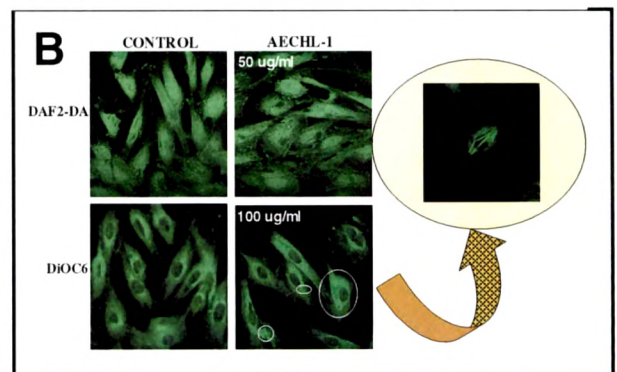
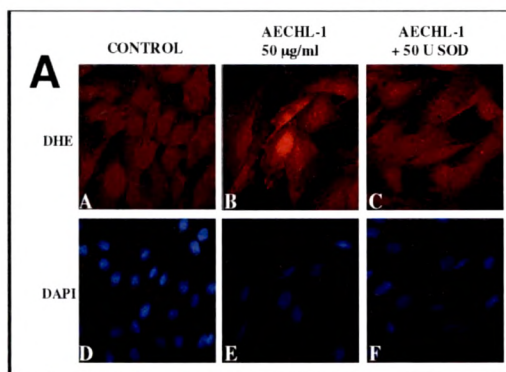
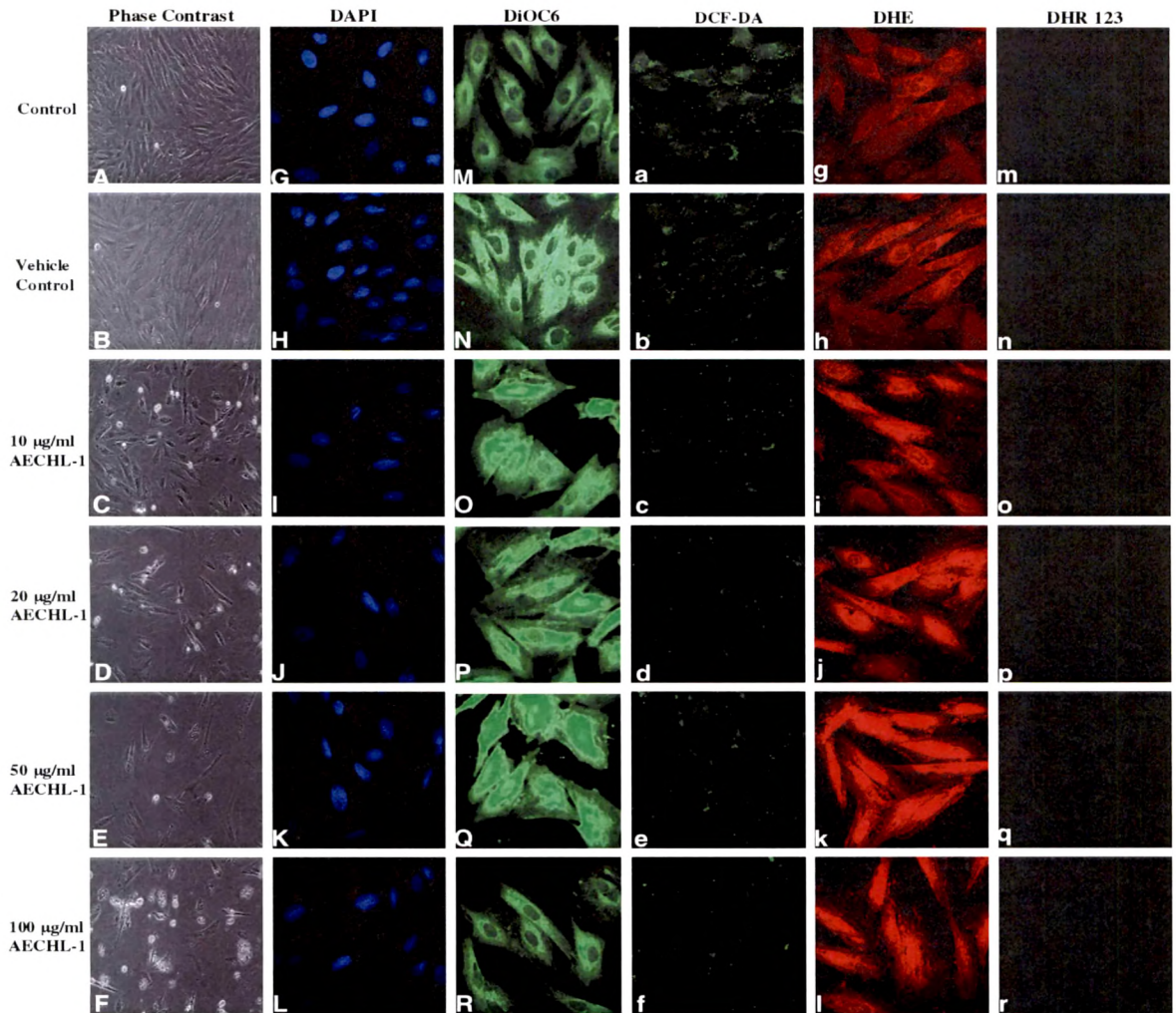


**Fig-3.37 (A-F) Phase contrast images of H9c2 cells showing the effect of AECHL-1**  
**Fig-3.38 (G-r) Confocal images of H9c2 cells showing the effect of AECHL-1.**  
**Fig-3.38A-Effect of SOD on AECHL-1 generated superoxide radicals**  
**Fig-3.38B-DAF2DA and DiOC6 stained cells after treatment with AECHL-1**

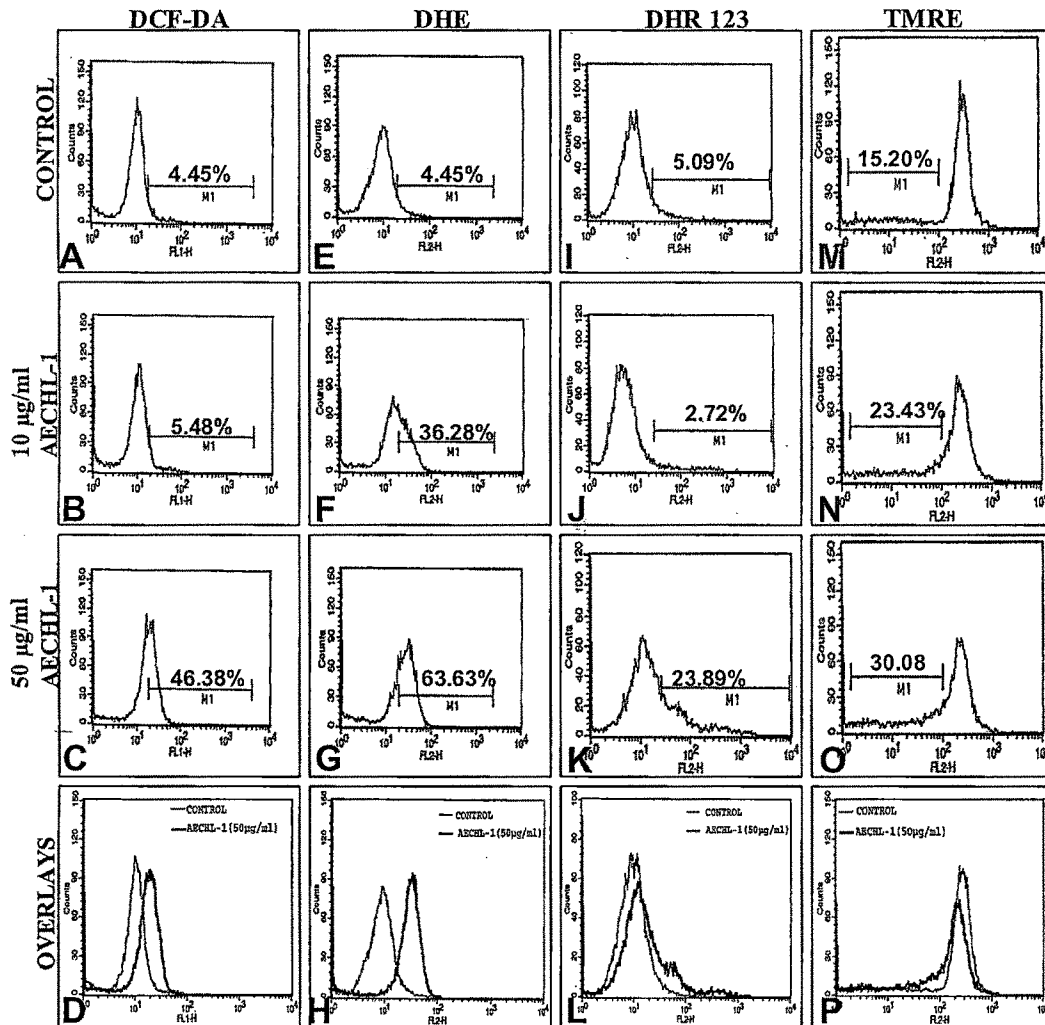


**Fig-3.39 (A-R) Flow activated cytometric analysis of H9c2 cells pretreated with different concentration of AECHL-1.**

### **3.2.6.10 Flow cytometry analysis of DNA content for cell cycle treated with different concentrations of AECHL-1 (Fig-3.40 & Fig- 3.41)**

Cell cycle analysis based on measurements of DNA content, generates a clear pattern of distribution of G<sub>0</sub>/G<sub>1</sub> phase, S phase and G<sub>2</sub>/M phase. DNA content was measured using fluorescent; DNA-selective stains propidium iodide (PI), that exhibit emission signals proportional to DNA mass. Flow cytometric analysis of these stained populations was used to produce a frequency histogram that reveals the various phases of the cell cycle.

H9c2 cells were incubated with AECHL-1 for 24, 48, 72 hr and cell cycle analysis was performed. The percentage of cells in G<sub>0</sub>/G<sub>1</sub>, S, and G<sub>2</sub>/M of the cell cycle was analyzed by flowcytometry and quantitated by Modfit software. The X axis represents the DNA content and Y axis represents the cell count (Fig-3.40 & Fig- 3.41).

In the present study Control cells showed a typical pattern of DNA content that reflected G<sub>0</sub>/G<sub>1</sub>-, S- and G<sub>2</sub>/M- phase of the cell cycle.

After 24 hrs treatment vehicle treated cells showed slight increase in cell count in G<sub>0</sub>/G<sub>1</sub> phase ie. 74.05% to that of control 69.44%. It also showed slight decrease in S phase cell count ie. 13.47% to that of control 17.80%. No change was occurred in G<sub>2</sub>/M phase compared to the control.

After 24 hrs of AECHL-1 (10, 20, 50 and 100µg/ml) showed significant increase in cell count of G<sub>0</sub>/G<sub>1</sub> phase ie. 80, 83.5, 80.59 and 79.28% to that of vehicle control 74.05% respectively. Cell count in G<sub>2</sub>/M phase was found to be decreased with AECHL-1 treatment at the above concentration range ie 10.94, 8.77, 6.85, and 8.70% compared to vehicle treatment 12.47%. AECHL-1 also decreased the cell count in S- phase ie 9.06, 7.58, 12.55 and 12.02% at the concentration of 10, 20, 50, 100 µg/ml respectively compared to control 13.47% respectively. AECHL treatment showed occurrence of debris ie 9.05, 6.29, 20.30 ad 22.57% in the concentration range of 10, 20, 50 and 100µg/ml respectively compared to vehicle control 3.65%.

After 48 hours of AECHL-1 treatment control cells showed a typical pattern of DNA content that reflected G<sub>0</sub>/G<sub>1</sub>-, S- and G<sub>2</sub>/M- phase of the cell cycle.

Vehicle treated cells showed slight increase in cell count in G0/G1 phase ie. 81.52% to that of control 79.71%. It also showed slight decrease in G2/M phase cell count ie. 7.79% to that of control 9.07%. No change occurred in S phase count compared to the control.

Treatment with AECHL-1 10 µg/ml showed slight increase in G0/G1 phase cell count ie 82.32% compared to that of vehicle control 81.52% respectively. While at the higher concentration (20, 50 and 100µg/ml) G0/G1 phase cell count were found to be significantly decreased ie. 72.27, 67.53 and 58.48% respectively compared to vehicle treatment 81.52%. Synthesis phase cell count was found to be increased with increasing concentration of AECHL-1, ie. 4.17, 5.96, 6.32 and 7.87% but found to be less to that of vehicle control 8.54% respectively. G2/M phase was found to be decreased with AECHL-1 treatment (10, 20, 50 and 100µg/ml) ie 6.24, 4.49, 4.59 and 5.45% compared to that of vehicle control 7.79%. As the concentration of AECHL-1 amount of necrotic cells were found to be increased ie. 7.40, 17.54, 21.89 and 28.157% when compared to that of vehicle treated 2.33%.

After 72 hours of AECHL-1 treatment control cells showed a typical pattern of DNA content that reflected G0/G1-, S- and G2/M- phase of the cell cycle.

In 72 hrs treatment vehicle treated cells showed slight increase in cell count in G0/G1 phase ie. 83.07% to that of control 81.08%. It also showed slight decrease in G2/M and S- phase cell count ie. 6.92% and 6.69% to that of vehicle control, 7.94% and 7.36% respectively.

72 hrs incubation of H9c2 with AECHL-1 (10, 20, 50, 100µg/ml) showed decrease cell count of G0/G1 phase ie.75.38, 68.81, 57.98, and 47.47% respectively compared to that of vehicle control 83.07%. Synthetic phase cell count was also found to be decreased ie. 5.71, 4.63, 4.82, and 5.46% respectively with that of vehicle control 7.36%. Same effect was observed in G2/M phase cell count.

After 72 hrs of incubation as the concentration of AECHL-1 increased necrotic cell count was found to be increased ie. 13.66, 21.37, 33.77, and 43.39% respectively compared to that of vehicle control 3.41%.

In the present study, AECHL-1 induced G2/M arrest in a concentration- and time-dependent manner.

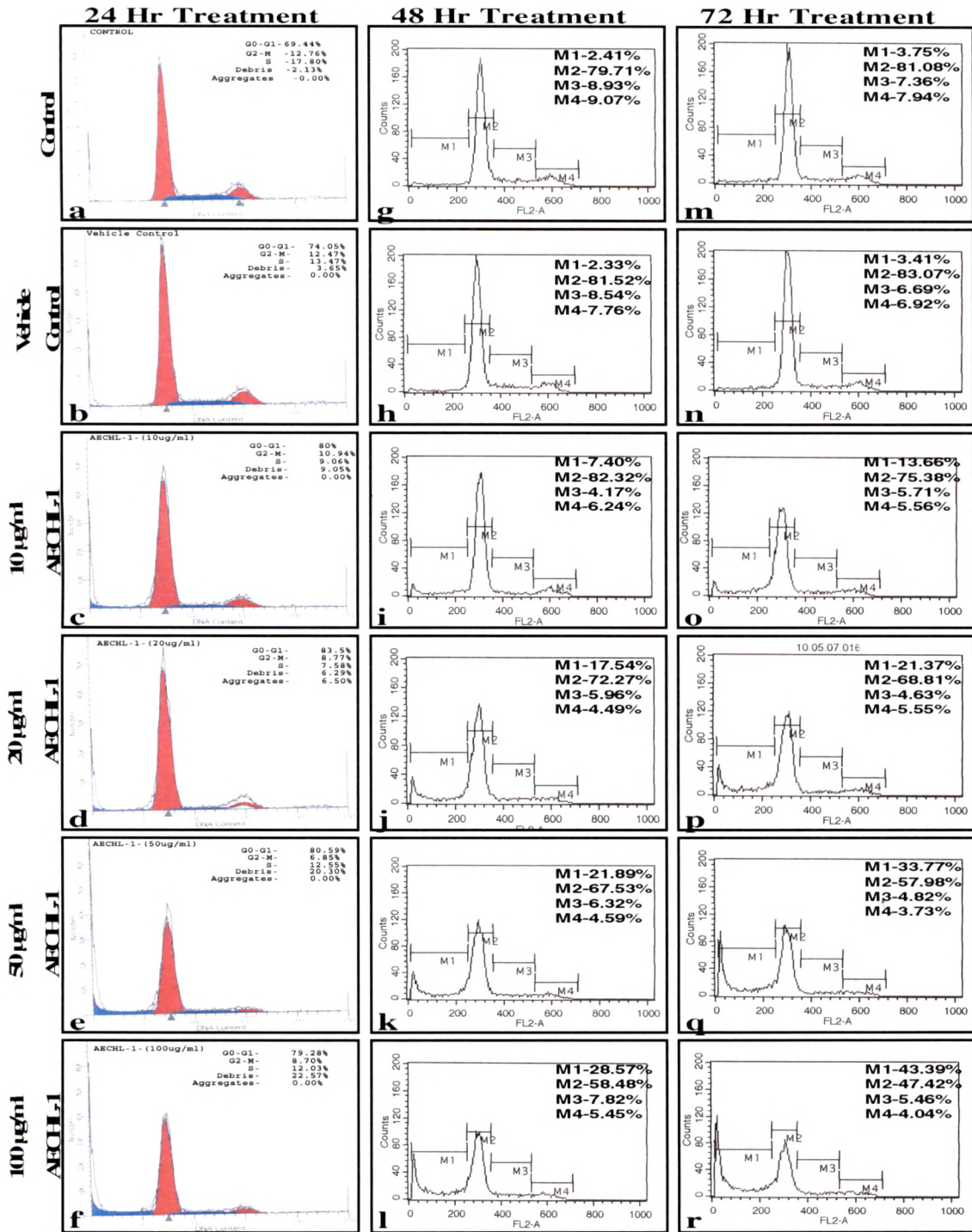


**Fig-3.40 Effect of AECHL-1 on DNA distribution in different phases of cell cycle of H9c2 cells**

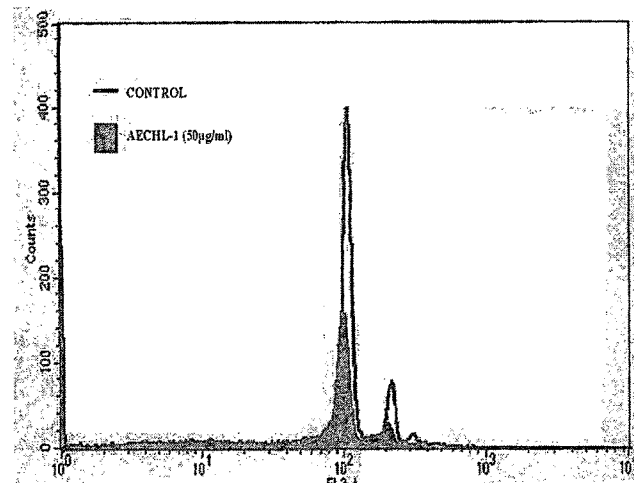


**Fig- 3.41 Cell cycle arrest with AECHL-1 after 48hrs incubation**

24 hrs treatment of AECHL-1, showed that cell proliferation was arrested in G<sub>0</sub>/G<sub>1</sub> phase confirmed by increased cell count in this phase and decreased cell count in S, G<sub>2</sub>/M phase. At higher concentration AECHL-1 forms necrotic cells due which variation in G<sub>0</sub>/G<sub>1</sub> and S phase occurred compared with the cells treated with lower concentration of AECHL-1.

After 48 hrs of treatment cell cycle get arrested in G<sub>0</sub>/G<sub>1</sub> phase at the low concentration (10µg/ml), but as the concentration of AECHL-1 increased formation of necrotic cells was found to be increased and this is the main reason for cell cycle arrest.

After 72 hrs of AECHL-1 treatment again the cell growth was found to be arrested due to the necrosis that's why the cell counts in all the phases was found to be decreased. No signs of apoptosis were observed.

### 3.2.7 Antitumor activity of AECHL-1 isolated from root bark of *Ailanthus excelsa*

Antitumor activity of AECHL-1 was evaluated in PC3 (prostate cancer cell line), MDA-MB (breast cancer cell line) and B16 (melanoma cells) using various *in vitro* and *in vivo* methods

#### 3.2.7.1 In vitro antitumor activity of AECHL-1

##### 3.2.7.1.1 Effect of AECHL-1 on viability of PC3, MDA-MB and B16 cell lines

###### a) Effect on viability - B16 Cells

Incubation of B16 cells with AECHL-1 (5-100µg/ml) showed concentration dependent effect on its viability.

Vehicle treated cells did not show any significant effect on viability of cells when compared with control. Incubation for 12 hrs showed 97, 50, 26, 11 and 6.06% cell viability, 24hrs incubation showed 89.49, 73.13, 46.33, 20.17, 7.51% of viable cells, while 48 hrs treatments with AECHL-1 showed 89.17, 78.83, 57.56, 18.76 and 3.62% cell viability at the concentration of 5, 10, 20, 50 and 100µg/ml respectively when compared with vehicle treated cells. (Table-1.24, Fig-3.42A)

Thus AECHL-1 showed concentration dependent effect on viability of B16 cells. The effect was nearly same at 12, 24 and 48 time interval. (Fig-3.42C)

**Table-1.24 Effect of AECHL-1 on % viability of B16 cells**

AECHL-1 (µg/ml)	12Hr	24Hr	48Hr
Control	100±4.5	100±2.9	100±6.8
V. Control	108.38±2.5	98.72±1.58	90.99±3.9
5µg	97.09±7.2	89.49±2.77	89.17±3.0
10µg	50.58±2.1	73.13±2.64	78.83±2.8
20µg	26.079±0.6	46.33±1.13	57.56±2.6
50µg	11.54±0.7	20.17±1.20	18.76±1.1
100µg	6.063±0.4	7.51±0.7	3.62±0.2

Values are expressed as mean ± SD of % cell viability (average of three determinations)

**b) Effect on viability – PC3 Cells**

PC3 cells were incubated with various concentration of AECHL-1 (5-100µg/ml) for different time interval. At 12hr of treatment 84.55, 70.18, 62.05, 49.32, 40.37% viable cells were observed, after 24hrs treatment 81.53, 66.19, 65.62, 51.70, 38.92%, while after 48hrs treatment 92.26, 62.98, 58.83, 42.26 and 33.42% of cell viability was observed at 5, 10, 20, 50 and 100µg/ml concentration respectively when compared with vehicle treated cells. AECHL-1 showed concentration dependent effect on viability of PC3 cells. (Table-1.25, Fig-3.42A) (Fig-3.42C)

**Table-1.25 Effect of AECHL-1 on % viability of PC3 cells**

<b>AECHL-1 (µg/ml)</b>	<b>12Hr</b>	<b>24Hr</b>	<b>48Hr</b>
Control	100±2.5	100±2.6	100±4.4
V. Control	101.35±2.0	101.98±3.4	107.73±4.9
5µg	84.55±2.2	81.53±1.2	92.26±1.2
10µg	70.18±4.5	66.19±4.1	62.98±2.4
20µg	62.05±1.8	65.62±2.9	58.83±3.5
50µg	49.32±2.4	51.70±1.9	42.26±2
100µg	40.37±2.8	38.92±0.1	33.42±0.6

Values are expressed as mean ± SD of % cell viability (average of three determinations)

**c) Effect on viability – MDA-MB Cells**

MDA-MB cells when incubated for 12hrs with AECHL-1 showed 88.88, 44.44, 54.16, 66.66% of cell viability, while 24hrs treatments showed 75.82, 48.35, 78.02, 70.32, and 62.63% when compared with vehicle treated cells. After 48hrs of treatment AECHL-1 showed 56.63, 34.51, 31.85, 46.9 and 43.36% of cell viability at conc. 5, 10, 20, 50 and 100µg/ml respectively, when compared with vehicle treated cells.

Thus it showed concentration and time dependent effect on the viability of MDA-MB cells. At lower concentration ie 5-10µg cell viability was found to be decreased when compared with vehicle treated cells which further increases with increasing concentration. (Table-1.26, Fig-3.42A) (Fig-3.42C)

**Table-1.26 Effect of AECHL-1 on % viability of MDA-MB cells**

<b>AECHL-1 (<math>\mu\text{g/ml}</math>)</b>	<b>12 Hr</b>	<b>24 Hr</b>	<b>48 Hr</b>
Control	100 $\pm$ 1.42	100 $\pm$ 10.9	100 $\pm$ 9.18
V. Control	102.85 $\pm$ 11.42	90.09 $\pm$ 9.9	115.3 $\pm$ 5.1
5 $\mu\text{g}$	88.88 $\pm$ 11.03	75.82 $\pm$ 7.69	56.63 $\pm$ 5.3
10 $\mu\text{g}$	44.44 $\pm$ 4.16	48.35 $\pm$ 2.1	34.51 $\pm$ 3.77
20 $\mu\text{g}$	54.16 $\pm$ 10.15	78.02 $\pm$ 9.41	31.85 $\pm$ 4.9
50 $\mu\text{g}$	55.55 $\pm$ 8.54	70.32 $\pm$ 13.86	46.9 $\pm$ 3.9
100 $\mu\text{g}$	66.66 $\pm$ 6.66	62.63 $\pm$ 10.76	43.36 $\pm$ 4.09

Values are expressed as mean  $\pm$  SD of % cell viability (average of three determinations)

### 3.2.7.1.2 Tritiated thymidine ( $[^3\text{H}]\text{-TdR}$ ) incorporation assay in PC3, MDA-MB and B16 cell lines

$^3\text{H}$ -thymidine when supplied to proliferating cells, gets incorporated into nascently synthesized DNA, which provides an accurate indicator of DNA synthesis. Quantitation was done by scintillation counting of labeled cells collected by aspiration upon membrane filters.

#### a) Effect of AECHL-1 on % proliferation of PC3 cell lines

To examine whether AECHL-1 affected cell growth, cell proliferation was measured by tritiated thymidine incorporation assay. In case of PC3 cell lines AECHL-1 (5-100 $\mu\text{g/ml}$ ) induced a concentration-dependent inhibition of cell proliferation. AECHL-1 at (conc. 5, 10, 20, and 50 $\mu\text{g/ml}$ ) showed 96.12, 40.96, 20.73, and 6.82% cell proliferation after 24 hrs treatment, while 53.52, 32.57, 20.059, and 3.57% proliferation after 48hrs of treatment when compared with control (Table 1.27-, Fig-3.42B).

**Table-1.27 Effect of AECHL-1 on % proliferation of PC3 cells**

<b>PC3</b>		
<b>Conc. <math>\mu\text{g/ml}</math></b>	<b>24Hr Treatment</b>	<b>48 Hr Treatment</b>
0	19466.6 $\pm$ 2722.07	40500.47 $\pm$ 319.57
5	18711.4 $\pm$ 1802.68	21679.6 $\pm$ 2781.57
10	7974.13 $\pm$ 3050.25	13193.4 $\pm$ 3772.56
20	4036.66 $\pm$ 887.18	8340.13 $\pm$ 1692.19
50	1328.33 $\pm$ 166.56	1446 $\pm$ 294.66

Values are expressed as mean  $\pm$  SD of % cell viability (average of three determinations)

**b) Effect of AECHL-1 on % proliferation of B16 cell lines**

In B16 cells AECHL-1 showed concentration dependent effect. At 5, 10, 20, and 50µg/ml concentration AECHL-1 showed 95.94, 77.62, 27.73 and 1.2% of cell proliferation after 24hrs of treatment, while after 48hrs of treatment it showed 96.32, 86.09, 54.36 and 1.36% of cell proliferation when compared with control (Table-1.28, Fig-3.42B).

**Table-1.28 Effect of AECHL-1 on % proliferation of B16 cells**

<b>B16</b>		
<b>Conc. µg/ml</b>	<b>24Hr Treatment</b>	<b>48 Hr Treatment</b>
0	115629.3±13191.93	121459.7±8509.78
5	110941.3±2214.69	116993.7±10264.08
10	89754.13±8301.16	104566.5±7764.31
20	32068.4±2255.4	66026.13±7963.04
50	1398.33±208.92	1660.6±734.47

Values shown are average of three determinations and are expressed as mean ± SD.

**c) Effect of AECHL-1 on % proliferation of MDA-MB cell lines**

In case of MDA-MB cells AECHL-1 showed concentration and time dependent response. At 5, 10, 20, and 50µg/ml concentration AECHL-1 showed 92.68, 85.26, 75.26, and 70.22% cell proliferation after 24 hrs of treatment. While after 48 hrs treatment AECHL-1 showed 93.66, 65.93, 61.77 and 55.11% cell proliferation when compared with control (Table-1.29, Fig-3.42B).

**Table-1.29 Effect of AECHL-1 on % proliferation of MDA-MB cells**

<b>MDA-MB</b>		
<b>Conc. µg/ml</b>	<b>24Hr Treatment</b>	<b>48 Hr Treatment</b>
0	3417.067±583.10	3621.067±197.72
5	3167.205±179.84	3391.733±324.82
10	2913.4±334.88	2387.667±32.50
20	2571.733±120.40	2237.067±229.87
50	2399.667±49.7	1995.667±167.78

Values shown are average of three determinations and are expressed as mean ± SD.

Cell proliferation is the measurement of the number of cells that are dividing in a culture and is measured by analyzing the DNA synthesis by incorporating the labeled DNA precursors ( $^3\text{H}$ -thymidine) in cells and quantifying with liquid scintillation counter. Amount of the labeled precursor into DNA is directly proportional to the amount of cell division occurring in the culture.

AECHL-1 showed concentration and time dependent effect on the growth of these cancer cell lines. The effect was very much significant in PC3 and B16 cells, compared to MDA-MB cells. AECHL-1 showed significant inhibition in cell proliferation.

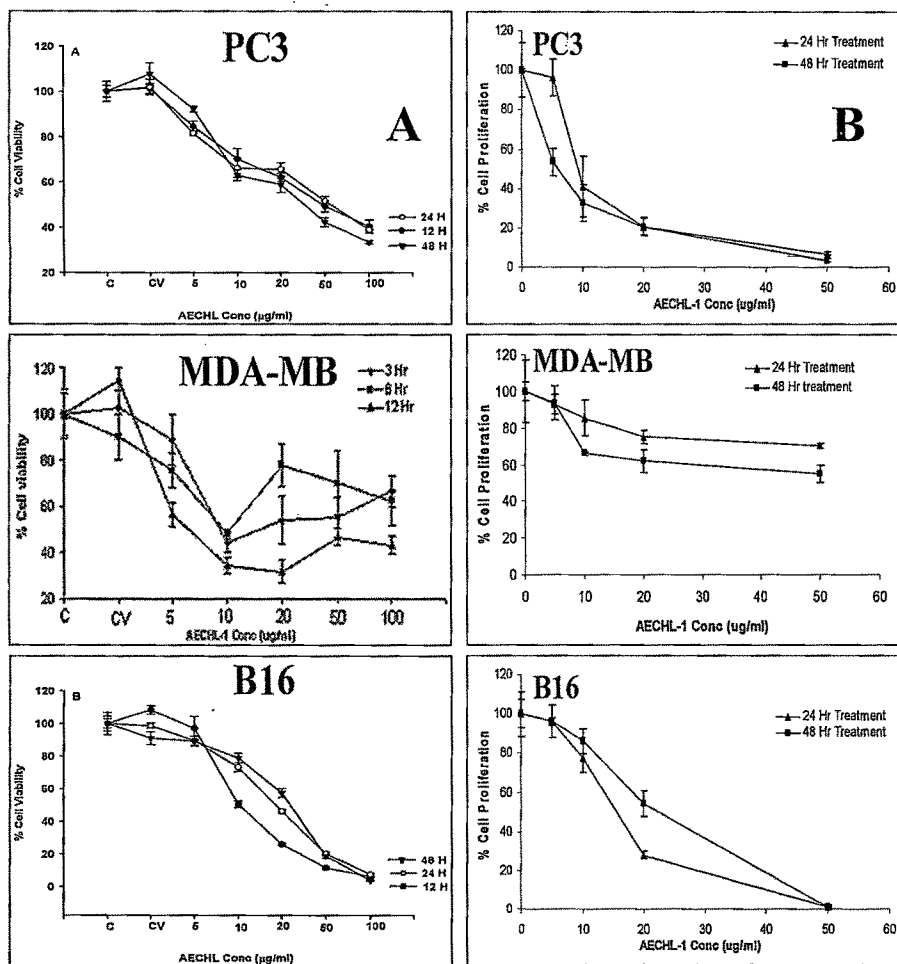


**Fig-3.42 Effect of AECHL-1 on A) viability and B) proliferation of PC3, MDA-MB and B16 cell lines at different time interval**

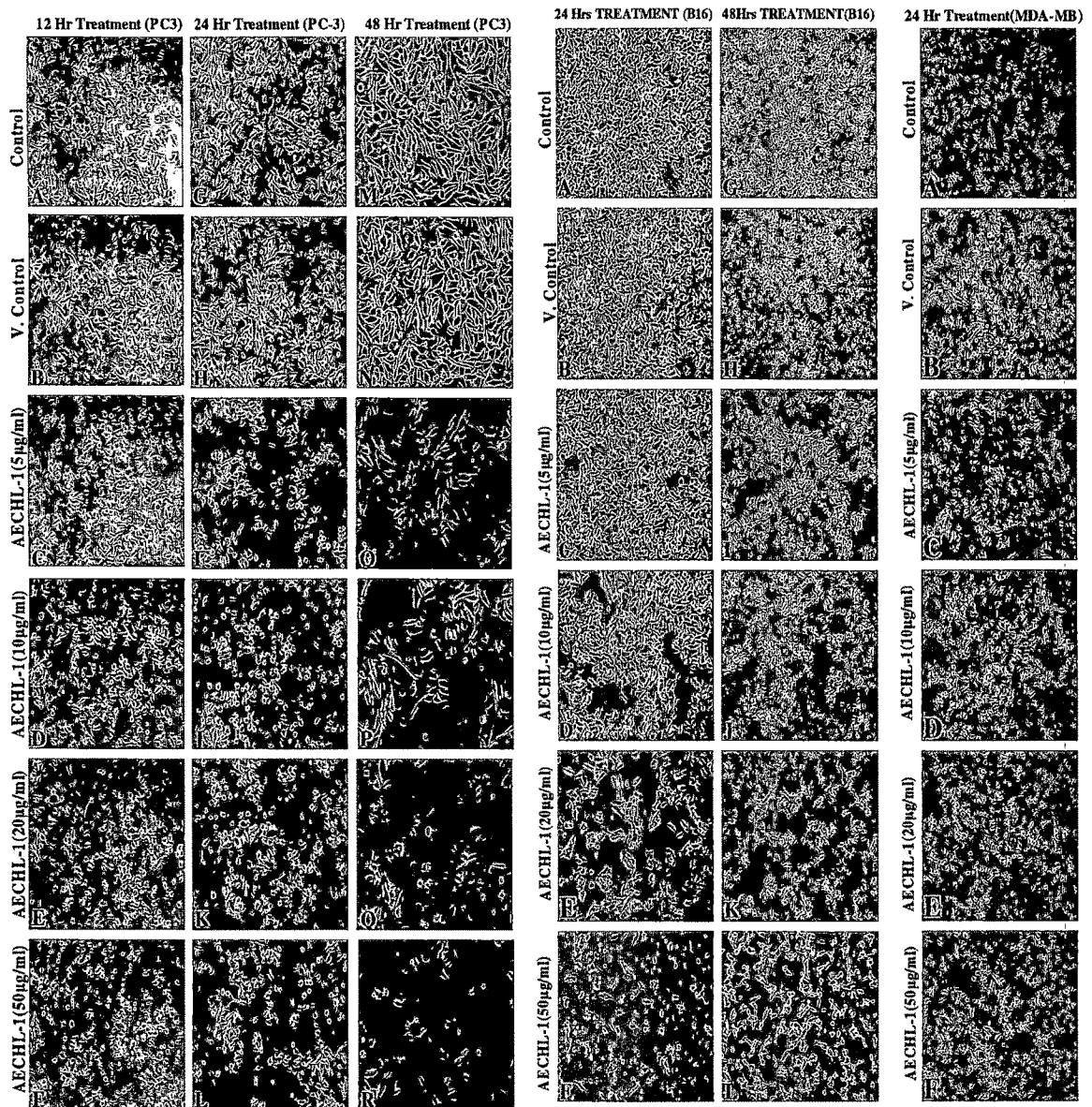


**Fig-3.42C-Phase contrast images showing the effect of AECHL-1 on different cancer cell lines**

### **3.2.7.1.3 Effect of AECHL-1 on DNA distribution in different phases of cell cycle**

Cell cycle analysis based on measurements of DNA content, generates a clear pattern of distribution of G0/G1 phase, S phase and G2/M phase. DNA content was measured using fluorescent DNA-selective stains propidium iodide (PI), that exhibit emission signals proportional to DNA mass. Flow cytometric analysis of these stained populations was used to produce a frequency histogram that reveals the various phases of the cell cycle.

#### ***a) Cell cycle analysis of PC3 cells***

PC3 cells treated with AECHL-1 (conc. 5, 10, 20, 50 $\mu$ g/ml) for 24 hours. Control cells showed a typical pattern of DNA content that reflected G0/G1-, S- and G2/M- phase of the cell cycle. Normal PC3 cells showed apoptotic cells. Vehicle treatment did not show any significant change in the distribution of the cells in the cycle.

Treatment with AECHL-1 (5 & 10 $\mu$ g/ml) showed increase in cell count of G0/G1 ie. 59% and 60.49% to that of the vehicle treated cells (58.45%) respectively. The cell count in S-phase was found to be decreased (12.36%) to that of vehicle treatment (14.52%). G2/M phase cell count was also found to be decreased (19.32 and 19.44%) to that of vehicle treatment (21%). Increased concentration of AECHL-1 (20 and 50 $\mu$ g/ml) showed increased percentage of apoptotic cell death ie. 12.06 and 12.11% to that of vehicle treatment 6.52% respectively. At these concentration, G0/G1 cell count was found to be slightly decreased ie. 56.87% to that of vehicle treatment 58.21%. While cell count in S-phase was found to be increase ie 15.53% to that of vehicle 14.52%. At 20 and 50 $\mu$ g/ml, significant reduction in G2/M phase cell count were observed ie. 15.85, 16.03 to that of vehicle treatment 21% (Fig-3.43).

### Flow Cytometry profile of PI stained (PC3) cells

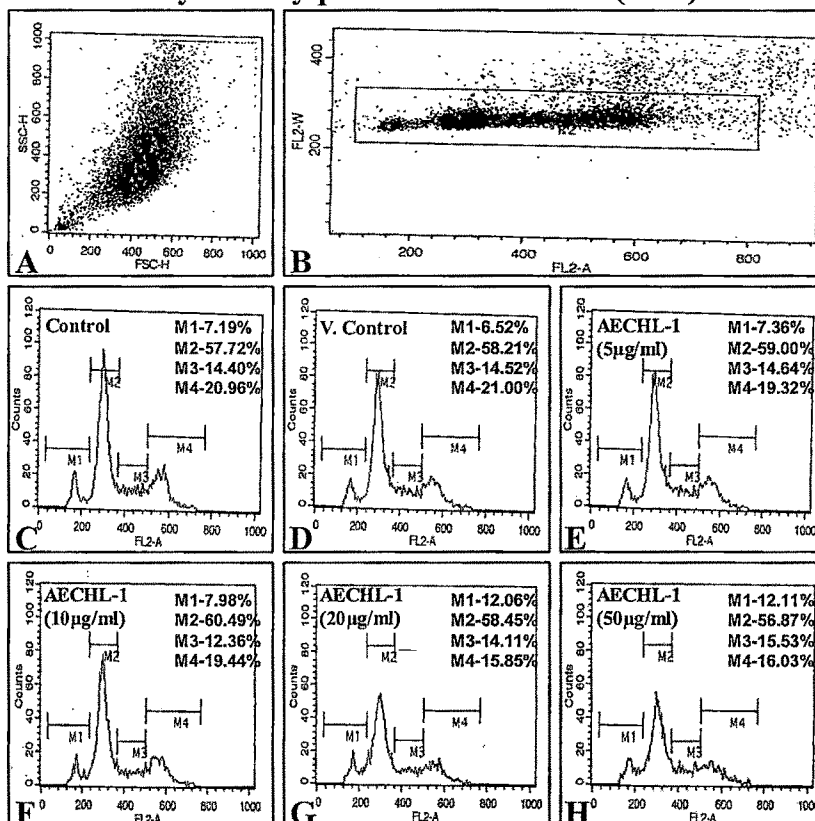


**Fig-3.43 Effect of AECHL-1 on DNA distribution in different phases of cell cycle of PC3 cells**

Treatment of PC3 cell lines with higher concentration of AECHL-1 showed apoptotic cell death with decreased cell count in G2/M phase thus inhibiting the cell cycle proliferation. While at lower concentration it showed apoptotic cell death and the cell growth was found to be arrested in G0/G1 phase, confirmed from increased cell count in G0/G1 and decreased cell count in S-G2/M phase. Thus AECHL-1 showed inhibition in cell proliferation by arresting cell cycle in G0/G1 with significant apoptotic cells.

**b) Cell cycle analysis of MDA-MB cells**

Treatment of MDA-MB cells with AECHL-1 (conc. 5, 10, 20, 50µg/ml) for 24 hours.

Control cells showed a typical pattern of DNA content that reflected G0/G1, S and G2/M phase of the cell cycle. Vehicle treated cells did not show any significant change in cell distribution pattern when compared with control.

Treatment with AECHL-1 (5, 10, 20, 50µg/ml) showed decreased cell count in G0/G1 phase ie.43.03, 33.18, 26.66 and 22.82% as compared to that of vehicle control 49.16% respectively. Cell count in S- phase was found to be increased with increasing concentration of AECHL-1 ie. 24.06, 28.63, 28.12, 30.99% to that of vehicle treated 25.73% respectively. Even treatment increased the cell count in G2/M phase ie. 32.21, 38.01, 45.14, 46.17% compared to that of vehicle treatment 24.10% respectively. AECHL-1 did not show any signs of necrosis in the cytogram (Fig-3.44).

**Flow Cytometry profile of PI stained (MDA-MB) cells**

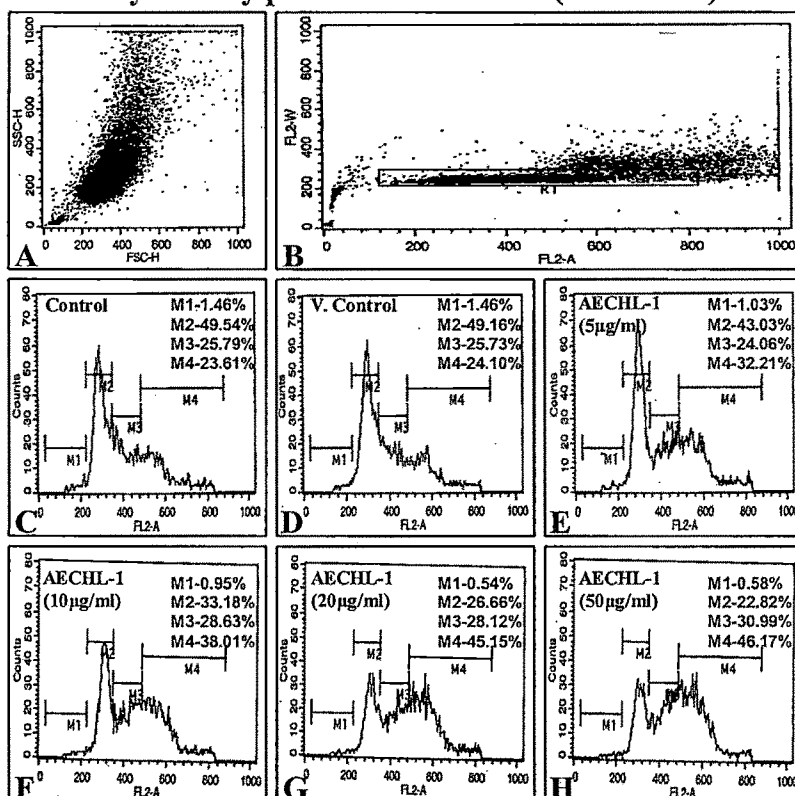
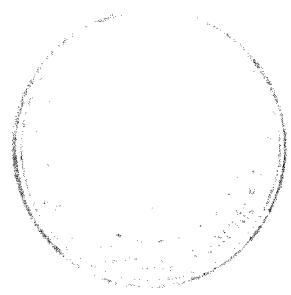


**Fig-3.44 Effect of AECHL-1 on DNA distribution in different phases of cell cycle of MDA-MB cells**

24 hr treatment of MDA-MB cells with different concentration of AECHL-1, showed cell cycle arrest in S-G2/M phase, confirmed by accumulation of cells in these phases and decreased cell count in G0/G1 phase. Most of the cells were found to be arrested in G2/M phase of the cell cycle. The effect was found to be concentration dependent. AECHL-1 did not show any signs of necrosis in MDA-MB

**c) Cell cycle analysis of B16 cells**

Treatment of B16 cells with AECHL-1 (conc. 5, 10, 20, 50 $\mu$ g/ml) for 24 hours. Control cells shows a typical pattern of DNA content that reflected G0/G1, S and G2/M phase of the cell cycle. Vehicle treated cells did not showed any significant change in cell distribution pattern, except slight decrease in G0/G1 phase ie 52.18% to that of control 55.64% and increase in G2/M phase cell count ie. 26.59% to that of control cell count 22.98% respectively when compared with control. Treatment with AECHL-1 showed marked increase in G0/G1 cell count ie. 56.55, 57.67, 72.08%, at the concentration of (5, 10, 20 $\mu$ g/ml) to that of Vehicle control 52.18% respectively. It also showed decrease cell count in S- phase ie. 20.46, 18.40, 11.43 (for the conc. 5, 10, 20 $\mu$ g/ml) to that of vehicle control 21.39% respectively. Cell count in G2/M phase was also found to be decreased ie. 23.02, to 14.73% to that of vehicle treated 26.59% respectively. For the concentration range 5-10 $\mu$ g/ml of AECHL-1 no apoptotic or necrotic cells were observed. But at higher concentration ie 50 $\mu$ g/ml cell growths was found to be inhibited due to apoptosis ie 7.82% to that of vehicle control 0.24% respectively. At 50  $\mu$ g/ml, the cell distribution was found to be, like, G0/G1-64.04%, S-15.41% and G2/M phase 13.23% respectively (Fig-3.45).



**Flow Cytometry profile of PI stained (B16) cells**

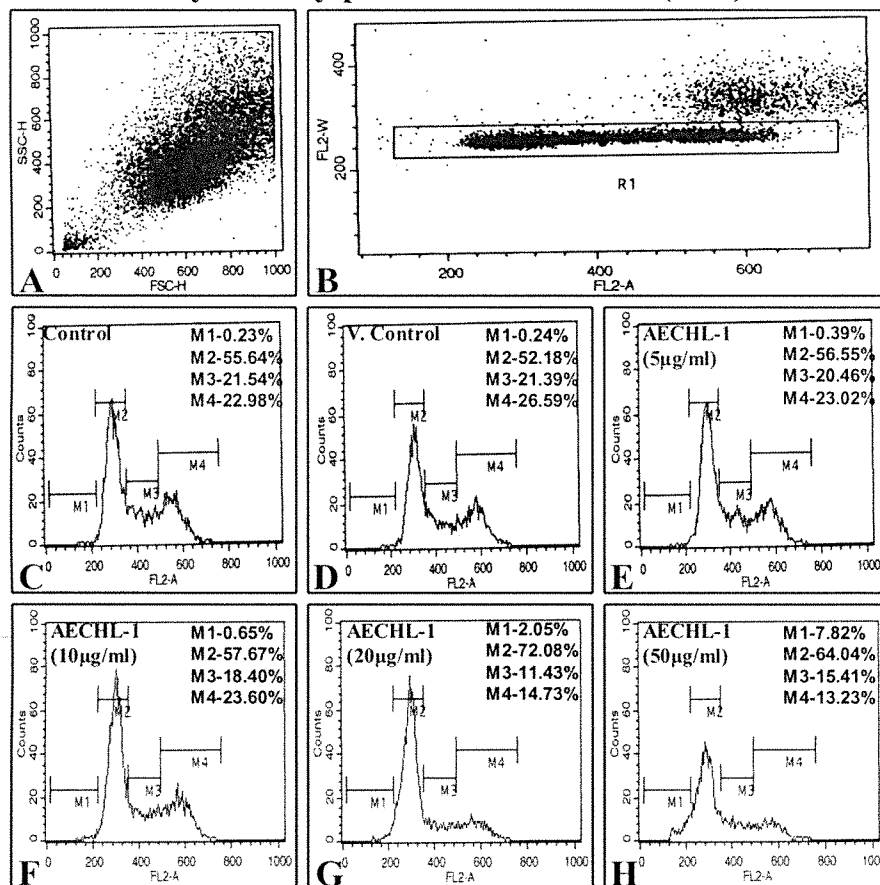


**Fig- 3.45 Effect of AECHL-1 on DNA distribution in different phases of cell cycle of B16 cells**

AECHL-1 arrests the cell cycle in G0/G1 phase, marked with increased cell count in this phase and decrease cell counts in S- and G2/M- phase. At higher concentration marked signs of apoptosis occur. Thus AECHL inhibits cell proliferation in concentration dependent manner, showing G0/G1 phase arrest at lower concentration while Go/G1 phase arrest with marked apoptosis at higher concentration.

### **3.2.7.2 In vivo antitumor activity in C57 mice**

#### **3.2.7.2.1 Toxicity study of AECHL-1**

C57 mice were injected with different concentrations of AECHL-1 (conc. 20, 50 and 100 $\mu$ ) by I.V. route and were observed for any signs of mortality. No mortality occurred during 21 days of observations. 50 and 100 $\mu$ g of AECHL-1 concentration were used for further studies based on *in vitro* studies.

#### **3.2.7.2.2 Antitumor activity**

5x10<sup>5</sup> B16-F10 melanoma cells in 100 $\mu$ l PBS were injected subcutaneously in the flank of C57Bl/6 mice. 15 days after inoculation animals were divided into four groups like control, AECHL-1 (50 $\mu$ g), AECHL-1 (100 $\mu$ g) and cis-platin (100 $\mu$ g) respectively with (n=6) in each group. Animals were given intratumor injections of AECHL-1 and cis-platin in PBS while control received only PBS for 15 days. Tumor volume was measured at definite interval during the study. At the termination of the experiment animals were sacrificed with ether anesthesia and tumor sample were prepared for biopsy and western blotting.

#### **a) Effect of AECHL-1 on tumor volume**

Intra group comparison of tumor volume showed, increase in tumor volume in control (p<0.001), AECHL-1 (50 $\mu$ g) (p<0.01), AECHL-1 (100 $\mu$ g) (p<0.01) and cis-platin (p<0.001) group on day 18<sup>th</sup> when compared to that of day 12<sup>th</sup>. On day 24<sup>th</sup> tumor volume in control, AECHL-1 (50 $\mu$ g) and AECHL-1 (100 $\mu$ g) was found to be increased (p<0.001), while that in cis-platin treated group volume was found to be decreased (p<0.001).

Inter group comparison in tumor volume showed no significant change in tumor volume on day 12<sup>th</sup> as the treatment was not started at this point, but on day 18<sup>th</sup> and significant decrease in tumor volume occurs in AECHL-1 (50 $\mu$ g) (p<0.001), AECHL-1 (100 $\mu$ g) (p<0.001) and cis-platin (p<0.001) treated groups (Table-1.30, Fig-3.46, Fig-3.49, 3.50)

Cis-platin was found to be extremely significant than AECHL-1 (50 $\mu$ g) and AECHL-1 (100 $\mu$ g). AECHL-1 (50 $\mu$ g) vs. AECHL-1 (100 $\mu$ g) was found to be non Significant (P>0.05).

Thus AECHL at both the concentrations prevents the growth of tumor cells with reduction in tumor volume when compared with control group.

**Table-1.30 Effect of AECHL-1 and Cis-platin on tumor volume during treatment**

<i>Treatment</i>	<i>12<sup>th</sup> Day</i>	<i>18<sup>th</sup> Day</i>	<i>24<sup>th</sup> Day</i>
Control	469.48±64.21	2344.3±141.14###	3891.9±361.12###
AECHL-1(50ug)	389.14±33.97	1012.9±60.17****	2167.7±202.89****
AECHL-(100ug)	484.58±76.82	888.07±111.17****	1906.5±49.52****
Cis-platin	376.93±23.84	1030.2±168.27****	267.35±20.93****

Statistical analysis was done by using ANOVA

Post test applied: Tukey-Kramer multiple comparison Test

Values are expressed as mean ± SEM.

\*p<0.05; \*\*p<0.01; \*\*\*p<0.001; <sup>ns</sup>p>0.05, (n=6)

#Intra group Comparison (<sup>ns</sup> P>0.05, #<0.05, ##P<0.01, ###P<0.00.1)

\*Inter group comparison (<sup>ns</sup> P>0.05, \*<0.05, \*\*P<0.01, \*\*\*P<0.00.1)

**Comparison:** 12th day Treatments with 12th day control, 18<sup>th</sup> day treatments with 18<sup>th</sup> day Control, 24<sup>th</sup> day treatments with 24<sup>th</sup> day Control

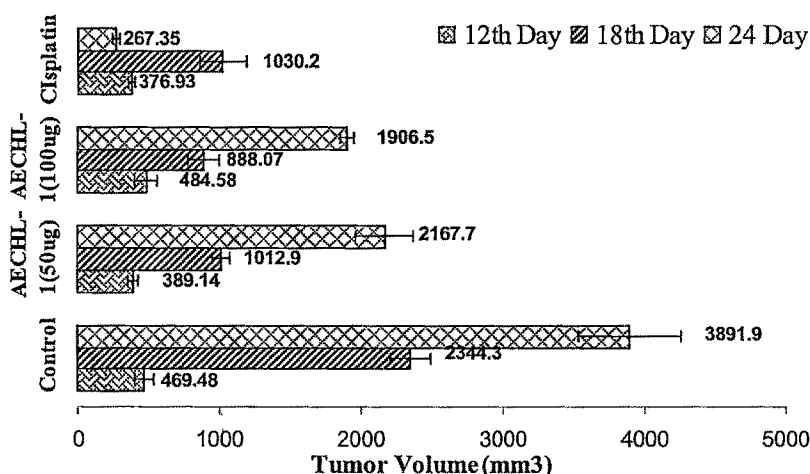


**Fig- 3.46 Effect of AECHL-1 and Cis-platin on tumor volume in C57 mice**

**b) Effect of AECHL-1 on tumor weight/Body weight ratio**

Treatment with AECHL-1 50µg, 100µg and cis-platin showed significant reduction in tumor weight to body weight ratio after 12 days treatment (p<0.01) when compared with control group.

Compared to AECHL-1 (100 µg) effect was more in AECHL-1 (50µg). Cis-platin treated group showed significant reduction in ratio, when compared with AECHL-1 and control groups (Fig-3.47, 3.50).

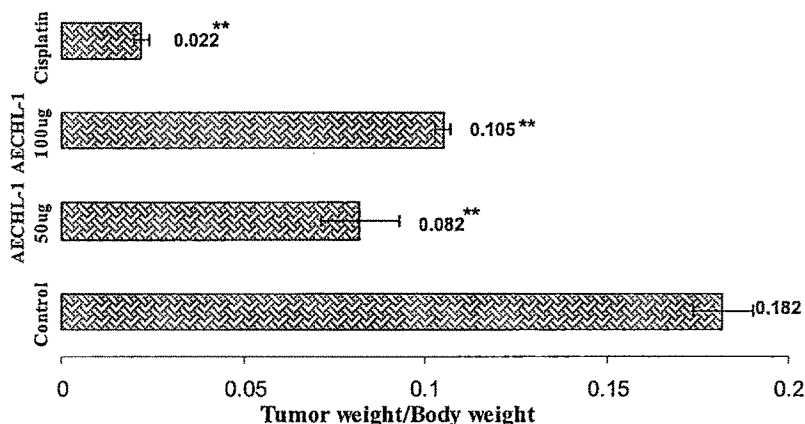


**Fig-3.47 Effect of AECHL-1 on tumor weight to body weight ratio**

Statistical analysis was done by using ANOVA  
 Post test applied: Dunnett multiple comparisons test.  
 Values are expressed as mean  $\pm$  SEM.  
 \* $p < 0.05$ ; \*\* $p < 0.01$ ; \*\*\* $p < 0.001$ ;  $^{ns}p > 0.05$ , (n=6)  
 Comparison made with control group ratio.

**c) Effect on Body weight**

**Table-1.31 Weight variations during treatment**

DAYS	Body weight (Gms)			
	Control	AECHL-1 (50 $\mu$ g)	AECHL-(100 $\mu$ g)	Cis-platin
0	27.6 $\pm$ 0.22	24.55 $\pm$ 0.3	27.47 $\pm$ 0.28	20.43 $\pm$ 0.69
12	28.47 $\pm$ 0.64 $^{ns}$	26.45 $\pm$ .32**	28.02 $\pm$ 0.35 $^{ns}$	21.9 $\pm$ 0.68 $^{ns}$
18	27.15 $\pm$ 0.37 $^{ns}$	26.47 $\pm$ 0.33 $^{ns}$	28.56 $\pm$ 1.19 $^{ns}$	18.77 $\pm$ 0.8*
24	27.57 $\pm$ 0.44 $^{ns}$	24.57 $\pm$ 0.28**	30.19 $\pm$ 0.98 $^{ns}$	18.65 $\pm$ 0.81*

Statistical analysis was done by using ANOVA  
 Post test: Tukey-Kramer multiple comparison Test  
 Values are expressed as mean  $\pm$  SEM.  
 \* $p < 0.05$ ; \*\* $p < 0.01$ ; \*\*\* $p < 0.001$ ;  $^{ns}p > 0.05$  = non significant, (n=6)  
 #”12<sup>th</sup> day compared with “0” day weight  
 \*18<sup>th</sup> and 24<sup>th</sup> day compared with 12<sup>th</sup> day animal weight

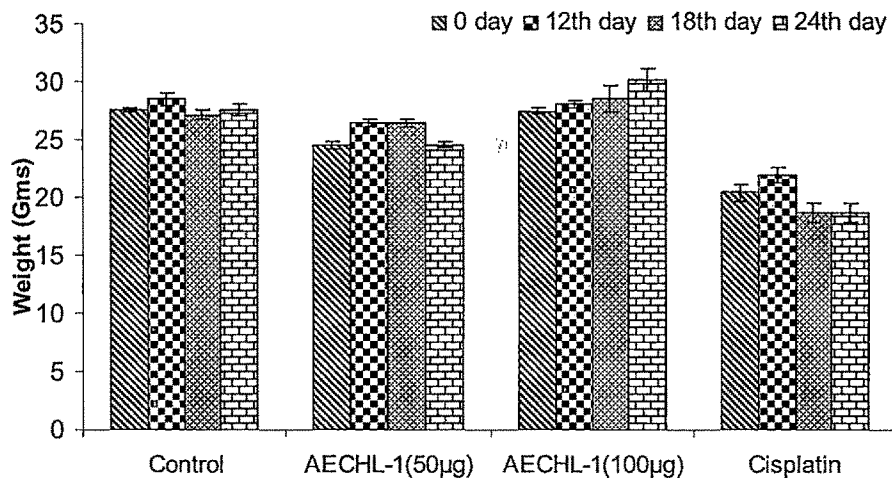


**Fig-3.48 Effect of AECHL-1 on body weight of mice**

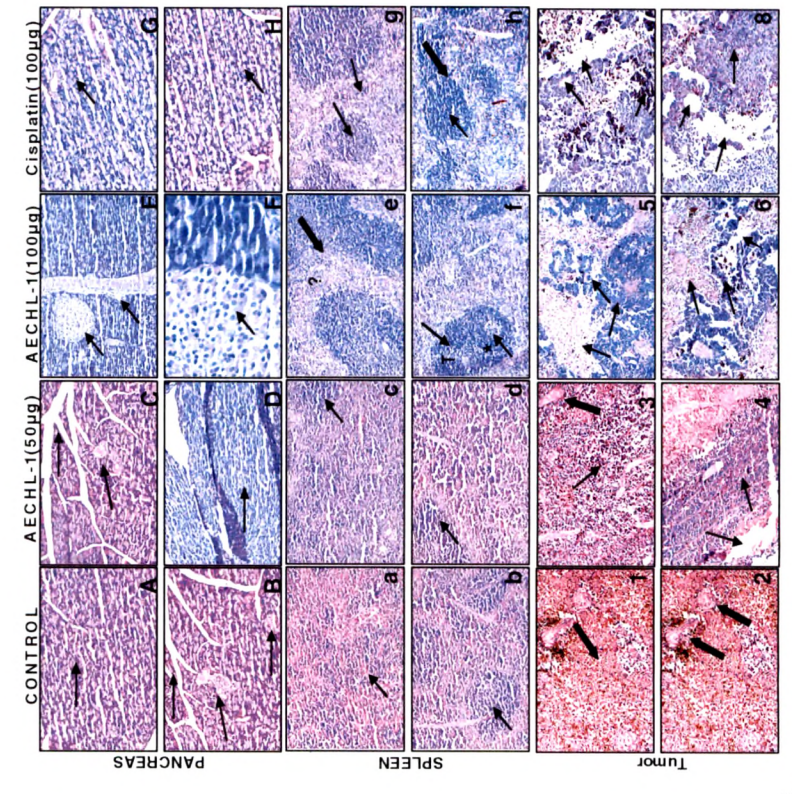
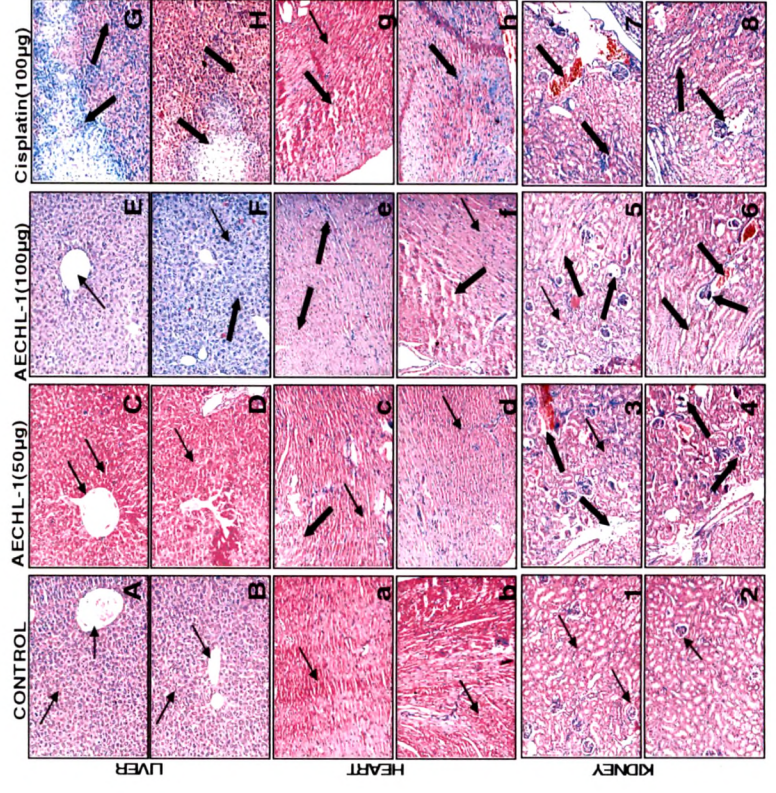
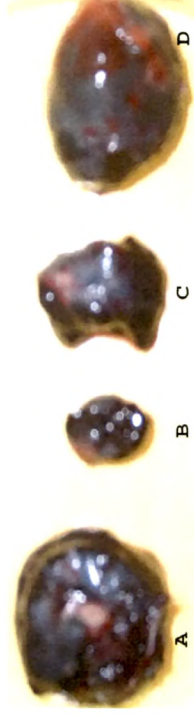
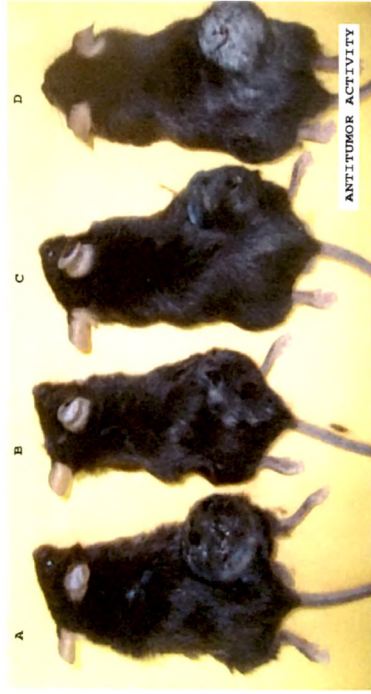


**Fig-3.49 C57 mice bearing solid tumor, A) Control mice (administered with PBS), B) Cis-platin treated(100µg) C) AECHL-1 treated (50µg), D) ACHL-1 treated (100µg),**

**Fig-3.50 Tumors isolated from mice, A) Control, B) Cis-platin treated, AECHL-1 (50µg) treated, D) ACHL-1 (100µg) treated,**

**Fig-3.51 Microscopic examination of liver, heart, kidney, pancreas, spleen and tumors from, control, AECHL-1 and cis-platin treated group**

***d) Histological studies of organs***

Liver from control group showing the central vein with portal triads at the periphery of the lobule. Kupffer cells were normally appeared (Fig-3.51A, B). AECHL-1 (50µg) did not affect the normal architect of the liver (Fig-3.51C, D). AECHL-1 (100µg) retains the normal architect of the liver with hypertrophic cell nucleus (Fig-3.51E, F). In cis-platin treated group there was extensive hepatocytes necrosis seen. The hepatocytes shown with arrow at the right are dead. This pattern can be seen with a variety of hepatotoxins. There focal hepatocytes necrosis with lymphocytic infiltration occurs. Histopathologically, lesions look like that of Tyzzer's disease characterised by necrosis with varying degrees of inflammation in response to the necrosis. Acute hepatic lesions consist of necrotic foci surrounded by minimal, primarily neutrophilic, inflammation (Fig-3.51G, H).

Heart from control group showed parallel fibers with prominent centrally placed nuclei indicating individual cells (Fig-3.51a, b). Treatment with AECHL-1 (50µg) showed necrosis of myocardial fiber with lymphocytic infiltration (Fig-3.51c, d). Treatment with AECHL-1 (100µg) showed extensive myocardial fiber necrosis with contraction bands and loss of nuclei. The fragmentation and smudging of the muscle fibers occur which is characteristic of coagulative necrosis (Fig-3.51e, f).

Cis-platin treated mice showed necrosis of myocardial fiber occurs with slight lymphocytic infiltration. Here again the fragmentation and smudging of the muscle fibers characteristic of coagulative necrosis (Fig-3.51g, h).

In control mice kidney showed well demarcated cortex and medulla, and the intact capsule with well formed glomeruli (Fig-3.51-1, 2).

Treatment with AECHL-1 (50µg) showed tubular vacuolization and tubular dilation with hemorrhagic areas, which is representative of acute tubular necrosis, normal glomeruli appears at the lower part. The glomeruli are sclerotic, there are scattered chronic inflammatory cell infiltrates, and the arteries are thickened with increased bowman's space (Fig-3.51-3, 4).

Treatment with AECHL-1 (100µg) showed tubular vacuolization and tubular dilation with hemorrhagic condition, tubules were dilated with scattered chronic inflammatory cell infiltrates (Fig-3.51-5, 6).

In Cis-platin treated mice lymphocytes are scattered in and around the vessel. The glomerulus is hypercellular and capillary loops are poorly defined which is a type of proliferative glomerulo nephritis. Many neutrophils are seen in the tubules and interstitium ie. Pyelonephritis (Fig-3.51-7,8).

No significant changes occur in the cellular architecture of pancreas histology (Fig-3.51A-H).

Representative spleen sections from a control mice showed different compartments of the white pulp indicated by (\*)-periarteriolar lymphatic sheaths; (⊙)-follicles; and (Ψ)-marginal zones. Control and AECHL-1 (50µg) showed normal spleen architect. Note the hyperplasia of the white pulp, especially of the follicles; and marginal zone. Histology showed increased numbers of granulocytes in the marginal zones (Fig.3.51 E-H).

#### ***e) Histological examination of tumor tissue***

To evaluate the effects of treatment on tumor histology, was compared with H & E stained sections of B16.F10 tissues from the AECHL-1 and Cis-platin treated with that of vehicle treated mice. Treatment was initiated when the tumors became palpable and tumors were evaluated after 15 days of treatment. As this was the time frame in which pronounced neovascularization occurred. It is thought that inhibition of this neovascularization forms the basis of the antitumor effects of test material. Tumor sections were evaluated regarding tumor cell density, location, number, and structure of blood vessels to assess possible changes related to angiogenesis; the presence of hemorrhagic areas to determine the vascular integrity of capillaries; and the presence, size, and location of picnotic/ necrotic cell areas to investigate tumor viability.

Treatment with AECHL-1 and Cis-platin pronounced effects on tumor size and produced necrotic areas in the core of the tumor, but overall has remarkably limited effects on tumor morphology.

Tumors from the vehicle treated group showed increased neovascularization with increased cell density with presence of hemorrhagic areas which showed probable signs of angiogenesis with increased threat of metastasis. The blood vessels were found to be well developed (Fig-3.51-1, 2)

AECHL-1 (50 $\mu$ g) did not show that much influence on the tumor vascularization with less occurrence of hemorrhagic areas. Tumor cell density was found to be decreased with occurrence of picnotic/ necrotic cells in the center of the tumor. Although we did not directly assess the functionality of blood vessels in this area, as vessels seemed perfused as indicated by the presence of erythrocytes. Therefore, necrosis in these areas did not seem to be the result of lack of vascularization (Fig-3.51-3, 4).

AECHL-1(100 $\mu$ g) showed increase necrotic nuclei through out the tumor area, with disappearance of neovasulization and hemorrhagic areas so reduced chances of angiogenesis and metastasis. Tumor cell density was found to be lowered compared to that of AECHL-(50 $\mu$ g) and vehicle treated animals (Fig-3.51-5, 6).

Cis-platin treated group showed significant increase in necrotic nuclei with decreased tumor cell density (Fig-3.51-7, 8).Tumor volume was also found to be reduced. There is no sign of neovasulization and hemorrhagic areas. Most of the cells were found to be dead when compared with control and AECHL-1 (50 $\mu$ g).

The absolute number of blood vessels determines the number of tumor cells that can be supported (Bergers G, 1999). Acquisition of blood vessels is a critical step in the survival and progression of many types of cancer (Folkman, J. 2002, Carmeliet, P. 2003). Through production of pro-angiogenic factors and down-regulation of angiostatic factors, tumors recruit new blood vessels from surrounding host tissue through both angiogenesis and vasculogenesis (Rossant, J, 2002; Patan, S. 2004). These blood vessels enable tumor growth, survival, and a point of entry into circulation for metastatic dissemination. Indeed, tumor vascularity correlates with a poor prognosis in cancer patients (Weidner, N, 1992; Tsutsui, S, 2003, Uzzan, B, 2004). When angiogenesis is induced, metastatic tumor cells grow rapidly. Therefore, inhibition of

angiogenesis prevents tumor growth, proliferation, and secondary metastasis. Inhibition of angiogenesis and suppression of invasion, motion and proliferation of tumors, and growth of endothelial cells of blood vessel, are essentially required for cancer prevention, AECHL-1 prevents the progression of angiogenesis by blocking neovasulization, thus reducing the risk of metastasis.

***f) Western blot analysis of tumor cells isolated from animals.***

Tissue samples were lysed in sample buffer and resolved on a 4–12% gradient SDS–polyacrylamide-gel electrophoresis gel. The proteins were transferred to a nitrocellulose membrane, blocked, and probed with the appropriate primary antibodies and secondary horseradish peroxidase-labeled antibodies. Proteins were detected by chemiluminescence and quantified with a Kodak 2000 gel-imaging system.

***Role of cyclin D1/cdk4 and p53 in AECHL-induced cell cycle arrest***

Cyclin D1 (also known as *bcl-1*, *PRAD1*) is a proto-oncogene that is overexpressed and/or amplified in numerous neoplasias (Raffeld M, 1991; Weinstat-Saslow D., 1995; Jadayel DM, 1997; Pelosio P, 1996; Fredersdorf S, 1997; Bartkova J, 1995). Ectopic expression of cyclin D1 and microinjection studies with neutralizing cyclin D1 antibodies and/or cyclin D1 antisense constructs support the notion that cyclin D1 is an important determinant in the progression through the G<sub>1</sub> phase of the cell cycle (Tam SW, 1994; Musgrove EA, 1994). The expression of cyclin D1 in normal cells varies with the phase of the cell cycle. A peak induction of cyclin D1 in early G<sub>1</sub> of normal cells is followed by a decline during S and G<sub>2</sub>-M Phases.

Also p53 is a transcription factor whose activity gives rise to a variety of cellular outcomes, most notably cell cycle arrest and apoptosis, eliminating cancer-prone cells from the replicative pool. Usually, p53 protein is present within a cell in minute amounts. It is very labile, with a half-life sometimes as short as a few minutes. In normal cells p53 protein is present in its latent form and levels are very low. DNA damage acts as a stimulus for p53 (Soussi T, 2000). In response, p53 expression is upregulated and p53 protein accumulates in the cell and has increased transcriptional activity. In response the cell may

undergo cell-cycle arrest (to allow for DNA repair) or undergo apoptosis (Janus F, 1996).

Treatment of solid tumors with 50  $\mu$ g of AECHL for 12 days reduced cyclin D1 protein levels, as detected by a pan D-cyclin antibody, increased p53 expression levels and decreased Bcl-2 levels (Fig-3.52).

These data suggest that inhibition of cyclin D1 expression and expression of p53 contributes to the growth inhibition induced by AECHL in B16F10 tumors through a cyclin D1/Cdk4/pRB signaling pathway.

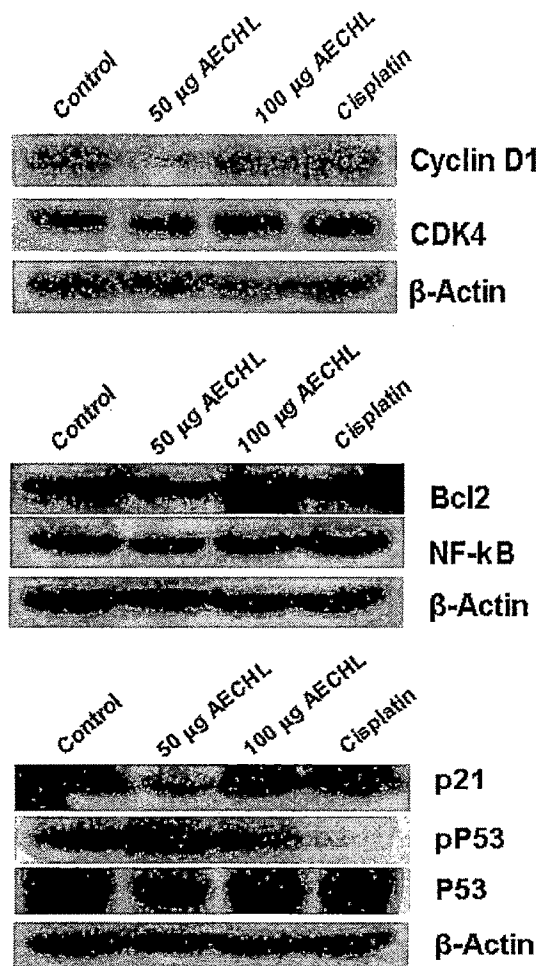


**Fig-3.52 Western blot analysis of proteins isolated from animal tumors**

### 3.2.7 Studies on AECHL-2 isolated from Root bark of *Ailanthus excelsa*

#### 3.2.7.1 Effect of AECHL-2 on % Cell viability of H9c2 cells

MTT assay was performed to determine the effect of AECHL-2 on cell viability. H9c2 cells were incubated with varying concentration of AECHL-2 (1, 2, 5, 10, 20, 50 and 100µg/ml) for different time period i.e. 12, 24, and 48h. At 5µg/ml concentration no significant change in cell viability was observed i.e. 94.48, 93.2, 94.59%, after 12, 24 and 48 hrs of treatment when compared with that of vehicle control. At 100µg/ml concentration cell viability was found to be decreased to 62.24, 57.02, and 49.83% respectively at 12, 24 and 48hrs of treatment (Table-1.32, Fig-3.53 & 3.57).

**Table-1.32 Effect of AECHL-2 % - viability of H9c2 cells**

<b>Conc.</b> <b>(µg/ml)</b>	% Cell viability		
	12 Hr	24 Hr	48 Hr
Control	100±0.43	100±6.57	100±9.59
V. Control	106.52±3.04	103.28±3.07	103.31±2.44
0.5	97.75±1.63	93.2±8.49	97.46±1.85
1	99.18±1.22	98.72±1.48	101.85±5.57
2	92.04±0.20	93.2±2.12	93.75±3.71
5	94.48±2.85	93.2±2.97	94.59±2.19
10	90.4±4.28	82.59±3.39	86.31±0.50
20	92.04±5.71	89.8±2.54	81.75±1.52
50	69.79±1.63	64.96±9.76	62.66±4.56
100	62.24±1.22	57.02±0.63	49.83±1.52

Values are expressed as mean ± SD of % cell viability (average of three determinations)

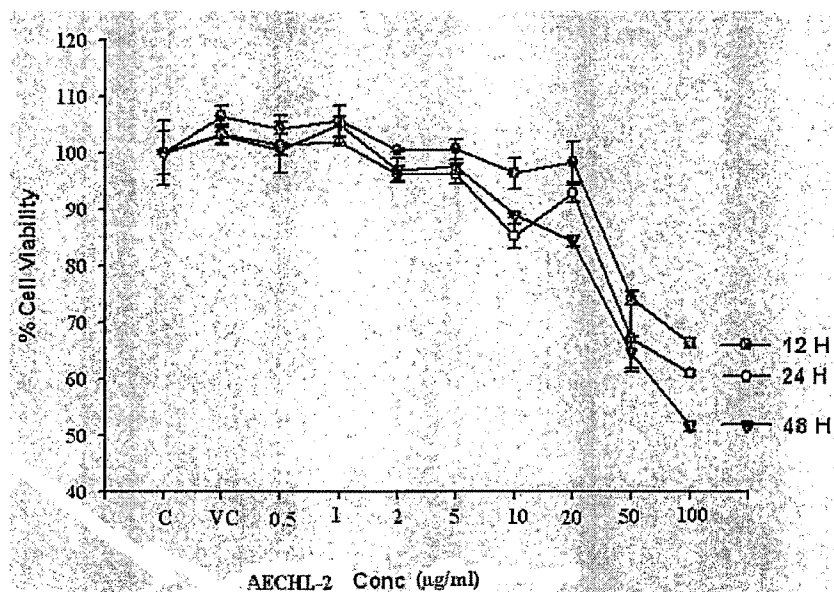


**Fig-3.53 Effect of various concentration of AECHL-2 on %-viability of H9c2 cells at different time interval**

AECHL-2 showed concentration dependent repose on the viability of H9c2. Even after treatment upto 48hrs it did not showed any significant effect on cell viability at lower concentration, but at higher concentration cell viability was found to be decreased with increased concentration and time. Thus AECHL-2 was found to be cytotoxic at higher concentration.

### 3.2.7.2 Annexin V- PI- Staining for AECHL-2

Annexin V- PI staining was done in order to study the nature of cell death caused by AECHL-2

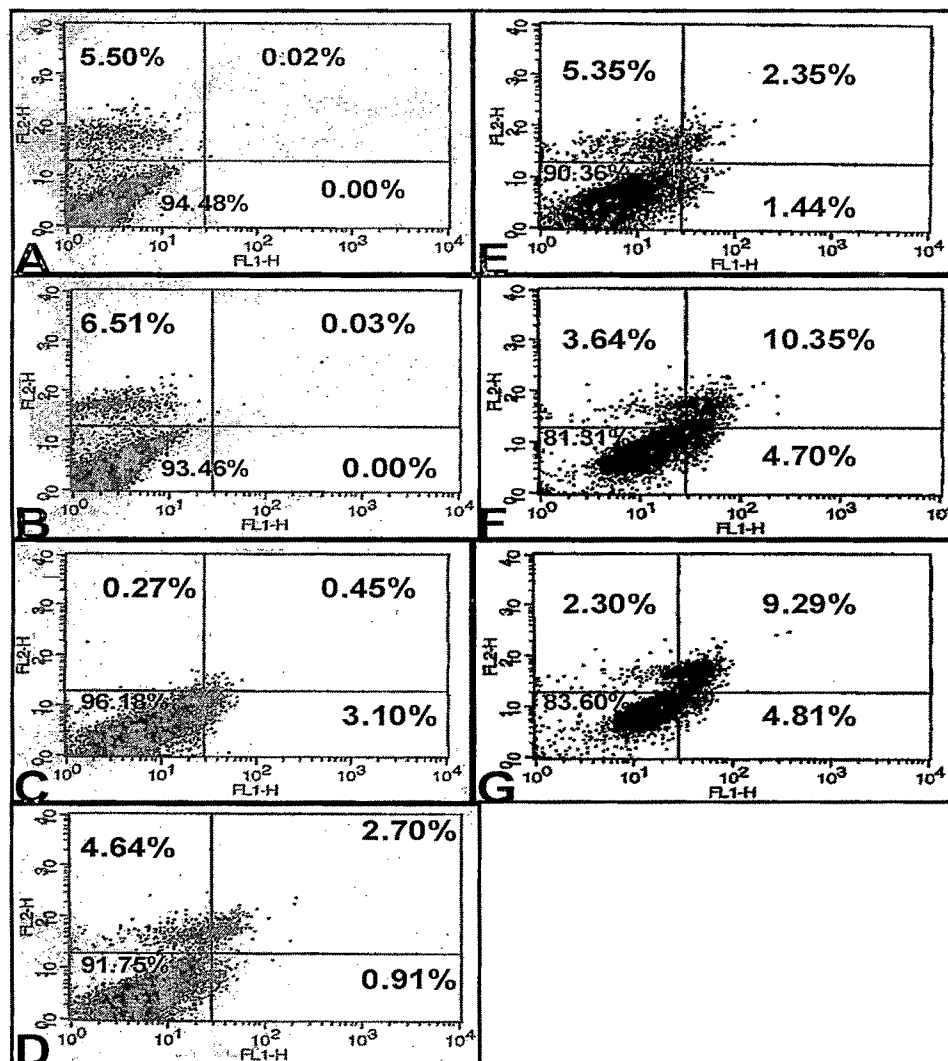


**Fig-3.54 Annexin-V and PI staining of the H9c2 cells treated with AECHL-2 for 48hrs.** A) Unstained cells, B) PI stained cells, C) Annexin stained cells, D) Both Annexin and PI stained cells considered as control E) Annexin + PI treated with 0.2% DMSO considered as Vehicle control, F) Treated with AECHL-2 (50µg/ml) G) AECHL-2 (100µg/ml). The percentage of cells in each quadrant is indicated.

In the above cytogram unstained and PI stained cells did not showed any apoptotic/ necrotic cells (fig-3.54 A & B). vehicle control (0.2% DMSO) group (fig-3.54 E) showed 1.44% of apoptotic cells and 2.35% necrotic cells with no significant change compared to that of control group (stained with Annexin V

along with PI) (fi-3.54 D) with 0.91%, 2.70 respectively. 48 hrs treatment with AECHL-2 (50 and 100µg/ml) showed increased both necrotic ie. 10.35, 9.29% and apoptotic 4.70, 4.81% cells respectively. Necrotic cells are more prominent than the apoptotic cells (fig-3.54F & G) when compared with the vehicle control (fig-3.54 E).

Annexin-V and PI staining of the H9c2 cells treated with AECHL-2 for 48hrs was done and analyzed by FACs at the excitation wavelength 488nm. No significant difference was observed between the control and vehicle treated group. Treatment with AECHL-2 showed increase in both apoptotic and necrotic/late apoptotic cell death. As the concentration of AECHL-2 increased from 50 to 10µg/ml both necrotic and apoptotic cell percentage increased. Necrosis was found to be more prominent compared to apoptotic cells.

#### **3.2.7.3 Effect of AECHL-2 on intracellular ROS level**

In order to detect the effect of AECHL-2 on intra cellular ROS, H9c2 cells, were treated with AECHL-2 (50 & 100µg/ml) and incubated for 24hrs. ROS was assessed by flow cytometric analysis after loading the cells with the ROS-sensitive dye DCFH-DA. As shown in (Fig-3.58 A-D), an increase in DCF was observed in the AECHL-2 treated cells, with the mean fluorescence intensity increased from 4.45% to 59.49%. For further confirmation, the cells treated with AECHL-2 (100µg/ml) under the same conditions were subjected to confocal microscopy. As shown in (Fig-3.55 A-B), no change in fluorescence intensity was observed when compared with the control cells.

#### **3.2.7.4 Effects of AECHL-2 on mitochondrial membrane potential ( $\Delta\Psi_m$ )**

$\Delta\Psi_m$  was measured by using cell permeable cationic dye Tetramethyl Rhodamine (TMRE). AECHL-2 (50 & 100µg/ml) reduced the membrane potential in H9c2 cells marked with increase fluorescence intensity from 13.62 to 19.32% when assessed by flow cytometric analysis after loading the cells with the  $\Delta\Psi_m$ -sensitive dye TMRE (Fig-3.58 M & P).

No significant change in fluorescence intensity was observed in confocal imaging of H9c2 after loading with TMRE (Fig-3.55 I & J). Thus AECHL-2

(100µg/ml) showed non significant change in mitochondrial membrane potential.

#### **3.2.7.5 Effect of AECHL-2 on endogenous Nitric oxide (NO) in H9c2 cells**

H9c2 cells treated with AECHL-2 (100µg/ml) for 24hrs after loading with DAF-2DA showed increase fluorescence intensity when analyzed by confocal microscopy. AECHL-2 generation of nitric oxide radicals in H9c2 cells (Fig-3.55 E-F).

#### **3.2.7.6 Effect of AECHL-2 on generation of superoxide radicals in H9c2 cells**

AECHL-2 treatment causes generation of  $O_2^{\cdot-}$ . Dihydroethidium (DHE) is a specific fluorescent dye for  $O_2^{\cdot-}$  was added to cells for tracking generation of ROS. Treatment of H9c2 cells with AECHL-2 (50 & 100µg/ml) increases the fluorescence intensity from 4.45 to 85.02% when assessed by flow cytometric analysis after loading the cells with the ROS-sensitive dye DHE (Fig-3.58 E to H). This effect was further confirmed by confocal microscopy which showed  $O_2^{\cdot-}$  was dramatically enhanced in AECHL-2 (100µg/ml) exposed cells when compared with the untreated cells (Fig-3.55 C & D).

Thus AECHL-2 was found to increase the intracellular superoxide radical formation.

#### **3.2.7.7 Effect of AECHL-2 on peroxynitrite formation in H9c2 cells.**

DHR 123 is used as an indicator of peroxynitrite formation. Pretreatment of H9c2 cells with AECHL-2 (50-100µg/ml), showed increased fluorescence intensity from 5.09 to 97.91% after loading with DHR 123 and assessing with FACs (Fig-3.58 I-L). This effect of AECHL-2 was confirmed when observed by confocal microscopy, where intensity of fluorescence was found to be increased in AECHL-2 pretreated cells (Fig-3.55 G-H). AECHL-2 showed concentration dependent effect on generation of peroxynitrite radicals in H9c2 cells.

Peroxynitrite (ONOO<sup>-</sup>) is a potent oxidant and nitrating species proposed as direct effectors of myocardial damage in numerous cardiac pathologies. This reactive species can be formed by the combination of superoxide ( $O_2^{\cdot-}$ ) and

nitric oxide ( $\cdot\text{NO}$ ) radicals, generated *in vivo* (Balavoine, 1999) by, for example, endothelial cells, Kupffer cells, neutrophils and macrophages.  $\text{ONOO}^-$  is a relatively stable species compared with free radicals but once protonated gives highly reactive peroxy-nitrous acid ( $\text{ONOOH}$ ) (Balavoine, 1999), decomposing with a very short half-life (1.9 s) at  $37^\circ\text{C}$  to form various cytotoxicants (Patel, 1999).  $\text{ONOO}^-$  can induce the oxidation of thiol ( $-\text{SH}$ ) groups on proteins, nitration of tyrosine, lipid peroxidation and also nitrosation reactions, affecting cell metabolism and signal transduction. It can ultimately contribute to cellular and tissue injury with DNA strand breakage and apoptotic cell death.

PN generation is favored when the production of both  $\text{NO}$  and  $\text{O}_2^-$  is enhanced, as may occur during inflammation, circulatory shock and reperfusion injury (Liaudet L, 2000). In the heart, PN generation occurs during myocardial infarction (Liaudet L, 2001), heart failure (Pacher P., 200) and cardiomyopathy due to anthracyclines (Pacher P, 2003) PN is generated in large amounts in the myocardium during myocardial reperfusion injury (Liaudet L, 2001), chronic heart failure (Pacher P, 200), circulatory shock (Lancel S, 2004) and anthracycline cardiomyopathy (Pacher P, 2003). PN has generally been considered as directly biotoxic towards cardiomyocytes.

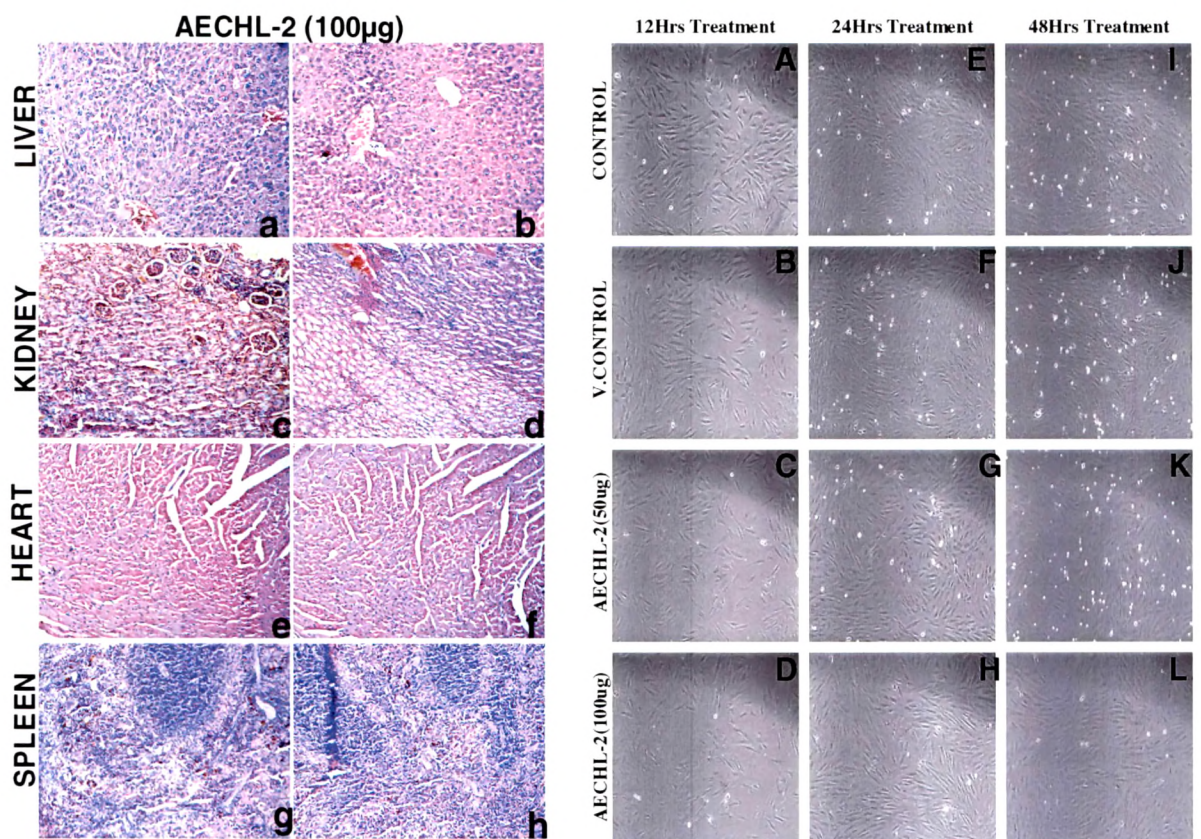
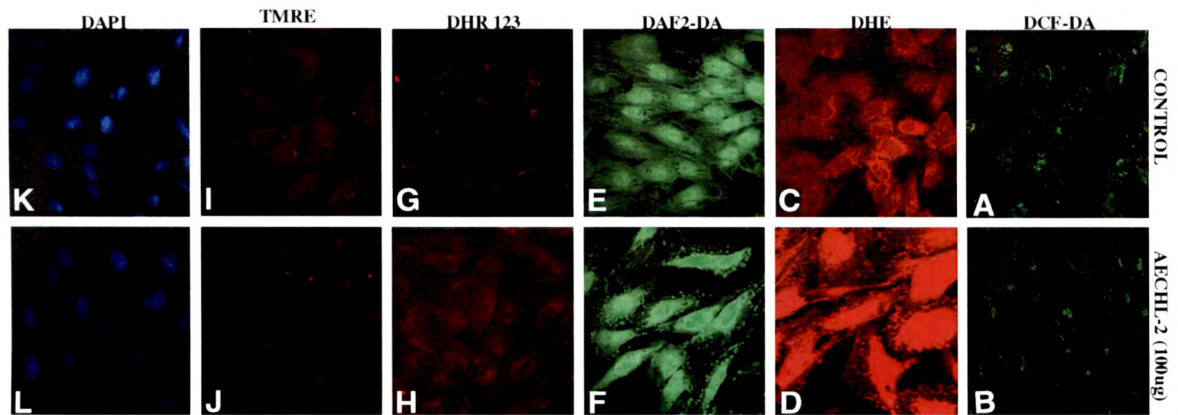


**Fig-3.55 Effect of AECHL-2 on generation of ROS in H9c2 cells after loading with specific molecular probes**

**Fig-3.56 Microscopic slides showing effect of AECHL-2 on different organs in C57 mice**

**Fig-3.57 Phase contrast photos showing effect of AECHL-2 on H9c2 cells**

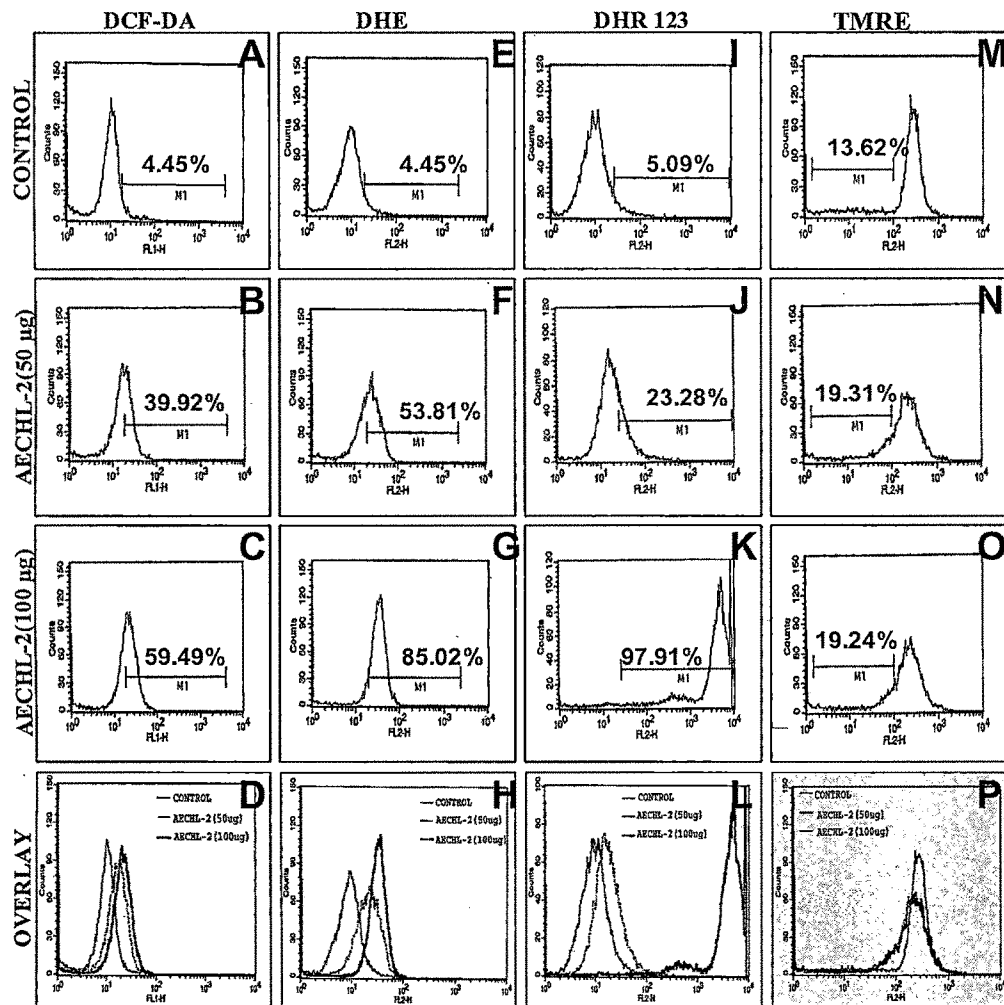


**Fig-3.58 (A-R) Flow activated cytometric analysis of H9c2 cells pretreated with different concentration of AECHL-2 after loading with different molecular probes.**

### **3.2.7.8 Effect of AECHL-1 on cytosolic and nuclear calcium in H9c2 cells**

Flow activated cytometry and confocal analysis of H9c2 cells treated with AECHL-2 and stained with the molecular probe fluo 3 AM was done in order to analyze the effect of AECHL-2 on intracellular calcium uptake. With fluo 3-AM, the baseline fluorescence was located in the cytoplasm and with increasing concentration of AECHL-2 calcium concentration in the perinuclear was found to be significantly increased when compared with the control cells.

After 20 and 60mins incubation of H9c2 cells with AECHL-2 (25 $\mu$ g/ml) increases the fluorescence intensity to 11.91 and 41.74% respectively (Fig-3.59 a & c), while treatment with 50 $\mu$ g/ml for the same period increased the fluorescence intensity to 11.77 and 54.83% respectively (Fig-3.59 b & d) compared to that of untreated (1.80%). Thus AECHL-2 showed time and concentration dependent increase in intracellular calcium uptake.

The results were confirmed by using data analyzed for unstained (0.00%), stained (1.80%), EGTA (0.10%), calcium (16.44%), ionomycin (17.59%), Calcium + Ionomycin (65.36%) respectively (Fig- 335a-i).

Where, cells after loading with fluo-3 shows increased fluorescence intensity in the perinuclear region of cells, unstained cells did not showed any region of fluorescence. Addition of EGTA showed decrease in fluorescence intensity in the perinuclear region and increased intensity in nucleus with death of cells. Calcium supplement showed increased fluorescence intensity which further increased after incubation with Ionomycin (Fig-3.35A-E).

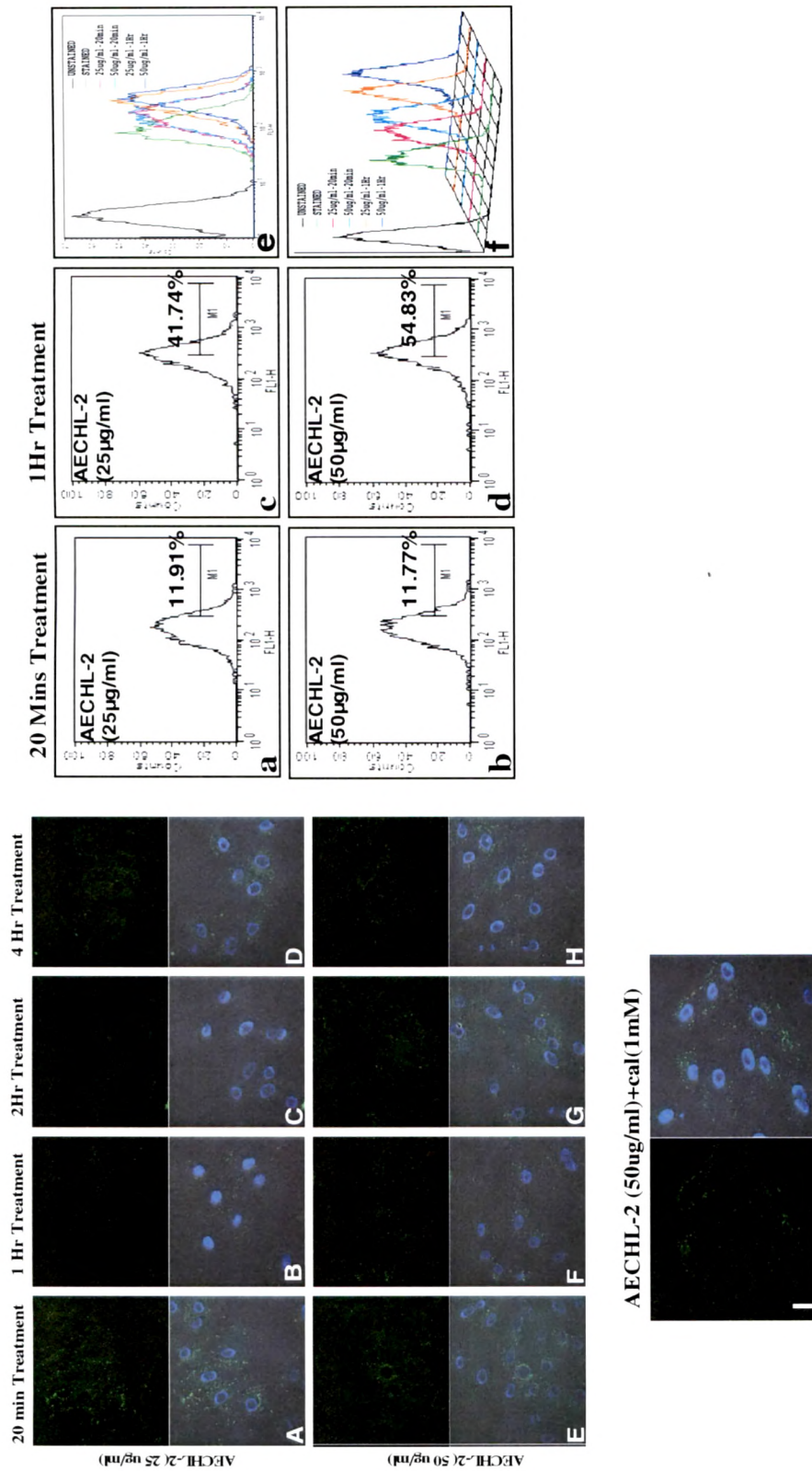


**Fig-3.59** Effect of AECHL-2 on intracellular calcium levels in H9c2 cell lines after loading with fluo 3 AM. A-I) Confocal images, a-f) FACS images of H9c2 cells after pretreatment with AECHL-2 and loaded with fluo 3 AM

The above data was further confirmed by confocal analysis, where after 4 hrs of treatment EGTA treated cells found dead (fig-3.35B), and fluorescence intensity of calcium marker probe fluo-3 AM was increase as Untreated < Calcium 1mM < Ionomycin 3 $\mu$ M < Calcium + Ionomycin.

In the same way H9c2 cells were incubated with AECHL-2 (25 and 50 $\mu$ g/ml) for different time period ie 20min, 1, 2, and 4 hrs respectively. After incubation time cells were treated with fluo 3 AM for the detection of intracellular calcium.

Incubation with 25 $\mu$ g/ml of AECHL-2 showed increased intracellular calcium level at 20mins and 4 hr based on the intensity of fluorescence seen in (fig-3.59 A-D). While incubation with 50 $\mu$ g/ml of AECHL-2 showed increased calcium level after 20-4hrs incubation (fig-3.59 E-H).

Incubation with 20 $\mu$ g/ml of AECHL-2 and 1mM of calcium did not show any significant change after 4hrs of treatment (fig-3.59 I).

Thus AECHL-1 was found to increase an intracellular calcium level in perinuclear area.

Calcium ions have a wide variety of important functions in the activity of the cardiovascular system. They control transmitter release, synaptic plasticity; firing rate, gene expression, and cell death (Meir A, 1999; Clapham DE, 1995). There is no doubt that calcium ions entering through the surface membrane have a major function in many of these processes. In recent years, however, a growing body of evidence suggests that calcium released from intracellular stores may play an important role in calcium control of neuronal function (David G, 1998; Eilers J 1996). Hence, the study of intracellular calcium dynamics is significant in this context. Thus it is an exciting way to study such dynamics is through the examination of calcium sparks.

#### **3.2.7.9 Effect of AECHL-2 on rat neonatal myocytes**

To study the effect of AECHL-2 on cardiovascular system, rat neonatal ventricular myocytes were isolated and after treatment with AECHL-2, mechanical properties of myocytes were assessed using an IonOptix MyoCam

system. Cell mechanics were assessed using the peak shortening (PS), time-to-90% peak shortening (TPS), time-to-90% relengthening ( $TR_{90}$ ) along with maximal velocities of shortening ( $+dL/dt$ ) and relengthening ( $-dL/dt$ ). (Table-1.33, Fig-3.60)

**Table-1.33 Effect of AECHL-2 on mechanical properties of rat neonatal myocytes**

Treatment	Cell length	PS	TPS	TR <sub>90</sub>	+dL/dt	-dL/dt
V. Control	60.03±2.2	19.79±2.75	4.31±1	4.64±0.85	235.85±8.007	91.035±4.11
AECHL-2 (1µg)	47.28±0.89***	18.08±2.22 <sup>ns</sup>	9.25±0.33*	8.19±0.26*	124.69±7.65***	106.81±6.59
AECHL-2 (2µg)	42.9±0.22***	13.52±1.93 <sup>ns</sup>	8.19±0.61*	8.85±0.46*	107.94±7.002***	197.2±5.4***
AECHL-2 (4µg)	48.71±1.45***	12.78±1.62 <sup>ns</sup>	4.5±0.97 <sup>ns</sup>	4±0.81 <sup>ns</sup>	111±11.86***	66.152±2.29**
AECHL-2 (6µg)	49.06±0.25***	4.85±0.46**	6.78±0.75 <sup>ns</sup>	4.96±0.87 <sup>ns</sup>	24.11±2.17***	83.03±3.02
AECHL-2 (6µg+Cal)	61.24±0.22 <sup>ns##</sup>	6.84±1.17***	6.06±1.16 <sup>ns</sup>	6.64±1.08 <sup>ns</sup>	87.64±3.91***##	95.134±5.91

Statistical analysis was done by using ANOVA

Post test applied: Tukey-Kramer multiple comparison Test

Values are expressed as mean ± SEM.

\*p<0.05; \*\*p<0.01; \*\*\*p<0.001; <sup>ns</sup>p>0.05 = non significant, (n=20-25 myocytes)

For TPS: P value is 0.0087 is considered very significant.

For Other parameters: P value is < 0.0001, considered extremely significant

\*Compared with the Control group

#Compared with AECHL-2 (5µg)

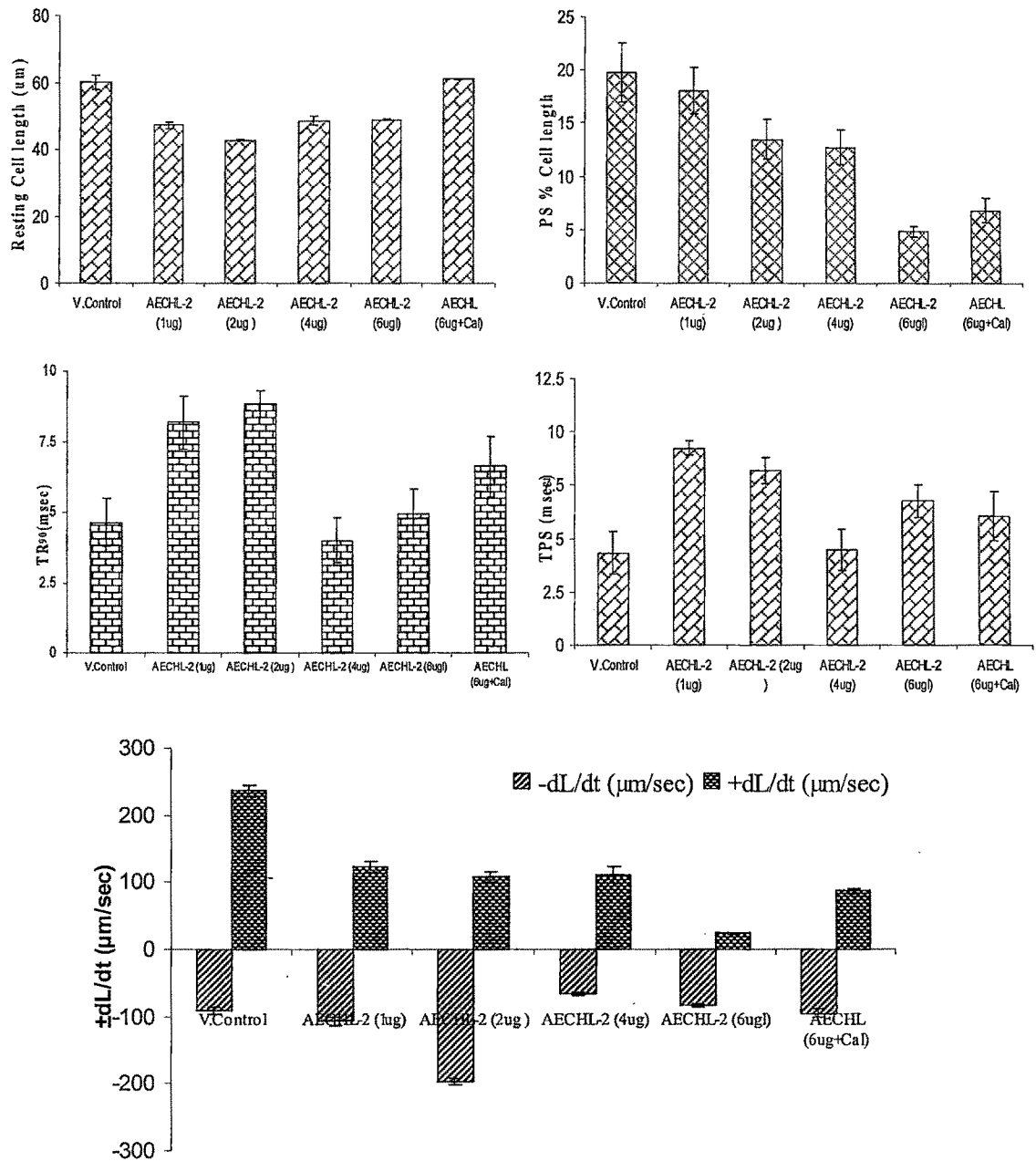


**Fig-3.60. contractile properties of ventricular myocytes from 2-3 days old infants.** A: resting cell length. B: peak shortening (PS; as percentage of resting cell length). C: time to peak shortening (TPS). D: time to 90% relengthening (TR90). E: maximal velocity of shortening (+dL/dt). F: maximal velocity of relengthening (-dL/dt). Values are means  $\pm$ SEM ;( n=20-25myocytes).

Time to peak shortening (TPS was) increased to 9.25msec at the initial concentration of 1ng ( $P<0.01$ ), which comes to normal with increasing concentration ie. 8.19 ( $p<0.05$ ), 4.5 ( $p>0.05$ ) and 6.78 msec ( $p>0.05$ ) at 2, 4 and 6ng respectively when compared with control 4.31msec. While 1mM calcium supplement rise TPS to 6.06 ( $p>0.05$ ) compared to that of control and AECHL-2 (6 $\mu$ g) respectively.

Time to 90% of relengthening  $TR_{90}$  was increased to 8.19, 8.85msec ( $p>0.05$ ) at 1 and 2 $\mu$ g of AECHL-2, but comes to normal with further increase in concentration ie 4 and 4.96 msec ( $p>0.05$ ) at 4 and 6 $\mu$ g respectively when compared to that of control 4.64. While with calcium  $TR_{90}$  found to be increased when compared to that of control and AECHL-2 (6 $\mu$ g) respectively.

AECHL-2 showed significant changes in mechanical properties of primary culture of neonatal myocytes measured by using IonOptix. The effect of AECHL-2 was similar to that of AECHL-1 on neonatal myocytes ie initial stimulation and later on depressant action on neonatal myocytes.

#### **3.2.7.10 Effect of single dose administration of AECHL-2 in Balb/C mice**

AECHL-2 at 100 $\mu$ g intravenous dose showed no mortality in Balb/C mice when observed for 21 days. Significant histological changes occur in liver, heart and kidney anatomy. In all cases leucocytic infiltration was common (Fig-3.56).

#### **3.2.7.11 Quantification of AECHL-2 in different extracts of Ailanthus root bark by HPTLC.**

Stock solution of AECHL-2 prepared in methanol.

Stock solutions of extracts were prepared in methanol.

Solvent system- Chloroform: Methanol (9: 1 v/v)

Calibration range for AECHL-2 (250 to 6000 ng)

Scanning wavelength-366nm

**Table-1.34 Estimation of AECHL-2 in different extracts of Ailanthus root bark.**

<b>Extracts</b>	<b>Concentration of extract applied</b>	<b>AECHL-2 present with respect to height</b>	<b>AECHL-2 present with respect to area</b>
Chloroform	2000ng	89.8%	83.25%
Benzene	3000ng	57.7%	50.8%
Ethyl acetate	3000ng	<225ng	<225ng
Methanol	3000ng	<225ng	<225ng

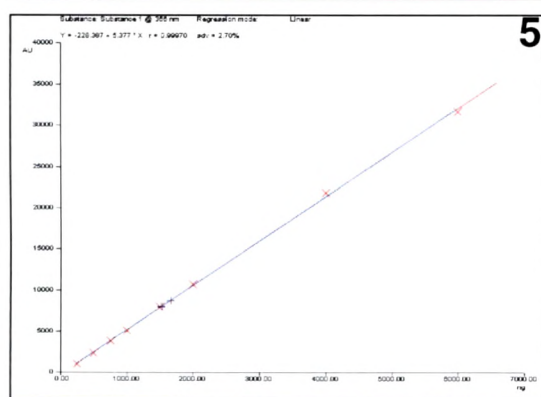
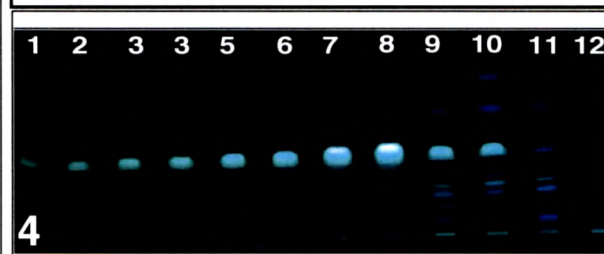
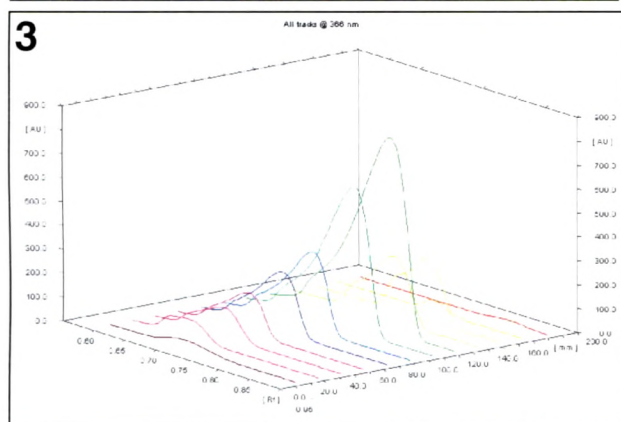
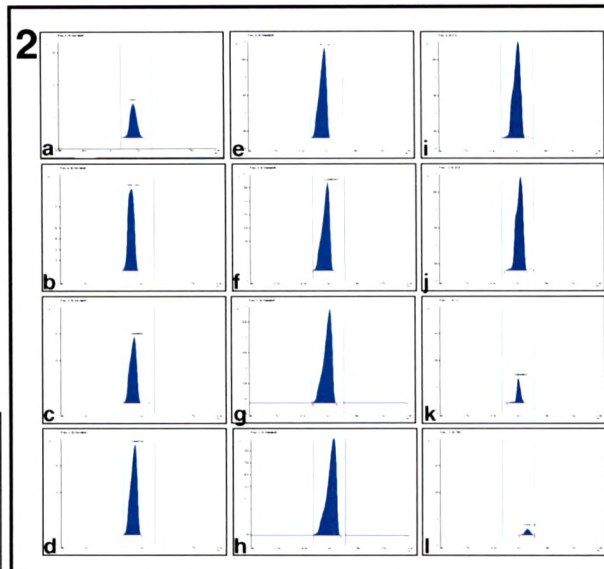
Chloroform extract of root bark contains 89.8 and 83.25% of AECH-2 with respect to height and area of chromatogram. Benzene extract showed 57.7 and 50.8% of AECHL-2 with respect to height and area, which is lesser than that of chloroform extract. Concentration of AECHL-2 was very low in ethyl acetate and methanol extract ie below 225ng, so not get quantified (Table-1.34, fig-3.61)

Spectrofluorometric analysis of AECHL-2 was done in order to quantify minimum amount of AECHL-2 in these extracts.

Substance: Substance 1 @ 366 nm      Regression mode: Linear

Regression via Height     $Y = 26.228 + 0.136 \cdot X$        $r = 0.99564$        $sdv = 9.25\%$   
 Area     $Y = -228.387 + 5.377 \cdot X$        $r = 0.99970$        $sdv = 2.70\%$

Track	Vial	Rf	Amount / Fraction	Height	X(calc)	Area	X(calc)	Sample ID / Remark
1	1	0.71	250.00 ng	32.00		1003.54		
2	1	0.71	500.00 ng	76.65		2277.44		
3	1	0.70	750.00 ng	122.84		3804.42		
4	1	0.70	1000.00 ng	168.34		5046.38		
5	1	0.71	1500 ug	250.26		7954.50		
6	1	0.71	2000 ug	325.22		10687.93		
7	2	0.72	4000 ug	605.92		21775.96		
8	3	0.72	6000 ug	810.30		31658.63		
9	4	0.72		271.16	1.796 ug	6727.40	1.665 ug	CHL
10	5	0.70		262.22	1.731 ug	7965.60	1.524 ug	BEZ
11	6	0.72		45.92	<225.00 n	821.29	<225.00 n	EA out of permitted range
12	7	0.72		12.06	<225.00 n	286.60	<225.00 n	TME out of permitted range



ESTIMATION OF AECHL-2

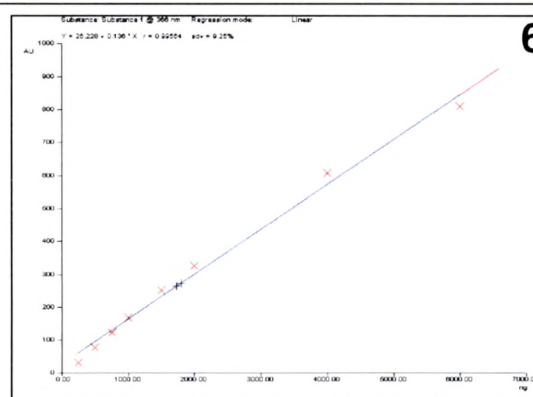


**Fig-3.61 Estimation of AECHL-2 in different extracts of Ailanthus root bark.** 1) Table detailing the concentration range and Rf of AECHL-2 along with amount detected in extracts. 2) Chromatograms for isolated AECHL-2 and that detected in chloroform and benzene extracts. 3) 3- D spectra of AECHL-2. 4) TLC plate showing AECHL-2 in extracts. 5-6) Linearity plot of AECHL-2 with respect to area and height of chromatogram

### 3.2.7.12 Fluorimetric analysis of AECHL-2

Calibration range (5-50ng/ml)

Excitation wavelength: 404

Emission wavelength: 462

Scale:  $\delta$ - Scale5

Concentration of Fractions used (50ng/ml).

Fluorimetric estimation of AECHL-2 showed 65.60% and 15.72% of AECHL-2 in chloroform and benzene extracts respectively. AECHL-2 was not quantified in ethyl acetate and methanol extracts. (Table-1.35, Fig-3.62)

**Table-1.35 Spectrofluorometric analysis of AECHL-2 in extracts from root bark**

Sr No.	Extract (50ng/ml)	% Relative Intensity		
		Conc. ng/ml	% present	
1	CHL	60.6	32.80165	<b>65.60%</b>
2	BZ	26.7	7.860506	<b>15.72%</b>
3	EA	---	---	---
4	TM	---	---	---

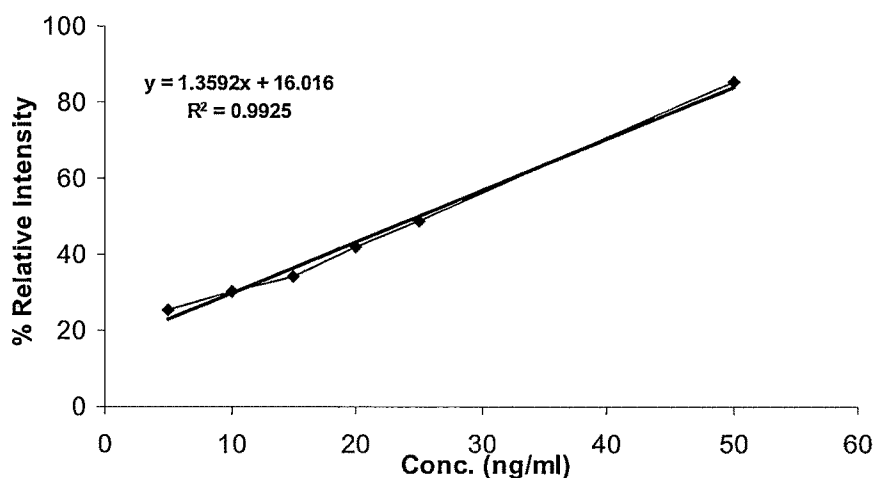


**Fig-3.62 Linearity plot for AECHL-2 by Spectrofluorometric method**

### 3.3 Studies on *Butea monosperma* flowers

#### 3.3.1 Preparation of extract

Coarse powder of the shade dried flowers was extracted with methanol in a soxhlet extractor; the extract was concentrated and dried under vacuum (yield 19.93 %w/w). The vacuum dried extract was suspended in water and then extracted with ethyl acetate and n-butanol (yield 5.82 and 19.98%w/w, respectively). The remaining aqueous portion was concentrated and dried (yield 48.54%). The total methanol extract along with its fractions were taken for further studies.

#### 3.3.2 Qualitative chemical tests

Ethyl acetate and butanol extracts showed the presence of sugars, amino acids, flavonoids, steroids and tannins, whereas aqueous extract contains sugars, amino acids, phenolics and tannins.

Ethyl acetate and butanol fractions showed flavonoids as a major class of components.

#### 3.3.3 Elemental analysis

Elemental analysis of *Butea* flowers was done by Atomic absorption spectrophotometer, where it showed high concentration of potassium, while cadmium was absent. (Table-1.36)

**Table-1.36 Elemental analysis of *Butea* flowers**

	Elemental analysis							
	Manganese	Zinc	Copper	Sodium	Potassium	Iron	Lead	Cadmium
<i>Butea</i> flowers	31.66	106.92	10.29	221.9	2830.16	29.47	7.58	NIL

All parameters are expressed in PPM

### **3.3.4 Evaluation of Antioxidant activity of Butea monosperma flowers**

#### **3.3.4.1 In-vitro antioxidant activity**

All the fractions of flowers along with total methanol extract were screened for in-vitro antioxidant activity.

##### **a) Reducing power assay**

Methanol extract along with its ethyl acetate and butanol fractions were found to possess significant reducing power. Ethyl acetate fraction was more active compared to butanol fraction and total methanol extract. Aqueous fraction did not show any activity. The extracts exhibited a concentration dependent increase in reducing power. Compared with ascorbic acid the reducing powers of the three fractions were lesser (Fig- 3.64A).

##### **b) Scavenging of DPPH radical**

Methanol extract along with its ethyl acetate and butanol fractions showed a concentration dependent antiradical activity by scavenging DPPH radical with an EC<sub>50</sub> value of 22.88, 15.44 and 41.53µg/ml, respectively. Ethyl acetate fraction was found to be more potent compared to butanol fraction and total methanol extract. Aqueous fraction did not show any inhibition. Compared with reference standard rutin (EC<sub>50</sub>: 2.85 µg/ml), the scavenging effects were lesser. (Fig- 3.64B)

##### **c) Inhibition of superoxide radical**

Ethyl acetate and butanol fractions were found to exhibit better inhibition of superoxide radical with an EC<sub>50</sub> value of 4.03 and 18.49µg/ml, respectively, while total methanol extract showed 50% inhibition at a higher concentration of 91.89µg/ml. The aqueous fraction did not show any inhibition of superoxide radical. The results were compared with reference standard quercetin (EC<sub>50</sub>:10.84µg/ml; Fig- 3.64C). Ethyl acetate fraction was more effective than the standard, quercetin.

**d) Inhibition of hydroxyl radical**

Effect of methanol extract along with its ethyl acetate, butanol and aqueous fractions on deoxyribose damage induced by  $\text{Fe}^{3+}/\text{H}_2\text{O}_2$  is shown in (Fig-3.64D). The ethyl acetate fraction was found to show better inhibition compared to butanol fraction and methanol extract, with  $\text{EC}_{50}$  15.45, 43.55 and 63.61  $\mu\text{g}/\text{ml}$ , respectively. Aqueous fraction did not show any inhibition in deoxyribose damage. The results were compared with reference standard curcumin ( $\text{EC}_{50}$ : 0.96 $\mu\text{g}/\text{ml}$ ), which was more effective than the fractions tested.

**e) Inhibition of nitric oxide radical**

Concentration of ethyl acetate, butanol fractions and total methanol extract required for 50% inhibition were found to be 225.66, 66.20 and 281.74  $\mu\text{g}/\text{ml}$  respectively. Butanol fraction was found to be more potent compared to methanol extract and its ethyl acetate fraction. Aqueous fraction did not show any inhibition of nitric oxide. Curcumin which was used as a reference compound, showed 50% inhibition at 34.23 $\mu\text{g}/\text{ml}$  (Fig- 3.64E).

**f) Inhibition of erythrocyte hemolysis**

The methanol extract along with its ethyl acetate and butanol fractions were found to inhibit the hemolysis of erythrocytes. Butanol and ethyl acetate fractions were found to be more potent compared to total methanol extract with  $\text{EC}_{50}$  values of 2.26, 8.35 and 11.41  $\mu\text{g}/\text{ml}$ , respectively. The results are comparable to that of ascorbic acid ( $\text{EC}_{50}$ : 3.07 $\mu\text{g}/\text{ml}$ ). The butanol fraction was found to be more potent than the ascorbic acid. Aqueous fraction did not show any inhibition in AAPH induced erythrocytes hemolysis (Fig-3.64F).

**g) Rapid screening for antioxidant compound**

Total methanol extract and its fractions *viz.*, ethyl acetate and butanol were found to contain antiradical components with ethyl acetate fraction containing higher concentration than butanol fraction and methanol extract (Fig-3.80d)

**h) Total phenolic content**

The total amount of phenolic content present in total methanol extract and its ethyl acetate, butanol and aqueous fractions was found to be 16.1, 25.29, 17.74 and 0.9% w/w, respectively. (Fig-3.63)

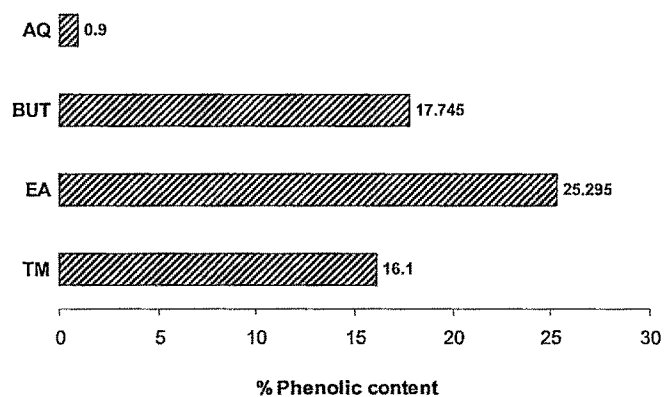


**Fig-3.63 Total phenolic content in different extracts of Butea flowers**

**Abbreviations:** TM-Total methanol extract, BUT-Butanol extract, EA-Ethyl acetate extract, AQ-Successive aqueous extract.

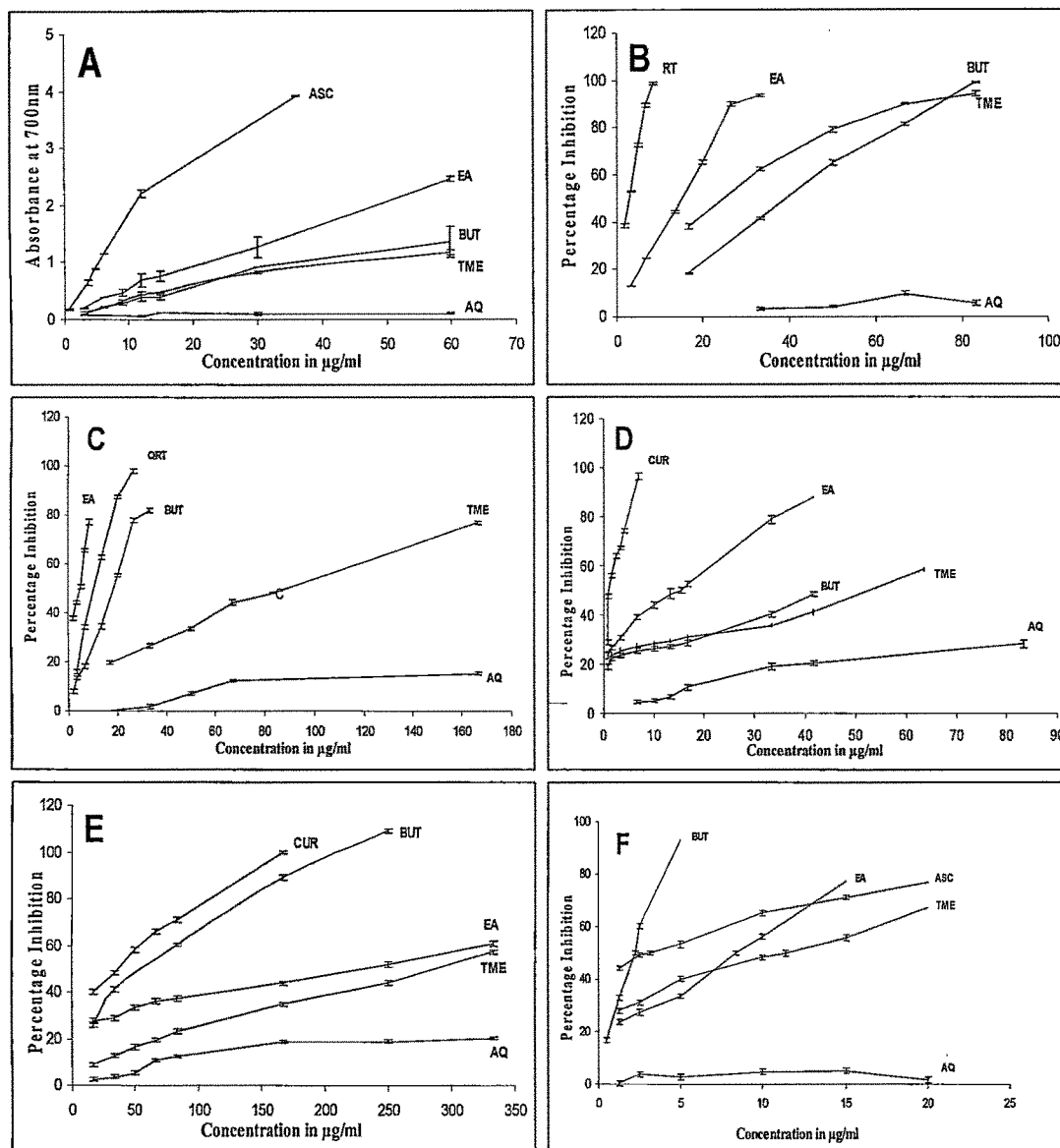


**Fig-3.64 XY- Scatters for *in vitro* studies on different extracts of Butea flowers.** Results are average of three determinations and shown as Mean  $\pm$  SD. A) Reducing power assay, B) DPPH radical scavenging assay, C) Superoxide radical scavenging assay, D) Hydroxyl radical scavenging assay, E) Nitric oxide radical scavenging assay, F) Inhibition of erythrocytes lysis by extracts.  
**Abbreviations used in figure:** EA-Ethyl acetate extract, AQ-Successive aqueous extract, TM-Total methanol extract, ASC-Ascorbic acid, CUR-Curcumin, RT-Rutin, QUR-Quercetin.

From the results it was observed that the methanol extract of the *B. monosperma* and its various fractions were found to act as radical scavengers against different free radicals under the conditions of oxidative stress. Most nonenzymatic antioxidative activity like scavenging of free radicals, inhibition of lipid peroxidation, etc. is mediated by redox reactions.

The reducing power determined in the present study depends on the redox potentials of the compounds present in different fractions. The highest amount of reducing power was observed in ethyl acetate and butanol fractions followed by total methanol extract. Thus, it can be expected that the fractions may have scavenging activity against other oxidizing agents.

DPPH radical has been widely used to test the radical scavenging ability of various natural products and has been accepted as a model compound for free radicals originating in lipids. Ethyl acetate and butanol fractions along with total methanolic extract showed a concentration dependent antiradical activity by reducing DPPH radical.

Superoxide anion, which is a reduced form of molecular oxygen, has been implicated in initiating oxidation reactions associated with aging. It plays an important role in the formation of other reactive oxygen species such as hydrogen peroxide, hydroxyl radical, and singlet oxygen, which induce oxidative damage in lipids, proteins, and DNA.

Ethyl acetate and butanol fractions were found to be good scavenger of superoxide radicals. The decrease of absorbance in the presence of these fractions indicates the consumption of superoxide anion in the reaction mixture. Hydroxyl radicals are reported to cause oxidative damage to various biomolecules like DNA, lipids and proteins.

Ethyl acetate and butanol fractions were capable of reducing the damage to deoxyribose more effectively than the total methanol extract. Sodium nitroprusside serves as a main source of nitric oxide radicals. Butanol and ethyl acetate fractions, scavenges the NO formed from the sodium nitroprusside by inhibiting the chromophore formation and hence the absorbance decreases as the concentration of the fractions increases.

The present study was further supported by the finding that the ethyl acetate and butanol fractions strongly inhibited erythrocyte hemolysis induced by

AAPH, where lysis occurs mainly by two events, lipid peroxidation and redistribution of oxidized band 3 within the cell membrane. It is considered that AAPH attack the membrane to induce the chain oxidation of lipids and proteins leading to the damage of spectrin, a membrane protein, by oxidative cross linking which may ultimately result in hemolysis. Band 3 in erythrocyte membranes plays an important role in a rapid exchange of  $\text{HCO}_3^-$  and  $\text{Cl}^-$  across the membrane. Butea fractions may block hemolysis by inhibiting the formation of hemolytic holes in the erythrocytes cell membrane by blocking oxidation and redistribution of band 3 proteins.

Rapid screening for antioxidants by TLC revealed the presence of many constituents with radical scavenging properties in varying proportions in all the fractions other than aqueous. These constituents can be isolated and can be used for future structural elucidation.

These studies suggest that specific constituents in ethyl acetate and butanol fractions contribute to the antioxidant activity of the flowers. Phenolic compounds are reported to be potent free radical terminators and thus, the results are further supported by the varying amounts of total phenolic content in different fractions of flowers.

Ethyl acetate and butanol fractions were found to have potent free radical scavenging activity and can also act by inhibiting the AAPH mediated erythrocyte hemolysis. The observed activity may be mainly due to their total phenol content. However, in case of erythrocyte hemolysis, butanol fraction with lower phenolic content was found to be more effective than ethyl acetate fraction with higher phenolic content, which may be due to the presence of two antihepatotoxic principles *viz.*, butrin and isobutrin.

#### **3.3.4.2 Toxicity study**

Ethyl acetate (EA), butanol fractions (BUT), did not show any mortality at a single oral dose of 2000mg/kg body weight. Histopathological examination of the visceral organs did not show any signs of necrosis or damage. Fractions did not affect the normal architect of liver, heart and kidney. BFEA and BUT treated

mice did not show any change in body weight. No signs of reactions like tremors, convulsions, salivation, and diarrhoea were observed. Safe dose 100 and 200mg/kg body weight was used for further in vivo studies.

### 3.3.4.3 In-vivo antioxidant activity

#### 3.3.4.3.1 Isoproterenol induced myocardial infarction

The ethyl acetate and butanol fractions were screened for their in-vivo antioxidant activity using ISO induced myocardial infarction and liver damage in rats. Results are shown in (Table-1.37, 1.38 & Fig-3.65, 3.66)

**Table-1.37 Effect of extracts on endogenous antioxidant enzymes in heart**

Groups	SOD	CAT	GSH	LPO
CONTROL	18.29±1.71	798.76±33.63	14.95±0.67	1.38±0.13
ISO	10.24±0.78*	368.11±33.33***	11.87±0.38**	4.59±0.22***
EA100	23.42±2.34 <sup>ns</sup>	801.26±41.43	17.48±0.44*	1.68±0.09 <sup>ns</sup>
EA100+ISO	20.77±0.96 <sup>#</sup>	705.15±66.78 <sup>###</sup>	21.09±0.52 <sup>###</sup>	2.4±0.15 <sup>###</sup>
EA200	9.95±1.33*	475.63±32.48***	7.79±0.79***	3.27±0.25***
EA200+ISO	9.13±1.54 <sup>ns</sup>	302.47±28.05 <sup>ns</sup>	4.59±0.19 <sup>###</sup>	4.07±0.2 <sup>ns</sup>
BUT	22.17±2.78 <sup>ns</sup>	775.68±51.59	13.24±0.21 <sup>ns</sup>	2.74±0.15**
BUT+ ISO	19.77±1.25 <sup>#</sup>	758.73±58.48 <sup>###</sup>	20.46±0.72 <sup>###</sup>	8.43±0.43 <sup>###</sup>

Statistical analysis was done by using ANOVA

Post test applied: Tukey-Kramer multiple comparison Test

Values are expressed as mean ± SEM.

\*p<0.05; \*\*p<0.01; \*\*\*p<0.001; <sup>ns</sup>p>0.05 = non significant, (n=6)

ISO treated group and extract alone pretreated groups were compared with control group (\*Compared with control group).

Extract pretreated group injected with ISO were compared with ISO group (#compared with ISO treated group).

**Table-1.38 Effect of extracts on cardiac and liver serum marker enzymes**

Groups	CKMB	LDH	SGPT	SGOT	ALKP	Uric acid
CON	585.47±41.58	1417.3±63.91	60.66±1.45	131±11.59	312.5±21.11	0.99±0.05
ISO	850.86±31.89**	1877.8±42.94***	60.66±0.88 <sup>ns</sup>	182.33±18.19**	475±22.58***	1.55±0.06***
EA100	573.6±29.85 <sup>ns</sup>	745.25±46.25***	59.25±0.48 <sup>ns</sup>	127.8±5.45 <sup>ns</sup>	325.96±25.27 <sup>ns</sup>	0.94±0.07 <sup>ns</sup>
EA100+ISO	591.88±39.5##	1265.3±54.85##	63.5±2.12 <sup>ns</sup>	118.68±1.55###	337.7±31.46##	1.08±0.08##
EA200	654.08±54.23 <sup>ns</sup>	1774.3±53.8*	75.91±1.5***	169.27±4.29 <sup>ns</sup>	406.67±19.41 <sup>ns</sup>	1.68±0.11***
EA200+ISO	670.33±62.95 <sup>ns</sup>	2126.8±83.75 <sup>ns</sup>	85.25±1.52###	176.9±5.81 <sup>ns</sup>	462.67±3.21 <sup>ns</sup>	1.47±0.13 <sup>ns</sup>
BUT	597.17±12.83 <sup>ns</sup>	1761.7±76.12*	59.91±0.58 <sup>ns</sup>	137.1±2.77 <sup>ns</sup>	332.72±17.48 <sup>ns</sup>	1.1±0.029 <sup>ns</sup>
BUT+ ISO	460.67±50.55###	2620.4±92.55###	60.66±2.23 <sup>ns</sup>	122±5.92##	366.67±14.87#	1.31±0.058 <sup>ns</sup>

Statistical analysis was done by using ANOVA

Post test applied: Tukey-Kramer multiple comparison Test

Values are expressed as mean ± SEM.

\*p<0.05; \*\*p<0.01; \*\*\*p<0.001; <sup>ns</sup>p>0.05 = non significant, (n=6)

ISO treated group and extract alone pretreated groups were compared with control group (\*Compared with control group).  
Extract pretreated group injected with ISO were compared with ISO group (#compared with ISO treated group).

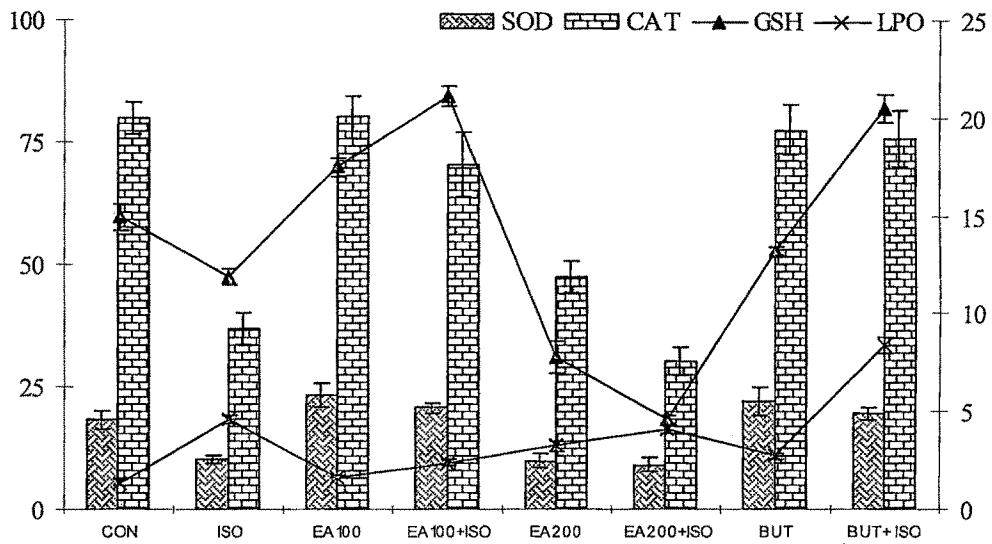


**Fig-3.65 Effect of Butea extracts on endogenous antioxidant enzymes in ISO induced myocardial infarction.**

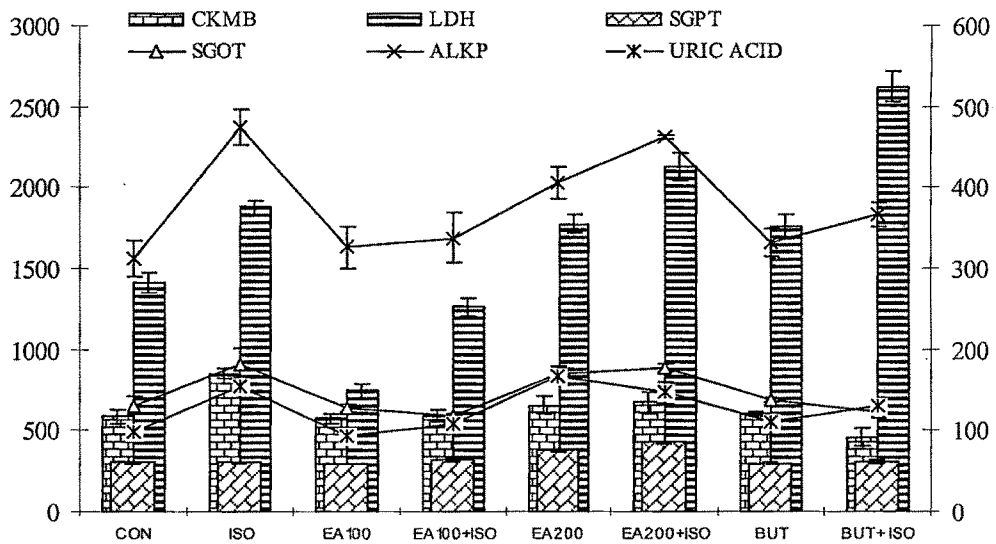


**Fig-3.66 Effect of Butea extracts on serum cardiac and liver marker enzymes.**

**a) Effect on Body weight**

No significant variation in body weight was observed, except BFEA, which at 200mg/kg b.w. showed significant decrease in body weight after 15 days treatment. This effect was observed both in BFEA+ISO and BFEA alone pretreated rats (Table-1.39, Fig-3.67)

**b) Effect on Heart weight/ Body weight ratio**

ISO group showed increase in Heart/body weight ratio compared to control group. BUT pretreated group injected with ISO showed significant reduction in the ratio compared to ISO group. BFEA at 100mg/kg b.w showed reduction in the ISO affected ratio, even BFEA alone showed reduction in this ratio. (Fig-3.68)

**c) Histopathological studies**

Microscopic examination of ISO treated rats showed myocardial necrosis foci intercalated among normal muscle fibers. In the necrosis foci there were lymphocytic exudates, atrophy of the remaining normal muscle and also elongation, undulation of the fibers and formation of contractile band lesions characteristic of the pre-infarction stage.

The rats pretreated with ethyl acetate (100mg/kg b.w) and butanol extracts of flowers reverse these changes. Ethyl acetate extract (200mg/kg b.w) treated heart showed non significant protection to the myocardium observed from presence of damaged myocardium blood pooling in certain areas of heart. (Fig-3.69)

**Table-1.39 Effect of Butea extracts on weight of rats during treatment.**

Groups	Animal Weights (Gms)							
	CON	ISO	BFEA100	BFEA100+ISO	BFEA200	BFEA200+ISO	BT	BT+ISO
1st day	343.33±8.72	313.33±3.63	293.33±16.91	250±1.44	320±6.23	319.17±5.23	331.67±11.66	336.67±12.27
8th day	333.33±11.15	323.33±3.63	297±16.53	256±1.52	301±2.15	290.83±3.74	328.33±13.01	330±13.76
15th day	343.33±7.37	330±5.2	298±16.37	262±1	285±5.65*	283.33±14.24*	341.67±13.01	330±16.64
17th day	353.33±4.94	328.33±6.5	304±15.63	262±0.66	272±9.58**	276.67±6.54**	343.33±13.09	335±11.45

Statistical analysis was done by using ANOVA  
 Post test applied: Dunnett multiple comparisons test.  
 Values are expressed as mean ± SEM.  
 \*p<0.05; \*\*p<0.01; \*\*\*p<0.001; nsp>0.05 = non significant, (n=6)  
 \* Compared with first day weight.

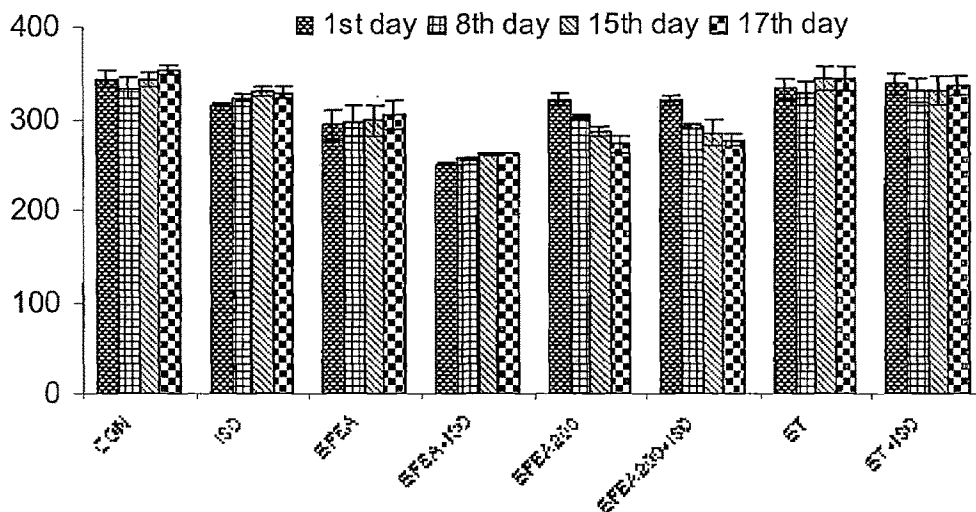


**Fig-3.67 Effect of Butea extracts on body weight of rats during treatment.**

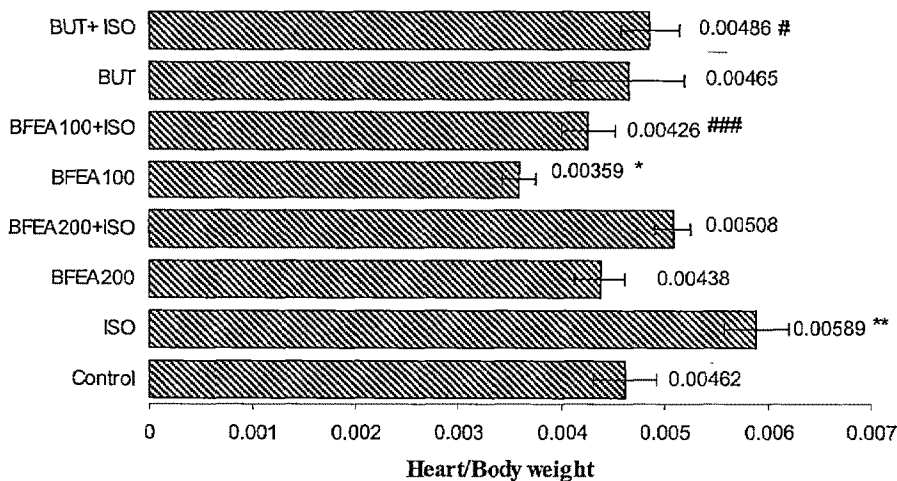


**Fig-3.68 Effect of Butea extracts on Heart weight/body weight ratio during treatment.**

Statistical analysis was done by using ANOVA

Post test: Tukey-Kramer multiple comparison Test

Values are expressed as mean  $\pm$  SEM.

\* $p < 0.05$ ; \*\* $p < 0.01$ ; \*\*\* $p < 0.001$ ;  $^{ns}p > 0.05$  = non significant, (n=6)

#compared with ISO treated group

\*Compared with normal group

The ethyl acetate extract (EA) (200mg/kg b.w.) showed decline in antioxidant enzyme levels in heart homogenate when compared to both control and ISO control group. The fraction also failed to decrease the ISO induced myocardial damage, marked with increased serum marker enzymes like LDH and uric acid, but only manage to reduce the serum CK-MB level as compared to ISO control. At a lower dose of 100mg/kg b.w. ethyl acetate extract was found to reverse the ISO induced damaging effect marked with increase in endogenous antioxidant enzymes with decreased serum cardiac marker enzymes. The study was further supported with the histopathological observations (Fig-3.65 & 3.66).

Butanol extract (BUT) the flowers showed marked increase in antioxidant enzyme levels in the heart homogenate with significant decrease in serum cardiac marker enzymes when compared with ISO group. Butanol extract alone pretreated rats showed a non-significant change when compared to control rats. No variation in body weight and heart to body weight ratio was observed in butanol extract treated group. It also reversed the ISO induced histopathological changes in cardiac muscles.

Ethyl acetate extract at a dose of 100mg/kg. b.w reversed the ISO induced cardiac and liver damage. At higher dosage it failed to provide any protection which may be due to its prooxidant effect. Butanol extract showed significant protection against ISO induced cardiac and liver damage. Increased endogenous antioxidant enzyme levels with BUT and EA may be contributes for its cardioprotective activity.

As weight loss occurred during the ethyl acetate treatment in rats, lipid profile of these animals was also measured.

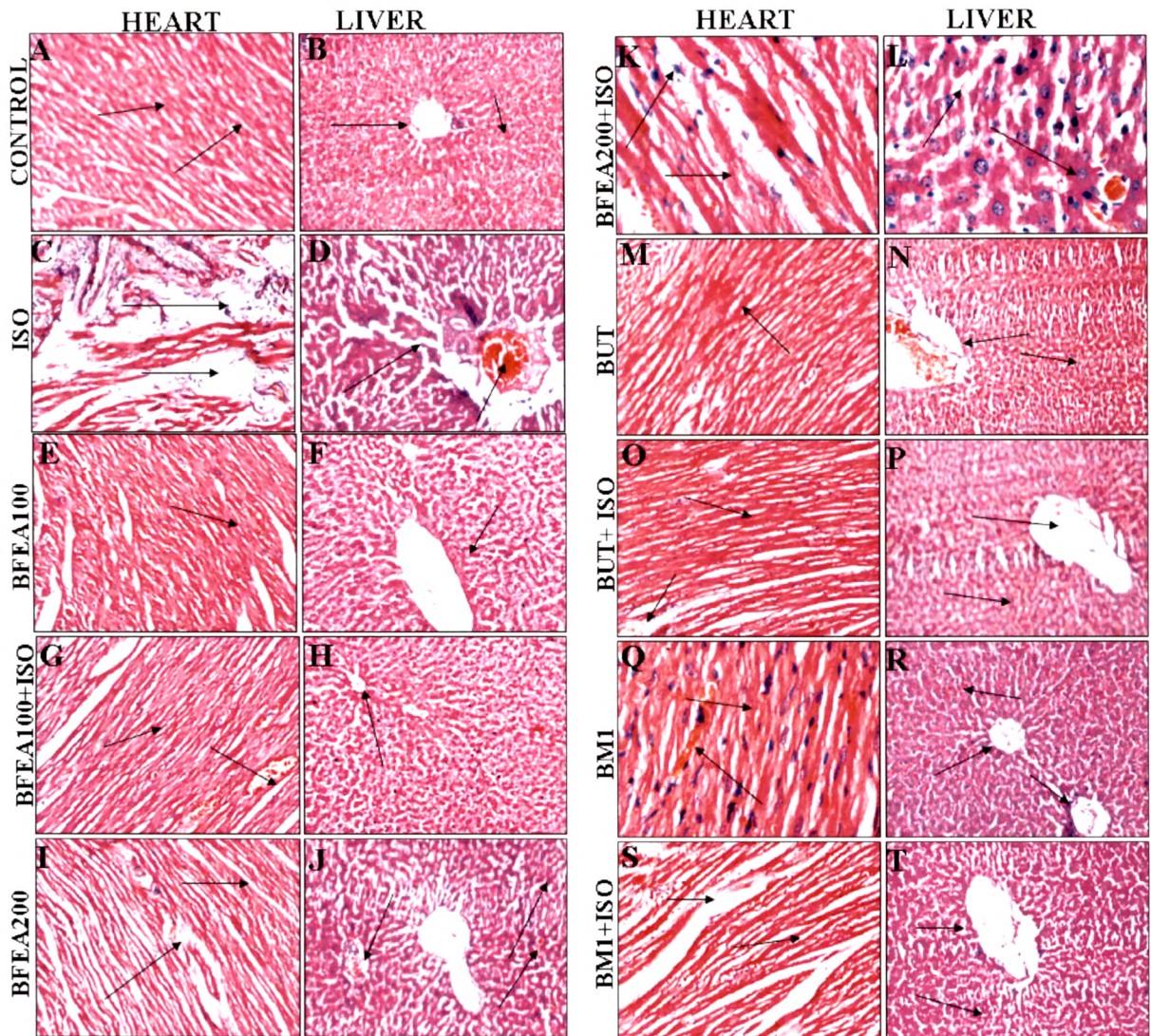


**Fig-3.69** Histopathology of heart and liver showing effect of *Butea* flower extracts in ISO induced myocardial and liver damage.

### 3.3.4.4 Isoproterenol induced Hyperlipidemia

As the weight loss occurred in ethyl acetate extract treated rats, the effect of *Butea monosperma* flowers were studied in ISO induced hyperlipidemia. Results are shown in (Table-1.40, Fig-3.70)

**Table-1.40 Effect of *Butea* extracts on serum lipid profile of extract treated rats.**

Groups	TC	TRIG	LDL	HDL	VLDL	TC/HDL	LDL/HDL
CONTROL	61±1.5	81.08±5.49	-0.58±1.61	40.33±0.44	9.93±0.43	1.51±0.05	-0.015±0.04
ISO	113.64±4.21***	153.17±0.97***	9.33±0.55***	35.33±0.49***	17.82±0.33***	3.21±0.11***	0.26±0.017***
EA100	68.75±0.4 <sup>ns</sup>	85.68±2.96 <sup>ns</sup>	-4.91±0.45*	41.95±1.06 <sup>ns</sup>	9.67±0.48 <sup>ns</sup>	1.65±0.06 <sup>ns</sup>	-0.11±0.008 <sup>ns</sup>
EA100+ISO	74.66±0.72###	53±2.97###	1.25±0.04###	41.55±0.64###	10.5±0.6###	1.79±0.01###	0.03±0.001###
EA200	98.67±5.12***	125.67±3.08***	19.73±1.37***	37.3±1.2 <sup>ns</sup>	18.16±0.23***	2.66±0.18***	0.52±0.03***
EA200+ISO	78.25±3.81###	100.33±1.64###	28.13±1.45###	39.9±0.57##	25.35±0.13###	1.96±0.11###	0.7±0.04###
BUT	65.5±1.29 <sup>ns</sup>	85.63±0.22 <sup>ns</sup>	3.95±0.01*	40±0.57 <sup>ns</sup>	10.95±0.48 <sup>ns</sup>	1.63±0.008 <sup>ns</sup>	0.09±0.001*
BUT+ ISO	59±0.86###	67.33±3.76###	5±0.28#	40.33±0.22###	12.16±0.3###	1.46±0.02###	0.12±0.006##

Statistical analysis was done by using ANOVA

Post test: Tukey-Kramer multiple comparison Test

Values are expressed as mean ± SEM.

\*p<0.05; \*\*p<0.01; \*\*\*p<0.001; <sup>ns</sup>p>0.05 = non significant, (n=6)

#compared with ISO treated group

\*Compared with normal group

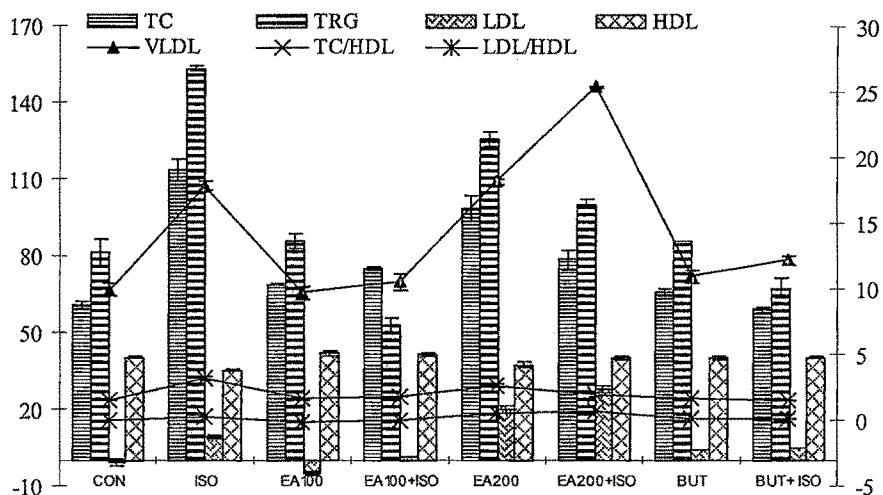


**Fig-3.70 Effect of Butea extracts on serum lipid profile.**

ISO treated group (25mg/kg.b.w) showed significant increase in serum total cholesterol, LDL, VLDL and triglycerides with marked decrease in HDL cholesterol level. It also showed an increase in TC/HDL and LDL/HDL value which is considered to be the risk factor for the heart.

Butanol extract of flower showed significant decrease in serum TC, LDL, TG, and VLDL with marked increase in HDL level. It also reduced the risk factor associated with the TC/HDL and LDL/HDL value, compared to ISO control group. Butea extract alone pretreated group did not show any change in serum lipid profile of the rat when compared to control group.

Ethyl acetate extract (200mg/kg) of flower showed significant increase in serum TC and LDL level. The fraction also increased the risk factor associated with TC/HDL and LDL/HDL value. But the extract reduced the serum TG and VLDL level significantly with marked increase in serum HDL level when compared to ISO control group. At 100mg/kg b.w. ethyl acetate extract showed significant protection against ISO induced hyperlipidemia.

**3.3.4.5 Evaluation of antioxidant activity of Butea flower ethyl acetate extract (BFEA) on cardiac cell line-H9c2**

**3.3.4.5.1 Percentage cell viability (H9c2)**

H9c2 cells were incubated with varying concentration of BFEA ie. (2, 5, 10, 20, 50, 75 and 100µg/ml) for different time interval ie. 3, 6, and 12h respectively and cell viability was determined by MTT assay. BFEA showed 80.65, 69.67, 78.68, 101.63, 97.13, 104.09, and 89.75% cell viability at the above concentration after 3hrs of incubation, while after 6hrs of incubation there was no significant change in viability of H9c2 cells, ie 100, 101, 102, 103, 109, 110, and 91.71%. BFEA showed 90.4, 88.95, 90.62, 88.95, 87.29, 83.33, and 72.08% of cell viability at the above concentration range after 12hrs of treatment. (Table-1.41, Fig-3.71)

**Table-1.41 Effect of BFEA from Butea flowers on % - viability of H9c2 cells**

BFEA (µg/ml)	3 Hr	6 Hr	12 Hr
<b>Control</b>	100±6.96	100±1.06	100±1.66
<b>2</b>	80.65±10.89	100±4.54	90.41±0.83
<b>5</b>	69.67±3.68	101.87±6.68	88.95±4.16
<b>10</b>	78.68±3.68	102.67±2.94	90.62±2.08
<b>20</b>	101.63±11.88	103.2±6.68	88.95±1.25
<b>50</b>	97.13±10.65	109.62±4.27	87.29±3.33
<b>75</b>	104.09±2.04	110.96±2.40	83.33±2.08
<b>100</b>	89.75±6.55	91.71±1.33	72.08±1.25

Values are expressed as mean ± SD of % cell viability (average of three determinations)

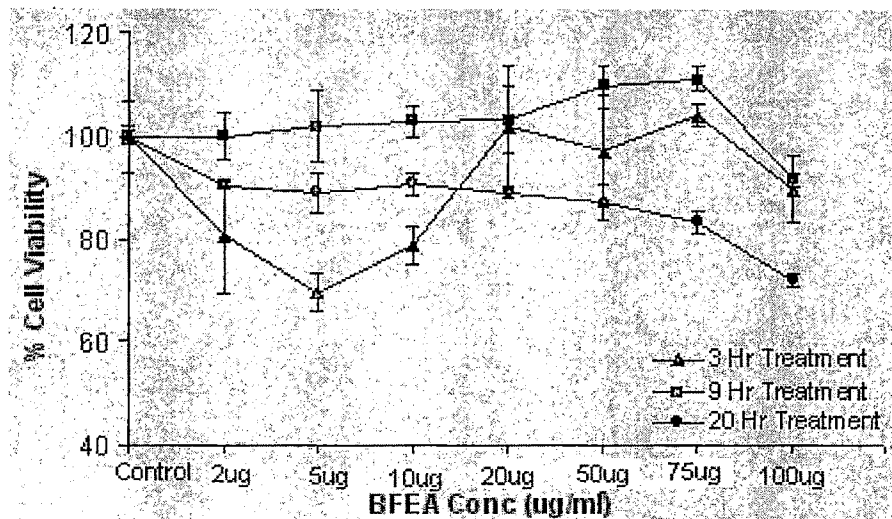


**Fig-3.71 Effect of various concentration of BFEA on %- viability of H9c2 cells at different time period**

BFEA showed concentration and time dependent repose on the viability of H9c2 after 12 hrs of treatment. It did not show any significant effect on cell viability after incubating for short duration. The results obtained for BFEA provides a lead for dose fixation for further studies carried out as stated below.

#### **3.3.4.5.2 Effect of BFEA from Butea flowers on H<sub>2</sub>O<sub>2</sub> induced stress in H9c2 cells**

H<sub>2</sub>O<sub>2</sub> lowers the cell viability to 21.13% after 3 hrs of treatment. Treatment with BFEA (1, 2, 5, 10, 15, 20, and 50µg/ml) showed 24.83, 36.38, 47.05, 56.42, 59.91, 71.24, and 95.42% of cell viability when compared with that of H<sub>2</sub>O<sub>2</sub> (21.13%).

BFEA after 6 hrs of treatment showed 27.01, 29.57, 31.59, 34.42, 36.38, 45.75 and 70.37% cell viability to that of H<sub>2</sub>O<sub>2</sub> (25.49%), while after 12 hrs of treatment the cell viability was found increased to 18.95, 21.78, 22.44, 25.7, 32.46, 45.53, and 62.96 respectively when compared to that of H<sub>2</sub>O<sub>2</sub> (27.66%) (Table-1.42, Fig-3.72 & 3.75 A-G).

BFEA showed concentration dependent protection against H<sub>2</sub>O<sub>2</sub> produced stress on H9c2 cells.

**Table-1.42 Effect of H<sub>2</sub>O<sub>2</sub> on BFEA pretreated H9c2 cell viability.**

BFEA ( $\mu\text{g/ml}$ )	3 Hr	6 Hr	12 Hr
Control	100 $\pm$ 5.01	100 $\pm$ 2.55	100 $\pm$ 4.61
H <sub>2</sub> O <sub>2</sub>	21.13 $\pm$ 2.61	25.49 $\pm$ 5.01	27.66 $\pm$ 1.74
1	24.83 $\pm$ 3.70	27.01 $\pm$ 5.66	18.95 $\pm$ 3.70
2	36.38 $\pm$ 6.97	29.57 $\pm$ 1.74	21.78 $\pm$ 1.30
5	47.05 $\pm$ 6.31	31.59 $\pm$ 0.87	22.44 $\pm$ 1.96
10	56.42 $\pm$ 6.10	34.42 $\pm$ 3.26	25.7 $\pm$ 1.30
15	59.91 $\pm$ 3.26	36.38 $\pm$ 4.13	32.46 $\pm$ 3.70
20	71.24 $\pm$ 6.53	45.75 $\pm$ 3.48	45.53 $\pm$ 3.05
50	95.42 $\pm$ 2.61	70.37 $\pm$ 2.39	62.96 $\pm$ 6.97

Values are expressed as mean  $\pm$  SD of % cell viability (average of three determinations)

BFEA showed significant protection against H<sub>2</sub>O<sub>2</sub> induced stress in H9c2 cells. The Protection was concentration and time dependent. As the incubation time was increased ie (12hrs) cell viability was also decreased when compared with 3hrs and 6hrs of treatment.

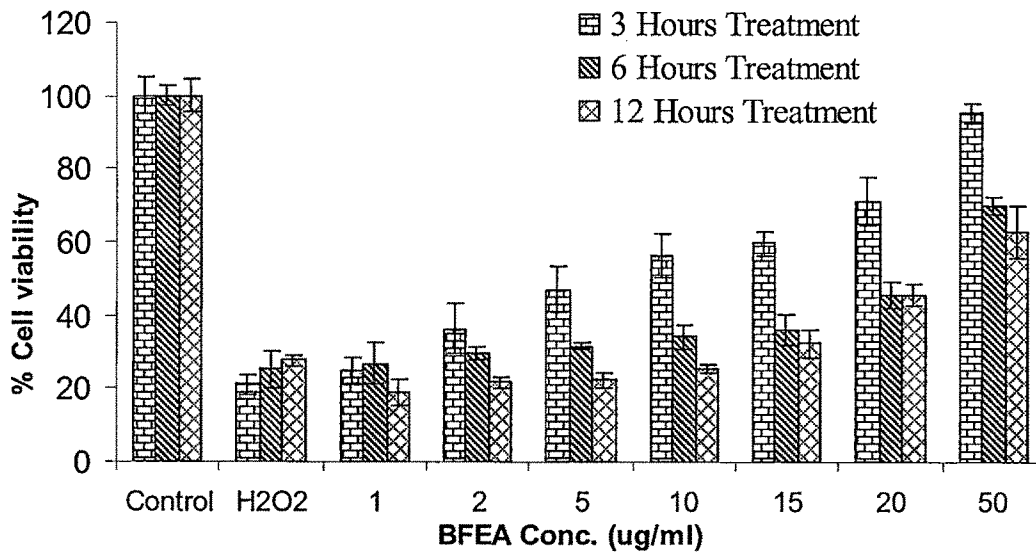


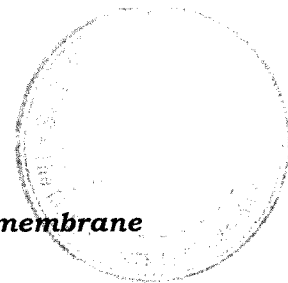
**Fig-3.72 Effect of H<sub>2</sub>O<sub>2</sub> on %- viability of BFEA pretreated H9c2 cell.**

#### **3.3.4.5.3 Effect of BFEA pretreatment on H<sub>2</sub>O<sub>2</sub> induced increase in intracellular ROS level**

H9c2 cells, pretreated with BFEA were exposed to H<sub>2</sub>O<sub>2</sub>, and ROS was assessed by flow cytometric analysis after loading the cells with the ROS-sensitive dye DCFH-DA. As shown in (Fig-3.74B), an increase in DCF was observed in the H<sub>2</sub>O<sub>2</sub>-treated cells, with the mean fluorescence intensity increased from 4.82% to 33.78% (Fig- 3.74A & 3.74B). This effect of H<sub>2</sub>O<sub>2</sub> was attenuated by BFEA pretreatment. Treatment of H9c2 cells with 2-5 µg/ml concentration of BFEA caused the mean fluorescence intensity to decrease from 33.78% to 5.24% (Fig - 3.74B, C, D & E). But further increase in BFEA concentration (15µg/ml) increased the fluorescence intensity to 25.37% compared to that of (2-5µg/ml) (Fig- 3.74 F), which might be due the prooxidant effect of extract. The cells treated under the same conditions were further subjected to confocal microscopy. A dramatic increase in fluorescence intensity was observed in the H<sub>2</sub>O<sub>2</sub> treated cells (Fig- 3.73 B), which was reversed by pretreatment with different concentration of BFEA (2-10µg/ml) (Fig- 3.73 B, C, D, & E), while at 15µg/ml, fluorescence was found to be increased which might be due to the prooxidant effect of BFEA on H9c2 cells (Fig- 3.73 F).

#### **3.3.4.5.4 Effect of BFEA on xanthine-xanthine oxidase induced increase in intracellular ROS level**

Treatment of H9c2 cells with (X+XO) increases the fluorescence intensity from 5.02 to 55.06% when assessed by flow cytometric analysis after loading the cells with the ROS-sensitive dye DHE (Fig- 3.74G to H). This effect of X+XO was reversed in cells pretreated with different concentration of BFEA (2-5µg/ml) with decrease in fluorescence intensity of DHE from 55.06 to 4.34% respectively (Fig-3.74 H to 3.74J), while at higher concentration ie (10-15µg/ml) BFEA showed increased intensity compared to (2-5µg/ml), which might be due to its prooxidant effect on H9c2 cells (Fig- 3.74K & 3.74L). The confocal examination showed O<sub>2</sub><sup>-</sup> was enhanced in X-XO exposed cells (Fig- 3.73M & 3.73N). BFEA pretreated cells (2-10µg/ml) found to reverse this X+XO induced changes, confirmed by decreased fluorescence intensity in BFEA pretreated cells (Fig- 3.73O to 3.73Q). BFEA showed prooxidant effect at 15µg/ml concentration with increased fluorescence intensity (Fig-3.73 R)



#### **3.3.4.5.5 Effects of BFEA on H<sub>2</sub>O<sub>2</sub> affected mitochondrial membrane potential ( $\Delta\Psi_m$ ) in H9c2 cells.**

DiOC<sub>6</sub>, a mitochondrial voltage dependent dye was employed to observe the changes in  $\Delta\Psi_m$ . After exposing the cells H<sub>2</sub>O<sub>2</sub> (35 $\mu$ M) for 2hrs, DiOC<sub>6</sub> intensity was significantly reduced as observed in confocal microscopy when compared to untreated control cell (Fig- 3.73G & 3.73H). Pretreatment with BFEA (2-15 $\mu$ g/ml) increased the fluorescence intensity when compared with H<sub>2</sub>O<sub>2</sub> treated cells (Fig- 3.73G-3.73L).

Thus BFEA pretreatment was found to increase the H<sub>2</sub>O<sub>2</sub> affected mitochondrial membrane potential ( $\Delta\Psi_m$ ).

$\Delta\Psi_m$  was further measured by using Tetramethyl Rhodamine (TMRE). H<sub>2</sub>O<sub>2</sub> reduced the membrane potential in H9c2 cells marked with increase fluorescence intensity from 9.71 to 41.04% when assessed by flow cytometric analysis after loading the cells with the  $\Delta\Psi_m$ -sensitive dye TMRE (Fig- 3.74M & 3.74N). Pretreatment with various concentration of BFEA (2-5 $\mu$ g/ml) increased the  $\Delta\Psi_m$  confirmed by decreased fluorescence intensity from 41.08 to 9.35% (Fig- 3.74N- 3.74P), but at higher concentration 10-15 $\mu$ g/ml,  $\Delta\Psi_m$  gets reduced, which might be due to the prooxidant effect of BFEA (Fig- 3.74Q & 3.74R).

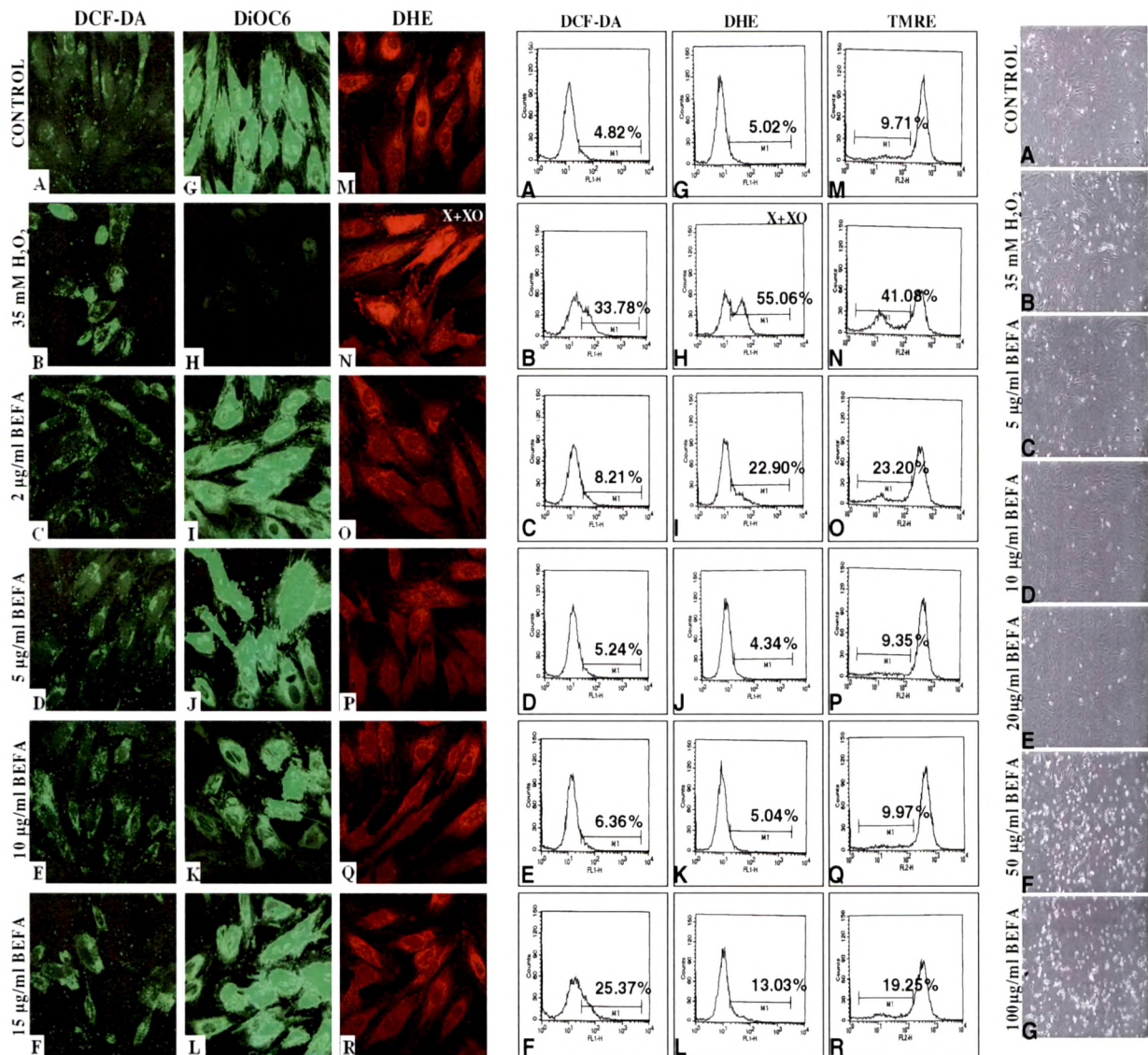


**Fig-3.73 (A-R) Confocal images of H9c2 cells loaded with different molecular probes showing the effect of BFEA on H<sub>2</sub>O<sub>2</sub> and Xanthine-xanthine oxidase induced stress.**

**Fig-3.74 (A-R) Flow activated cytometric analysis of H9c2 cells pretreated with different concentration of BFEA and challenged with H<sub>2</sub>O<sub>2</sub> and Xanthine-xanthine oxidase after loading with different molecular probes.**

**Fig. 3.75 (A-G) Effect of BFEA on H<sub>2</sub>O<sub>2</sub> induced stress in H9c2 cell lines**

### **3.3.5 Isolation of BFEA-1 from ethyl acetate fraction of Butea flowers (BFEA)**

BFEA-1 was isolated by preparative thin layer chromatography (PTLC) of ethyl acetate extract of flowers. PTLC was developed in Toluene: Glacial acetic acid: Ethyl acetate (40:20:20v/v). Dark black colored band visible at 254nm with R<sub>f</sub> 0.4 was scrapped and compound was dissolved in methanol. Silica was separated by centrifugation at 2500rpm. BFEA was further purified by recrystallization in methanol. White buff colored compound was obtained which shows single band on TLC in Toluene: Glacial acetic acid: Ethyl acetate (40:20:20v/v).

#### **3.3.5.1 Characterization of BFEA-1**

BFEA-1 isolated from Butea flowers was characterized by UV, <sup>1</sup>H NMR, <sup>13</sup>C NMR, and IR. BFEA showed following characteristic spectra's.

IR (KBr): 3365, 3387(hydroxyl group), 3065(C-H stretching), 1703(C=O stretching of carboxylic group), 1619(C-C stretching within ring), 1541(C-C stretching within ring), 1447(C=C stretching within the ring), 1340(O-H bending of hydroxyl group), 1310,(O-H bending of carboxylic acid) 1248(C-O stretching of hydroxyl group), 1026(C-O stretching of carboxylic acid), 867, 790, 703(aromatic compound), 765 nm (alcoholic compound).

<sup>1</sup>H NMR (D<sub>2</sub>O, 400 Hz): δ: 6.99 (2H, s, H-2, H-6). Chemical shifts are given in ppm on the δ-scale, s = singlet.

<sup>13</sup>C NMR (D<sub>2</sub>O, 100 MHz): δ: 109.98 (2C, C-2, C-6), 120.76(1C, C-1), 138(1C, C-4), 144.39(2C, C-3, C-5), 170.14(1C, C-7).

Compound BEFA, is a colourless solid, mp. 278-281°C was identified as 3, 4, 5-trihydroxy benzoic acid, i.e., *Gallic acid*. The UV spectrum gave the characteristic absorption maximum of gallic acid at 215nm and 272nm, further the R<sub>f</sub> value of the compound was matched with gallic acid. On TLC dark black bands of BEFA-1 and pure gallic acid were observed with methanolic FeCl<sub>3</sub>, which further confirmed BEFA-1 to be gallic acid. The IR spectrum

fingerprinting matched exactly with that of pure gallic acid. BFEA-1 showed the presence of hydroxyl(s) (3365nm, 3287nm), aromatic moiety (1619nm), and carboxylic acid (1703nm). The <sup>1</sup>H NMR spectrum of BEFA showed presence of aromatic protons at δ 6.99. The <sup>13</sup>C NMR showed peak at δ 109.98 for C-2 and C-6 and at δ 170.14 for carboxylic acid.

**3.3.5.2 Quantification of BFEA-1 in different extracts of Butea flowers by HPTLC.**

Stock solution of BFEA-1 prepared in methanol.

Stock solutions of extracts were prepared in methanol.

Solvent system- Toluene: Glacial acetic acid: Ethyl acetate (40:20:20v/v)

Calibration range for BFEA-1AECHE-2 (100 to 400ng)

Scanning wavelength-254nm

Regression vial height (r=0.99948, sdv= 1.85%)

Regression via area (r= 0.99573, sdv=5.80)

Ethyl acetate fraction of butea flowers contain 57.2 and 61.6% of BFEA-1 while butanol fraction showed 42 and 43.66% of BFEA-1 with respect to height and area. BFEA is present at higher concentration in ethyl acetate fraction. BFEA-1 was not get quantified in aqueous fraction (Table-1.43, Fig-3.76)

**Table-1.43 Estimation of BFEA-1 in different extracts of Butea flowers.**

<b>Extracts</b>	<b>Concentration of extract applied</b>	<b>BFEA-1 present with respect to height</b>	<b>BFEA-1 present with respect to area</b>
Ethyl acetate extract	200ng	57.2%	61.6%
Butanol extract	300ng	42.0%	43.66%
Methanol extract	300ng	45.33%	47.33%
S. aqueous extract	300ng	Not detected	Not detected

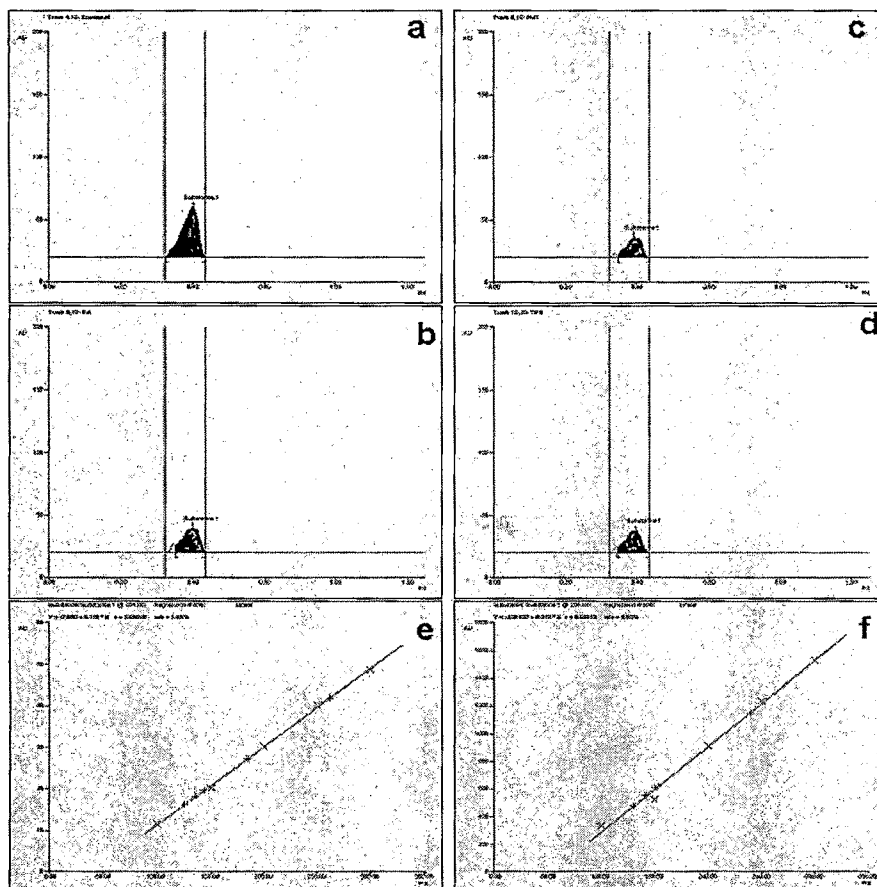


**Fig-3.76 Quantification of BFEA1 in different extracts of Butea flowers by HPTLC. Chromatogram for a) Isolated compound, b) Ethyl acetate fraction, c) Butanol fraction d) Total methanol extract, e) Regression via height ( $r=0.99948$ ), f) Regression via area ( $r=0.99573$ )**

Highest concentration of BFEA-1 was present in ethyl acetate extract as per height and area while it was less in butanol fraction. BFEA-1 was not detected in successive aqueous extract of flowers.

### 3.3.6 Chromatographic studies

TLC fingerprint profile of the ethyl acetate and butanol fractions were recorded. (Table- 1.44 & 1.45 2 and Figs- 3.77, 3.78, 3.79 & 3.80)

**Table-1.44 TLC fingerprinting for butanol fraction of *B. monosperma* flowers**

Scanning wavelength	<b>Solvent system 1*</b>			<b>Solvent system 2**</b>		
	R <sub>f</sub>	λ <sub>max</sub>	Relative % area	R <sub>f</sub>	λ <sub>max</sub>	Relative % area
254nm (Under UV)	0.13	366	2.01	0.07	200	5.87
	0.33	277	44.78	0.09	200	3.08
	0.52	370	40.51	0.14	278	47.33
	0.93	415	6.74	0.16	374	43.72
366nm (Under UV)	0.29	276	11.42	0.11	200	49.52
	0.45	406	27.31	0.14	278	23.43
	0.59	406	18.86	0.17	200	12.22
	0.76	586	17.43	0.18	200	14.84
	0.91	414	24.98			
520nm (After Derivatization)	0.11	480	1.52	0.57	476	86.13
	0.26	480	20.85	0.65	474	13.87
	0.39	558	31.04			
	0.60	480	8.90			
	0.68	525	10.25			
	0.77	468	15.10			
	0.84	523	11.22			
	0.94	525	1.13			

\*Solvent system 1—ethyl acetate: formic acid: glacial acetic acid: water (14.28:1.42:1.42:2.85 v/v) and treated with DPPH; \*\*Solvent system 2—butanol: acetic acid: water (4:1:5 v/v), treated with anisaldehyde sulphuric acid reagent.

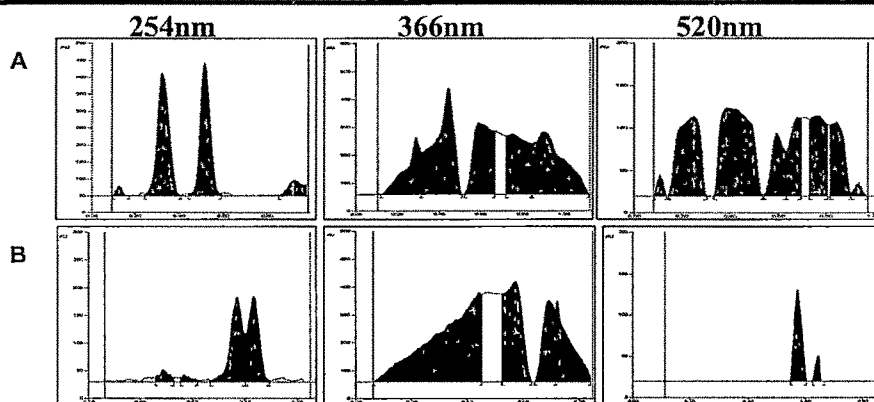


**Fig-3.77 TLC chromatogram for ethyl acetate fraction of *B. monosperma* flowers in ethyl acetate: formic acid: glacial acetic acid: water (14.28:1.42:1.42:2.85 v/v)**

**Table 1.45 TLC fingerprinting for ethyl acetate fraction of *B. monosperma* flowers**

Scanning wavelength	Solvent system-1*			Solvent system-2*		
	Rf	$\lambda_{\max}$	Relative %	Rf	$\lambda_{\max}$	Relative %
254nm (Under UV)	0.53	374	1.48	0.04	278	36.46
	0.76	370	6.25	0.68	283	13.40
	0.93	284	57.41	0.75	345	19.25
				0.94	280	30.89
366nm (Under UV)	0.48	406	18.27	0.03	700	0.14
	0.63	373	13.65	0.17	700	15.13
	0.76	372	24.23	0.20	700	48.96
	0.92	278	37.71	0.62	681	12.34
				0.85	682	7.24
				0.95	700	7.36
520nm (After Derivatization)	0.26	420	19.79	0.05	100	371
	0.38	540	22.53			
	0.54	480	34.25			
	0.78	480	5.75			
	0.92	535	17.68			

\*Solvent system 1: ethyl acetate: formic acid: glacial acetic acid: water (14.28:1.42:1.42:2.85 v/v) and treated with DPPH; Solvent system 2: chloroform: acetone: formic acid (14.85:3.36:1.78 v/v) and treated with anisaldehyde sulphuric acid reagent.

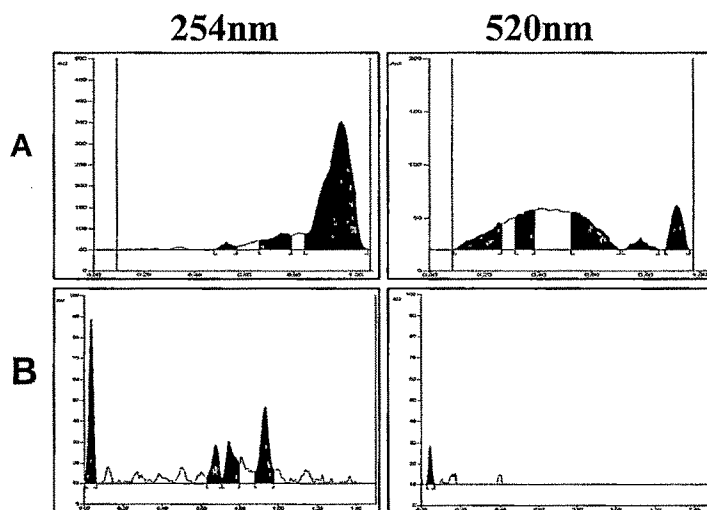


**Fig- 3.78 TLC chromatogram for ethyl acetate fraction of *B. monosperma* flowers in chloroform: acetone: formic acid (14.85:3.36:1.78 v/v)**

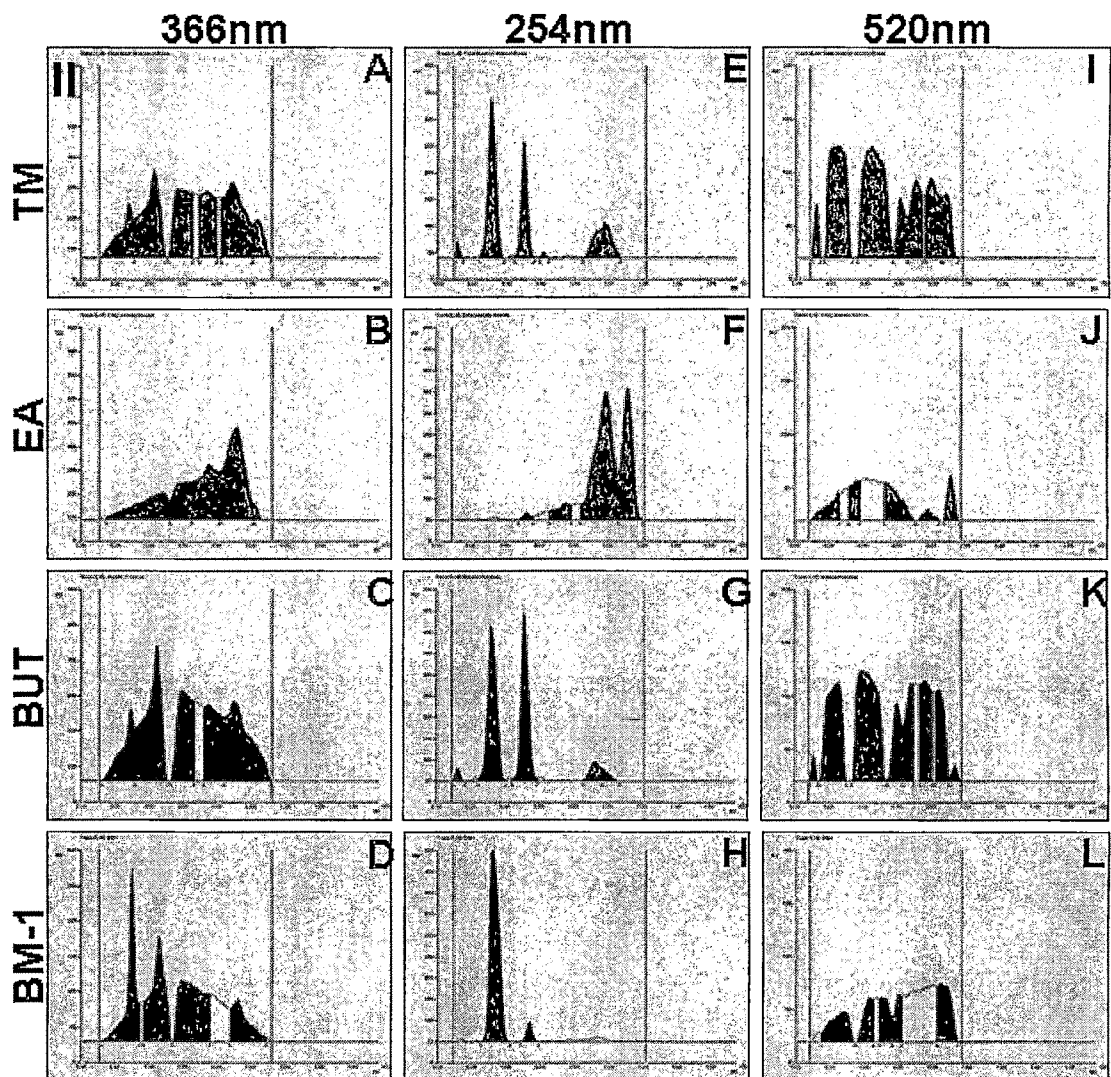
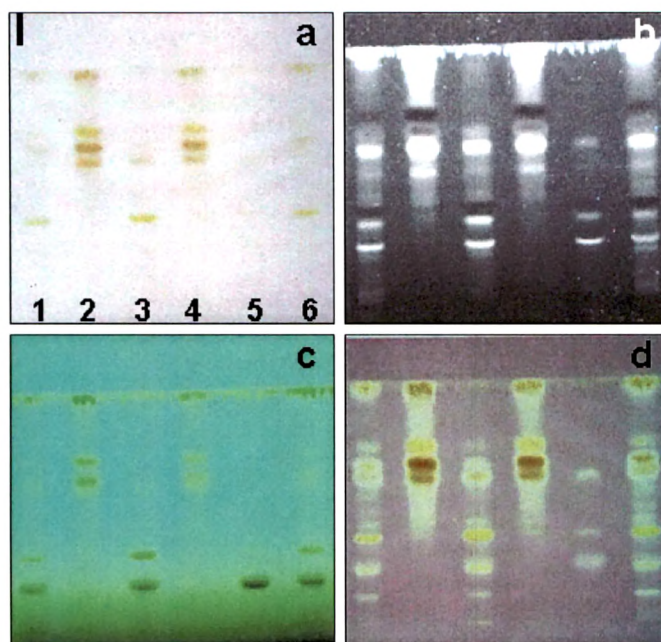


Fig-3.79 HPTLC Chromatogram for different extracts and fractions of Butea flowers scanned at 366 (A-D), 254 (E-H) and 520nm (I-L)-after treatment with anisaldehyde sulphuric acid reagent



**Fig-3.80** TLC showing- track-1- butanol extract, track-2- ethyl acetate extract, track-5 BM1 fraction of *Butea* flowers. Plate-a) Visible region, b) 366nm, c) 254nm, d) 520nm after treatment with DPPH reagent (Yellow coloration due to presence of radical scavengers).

TLC fingerprint of ethyl acetate and butanol extracts were derived in order to develop the standards and to know the compounds present. It will also help in designing the method of isolation and characterization of the bioactive components.

### **3.4 Studies of BM1 from *Butea monosperma* flowers**

During extraction of *Butea monosperma* flowers, with methanol, we found the yellow colored granular mass, which was filtered and washed several times with methanol. The mass was designated as BM1 for further studies.

Phytochemical investigation of BM1 reveals presence of flavonoids and sugars.

#### **3.4.1 Evaluation of antioxidant activity**

##### **3.4.1.1 In-vitro antioxidant activity**

BM1 was subjected for in-vitro antioxidant activity by above methods. It showed significant radical scavenging activity and it also inhibited the AAPH induced lysis of human blood erythrocytes. The results were compared with the reference standards.

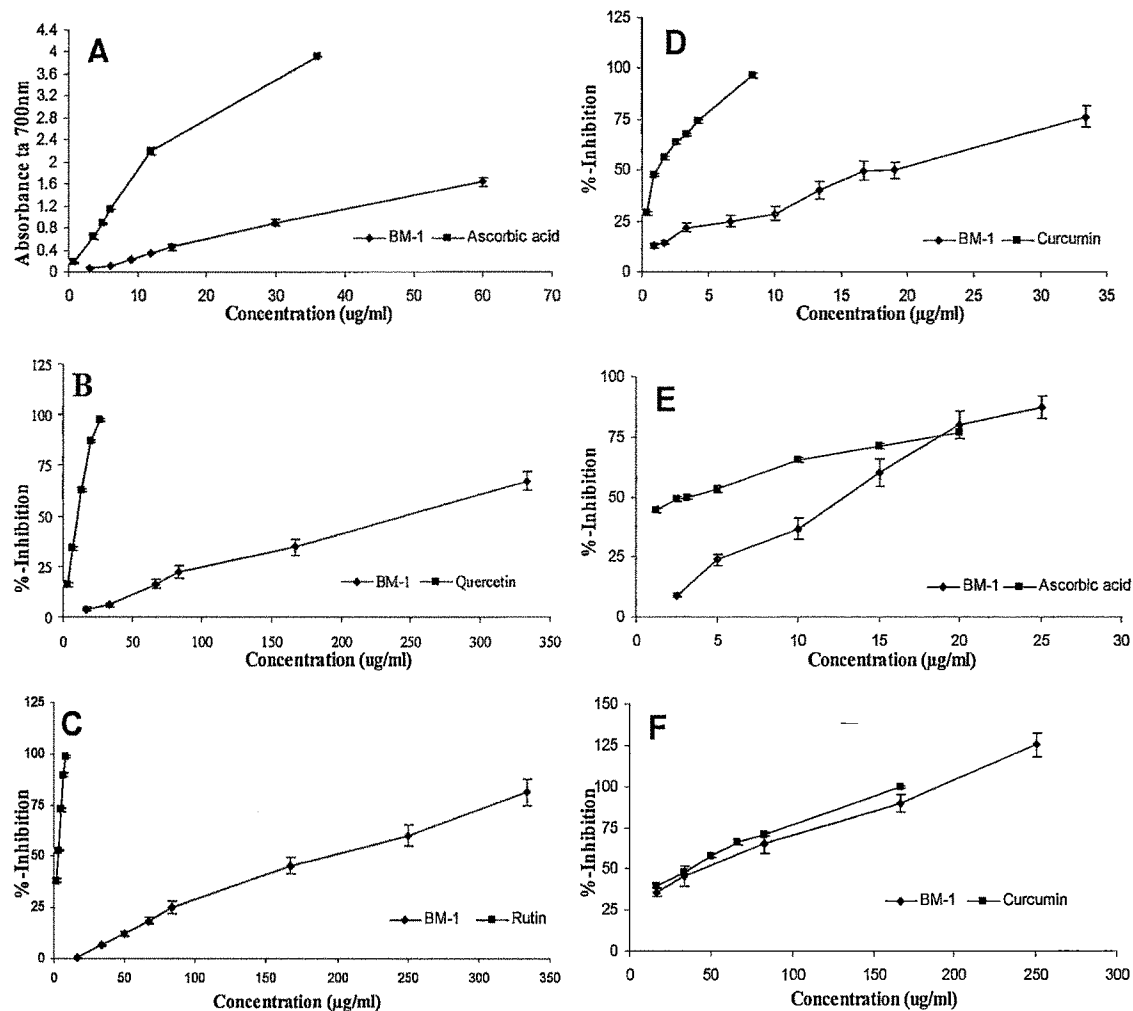


**Fig-3.81 XY- Scatters for *in vitro* studies on BM1 from butea flowers. Results are average of three determinations and shown as Mean  $\pm$  SD. A) Reducing power assay, B) Superoxide radical scavenging assay, C) DPPH radical scavenging assay, D) Hydroxyl radical scavenging assay, E) Inhibition of erythrocytes lysis F) Nitric oxide radical scavenging assay.**

**a) Reducing power assay**

BM1 exhibited concentration dependent increase in reducing power. Compared with ascorbic acid the reducing power of BM1 was lesser (**Fig-3.81A**).

***b) Inhibition of superoxide radical***

BM1 showed inhibition of superoxide radical with an EC<sub>50</sub> value of 242.01µg/ml. The scavenging effects was lesser compared to reference standard quercetin (EC<sub>50</sub>:10.84 µg/ml) (**Fig-3.81B**).

***c) Scavenging of DPPH radical***

BM1 showed a concentration dependent antiradical activity by scavenging DPPH radical with an EC<sub>50</sub> value of 185.45µg/ml. The scavenging effects were lesser compared to reference standard rutin (EC<sub>50</sub>: 2.85 µg/ml) (**Fig-3.81C**).

***d) Inhibition of hydroxyl radical***

BM1 showed 50% inhibition of hydroxyl radicals at the concentration of 19.04µg/ml. The results were compared with reference standard curcumin (EC<sub>50</sub>: 0.96µg/ml), which was more effective than the fractions tested (**Fig-3.81D**).

***e) Inhibition of erythrocyte hemolysis***

BM1 inhibits the AAPH induced hemolysis of erythrocytes with EC<sub>50</sub> values of 13.01µg/ml. The inhibitory effect was lesser than ascorbic acid (EC<sub>50</sub>: 3.07 µg/ml). (**Fig-3.81E**)

***f) Inhibition of nitric oxide radical***

Concentration of BM1 required for 50% inhibition of nitric oxide radicals was found to be 49.01µg/ml respectively. Curcumin was used as a reference compound, showed 50% inhibition at 34.23µg/ml. (**Fig-3.81F**)

***Rapid screening for antioxidant compounds***

BM1 contains antiradical components, when evaluated by TLC using DPPH reagent. (**Fig-3.80d**)

***g) Total phenolic content***

BM1 shows 16.7%w/w of phenolics, Gallic acid was used as a standard for the calibration.

### 3.4.1.1 Toxicity study

Toxicity study was carried out for BM1 as per OECD guidelines in female albino mice. No mortality was observed at a single oral dose of 2000mg/kg body weight. Histopathological examination of the visceral organs in mice did not show any signs of necrosis or damage. Safe dose 200mg/kg body weight was used for further studies.

### 3.4.1.2 In-vivo antioxidant activity

The fraction obtained from butea flowers BM1 was subjected to in vivo antioxidant activity. The results are shown in (Table-1.46 & 1.47, Fig-3.82 & 3.83)

**Table-1.46 Effect of BM1 on endogenous antioxidant enzymes in heart**

Groups	SOD	CAT	GSH	LPO
CON	18.29±1.71	798.76±33.63	14.95±0.67	1.38±0.13
ISO	10.24±0.78**	368.11±33.33***	11.87±0.38**	4.59±0.22***
BM	22.23±1.98 <sup>ns</sup>	777.1±59.31 <sup>ns</sup>	19.55±0.71***	2.02±0.12 <sup>ns</sup>
BM+ISO	21.39±1.49###	702.46±49.13###	14.67±0.78#	3.34±0.23###

Statistical analysis was done by using ANOVA

Post test applied: Tukey-Kramer multiple comparison Test

Values are expressed as mean ± SEM.

\*p<0.05; \*\*p<0.01; \*\*\*p<0.001; <sup>ns</sup>p>0.05 = non significant, (n=6)

ISO treated group and BM1 alone pretreated groups were compared with control group (\*Compared with control group).

BM1 pretreated group injected with ISO were compared with ISO group (#compared with ISO treated group).

**Table-1.47 Effect of BM1 on cardiac and liver serum marker enzymes**

Groups	CKMB	LDH	SGPT	SGOT	ALKP	Uric acid
CON	585.87±41.58	1417.3±63.91	60.66±1.45	131±11.51	312.5±21.11	0.99±0.05
ISO	850.86±31.89***	1877.8±42.94***	60.66±0.88 <sup>ns</sup>	183±7.08***	475±22.58***	1.55±0.06***
BM	599.17±14.23 <sup>ns</sup>	2168.3±76.94***	62±1.91 <sup>ns</sup>	135.67±5.71 <sup>ns</sup>	325±23.05 <sup>ns</sup>	1.3±0.02***
BM+ISO	709±13.02###	2702.7±84.05###	56.19±0.66 <sup>ns</sup>	145.08±3.07##	333±12.29###	1.35±0.01#

Statistical analysis was done by using ANOVA

Post test applied: Tukey-Kramer multiple comparison Test

Values are expressed as mean ± SEM.

\*p<0.05; \*\*p<0.01; \*\*\*p<0.001; <sup>ns</sup>p>0.05 = non significant, (n=6)

ISO treated group and BM1 alone pretreated groups were compared with control group (\*Compared with control group).

BM1 pretreated group injected with ISO were compared with ISO group (#compared with ISO treated group).

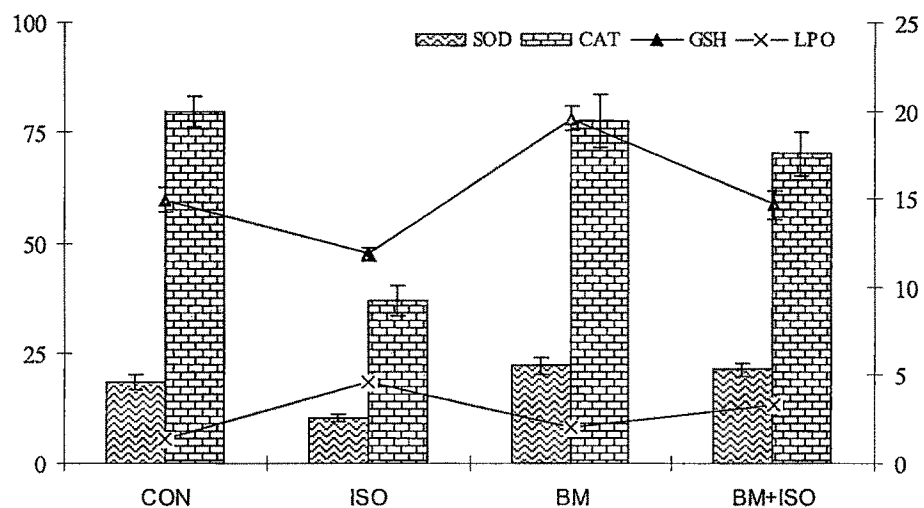


**Fig-3.82 Effect of BM1 on endogenous antioxidant enzymes in ISO induced myocardial infarction.**

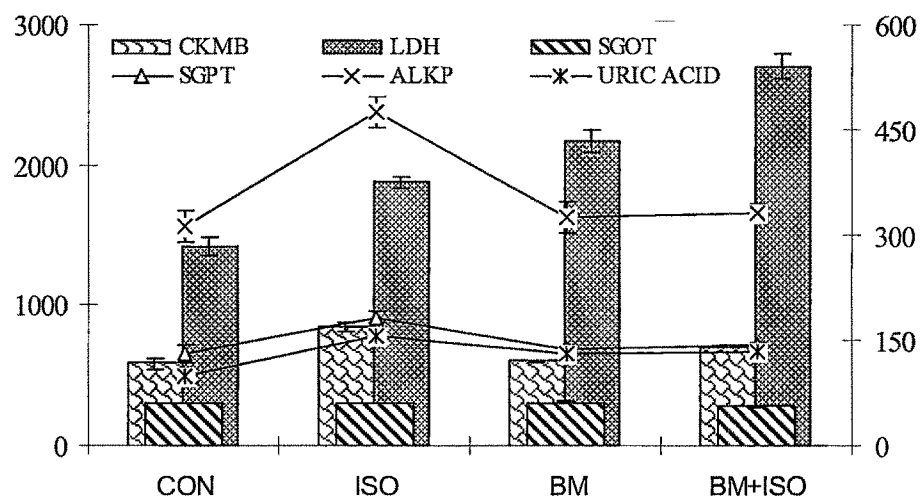


**Fig-3.83 Effect of BM1 on serum cardiac and liver marker enzymes**

**a) Effect on Body weight**

No significant variation in body weight was observed. (Table-1.48, Fig-3.84)

**b) Effect on Heart weight/ Body weight ratio**

ISO group showed increase in Heart/body weight ratio ( $p < 0.01$ ) when compared with control group. BM1 did not showed any change in ISO affected ratio. BM1 alone pretreated group showed no significant change in the ratio compared to control group (Fig-3.85).

**Table-1.48 Effect of BM1 on weight of rats during treatment**

Groups	Weight (Gms)			
	CON	ISO	BM	BM+ISO
1 <sup>st</sup>	343.33±8.72	313.33±3.63	280.5±5.05	333.33±13.41
8 <sup>th</sup>	333.33±11.15	323.33±3.63	276±4.48	335±10.10
15 <sup>th</sup>	343.33±7.37	330±5.2	276.33±4.17	335±11.81
17 <sup>th</sup>	353.33±4.94	328.33±6.5	290.91±4.42	331±12.61

Statistical analysis was done by using ANOVA

Post test applied: Dunnett multiple comparison test.

Values are expressed as mean ± SEM.

\* $p < 0.05$ ; \*\* $p < 0.01$ ; \*\*\* $p < 0.001$ ; <sup>ns</sup> $p > 0.05$  = non significant, (n=6)

\* Compared with first day weight.

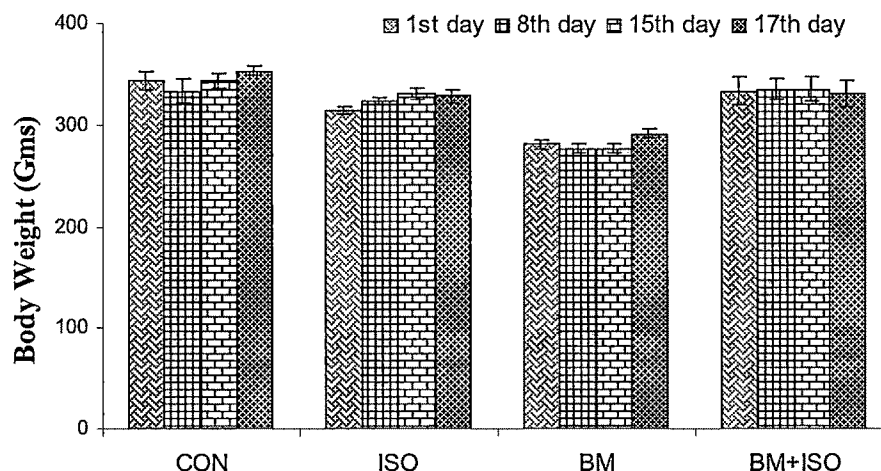


**Fig-3.84 Effect of BM1 on body weight of rats during treatment**

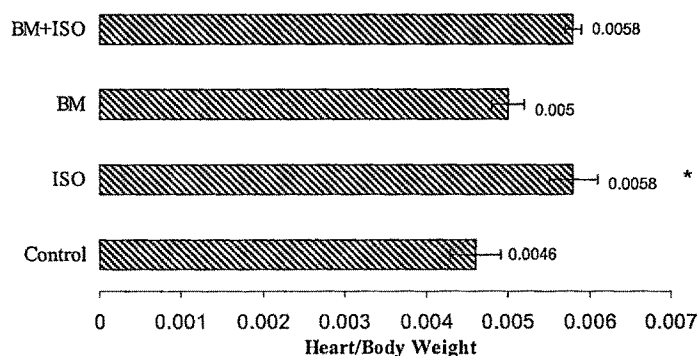


**Fig-3.85 Effect of BM1 on Heart weight/body weight ratio during treatment.**

Statistical analysis was done by using ANOVA

Post test: Tukey-Kramer multiple comparison Test

Values are expressed as mean  $\pm$  SEM.

\* $p < 0.05$ ; \*\* $p < 0.01$ ; \*\*\* $p < 0.001$ ; <sup>#</sup> $p > 0.05$  = non significant, (n=6)

#compared with ISO treated group

\*Compared with normal group

### **c) Histopathology of heart and liver**

Microscopic examination of ISO treated rats showed myocardial necrosis foci intercalated among normal muscle fibers. In the necrosis foci there were lymphocytic exudates, atrophy of the remaining normal muscle and also elongation, undulation of the fibers and formation of contractile band lesions characteristic of the pre-infarction stage. ISO further showed damaging effect on liver anatomy with several regions of necrotic foci. ISO also affects the central artery and triads. The rats pretreated with BM1 were found to reverse these changes. **(Fig-3.69)**

The BM1 fraction was subjected to screen for in-vivo antioxidant activity using isoproterenol (ISO) induced myocardial infarction in rats. Pretreatment with BM1 found to reverse the ISO affected levels of endogenous antioxidant enzymes. It also protects the liver and heart against ISO damage marked with significant reduction in marker enzymes like CKMB, SGOT, ALKP and uric acid. While BM alone treated group showed non significant change in enzymes and LPO level except significant rise in GSH, without ant significant change in

marker enzymes. The study was further supported by the histopathological examination of the heart and liver.

#### **3.4.2 Isolation and Characterization of BM from BM1 fraction**

Pale yellow colored BM1 obtained from extraction of Butea flowers with methanol, was further processed for isolation of active compounds. 500mg of BM1 dissolved in 5ml of distilled water by heating on water bath gave intense orange coloration, filtered and kept at room temperature for overnight. Broom shaped crystals got separated at the bottom of the flask, which was separated and washed with several quantities of water under vacuum (93.30mg). Chromatographic study showed two bands at Rf 0.2 and 0.25 when developed in ethyl acetate: formic acid: glacial acetic acid: water (100:11:11:26). Compound at Rf-0.25 gives light blue color at 366, while that with Rf- 0.2- dark blue color at 254 and light blue fluorescence at 366, it also gives dark orange color after treatment with anisaldehyde sulphuric acid reagent.

The compound obtained above was refluxed with methanol for 2hr̄s and filtered hot. Filtrate after keeping at 4-8°C gave 92mg of white granular mass after washing several times with cold methanol. This compound shows single spot on TLC using same solvent system which turns dark orange after spraying with anisaldehyde sulphuric acid reagent. For further studies this compound is designated as BM.

*Solubility:* BM was soluble in water and methanol in hot conditions while insoluble in petroleum ether, chloroform, ethyl acetate and benzene. It gave intense orange color in water. 1% solution of BM in water showed pH in between 5-6, but it did not show any effervescence after addition of few drops of 10% sodium bicarbonate solution, which revealed its phenolic nature. Its aqueous solution gets decolorized with addition of KMNO<sub>4</sub>/bromine water, which showed BM unsaturation. The compound gave intense orange colour on addition of concentrated H<sub>2</sub>SO<sub>4</sub>/ NaOH, indicating that BM may be phenolic in nature.

It gave sooty flame due to its aromatic nature. Nitrogen and sulphur were absent.

### 3.4.2.1 Characterization of BM

Compound BM when subjected to characterization showed following characteristic UV, IR, NMR and mass spectra.

UV spectra: Band Ia- 312nm, Band Ib-372nm, Band II- 270 nm. + NaOEt - 431nm (increased intensity), + AlCl<sub>3</sub>- 422 nm, +NaOAc- No change.

IR (KBr): 3313-3118 (hydroxyl group), 2972, 2923 (alkyl C-H stretch), 1670 (conjugation with alkene), 1612 (aromatic), 1571,1521,1444 (tri-substituted benzenes), 1419 (C-H bending in alkene), 1336 (O-H bending), 1280 (C-O stretching), 1251 (asymmetrical C-O-C stretching), 1114 (=C-H wagging), 1085 (symmetrical C-O-C stretching), 1076 (=C-H wagging), 680-453nm (substituted benzenes).

<sup>1</sup>H NMR (DMSO, 400 Hz)  $\delta$ : 2.79 (1H, d, H-7),  $\delta$ : 3.1(1H, t, H-8),  $\delta$ : 3.3-3.8 (6H, m, H-10, H-12, H-13, H-14, 2H-15),  $\delta$ : 4.37 (1H, t, 4'-OH),  $\delta$ : 4.44 (1H, d, 15-OH),  $\delta$ : 4.68 (1H, t, OH-2'),  $\delta$ : 4.86 (2H, s, OH-12, OH-13),  $\delta$ : 4.97 (1H, d, OH-4),  $\delta$ : 5.39 (1H, d, H-14),  $\delta$ : 6.67 (1H, t, H-3'),  $\delta$ : 6.71 (1H, t, H-5'),  $\delta$ : 6.85 (1H, d, H-6'),  $\delta$ : 7.01 (1H, t, H-5),  $\delta$ : 7.36 (1H, d, H-6),  $\delta$ : 7.76 (1H, d, H-2).

Chemical shifts are given in ppm on the  $\delta$ -scale, s = singlet, d = doublet, t = triplet, m-multiplet.

The m.s. showed the following principal peaks:  $m/z$ : 435.1 [M<sup>+</sup>], 274.3 [M- C<sub>6</sub>H<sub>9</sub>O<sub>5</sub>], 273.3 [M- C<sub>6</sub>H<sub>10</sub>O<sub>5</sub>], 259.3 [M- C<sub>6</sub>H<sub>11</sub>O<sub>6</sub>].

The compound (BM) found as white granular solid, m.p.176-178°C, molecular formula of C<sub>21</sub>H<sub>22</sub>O<sub>10</sub> as indicated by EI and ES mass spectra. The colour reaction (deep orange red fluorescence in UV light when exposed to ammonia) and U.V. spectra indicated it to be chalcone glycoside. Polyhydroxychalcones absorb strongly in the 300-400 nm region (Band I) and in 220-270 nm region (Band II). Band I consists of an intense peak (Band Ia) and a minor inflection (Band Ib). The UV spectra of BM showed maxima at 270 nm, 312 nm, and 372 nm. Addition of shift reagents showed free hydroxyl groups at 2', 4', 4 positions of the chalcone ring. The UV maxima shifted with AlCl<sub>3</sub> to 422 nm indicating

that 2' position is free. Bathochromic shift with increased intensity (Band Ia shifted to 431 nm) on addition of Sodium ethoxide showed the presence of free hydroxyl group at 4 position. Lack of change in the UV spectrum with sodium acetate and boric acid indicated that the glucose unit may be in the B- ring, linked to 3- hydroxyl group. (Fig-3.86, 3.87)

The IR spectrum showed the presence of hydroxyl(s) (3118-3313nm) region due to intermolecular hydrogen bonding), ketone in conjugation with alkene (1670nm), aromatic moiety (1612 nm).

The  $^1\text{H}$  NMR spectrum of BM 2 revealed the presence of aromatic protons ( $\delta$  6.677-7.77). Glucose protons are evident at  $\delta$  3.3- 4.0; H-1 of glucose resonates at  $\delta$  5.18.

Paper chromatography showed orange colour in UV light with ammonia. With NaOH, BM gives deep yellow while it gives brown color on addition of  $\text{FeCl}_3$ .

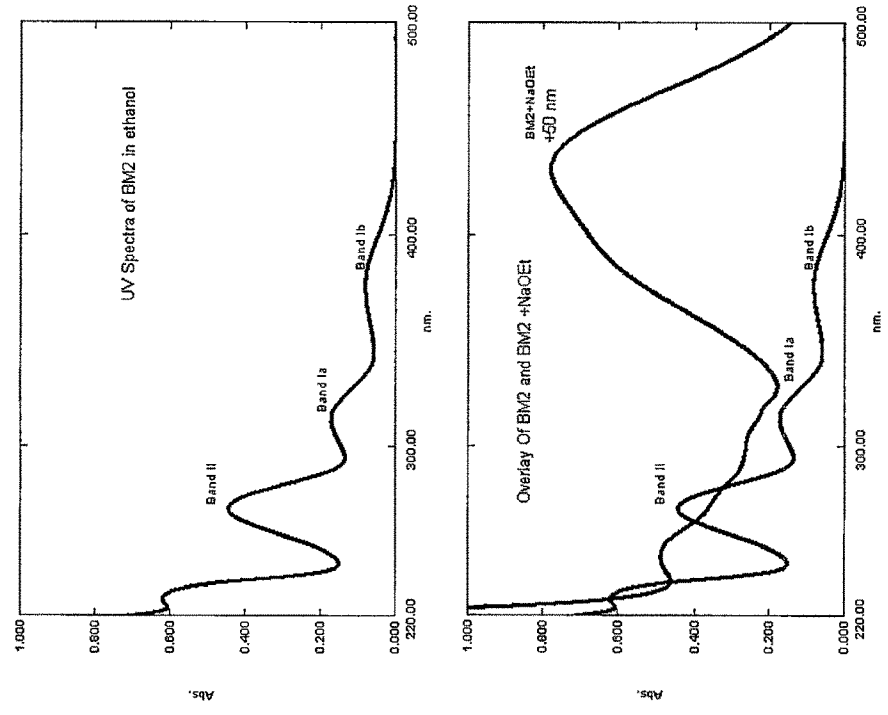
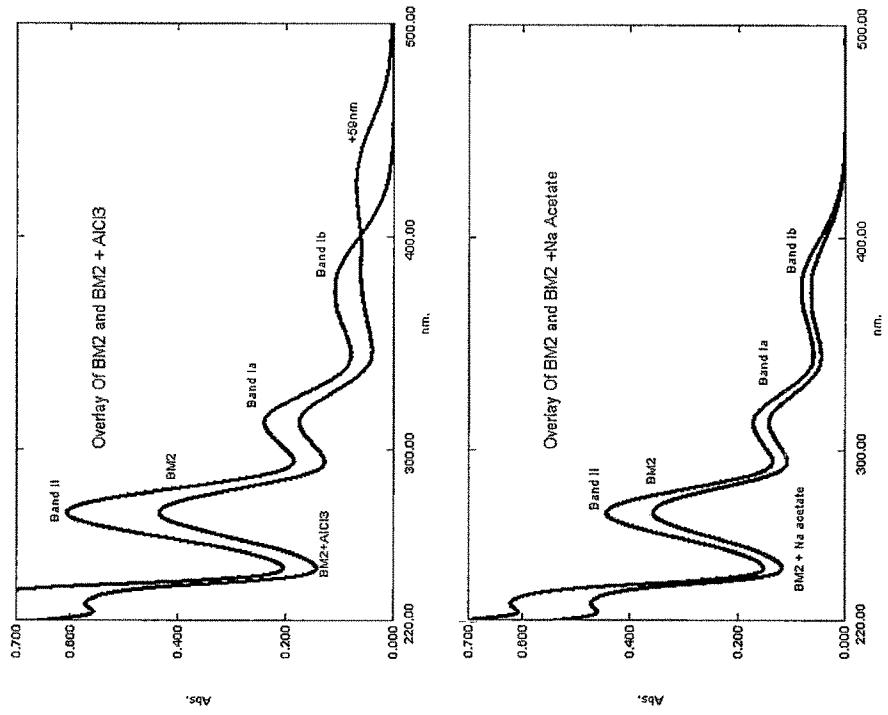
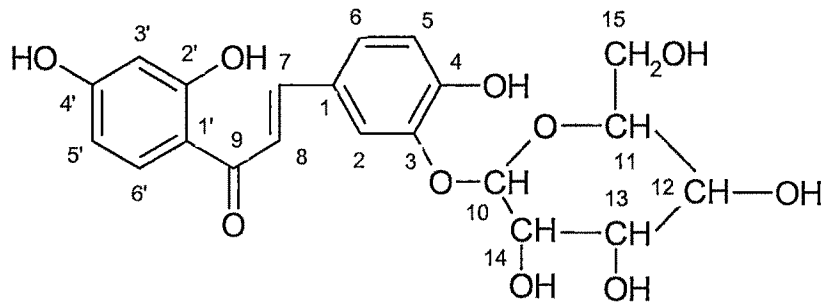
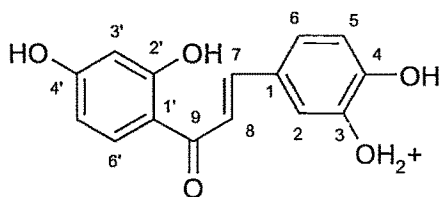


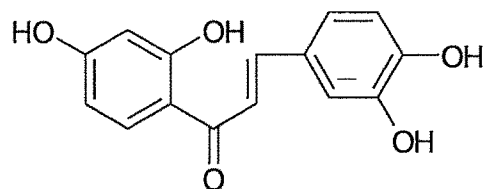
**Fig-3.86 Effect of addition of shifts reagent on UV absorption spectra of BM**



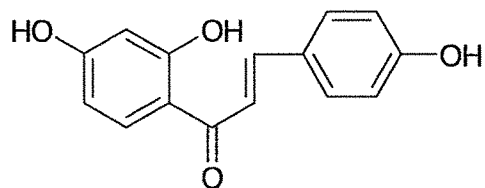
Butein-3-beta-D-glucoside (Monospermoside)



[m/z : 274]



[m/z : 273]



[m/z : 259]

Fig-3.87 Structure of BM

### 3.4.2 Evaluation of antioxidant activity of BM using cardiac cell line-H9c2

#### 3.4.2.1 Percentage cell viability (H9c2)

After 3 and 6hrs of treatment BM did not show any significant change in viability of H9c2 cell at 2-100 $\mu$ g/ml concentration. After 12 hrs of incubation cell viability was found to be reduced to 98.65, 93.95, 92.91, 92.08, 89.79, and 97.7% at the conc. 5-100 $\mu$ g/ml respectively when compared with control. Thus BM obtained from Butea flowers did not showed cytotoxicity in H9c2 cells, even after 12 hrs of incubation the reduction in cell viability was not significant. (Table-1.49, Fig-3.88).

**Table-1.49 Effect of BM on % - viability of H9c2 cells**

BM ( $\mu$ g/ml)	3 Hr	6 Hr	12 Hr
Control	100 $\pm$ 8.86	100 $\pm$ 1.06	100 $\pm$ 1.66
2	89.45 $\pm$ 4.64	105.61 $\pm$ 5.88	101.04 $\pm$ 4.58
5	90.29 $\pm$ 5.48	98.39 $\pm$ 3.20	98.65 $\pm$ 0.68
10	100 $\pm$ 8.43	98.12 $\pm$ 2.94	93.95 $\pm$ 4.37
20	101.26 $\pm$ 9.70	101.06 $\pm$ 7.75	92.91 $\pm$ 2.29
50	101.68 $\pm$ 2.10	101.87 $\pm$ 1.06	92.08 $\pm$ 1.45
75	104.21 $\pm$ 5.06	98.39 $\pm$ 6.68	89.79 $\pm$ 2.08
100	110 $\pm$ 5.69	96.79 $\pm$ 3.20	97.7 $\pm$ 3.33

Values are expressed as mean  $\pm$  SD of % cell viability (average of three determinations)

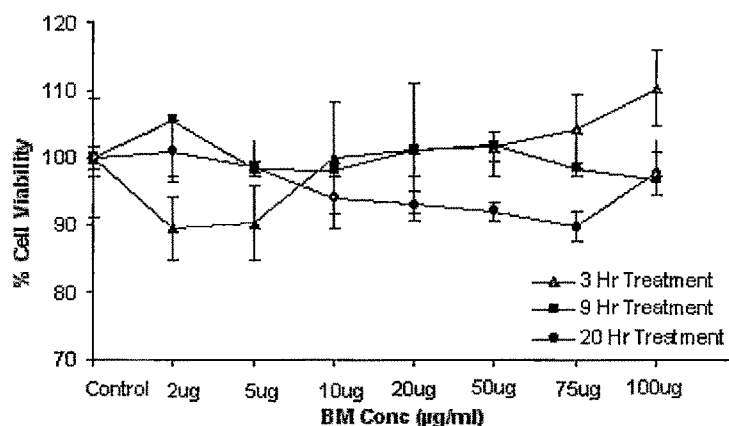


**Fig-3.88 Effect of various concentration of BM on %- viability of H9c2 cells at different time interval**

### 3.4.2.2 Effect of BM on H<sub>2</sub>O<sub>2</sub> induced stress in H9c2 cells

BM was found to reverse the H<sub>2</sub>O<sub>2</sub> induced stress in H9c2 cells. After 3 hrs of treatment, it showed 85.62, 93.56, 94.67, 115.18, 98.73, 92.4, and 89.26% of cell viability in between concentration range (2-100µg/ml) respectively when compared with H<sub>2</sub>O<sub>2</sub> control with 32.02% viability.

Even after 6 hrs incubation, BM showed 81.96, 76.96, 78.29, 76.98, 70.16, 69.56 and 56.98% cell viability when compared with that of H<sub>2</sub>O<sub>2</sub> control (41.06%) respectively.

After 12 hrs of treatment cell viability was found to be 64.16, 50.2, 40.83, 41.45, 35.83, 38.56 and 40% respectively for the same concentration range when compared to that of H<sub>2</sub>O<sub>2</sub> (49.82%) (Table-1.50, Fig-3.89 & 3.92 A-G).

**Table-1.50 Effect of pretreatment of BM on H<sub>2</sub>O<sub>2</sub> affected viability of H9c2 cells**

BM (µg/ml)	3 Hr	6 Hr	12 Hr
Control	100±8.43	100±1.06	100±1.66
H <sub>2</sub> O <sub>2</sub>	32.02±3.79	41.06±2.67	49.82±4.16
2	85.62±7.32	81.96±5.69	64.16±4.16
5	93.56±5.69	76.96±5.34	50.2±6.25
10	94.67±7.56	78.29±5.34	40.83±6.25
20	115.18±3.96	76.98±2.67	41.45±4.16
50	98.73±5.69	70.16±4.96	35.83±2.08
75	92.4±8.69	69.56±5.34	38.56±2.08
100	89.26±8.43	56.98±5.34	40±4.16

Values are expressed as mean ± SD of % cell viability (average of three determinations)

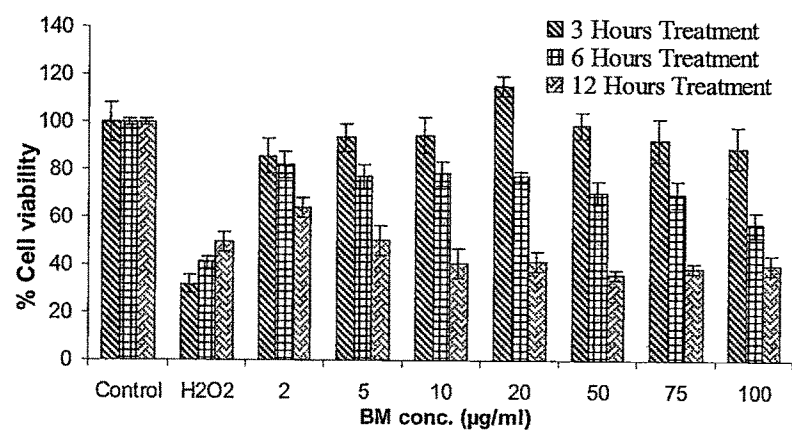


**Fig-3.89 Table-7 Effect of pretreatment of BM on H<sub>2</sub>O<sub>2</sub> affected viability of H9c2 cells**

BM showed concentration and time dependent protection against H<sub>2</sub>O<sub>2</sub> induced stress in H9c2 cells. As the concentration of BM increased cell viability was found to be increased, but above 20µg/ml, BM showed reduction in cell viability. This effect might be due to its prooxidant activity on H9c2 cells.

Cell viability was also found to be reduced with increased incubation time.

#### **3.4.2.3 Effect of BM pretreatment on H<sub>2</sub>O<sub>2</sub> induced increase in intracellular ROS level**

H9c2 cells, pretreated with BM were exposed to H<sub>2</sub>O<sub>2</sub>, and ROS was assessed by flow cytometric analysis after loading the cells with the ROS-sensitive dye DCFH-DA. As shown in (Fig- 3.90B), an increase in DCF was observed in the H<sub>2</sub>O<sub>2</sub>-treated cells, with the mean fluorescence intensity increased from 4.61% to 26.17% (Fig- 3.90A & 3.90B). This effect of H<sub>2</sub>O<sub>2</sub> was attenuated by BM pretreatment. Treatment of H9c2 cells with 10-100 µg/ml concentration of BM caused the mean fluorescence intensity to decrease from 26.17% to 4.04% (Fig- 3.90B - 3.90F). The cells treated under the same conditions were further subjected to confocal microscopy. An increase in fluorescence intensity was observed in the H<sub>2</sub>O<sub>2</sub> treated cells (Fig-3.91B), which was reversed by pretreatment with different concentration of BM (10-50µg/ml) (Fig-3.91B-3.91E), while at 100µg/ml, fluorescence intensity was found increased which might be due to the prooxidant effect of BM on H9c2 cells (Fig-3.91F).

#### **3.4.2.4 Effect of BM on xanthine-xanthine oxidase induced increase in intracellular ROS level**

Treatment of H9c2 cells with (X+XO) increases the fluorescence intensity from 5.50 to 55.08% when assessed by flow cytometric analysis after loading the cells with the ROS-sensitive dye DHE (Fig- 3.90G- 3.90H). This effect of X+XO was reversed in cells pretreated with different concentration of BM (10-100µg/ml) with decrease in fluorescence intensity of DHE from 55.08 to 4.74% respectively (Fig.3.902H to 3.90L). Confocal examination of cells showed O<sub>2</sub><sup>•-</sup> was enhanced in X-XO exposed cells (Fig- 3.91M & 3.91N). BM pretreated cells (10µg/ml) found to reverse this X+XO induced changes, confirmed by decreased fluorescence intensity in BM pretreated cells (Fig- 3.91I). Increasing the concentration (20-100µg/ml) increased the fluorescence intensity which might be due to prooxidant effect of BM on H9c2 cells. (Fig- 3.91J - 3.91L)

#### **3.4.2.5 Effects of BM on H<sub>2</sub>O<sub>2</sub> affected mitochondrial membrane potential (ΔΨ<sub>m</sub>) in H9c2 cells.**

DiOC<sub>6</sub>, a mitochondrial voltage dependent dye was employed to observe the changes in ΔΨ. After exposing the cells H<sub>2</sub>O<sub>2</sub> (35µM) for 2hrs, DiOC<sub>6</sub> intensity

was significantly reduced as observed in confocal microscopy when compared to untreated cell (Fig- 3.91S - 3.91T). Pretreatment with BM (10-50 $\mu$ g/ml) increase the fluorescence intensity, compared to H<sub>2</sub>O<sub>2</sub> treated cells (Fig- 3.91U-3.91W). Further increase in concentration of BM (100 $\mu$ g/ml) showed decrease fluorescence intensity which might be due to prooxidant activity of BM (Fig-3.91X)

Thus BM pretreatment was found to increase the H<sub>2</sub>O<sub>2</sub> affected mitochondrial membrane potential ( $\Delta\Psi_m$ ) but at higher concentration this effect gets abolished which might be due to its prooxidant effect.

$\Delta\Psi_m$  was further measured by using Tetramethyl Rhodamine (TMRE). H<sub>2</sub>O<sub>2</sub> reduced the membrane potential in H9c2 cells marked with increase fluorescence intensity from 10.89 to 42.76% when assessed by flow cytometric analysis after loading the cells with the  $\Delta\Psi_m$ -sensitive dye TMRE (Fig-3.90M & 3.90N). Pretreatment with various concentration of BM (10-50 $\mu$ g/ml) increased the  $\Delta\Psi_m$  confirmed by decreased fluorescence intensity from 42.76 to 10.10% (Fig-3.90N- 3.90P), but at higher concentration ie 100 $\mu$ g/ml,  $\Delta\Psi_m$  gets reduced, which might be due to the prooxidant effect of BM (Fig. 3.90Q & 3.90R).

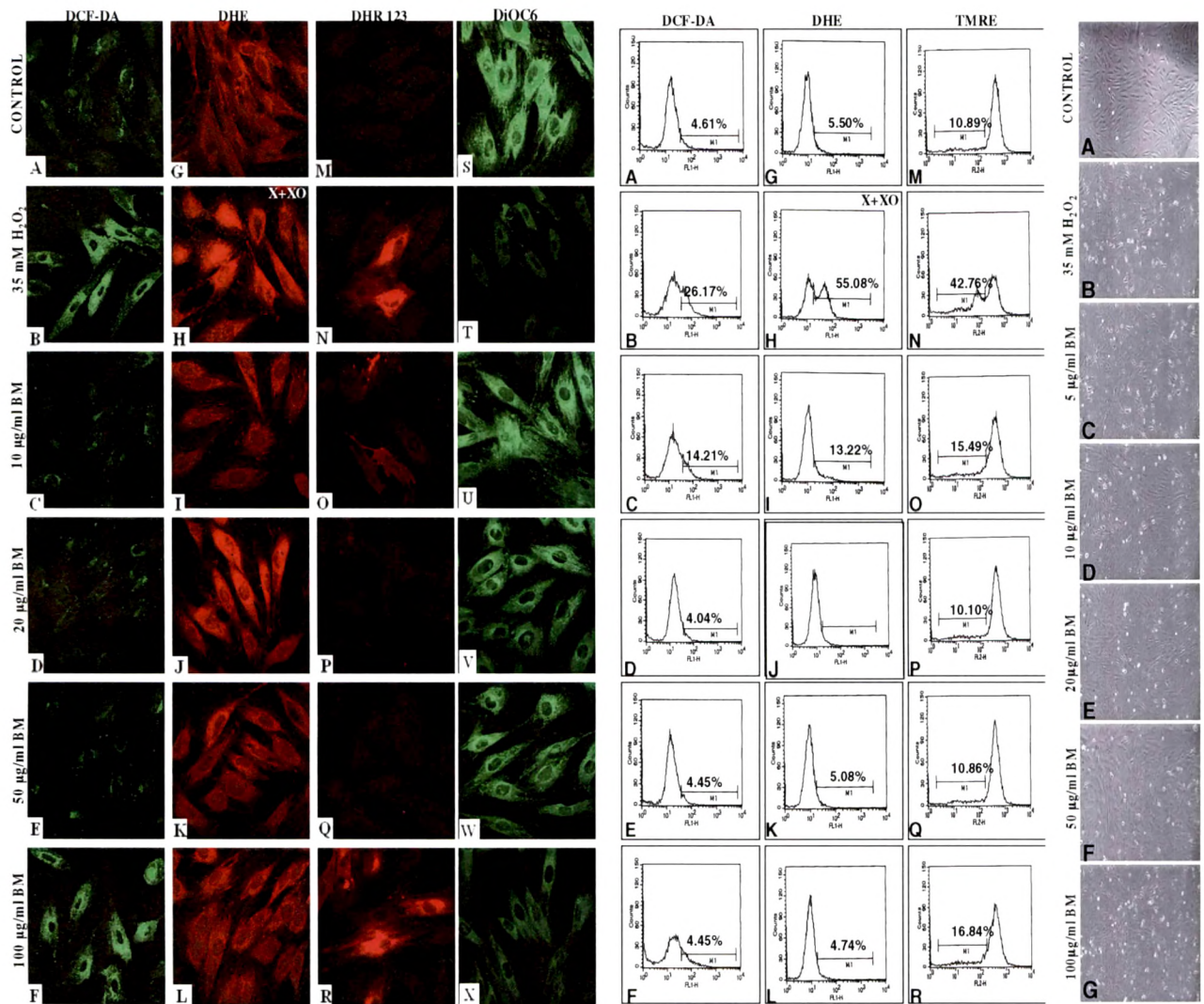


**Fig-3.90 (A-R) Flow activated cytometric analysis of H9c2 cells pretreated with different concentration of BM and challenged with H<sub>2</sub>O<sub>2</sub> and Xanthine-xanthine oxidase after loading with different molecular probes.**

**Fig-3.91 (A-X) Confocal images of H9c2 cells loaded with different molecular probes showing the effect of BM on H<sub>2</sub>O<sub>2</sub> and Xanthine-xanthine oxidase induced stress.**

**Fig. 3.92 (A-G) Effect of BM on H<sub>2</sub>O<sub>2</sub> induced stress in H9c2 cell lines-Phase contrast images.**

### 3.4.3 Estimation of BM in different fractions of butea flowers by HPTLC

BM was estimated in various extracts of Butea flowers (Table-1.51, Fig-3.93).

Stock solution of BM prepared in methanol (1mg/ml)

Concentration of extracts 1mg/ml

Scanning wavelength- 254nm (Lamp-D2)

Calibration plot for BM in the concentration range of 250-6000ng

Solvent system- Ethyl acetate: formic acid: Glacial acetic acid: water

**Table-1.51 Estimation of BM in various extracts of Butea flowers**

		% of BM present in extracts			
	Ethyl acetate extract (4µl)	Butanol extract (4µl)	Methanol extract (4µl)	BM1 (4µl)	Aqueous extract (7µl)
Height	Not detected	86.37	65.15	38.12	76.54
Area	Not detected	81.75	56.83	44	84.71

TLC quantification showed high concentration of BM in butanol and aqueous extracts, while it was not detected in ethyl acetate extract.

Substance: Substance1 @ 254 nm      Regression mode: Linear  
 Regression via Height  $Y = 75.354 + 0.039 \cdot X$        $r = 0.98523$        $sdv = 10.27\%$   
 Area  $Y = 2032.278 + 0.923 \cdot X$        $r = 0.99007$        $sdv = 7.84\%$

Track	Vial	Rf	Amount / Fraction	Height	X(calc)	Area	X(calc)	Sample ID/ Remark
1	1	0.20	250.00 ng	91.33		2245.57		
2	1	0.20	500.00 ng	96.85		2284.60		
3	1	0.19	750.00 ng	67.86		2217.19		
4	1	0.21	1000.00 ng	100.17		2523.86		
5	1	0.21	2.000 ug	178.65		4419.96		
6	2	0.21	4.000 ug	239.88		5360.53		
7	2	0.20	6.000 ug	301.53		7654.13		
8	3							EA not detected or del
9	4	0.20		210.93	3.455 ug	5048.30	3.269 ug	BM1
10	5	0.20		177.60	2.606 ug	4129.94	2.273 ug	TME
11	6	0.20		135.19	1.525 ug	3117.49	1.176 ug	BM1
12	7	0.20		265.57	5.358 ug	7503.90	5.930 ug	SAQ

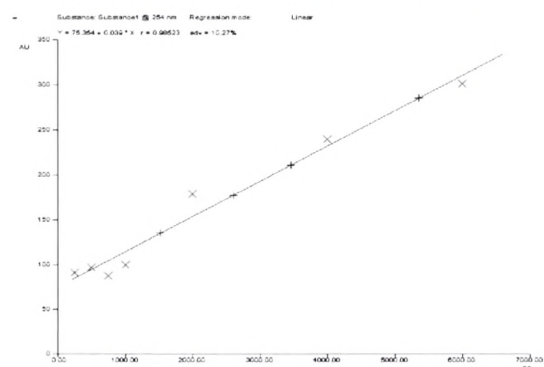
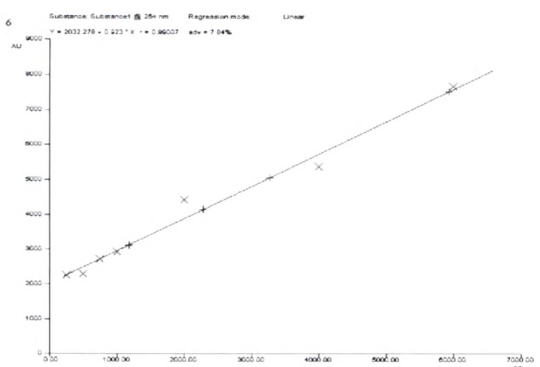
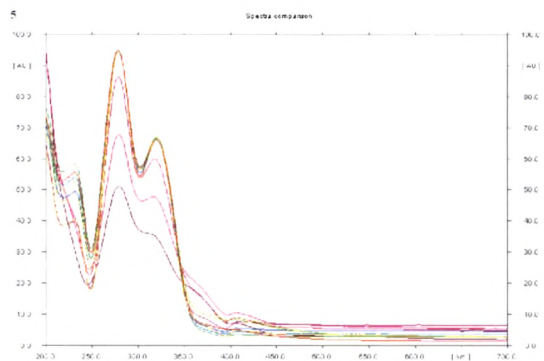
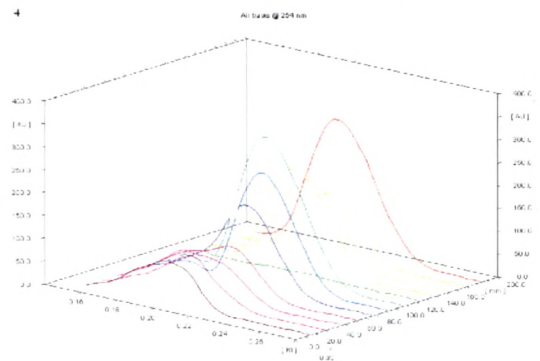
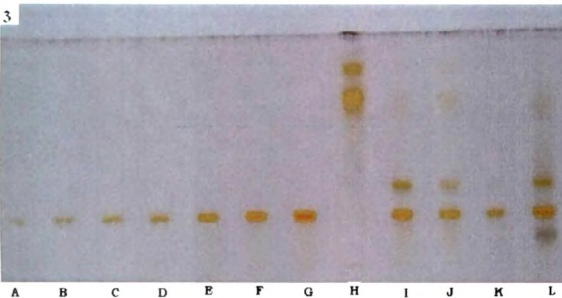
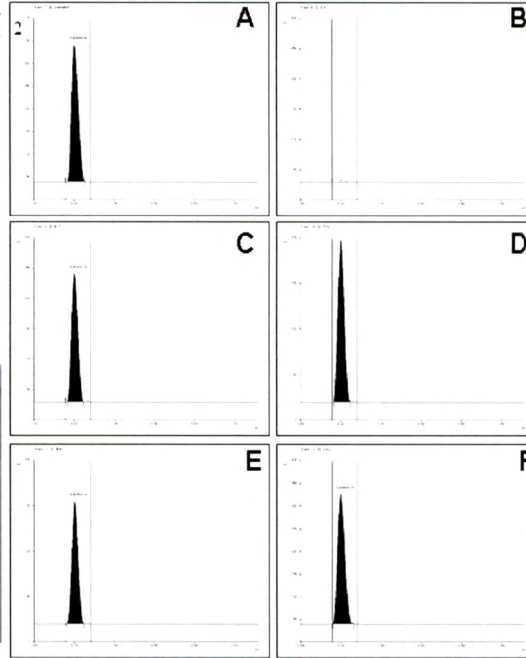


**Fig 3.93- 1 Substance applied, 2) Chromatogram for BM in different extracts of flowers, 3) TLC Plate showing track (A-G) for BM treated with Anisaldehyde-sulphuric acid reagent, (H-L) Ethyl acetate, butanol, total methanol, BM1 fraction and aqueous fraction of Butea flowers, 4) 3-D view of all tracks, 5) Spectra comparison of BM. 6-7) Linearity plot as per area and height.**

#### 3.4.4 Fingerprinting of BM1 by HPTLC

TLC fingerprint profile of the BM1 was established which comprises of the bands resolved, Rf values, spectral details and  $\lambda_{\max}$  when scanned in UV-254, 366 and 520nm. Data was recorded in (Table-1.52, Fig-3.94).

Solvent system- Ethyl acetate: formic acid: Glacial acetic acid: water (14.28:1.42:1.42:2.85 v/v)

Concentration of BM1- 1mg/ml

Volume applied 10 $\mu$ l

**Table-1.52 TLC fingerprinting for BM1 scanned at 254, 366 and 520nm.**

Scanning wavelength	Rf	$\lambda_{\max}$	Relative % area
254nm (Under UV)	0.09		11.11
	0.17		83.60
	0.32		5.29
366nm (Under UV)	0.08	200	2.56
	0.16	277	21.99
	0.26	406	21.43
	0.35	425	9.53
	0.41	433	14.40
	0.48	434	13.63
520nm (AS reagent)	0.61	406	15.37
	0.19	382	97.75
	0.35	385	2.25

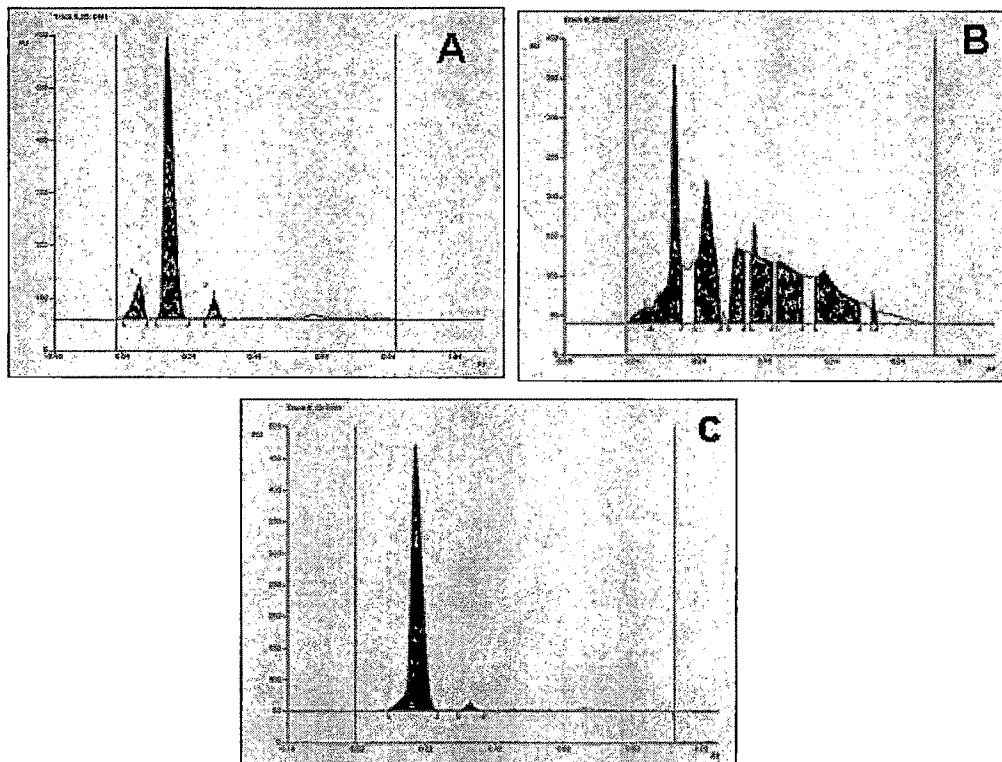


**Fig-3.94 HPTLC- chromatogram for BM1 developed in ethyl acetate: formic acid: glacial acetic acid: water and scanned at A) 254nm, B) 366nm and C) 520nm (after treatment with anisaldehyde- sulphuric acid reagent)**

These fingerprint data helps in asserting the total number of chemical moieties which are common in these extracts and also provides an idea regarding the isolation of these bioactive compounds.